European School of Molecular Medicine (SEMM)

University of Milan and University of Naples "Federico II"

PhD degree in Systems Medicine (curriculum in Molecular Oncology)

Settore disciplinare: BIO/11

Proteomic identification of the transcription factors Ikaros and Aiolos as new Myc interactors on chromatin

Chiara Veronica Locarno

Matricola: R10755

Center for Genomic Science IIT@SEMM, Milan

Supervisor: Bruno Amati, PhD
IEO, Milan

Added Supervisor: Arianna Sabò, PhD
IEO, Milan

Academic year 2017-2018

Table of contents

List of abbreviations

AchR	acetylcholine receptor
ACN	acetonitrile
ALL	acute lymphoblastic leukemia
Bcl-2/6	B cell lymphoma 2/6
BCR	B cell receptor
BET	bromodomain and extra-terminal motif proteins
Brd4	bromodomain containing 4
BrdU	5'-Bromo-2'Deoxyuridine
bHLH-LZ	basic helix-loop-helix leucine zippr
BPTF	bromodomain PHD Finger transcription factor
BSA	bovine serum albumin
CBP	CREB binding protein
CDK9	cyclin dependent kinase 9
cDNA	complementary DNA
CHD4	chromodomain helicase DNA binding protein 4
coIP	coimmunoprecipitation
CtBP	C-terminal binding protein
CTD	C-terminal domain
CtIP	CTBP-interacting protein
ChIP	chromatin immunoprecipitation
ChroP	chromatin proteomics
CK2	casein kinase 2
CLP	common lymphoid progenitors
CMP	common myeloid progenitors

CpG	cystein-phosphate-guanin
DC	dendritic cells
DEG	differentially expressed gene
DN	dominant negative
DNA	deoxyribonucleic acid
Dox	doxycycline
EBF1	early B-cell factor 1
E-box	enhancer box
EBV	Epstein-Bar virus
eRPKM	exonic reads per kilobase per milion
EtOH	ethanol
ELP	earliest lymphocytes progenitors
FA	formaldehyde
FACS	fluorescence-activated cell sorting
FC	fold change
FT	flowthrough
GC	germinal center
GFP	green fluorescent protein
GO	gene onthology
GSEA	gene set enrichment analysis
HAT	histone acetyltransferase
HCC	hepatocellular carcinoma
HDAC	histone deacetylase
HSC	hematopoietic stem cells
IFRD2	interferon related developmental regulator 2
Igll1	immunoglobulin lambda like polypeptide 1
IkarosER	Ikaros estrogen receptor

IL7	interleukin 7
IP	immunoprecipitation
LC-MS/MS	liquid chromatography coupled with tandem mass spectrometry
LFQ	label free quantification
LMPP	lymphoid-primed multipotent progenitor
Max	Myc-associated factor x
MB I-II-III –IV	Myc box I-II-III-IV
MCM2-7	minichromosome maintenance protein 2-7
Mga	Max gene-associated protein
Miz-1	Myc-interacting zinc finger protein 1
MPP	multipotent progenitors
mRNA	messenger ribonucleic acid
MS	mass spectrometry
Myc	myelocytomatosis
MZ	marginal zone
NCL	nucleolin
NF-Y	nuclear transcription factor Y
NGS	next generation sequence
NK	natural killer cell
Npm	nucleophosmin
NuRD	nucleosome remodeling deacetylase complex
NURF	nucleosome remodeling factor
OHT	4-hydroxytamoxifen
Ph+	Philadelphia chromosome
PI	propidium iodide
PIC	preinitiation complex
P-TEFb	positive transcription elongation factor b

Pol II	RNA polymerase II
qPCR	quantitative polymerase chain reaction
Ras	rat sarcoma virus oncogene
RNA	ribonucleic acid
ROS	reactive oxygen species
RT-PCR	reverse transcriptase polymerase chain reaction
SDS-PAGE	sodium dodecyl sulphate-polyacrylamide gel electrophoresis
SLC	surrogate light chain
SMAD2/3	Sma- and Mad-related protein 2/3
SP1/SP3	specificity protein 1
STAT5	signal transducer and activator of transcription 5
SWI/SNF	SWItch/Sucrose Non-Fermentable
TAD	transcriptional activation domain
TBP	TATA-box binding protein
TCR	T cell receptor
Tdt	terminal deoxynucleotidyltransferase
Tet	tetracycline
TFA	trifluoroacetic acid
TFII-I	general transcription factor II, I
TRIM28	tripartite motif containig 28
TRRAP	transformation/transcription domain associated protein
TSS	transcription start site
VDJ	variable-diversity-junction
WDR5	WD repeat domain 5
YY1	Yin and Yang 1 Protein
v-*myc*	viral myelocytomatosis
WB	western blot

List of figures

List of tables

Abstract

Myc is a transcription factor that plays a key role in many cellular functions. When deregulated, it becomes a potent oncogene and a hallmark of many human cancers. Although its activity has been proven to strongly depend on many cofactors, we are still far from a comprehensive understanding of Myc's mechanisms of action in transcriptional control. Moreover, since Myc itself is not easily druggable, targeting its cofactors or downstream effectors may constitute a more promising therapeutic strategy in Myc-driven tumors. Here, we have used the Chromatin Proteomics (ChroP) technology to identify new Myc interactors. Among the list of identified candidates, we have chosen to focus our attention on two lymphocyte specific transcription factors, Ikaros and Aiolos. We validated the interaction of Myc with these factors and started to study its functional meaning. Our working hypothesis is that Myc and Ikaros/Aiolos antagonize each other on chromatin at selected target loci. We were able to identify a subset of genes regulated in opposite manners by Ikaros and Myc, involved mainly in cell cycle regulation, metabolism of lipids and metabolic stress response; the next step will be to study more in depth the mechanisms behind their regulation and their functional significance.

1. Introduction

1.1 Myc

1.1.1 Myc discovery and structure

The *c-myc* oncogene was discovered as the cellular homologue of a viral oncogene isolated from the MC29 chicken virus (v-*myc*) (Sheiness & Bishop, 1979; Sheiness et al., 1978; Vennstrom et al., 1982). The MC29 virus causes myeloid cells transformation that results in myelocytomas, hence the name c-*myc* (myelocytomatosis).

The Myc family includes three related genes, c-, N- and L-*myc,* encoding the basic-helix-loop-helix leucine zipper transcription factors c-Myc, N-Myc and L-Myc. c-Myc (hereafter Myc) is broadly overexpressed in both blood-borne and solid tumors, N-Myc in solid cancers of neural origin such as neuroblastoma and glioma (Schwab et al., 1984), and L-Myc in small cell lung carcinomas (Nau et al., 1985; Wasylishen & Penn, 2010). Myc is 439 aminoacids in length and can be schematically divided into three main parts, organized in the same way in all the members of the family (figure 1), as follows:

1) an N-terminal transcriptional activation domain (TAD): this region is mostly unstructured (Andresen et al., 2012) and is required to sustain Myc-dependent cell transformation (Stone et al., 1987) and transcriptional activities, when fused to a DNA binding domain (Kato et al., 1990). Moreover, it also includes two conserved regions called Myc-boxes (MB): MBI, that contains a degron responsible of Myc ubiquitination and degradation, and MBII, implicated in protein-protein interactions and transcriptional activation (Conacci-Sorrell et al., 2014; Tansey, 2014);

2) a central part containing the nuclear localization sequence, together with a region rich in proline, glutamic acid, serine and threonine (PEST) and the conserved Myc box regions called MBIII and MBIV;

3) a C-terminal basic helix-loop-helix leucine zipper (bHLH-LZ) domain, a region of about 100 amino acids that mediates dimerization with the partner protein Max (Myc-associated factor x) and DNA binding.

Max is also a member of the bHLH-LZ family and, to date, is the only known dimerization partner of Myc. The Myc/Max interaction is essential for DNA binding and, in particular, to recognize the E-box consensus sequence CACGTG (or variant thereof) (Blackwell et al., 1993; Blackwell et al., 1990). Max is thus fundamental to accomplish the majority of Myc activities, such as transcriptional regulation and cell transformation (Amati et al., 1993a; Amati et al., 1992). While, at least at physiological levels, Myc cannot form homodimers, Max can do it and can also form heterodimers with other bHLH-LZ proteins, including the MXD proteins and Mga (Diolaiti et al., 2015). These interactions may antagonize the function of Myc at different levels: they may sequester Max in complexes other than the Myc/Max heterodimers, may compete for the same binding sites on DNA, and may recruit transcriptional repressors to common target loci (Grandori et al., 2000; Nair & Burley, 2003).

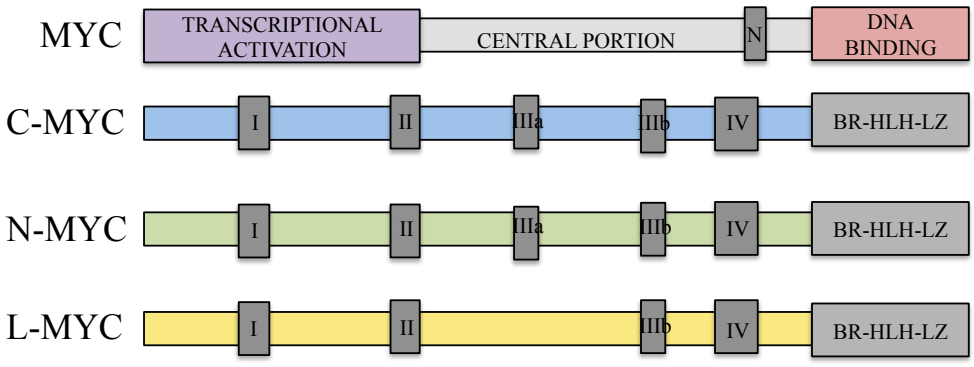

Figure 1. Structure of Myc family proteins. At the top of the image, a generic Myc protein is represented with the transcriptional activation domain, the central portion, the nuclear localization sequence (N) and the DNA binding domain. Below, the three members of the family with the conserved Myc box regions are depicted (adapted from Tansey, 2014)

1.1.2. Role of Myc in physiological and pathological conditions

Myc is a pleiotropic transcription factor that plays a fundamental role in several cellular functions such as cell cycle regulation, cell growth, apoptosis, cell differentiation and development (figure 2). One of its main functions is the regulation of cell proliferation. In fact, Myc activation is sufficient to induce quiescent cells to re-enter the cell cycle and can make cycling cells proliferate more rapidly and independently from growth factors (Amati et al., 1998). It also activates the expression of genes involved in mRNA maturation, ribosomal and mitochondrial biogenesis, nucleic acid synthesis and protein translation, providing the energy required by a cell to replicate (Arabi et al., 2005; Gomez-Roman et al., 2003; Iritani & Eisenman, 1999).

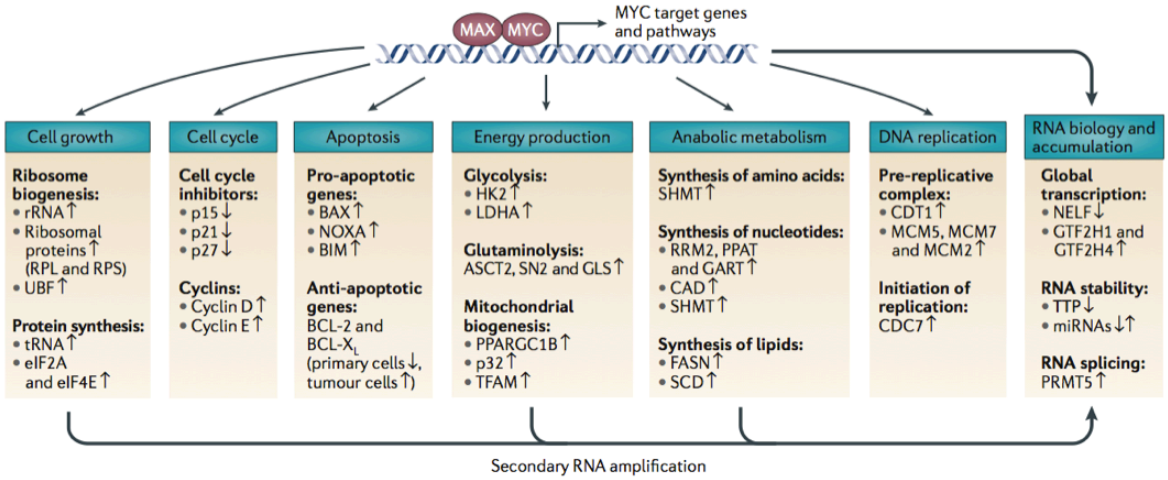

Figure 2. Myc transcriptional activation functions. Summary of the main pathways activated by the Myc/Max dimer (from Kress 2015).

Due to its crucial role in regulation of cell growth, cell transformation and tumorigenesis, Myc activity is strictly controlled in physiological conditions, at every step from gene expression to post-transcriptional modifications. Indeed, its expression is generally low in adult tissues and mainly restricted to cells with proliferative or regenerative potential.

To prevent uncontrolled cell proliferation as a consequence of Myc overexpression, Myc itself can induce apoptosis (Evan et al., 1992), either via the activation of p53 through the

upregulation of Arf (Zindy et al., 1998) or in a p53-independent way by regulating the balance between pro-apoptotic and anti-apoptotic proteins (Eischen et al., 2001). Loss of a tumor suppressor, such as p53 or Arf, or the activation of a second oncogene can abolish Myc-dependent apoptosis and favor tumorigenesis. For example, Bcl-2 overexpression inhibits Myc-mediated apoptosis but does not affect Myc-induced proliferation, providing an example of oncogene cooperation in sustaining tumor development (Bissonnette et al., 1992; Fanidi et al., 1992; Strasser et al., 1990).

Failure in Myc regulation induces a cascade of oncogenic signals that contribute to tumorigenesis and tumor maintenance, such as uncontrolled cell proliferation and growth, increased protein biogenesis, metabolic changes (Gabay et al., 2014). One way in which Myc deregulation occurs is by chromosomal translocation. This is characteristic of Burkitt's lymphoma, where the *Myc* gene is translocated under the control of the Igμ heavy chain enhancer, resulting in very high levels of Myc expression in B cells (Dalla-Favera et al., 1982). In other cancer types, instead, Myc is subjected to gene amplification (Little et al., 1983; Vita & Henriksson, 2006). Although mutational changes in the c-Myc coding sequence, often leading to stabilization of the Myc protein, are observed in a fraction of tumors (in particular Burkitt's lymphoma) (Bahram et al., 2000; Hemann et al., 2005), these are not obligatory and are generally secondary to a translocation event. Moreover, deregulated Myc expression in cancer can also occur in the absence of c-Myc alterations, due to mutations in upstream regulatory pathways such as Wnt, Notch and others (Meyer & Penn, 2008). In tumor cells, Myc can promote metabolic changes aimed to support a rapid growth, for example by enhancing the expression of genes involved in glucose uptake and glycolysis; indeed, Myc-transformed cells often become glucose and glutamine addicted (Gao et al., 2009; Hsieh et al., 2015; Shim et al., 1998). Moreover, Myc can improve angiogenesis, helping the tumor to develop its own vasculature (Baudino et al., 2002; Dews et al., 2009), can induce epithelial to mesenchymal transition (Smith et al., 2009; Trimboli et al., 2008) and adhesion independence (Frye et al., 2003), thus favoring

metastasis. An aberrant proliferation can also result in “replication stress”, collapse of DNA replication forks at fragile sites, followed by double strand breaks and chromosomal abnormalities (Felsher & Bishop, 1999; Prochownik & Li, 2007; Rohban & Campaner, 2015). Finally, Myc can be implicated in DNA damage and instability through the induction of reactive oxygen species (ROS) (Vafa et al., 2002).

Besides driving tumor initiation and progression, Myc is essential for tumor maintenance (Gabay et al., 2014). In several mouse models of Myc-driven malignancies, tumor cells become addicted to continuous Myc overexpression, as switching Myc off can result in growth arrest, apoptosis and differentiation. This is true not only in Myc driven tumors but also in cancers driven by other oncogenes like Ras (Felsher et al., 2010; Li et al., 2014; Soucek et al., 2013).

1.1.3. Myc interactions on chromatin

1.1.3.1. Myc binding to DNA

As we said, Myc requires the dimerization with Max to bind DNA and activate or repress the expression of its target genes. Myc/Max binding sites on DNA have been broadly studied thanks to the advent of the chromatin immunoprecipitation (ChIP) and more recently of ChIP-seq technique, and some common characteristic have been described:

- Myc-binding sites are always associated with open chromatin, characterized by the presence of specific histone marks such as H3K4me3 or H3K27ac, the presence of the basal transcription machinery and hypersensitivity to digestion by DNaseI (Guccione et al., 2006); other important genomic features often associated with Myc binding sites are CpG island, that are themselves sites of active chromatin, and the presence of Pol II (Fernandez et al., 2003; Zeller et al., 2006).
- The Myc/Max dimer is not only bound at E-box sequences and it can bind both promoters and distal sites (mostly active enhancers) according to its expression

level: at physiological levels, it preferentially binds to high-affinity, E-box containing promoters, while when it is overexpressed, it can also "invade" lower affinity sites even devoid of any E-box as far as they reside in an active chromatin state (Sabò et al., 2014, Zeller et al., 2006).

In our group, a model describing Myc/Max binding to DNA has been proposed. In this model, the Myc/Max dimer recruitment to the open chromatin is facilitated by protein-protein interactions with other chromatin-associated proteins; this leads to a first interaction with the double helix that is sequence independent, followed by a "scanning" phase of the DNA sequence that ends with the stabilization of the Myc/Max dimer in correspondence of high-affinity sites (Sabò & Amati, 2014). The fact that only a small fraction of all the Myc/Max bound regions contains the E-box consensus site strengthens the hypothesis that, besides DNA sequence specificity, Myc could be recruited to chromatin also through the interaction with other proteins as well as non sequence-specific interactions with DNA. For example, Myc binding is mainly found on pre-engaged RNAPol2 (Pol II) promoters, thus it is possible that Myc is recruited on DNA through components of the general transcriptional machinery; moreover, Myc is reported to interact with Pol II itself as well as with other general regulators such as TFII-I (Roy et al., 1993), TBP (Hateboer et al., 1993) and P-TEFb (Eberhardy & Farnham, 2002; Rahl & Young, 2014).

An example of the critical role played by protein-protein interactions in Myc target recognition is unveiled by WDR5, a component of many complexes involved in histone methylation, which mediates Myc recruitment on chromatin (Thomas et al., 2015). ChIP-seq experiments showed that Myc signal overlaps well with WDR5 binding, while this co-localization strongly decreases if the protein-protein interaction is disrupted (Thomas et al., 2015). Similarly, Myc interaction with BPTF, a core component of the NURF chromatin-remodeling complex, appears to be implicated in Myc target recognition: BPTF

knockdown, in fact, results in reduced Myc binding to chromatin and impaired activation of Myc transcriptional program (Richart et al., 2016).

1.1.3.2. Mechanisms of transcriptional control by Myc

The mechanisms through which Myc is able to activate and repress transcription are not completely defined yet. Since Pol II is the enzyme responsible for the transcription of protein-coding genes, the interplay between Myc and Pol II has been widely studied. The transcription cycle includes a first step (transcription initiation) in which Pol II is recruited at gene promoters, a second step (transcription elongation) in which the C-terminal domain (CTD) of Pol II must be phosphorylated by the CDK9/P-TEFb complex in order to have a successful processivity, and a third step (transcription termination) that concludes transcription through Pol II dissociation. Many studies showed that Myc is able to recruit P-TEFb to its target genes, thus facilitating Pol II elongation (Bouchard et al., 2004; Eberhardy & Farnham, 2001; Rahl & Young., 2014). More recently, Pol II recruitment was shown to be the primary step in Myc-activated transcription, followed by pause-release (de Pretis et al., 2017).

The capacity of Myc to recruit the general transcription factor P-TEFb and to increase Pol II processivity, together with its widespread genomic distribution, has been the basis of a new model in which Myc was proposed to act as a general amplifier of transcription at all the active sites, rather than as a regulator of specific target genes. This effect would also explain the increase in RNA quantity per cell ("RNA amplification") that is often observed upon Myc overexpression (Lin et al., 2012; Nie et al., 2012). Our group, instead, demonstrated that Myc can only regulate a specific set of genes in response to environmental stimuli, arguing that Myc-dependent transcriptional regulation and RNA amplification, when present, are two distinct processes. In this case, the global increase in RNA level would be a secondary effect following the regulation of Myc target genes, as

many of these genes are themselves involved in RNA biosynthesis and processing (Kress, Sabò, & Amati, 2015; Sabò et al., 2014).

The observation that Myc can invade most of the promoters located in open chromatin when overexpressed, but that only a small part of them is transcriptionally regulated, suggests that Myc binding to DNA is not sufficient to determine gene regulation, but that the interaction with other effectors is needed. For examples, Myc can recruit different histone acetyltransferase (HAT) containing complexes. Interaction with the adaptor protein TRRAP (McMahon et al., 1998), in particular, allows the recruitment of the STAGA (Zhang et al., 2014) and NuA4 (Frank et al., 2003) complexes that include the HAT subunits GCN5/PCAF and TIP60, respectively. Moreover, Myc can also interact with the CBP and EP300 HATs (Vervoorts et al., 2003). Myc has been reported to bind different components of the SWI/SNF complex (Cheng et al., 1999; Stojanova et al., 2016), which regulates transcription by remodeling chromatin in an ATP-dependent manner. In particular, the bHLH-LZ domain of Myc directly interacts with INI1/hSNF5, a key component of SWI/SNF complex, and this allows Myc mediated expression of reporter genes *in vitro* (Cheng et al. 1999). Myc can also interact with transcriptional repressors such as Sin3a, Sin3b (Garcia-Sanz et al., 2014) and components of the NuRD chromatin remodeler complex, including HDAC1 (Garcia-sanz et al., 2014), HDAC2, TRIM28 and CHD4 (Koch et al., 2007).

Myc-dependent repression is less characterized than activation, and is mostly related to Myc binding to chromatin through other transcription factors, among which Miz-1 (Peukert et al., 1997) SP1/SP3 (Gartel et al., 2001), NF-Y (Izumi et al., 2001) SMAD2/SMAD3 (Feng et al., 2002), YY1 (Shrivastava et al., 1993). The most studied mechanism regards Myc-interacting zinc finger protein 1 (Miz-1) which activates transcription by the association with p300 and nucleophosmin (Npn); Myc association with Miz-1 is able to displace Miz1 coactivators thus blocking the activation of target genes (Staller et al., 2001). It has been shown that Myc/Miz-1 complexes can recruit the

methylases Dnmt3 to the *cdkn1a* promoter, thus inducing DNA methylation and silencing of the target genes (Brenner et al., 2005); moreover, Myc is able to recruit the HDAC3 deacetylase (Kurland & Tansey, 2008), but whether the recruitment of corepressors and the formation of heterochromatin are common mechanism for Myc-dependent gene repression remains to be determined.

1.1.4. Myc and cancer therapy

Myc deregulation is one of the most common features of many cancer cells; moreover, the fact that many tumors become Myc-dependent makes the inhibition of Myc activity appealing for anticancer drugs. Unfortunately, Myc itself is not an easy target, in fact transcription factors, as a class of proteins, lack an active site that can be blocked by small molecules (Horiuchi et al., 2014; McKeown & Bradner, 2014).

Many strategies have been studied to interfere with Myc-dependent transcriptional activity at different levels. For example, Myc function can be impaired by acting on its interaction with Max (Amati et al., 1993a; Amati, et al., 1993b; Amati et al., 1992). Omomyc is a dominant negative, mutated version of Myc that can either form homodimers or heterodimers with Myc or Max, thus it can interfere with Myc activities at different levels: by sequestering Myc away from Max or by occupying the Myc/Max binding sites as inactive Omomyc homodimers (Jung et al., 2017; Soucek et al., 2008). Several small molecule inhibitors of Myc/Max dimerization as well as molecules that impair Myc/Max binding to DNA have also been developed (Koh et al., 2016).

Another example is provided by inhibitors of BET bromodomain proteins that recognize specific acetylated lysine residues in the N-terminal tails of histones and modulate gene expression by recruiting transcriptional regulators on chromatin. In particular, Brd4 was shown to directly interact with the positive elongation factor complex b (P-TEFb); the observation that also Myc regulates the pause release of Pol II at promoters by recruiting P-TEFb, settled the rationale to explore the effects of Brd4 inhibition on Myc

transcriptional program. Actually, blocking Brd4 function with small molecule inhibitors such as JQ1, i-BET and MMS417, have been shown to inhibit Myc-dependent transcription, but also to negatively regulate Myc expression in several systems. (Delmore et al., 2011; Donato et al., 2017; Mertz et al., 2011; Zuber et al., 2011) Finally, a recent work identified WDR5 as a critical factor in pancreatic cancer proliferation, thus building the rationale to consider inhibitors of the Myc-Wdr5 interaction for therapies (Carugo et al., 2016). Altogether, the above evidences suggest that, although direct pharmaceutical inhibition of Myc is a difficult goal, targeting upstream or downstream signals and protein-protein interactions could be an alternative strategy to inhibit Myc's oncogenic activity.

1.2. B-cell development

1.2.1. Early development

Hematopoiesis is the process through which the blood system is originated and maintained. In adult mammals, hematopoiesis begins from the few hematopoietic stem cells (HSC) that populate a specific niche in the bone marrow. These cells are mainly quiescent and characterized by the ability to self-renew; their direct progeny is composed by multipotent progenitors (MPP) that loose the self-renewal ability, but retain the potential to differentiate into various lineages. Indeed, the commitment of MPP can results either in the formation of common myeloid progenitors (CMP) or in the formation of lymphoid-primed multipotent progenitor (LMPP) which are the precursors of the earliest lymphocytes progenitors (ELP). In the ELP, Rag1 and Rag2 start to be expressed to allow the $D(diversity)_H$-$J(junction)_H$ rearrangement at the immunoglobulin heavy-chain locus. ELP are thought to originate early T lineage progenitors (ETP) in the thymus and common lymphoid progenitors (CLP) in the bone marrow. From the latter, all the lymphoid cells can originate, such as B-cells, T-cells and Natural killer (NK). The first identifiable B cell precursors are recognized thanks to the expression of the B220 surface marker and are

called pre/pro B cells (or fraction A, according to the Hardy classification) (figure 3) (Hardy et al., 1991; Li et al., 1996). The heavy-chain DJ rearrangement terminates in the early pro-B cell phase (fraction B/C). This is followed by the heavy-chain V(variable)DJ recombination that results in the surface expression of the Igμ heavy chain as part of the pre-B cell receptor (pre-BCR). The functional μ heavy chain will pair with a surrogate light chain (SLC) and, together with the Igα/β heterodimer will form the pre-B cell receptor (pre-BCR) on the surface of pre-BI cells (Fraction C'). The SLC is encoded by the *Igll1* (λ5) and *Vpreb* genes, and is similar to the final light chain but it is not variable (Melchers et al., 1993). The expression of the pre-BCR is proposed to be responsible of positive and negative selection of pre-B cells: only cells that express a functional μ heavy chain that is able to couple with a SLC are maintained. These events block the rearrangement mechanism to avoid that different heavy chains are produced (allelic exclusion) and compels the transition to the proliferative large pre-BII cell stage (fraction D) (Hess et al., 2001; Mårtensson et al., 2010; Melchers et al., 2000). Finally, the pre-BCR receptor promotes its own down-regulation, by silencing the genes coding for the SLC in order to start the recombination of the κ or λ Ig light chain; at this point, cells stop their proliferation and become small resting pre-B cells. The light chain, combined with the μ heavy chain, will form the IgM molecule that will be expressed on the surface of immature B cells (fraction E), constituting the B-cell receptor (BCR) (Ferreiros-Vidal et al., 2013; Mårtensson et al., 2007; Pieper et al., 2013).

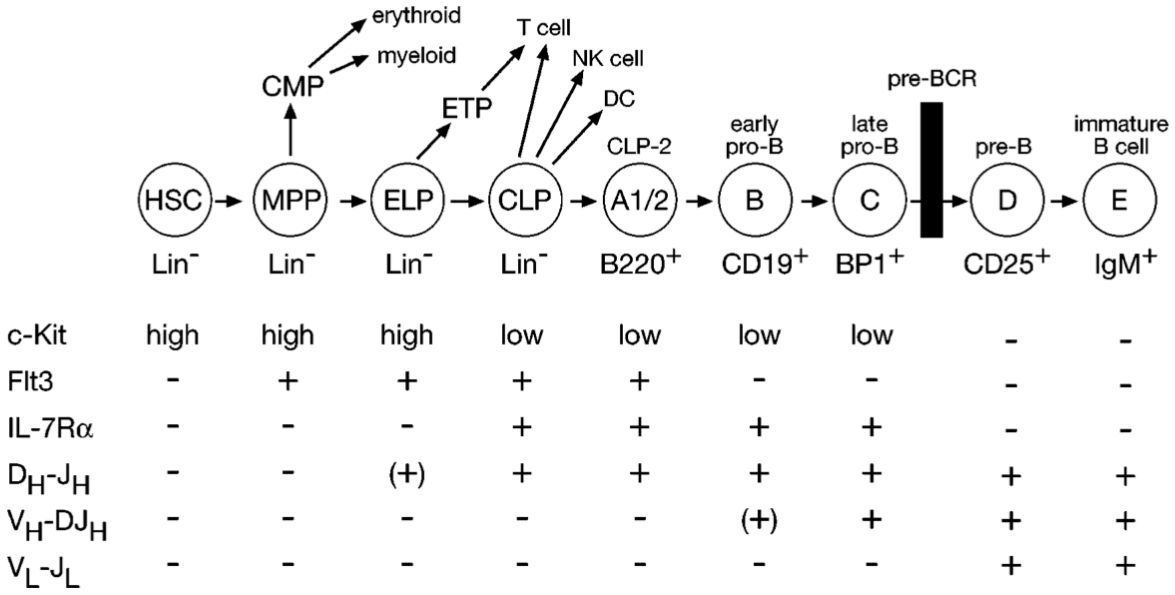

Figure 3. B cell development. Surface markers and the rearrangement status of immunoglobulin genes are reported for each stage of B lymphopoiesis (from Busslinger 2004).

1.2.2. Maturation

Only a small percentage of immature B cells will continue the maturation pathways, while most of them are negatively selected already in the bone marrow to avoid the development of auto-reactive, mature B cells (Pelanda & Torres, 2012). There are three possible mechanisms of negative selection: receptor editing, clonal deletion or anergy. The accepted model is that if an immature B cell strongly recognizes an auto-antigen, it starts a new round of recombination to change the BCR in order to avoid the self-reactivity (receptor editing); if it fails, it is eliminated (clonal deletion). Some cells that recognize only weakly an auto-antigen, could be positively selected, but if they recognize a self-antigen in the periphery, they become non-responsive (anergic) (Cancro & Kearney, 2004; Carsetti et al., 1995). Non-autoreactive cells can reach the spleen and proceed with the maturation. Nevertheless, they are also subjected to a positive selection, meaning that BCR expression must reach a certain level, inducing a tonic signal that promote the differentiation toward the next stage (King & Monroe, 2014; Levine et al., 2000; Melchers et al., 1995). Peripheral immature B cells are called transitional B cells. A transitional B cell could

differentiate either in a marginal zone (MZ) B cell or in a follicular B cell (Pillai & Cariappa, 2009). A small fraction of transitional B cells reaches the splenic marginal zone and is retained there as non-recirculating marginal zone B cells. These cells contribute to the first immunological response, since they are quickly activated. In accordance to this, their location is strategic for the recognition of blood-borne antigens and they mostly recognize antigens in a T-cell independent way (Allman & Pillai, 2008).

Follicular B cells, instead, are recirculating B cells and constitute the most abundant fraction of mature B cells. They migrate through blood and lymph and mainly home to the follicles in secondary lymphoid organs (B zone lymph nodes, Peyer's patches and spleen), that are located next to the T cell zones. Indeed, follicular B cells are preferentially activated by the interaction with T helper lymphocytes, even if they are also able to recognize blood-borne antigens in a T-cell independent manner (Allman & Pillai, 2008).

Another peculiar group of mature B cells, called B1 cells, exists. B1 cells are mainly found in peritoneal and pleural cavities and in the gut lamina propria. They are thought to follow an independent development pathway by originating from progenitors that are abundant in fetal liver but absent in adult bone marrow; in accordance to this, they are characterized by a unique self-renewing ability. B1 cells quickly respond to antigen in a T-cell independent manner and are a source of "natural" IgM, low affinity antibodies that contribute to the first lane response against an antigen: once B1 cells are activated, they migrate to the spleen or gut and become antibody-secreting plasma cells (Allman & Pillai, 2008; Casola et al., 2004).

1.2.3. Antibody production and memory

In presence of an antigen, the first cells that become active antibody producers (plasma cells) are B1 and marginal zone B cells. Circulating follicular B cells that encounter an antigen in a T-cell dependent or independent way, can also form extra-follicular foci of

plasmablasts where they undergo proliferation and secrete antibody in a couple of days after immunization. These kind of plasma cells are short-lived and do not have somatically mutated Ig genes, but provide a quick clearance of the antigen (Shapiro-Shelef & Calame, 2005).

As a second option, activated follicular B cells can establish a germinal center (GC), where they undergo affinity maturation and class-switch recombination while proliferating. In particular, it is possible to distinguish a dark zone in which B cells (called centroblasts) proliferate and undergo somatic hypermutation and a light zone in which B cells (called centrocytes) are subsequently selected according to their interaction with the antigen. The germinal centers allow the production of both plasma cells and memory cells with high affinity BCR. Differently from plasma cells, memory cells do not secret antibodies immediately, but are ready to react very quickly after a subsequent encounter of the antigen. Some plasma cells can migrate to the bone marrow to become long-lived plasma cells (Cyster, 2010; Nutt et al., 2015) (figure 4).

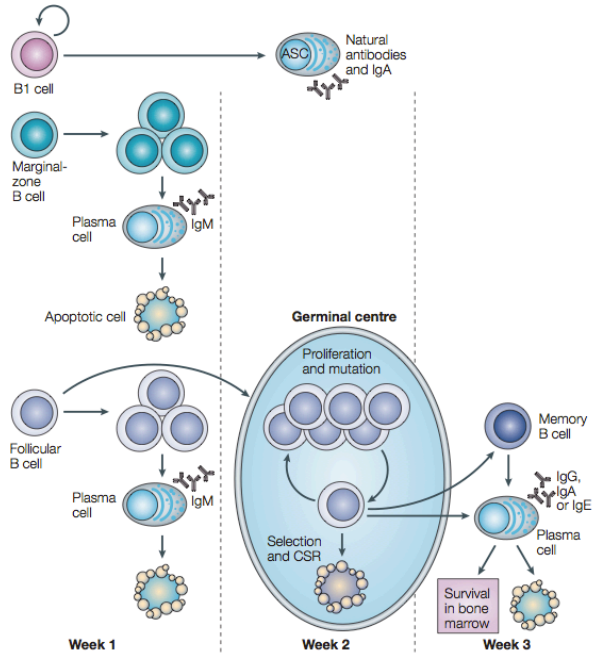

Figure 4. Plasma cell development. B1 cells, Marginal-zone B cells and Follicular B cells can develop into cells producing low affinity antibodies. Follicular B cells that form a germinal center can develop into high affinity plasma cells or memory B cells (from Shapiro 2005).

1.2.4. Role of Myc in B lymphopoiesis

Myc has been shown to play an important role in B-cell lymphopoiesis and to be deregulated in many B cell malignancies. Myc expression level changes in a strictly regulated manner during B cell development and maturation, defining the balance between proliferative and resting periods (Delgado & Leon, 2010). Myc-deficient embryos die at around day 10 and defective hematopoiesis seems to be the main reason for this lethality (Davis et al., 1993). Conditional deletion of Myc in the HSC compartment results in an accumulation of HSCs, caused by a failure in the normal differentiation process; on the contrary, enforced Myc expression causes a decrease in HSC numbers, while increasing proliferation of progenitors and cell differentiation (Wilson et al., 2004). Thus, Myc seems to control the balance between self-renewal and differentiation in HSCs (Delgado & Leon, 2010; Wilson et al., 2004).

Later, during B cells differentiation, Myc expression is induced by the pre-BCR and interleukin 7 (IL7) signaling to burst pro-B cell proliferation, while it is downregulated again in small resting pre-B cells. Constitutive expression of Myc results in an accumulation of pre-B cells and a consequent reduction in mature B cells numbers. Thus, at this stage, Myc seems to be required for the pro-B to pre-B cell transition (Habib et al., 2007; Iritani & Eisenman, 1999; Yasuda et al., 2008).

When mature B cells are activated by the encounter with an antigen, Myc expression becomes fundamental for the formation of the germinal center (Calado et al 2012). During the germinal center reaction, two areas are distinguishable in the GC: a dark zone in which B cells are proliferating and a light zone where B cells are positively selected by the interaction with the antigen. Surprisingly, c-Myc is found to be expressed only in a small fraction of B cells located in the non-proliferative light zone, while it is down-regulated by Bcl-6 in most of the other cells (Calado et al., 2012; Dominguez-Sola et al., 2012). Subsequently, Myc downregulation is required to proceed toward differentiation into plasma cells. In particular, Myc is downregulated by Blimp-1 (B lymphocyte-induced

maturation protein-1), a master regulator of terminal B cells differentiation. Ectopic expression of Myc at this stage, blocks terminal differentiation into plasma cells, often leading to tumorigenic effects (Lin et al., 2000).

In summary, the role of Myc in lymphopoiesis depends on cell stage: it drives differentiation in HSCs and early B cell progenitors, while it inhibits terminal differentiation of mature B cells (figure 5).

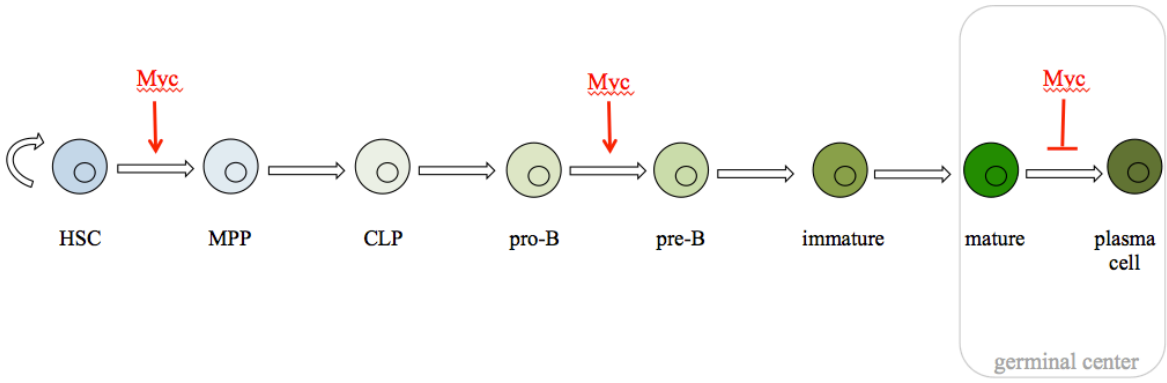

Figure 5. Myc role in B lymphopoiesis. During B cell development, Myc plays a crucial role in regulating cell proliferations. In particular, Myc promotes differentiation of hematopoietic stem cells (HSC) and pro-B cells, while must be downregulated to allow B cell differentiation into plasma cells.

1.3. Ikaros and Aiolos

1.3.1. Ikaros discovery and structure

Lymphocyte development and maturation is the result of tightly regulated events driven by specialized transcription factors, among which Ikaros and Aiolos, that will be the topic of this thesis. In the early 1990s, a protein able to bind the TdT promoter in T cells was identified and initially named LyF-1 (Lo et al., 1991); in parallel, the enhancer of the earliest definitive T cell differentiation marker, CD36δ, was used to screen a T cell expression library aimed at identifying transcription factors that prime T lymphocyte lineage in mice. A cDNA coding for an uncharacterized protein, that was able to bind and regulate this enhancer, was identified (Georgopoulos et al., 1992) and the corresponding

protein was named Ikaros. LyF-1 and Ikaros were then recognized to be the same protein (Hahm et al., 1994) and, few years later, the human ortholog was identified and cloned (Molnár et al., 1996). Ikaros is well conserved among species (Molnár et al., 1996) and is characterized by two groups of zinc-finger domains. The four zinc fingers in the N-terminal constitute the DNA binding domain and determine the recognition of the binding motif, the core of which is defined as GGGAA. Two zinc-fingers are present at the C-terminus and mediate omo- or hetero-dimerization with the other members of the family (Molnár & Georgopoulos, 1994; Sun et al., 1996).

The gene encoding Ikaros (*IKZF1*) gives rise to a number of different protein isoforms due to alternative splicing or deletions (figure 6) (Georgopoulos et al., 1994; Hahm et al., 1994; Molnár & Georgopoulos, 1994; Molnár et al., 1996). The isoforms all share the two C-terminal zinc fingers, but differ in the number of N-terminal zinc fingers: isoforms with 2 to 4 zinc fingers in the N-terminal domain can bind DNA, even if with different affinities and functions, conversely, isoforms with only one or no zinc fingers in the N-terminal domain cannot bind DNA. Since heterodimers containing an active isoform together with an isoform that cannot bind DNA are transcriptionally inert, the latter are called dominant negative (DN) isoforms and are thought to be implicated in Ikaros self-regulation (Sun et al., 1996). Of particular interest, the DN isoform Ik6 (figure 6) is overexpressed in many cases of pre-B acute lymphoblastic leukemia (ALL), especially associated with BCR/ABL translocation. For this reason, it is particularly studied as a possible diagnostic marker as well as a putative therapeutic target (Mullighan et al., 2008; Zhou et al., 2013).

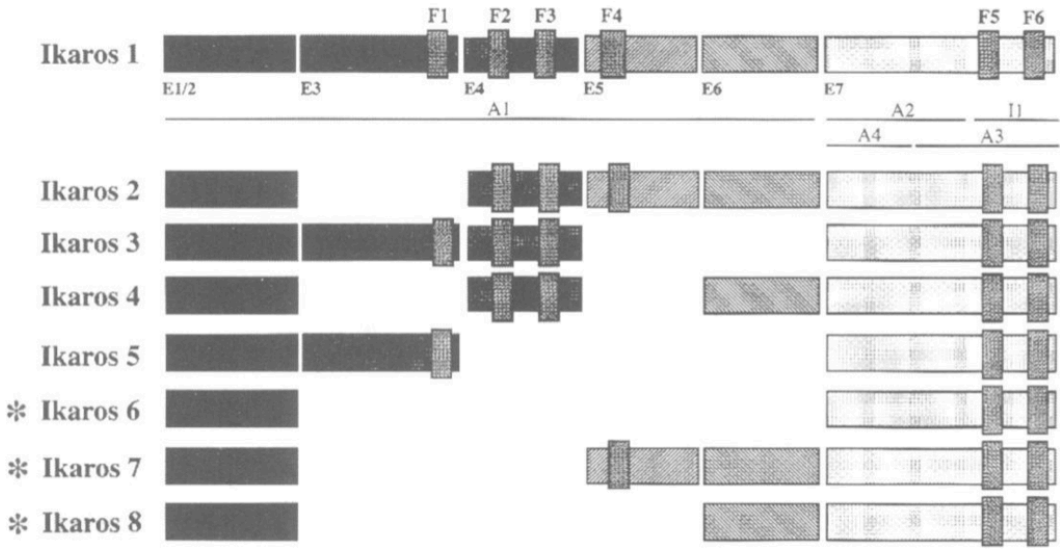

Figure 6. Ikaros isoforms. Schematic representation of Ikaros isoforms and their domains**.** E1-E7= exons; F1-F6= zinc fingers. * indicates dominant negative isoforms (generated by the mutant *Ikzf1* gene in which exons 3 and 4 are deleted) (adapted from Sun et al 1996).

1.3.2. Function of Ikaros and Aiolos in hematopoiesis

To study the role of Ikaros in hematopoiesis, transgenic mice bearing Ikaros mutations or inactivation have been created (Cortes et al., 1999; Katia Georgopoulos et al., 1997; Nichogiannopoulou et al., 1998). In the first model used, a region of 8.5 kb including part of exons 3 and exon 4 of the Ikaros gene was deleted and substituted with a neomycin-resistance cassette, resulting in the loss of three zinc fingers of the DNA-binding domain and production of a dominant negative isoform. This construct was inserted into embryonic stem cells and used to generate recombinant mice. In homozygous mice (DN-/-), B and T lymphocytes, as well as NK cells and progenitors, were absent at either fetal or postnatal stages, while the erythroid and myeloid compartments did not seem to be affected, indicating that Ikaros has a role at the very early stages of lymphopoiesis (Georgopoulos et al., 1994).

In heterozygous mice (DN +/-), an apparently normal phenotype during the first three months was followed by development of T cells leukemia and lymphomas with 100% penetrance. T lymphocyte expansion started in the thymus, suggesting that it arose from

maturing lymphocytes, and was accompanied by loss of the wild type *Ikzf1* allele, Conversely, no B cells were identified in spleen, lymph nodes or bone marrow. These results suggested that Ikaros plays a critical role not only in early development of lymphoid progenitors but also at later stages of T cell maturation (Winandy et al., 1995).

To obtain a real Ikaros null mouse model, a 1.35 kb region at the C-terminal was removed, by substituting part of exon 7 with a neomycin resistance cassette: in this way, the dimerization domain and an activation domain that mediates transcriptional effects were eliminated in the germ line, leading to production of an inactive protein that is unstable and rapidly degraded, not detected at cellular level; moreover, this mutant has been shown to be transcriptionally inactive and do not display dominant negative effects (Sun et al., 1996; Wang et al., 1996). In this mouse model, thymocytes and their precursors were not detected during gestation, but appeared only 3-5 days after birth; moreover, although they expanded reaching almost a normal number, they did not follow the canonical differentiation pathway and were skewed toward a CD4+CD8- phenotype. Lymphnode development was also impaired and NK cells were absent, while the erythroid and myeloid compartments were normal or even increased. Moreover, B lymphocyte differentiation was completely blocked in these mice, with no detectable formation of B cells and their precursors (Wang et al., 1996).

The results obtained with these models and, in particular, the fact that mice bearing the Ikaros DN isoform (Georgopoulos et al., 1994, Winandy et al., 1995) showed a more severe effect than Ikaros null mice (Wang et al., 1996), suggested that Ikaros is necessary for fetal HSC differentiation and lymphocyte specification, but that its function in the late fetal and postnatal hematopoiesis can be at least partially rescued by other proteins, which are similarly inhibited by the dominant negative isoforms (Morgan et al, 1997).

According with this hypothesis, Aiolos was identified as a zinc finger protein showing the highest similarity with Ikaros; the two transcription factors share a conserved structure and extended homology particularly through the DNA binding domain and the C-terminal

region (Caballero et al., 2007; Hosokawa et al., 1999; Morgan et al., 1997). To study Aiolos function in hematopoiesis, an Aiolos-null mouse model was generated by replacing exon 7 of the gene with a neomycin-resistance cassette, similarly to what had been done for Ikaros (Wang et al., 1996; Wang et al., 1998). Aiolos-null mice showed an accumulation of B cell precursors, increased B cell lymphomagenesis and auto-antibody production, while the number of recirculating B cells in bone marrow was reduced. Minor effects, instead, were visible in the T cell compartment. Thus, Aiolos is not required for early differentiation of B and T lymphocytes, but plays a more prominent role in B cell maturation (Wang et al., 1998).

Ikaros and Aiolos can form heterodimers in differentiating and mature B and T lymphocytes. To analyze their functional interaction, mice with mutations in both the genes were studied; the results suggested that the two transcription factors collaborate to set threshold for the control of antigen-mediated lymphocyte proliferation (Cortes et al., 1999).

After Aiolos, other members of the Ikaros family have been identified, with a conserved dimerization and activation domain: Helios (Hahm et al., 1998), Eos/Dedalus (Honma et al., 1999) and Pegasus (Perdomo et al., 2000).

1.3.3. Expression pattern of Ikaros family members

Although Ikaros proteins share a high degree of similarity, their expression pattern is quite different. Ikaros can be detected from the earlier stages of embryogenesis in the yolk sac, fetal liver, thymus and hematopoietic stem cells. In adults, Ikaros expression is restricted to bone marrow, thymus and spleen, it is constantly expressed during all the stages of lymphopoiesis, while it is present at low level in erythroid and myeloid precursors and not in terminally differentiated erythrocytes, monocytes and macrophages (Georgopoulos et al., 1992; Nichogiannopoulou et al., 1998). Aiolos is not expressed in multipotent

progenitors but is induced upon pre-BCR signaling in cycling pre-B cells and reaches the highest level in differentiated lymphocytes (Kioussis et al., 2007; Morgan et al., 1997).

The other members of the family are more widely detectable. Helios is found at low levels in HSC and does not seem to be involved in B cell development, in fact its expression is restricted to the T lymphocyte lineage; moreover, Helios is also expressed in epidermal keratinocytes (Georgopoulos, 2017; Hahm et al., 1998; Kelley et al., 1998). Eos/Dedalus is expressed at low level in the immune and neuro-epithelial system, having a role both in the hematopoietic and nervous system (Honma et al., 1999; Rieder & Shevach, 2013). Finally, Pegasus expression is spread in different tissues, thus it may play functions outside the lymphoid compartment (Perdomo et al., 2000).

1.3.4. Ikaros and Aiolos role in B lymphocyte development

1.3.4.1. Priming of the lymphoid lineage

Ikaros plays an important role in at least two defined stages or early lymphopoiesis, namely the development of LMPPs and at the transition to pre-B cell stage (Dovat, 2013). It has been hypothesized that Ikaros could drive the development of MLPPs by governing lineage regulators, such as Flt3 (Yoshida et al., 2006). In fact, Ikaros deficient progenitors lack Flt3 expression and MLPPs are present, but lose the potential to develop into B and T lymphocytes (Ng et al., 2007). HSCs can potentially develop into myeloid, erythroid or lymphoid lineage; the subsequent lineage restriction is dependent on the stabilization of the appropriate genetic program and concomitant inhibition of the alternative programs. For example, upon HSC restriction to MLPPs, the downregulation of erythroid transcripts is concomitant with the establishment of myeloid and lymphoid programs. This is dependent upon Ikaros, which initiates a cascade of lymphoid-promoting signals, comprising the expression of transcription factors such as Sox4, FoxP1 and signaling receptors such as Flt3 and Notch1, while negatively regulating genes implicated in self-renewal and

development of non-lymphoid lineages (Hu et al., 2016; Ng et al., 2009; Yoshida et al., 2006). Thus, Ikaros not only provides an important contribution in priming lymphoid lineage, but it is also implicated in the repression of genes driving stemness and self-renewal that, if deregulated, could lead to malignant cell growth.

1.3.4.2. Ikaros role in early B cell progenitors

A recent work dissected the role of Ikaros in early B cell progenitors and demonstrated that it specifically controls the transition from pro-B to pre-B cells, by inducing pre-BCR signaling. Without Ikaros, cells are blocked at an atypical pro-B cell stage, characterized by increased cell adhesion and defects in pre-BCR signaling (Schwickert et al., 2014). Of notice, Aiolos is not able to compensate the lack of Ikaros in early lymphomagenesis, suggesting that the two factors have also non redundant functions (Schwickert et al., 2014). When the pre-B cell receptor complex is assembled and expressed on the cell surface, pre-B cells undergo a massive proliferation step; to proceed toward the resting small pre-B cell stage, cells must exit the cell cycle, and start the rearrangement of the light chain. Ikaros family proteins are involved in this transition, which requires the suppression of pre-BCR signaling through down-regulation of the pre-BCR components, Igll1 (λ5) and Vpreb. Mechanistically, pre-BCR signaling induces a negative feedback loop through activation of Aiolos expression which, together with Ikaros, downregulates the expression of the pre-BCR components, thus keeping pre-B cell proliferation under strict control (Joshi et al., 2014; Kioussis, 2007; Ma et al., 2008; Thompson et al., 2007). Another way in which Ikaros could contribute in blocking cell proliferation at this differentiation stage is by binding to Myc promoter and repressing its transcription (Ma et al., 2010).

1.3.4.3. Role of Aiolos in mature B cells

While Aiolos is absent or lowly expressed in early lymphocyte progenitors, it seems to play a fundamental role in mature and recirculating B cells, where it is expressed at high levels (Georgopoulos, 2017). In Aiolos null mice, B cells appear to be more sensible to BCR activation; that leads to cell proliferation (Wang et al., 1998) and results in an increased number of germinal centers, independently from immunization (Cariappa et al., 2001). In a similar way, Ikaros loss in mature T cells facilitates their activation in response to T cell receptor (TCR) signals (Avitahl et al., 1999). Moreover, mice lacking Aiolos develop symptoms of Lupus Erythematosus, suggesting that Aiolos could be implied in the control of auto-immunity (Sun et al., 2003). In addition, Aiolos is involved in the production of high affinity long-lived plasma cells (Cortés & Georgopoulos, 2004) and other nonconventional B cells such as peritoneal B1 cells, marginal zone B cells and recirculating B cells (Wang et al., 1998).

1.3.5. Mechanisms of action

The first studies on Ikaros and Aiolos molecular functions revealed their capability to activate transcription of target genes by *in vitro* reporter assays (Georgopoulos et al., 1992; Molnár & Georgopoulos, 1994a; Morgan et al., 1997; Sun et al., 1996; Wargnier et al., 1998). Subsequent *in vivo* studies confirmed this role: for example, Ikaros was shown to activate the *CD8* gene either by increasing chromatin accessibility, thus facilitating the recruitment of other transcription factors, or by supporting the activity of already bound transcriptional regulators (Harker et al., 2002). Indeed, it was also proposed that Ikaros, instead of promoting gene activation *per se*, could act as a potentiator of other *bona fide* transcriptional activators (Koipally et al., 2002). Moreover, Ikaros and Aiolos are often found associated to centromeric heterochromatin, thereby suggesting that they could also have a role in gene repression, for example by relocating their target genes in proximity of

this transcriptionally inactive region (Brown et al., 1997; Cobb et al., 2000; Cortes et al., 1999; Klug et al., 1998). Nevertheless, other complementary or alternative mechanisms could to be exploited by these transcription factors to regulate gene repression, as reported below (Sabbattini et al., 2001).

Ikaros can interact with two chromatin remodeling complexes: the nucleosome remodeling and deacetylase (NuRD) complex and the SWItch/Sucrose Non-Fermentable (SWI/SNF) complex. Most of cellular Ikaros is associated with the NuRD complex (Kim et al., 1999; Sridharan & Smale, 2007) which contains the ATPase Mi-2b and the histone deacetylases HDAC1 and HDAC2. Therefore, NuRD can act both as an ATP-dependent chromatin remodeler and a histone deacetylase, leading to either opening or closing of the chromatin. Only a minor fraction of Ikaros has been found associated to the SWI/SNF complex containing Sin3/HDAC complex subunits (Busslinger, 2004; Kim et al., 1999). Although the interaction between Ikaros and chromatin remodeling complexes is well established, its functional consequences remain unclear. *In vitro* experiments showed that Ikaros and Aiolos, when fused to heterologous DNA binding domain, were able to support repression through HDACs recruitment (Koipally et al., 1999). Moreover, ChIP-seq experiments in thymocytes showed a variation of the NuRD complex genomic distribution upon Ikaros knockdown, thus supporting the idea of a functional relation between these factors (Oestereich & Einmann, 2012; J. Zhang et al., 2012). Further evidences suggested that, thanks to the interaction with the NuRD complex, Ikaros can regulate chromatin organization and accessibility and consequently affect transcription initiation (Bottardi et al., 2014). This idea is based on the observation that Ikaros can interact with P-TEFb (in particular with the CDK9 subunit) and recruit it on target gene promoters (Bottardi et al., 2011; Bottardi et al., 2013). P-TEFb is also part of an elongation-competent form of the NuRD complex, that exists besides the most abundant form, not associated with P-TEFb. Ikaros interaction with the NuRD/P-TEFb complex could induce chromatin remodeling, facilitating the recruitment of general transcription factors such as TFIIB and TBP (which

Ikaros itself can directly interact with; Koipally & Georgopoulos, 2002) and the assembly of the preinitiation complex (PIC) (Bottardi et al. 2014). Subsequently, Ikaros was suggested to promote CDK9 dephosphorylation by recruiting PP1 with the consequent P-TEFb activation; CDK9/P-TEFb can, in turn, phosphorylate the Pol II CDT inducing transcriptional elongation (Bottardi et al., 2014). Therefore, Ikaros could regulate gene activation by combining chromatin remodeling and Pol II elongation (Bottardi et al., 2014; Bottardi et al., 2015). Although this is an interesting hypothesis, the actual role of the Ikaros-NuRD/P-TEfb complex in transcriptional activation remains to be elucidated.

On the other hand, the cooperation between Ikaros and the NuRD complex was also proposed to exert an opposite effect, favoring transcriptional repression. It was already demonstrated that Ikaros could compete with the transcriptional activator EBF1 to bind and regulate the *Igll1* promoter (Thompson et al., 2007). A higher resolution study of the mechanism suggested that Ikaros could repress gene expression by interfering with Pol II recruitment. More in detail, Ikaros recruits the NuRD complex, where its ATPase subunit Mi-2b induces nucleosome invasion of the promoter; as a consequence, EBF1 binding is reduced and Pol II is evicted. Subsequently, HDAC1/2, are required to stabilize the repression and the recruitment of the *Igll1* allele to pericentromeric heterochromatin sites. The same mechanism was observed also on the *Myc* promoter (Liang et al., 2017).

Another way through which Ikaros may regulate target gene expression is through direct competition with other transcription factors. For example, Ikaros and STAT5 share many target genes that are inversely regulated. These two factors might exert their opposite regulation in two manners: by recruiting on chromatin different histone modifiers which regulate acetylation in an opposite way, or by directly competing for overlapping binding sites (Katerndahl et al., 2017). Ikaros competition with transcription factors for an overlapping binding site was also proposed for other target genes; for instance, Ikaros can repress TdT expression by competing with the Ets transcriptional activator to occupy the binding site present on *TdT* promoter (Trinh et al., 2001). Finally, Ikaros interaction with

corepressors such as CtBP and CtIP, could also subtend a deacetylase-independent mechanism for gene repression (Koipally & Georgopoulos, 2000).

In conclusion, Ikaros and Aiolos are transcription factors able to either activate or repress gene expression (Schwickert et al., 2014; Ferreiros-Vidal et al., 2013).

1.3.6. Pathologies and therapies

Studies on mice suggested a tumor suppressor role for Ikaros mainly in T cells: mice heterozygous for Ikaros DN mutation develop T cell lymphomas (in which the wildtype allele is lost) with 100% penetrance (Winandy et al., 1995). Nevertheless, in humans, Ikaros defects are identified only rarely in T cell malignancies. Interestingly, instead, Ikaros mutations are frequent in B cell Acute Lymphoblastic Leukemia (B-ALL). In this context, Ikaros deletions can result in haploinsufficiency, in a complete loss of Ikaros expression or in the expression of the dominant negative Ik6 isoform (Sun et al., 1996). These are the most frequently identified alterations and they preferentially appear in high risk B-ALL, characterized by the BCR/ABL translocation (Philadelphia chromosome, Ph+ALL), that constitute around 5% of pediatric B-ALL and 40% of adult B-ALL, or in Ph-like ALL. The presence of mutated Ikaros is considered a predictor of bad prognosis in both BCR/ABL positive and negative leukemia; moreover, it seems that certain Ikaros polymorphisms could define a predisposition to develop B-ALL (Mullighan et al., 2008; Mullighan et al., 2009). While the BCR/ABL translocation can also be linked to the development of chronic myelogenous leukemia (CML), Ikaros deletions are not identified in the chronic phase of this disease, while they are acquired during the progression to the blast crisis status (Mullighan et al., 2008).

Following the above observations, restoration of Ikaros levels and function could be an interesting therapeutic strategy, and different approaches have been studied in this direction. For example, Casein Kinase2 (CK2) is a proto-oncogene overexpressed in hematological malignancies that phosphorylates Ikaros, inducing its degradation (Song et

al., 2015). Preliminary studies *in vitro* and in preclinical models using CK2 inhibitors, showed a stabilization of Ikaros level and promising anti-leukemic effects (Gowda et al., 2017; Song et al., 2015). Another study shows that retinoids induce the upregulation of Ikaros expression and can reverse the leukemic phenotype in a pre-B ALL mouse model, thus it would be interesting to study more in depth their clinical effect on Ikaros-altered Ph+ ALL patients (Churchman et al., 2015).

While Ikaros deletion and loss of function are frequent in pre-B ALL, mature B-cell lymphomas, such as multiple myeloma, bear high levels of this transcription factor. Multiple myeloma is a blood malignancy derived from plasma cells, antibody producer mature B cells in which both Ikaros and Aiolos are expressed at high levels. It has been shown that Lenalidomide, a drug that has been extensively used to treat multiple myeloma as well as other blood malignancies, induces the specific recruitment of Ikaros and Aiolos to the ubiquitin ligase Cereblon ($CRL4^{CRBN}$), thus promoting their ubiquitination and degradation (Fink & Ebert, 2015; Kronke et al., 2014; Lu et al., 2014). Although the underlying mechanism is not known, Ikaros and Aiolos degradation in multiple myeloma results in downregulation of Irf4 and Myc, differently from what is observed during normal mouse-B cell development, suggesting a switch from a negative to a positive regulation of these target genes; thus, an hypothesis is that the regulation of this axis, directly or indirectly mediated by Ikaros and Aiolos, could explain the antiproliferative effect of the drug (Bjorklund et al., 2015).

Apart from the widely studied role of Ikaros family in blood tumors, some recent works examine the less known function of these transcription factors in solid tumors. In particular, Aiolos emerged to be overexpressed in lung cancer, where it confers resistance to anoikis (Frisch & Schaller, 2014; Zhang et al., 2013; Zhu et al., 2017; Terada & Liu, 2014), while pioneer studies on Ikaros role in hepatocellular carcinoma (HCC), suggest that patients affected by HCC have longer survival when Ikaros is present at higher level (Liu et al., 2017; Tian et al., 2017; Zhang, 2014).

Aim of the project

Myc deregulation is a hallmark of many human cancers and its function is essential for tumor maintenance. For this reason, it would be of great interest finding ways to inhibit Myc activity in the clinic. However, since Myc itself is not easily druggable, one possibility is to block Myc interaction with Max or other cofactors, impairing the regulation of its target genes. For this reason, the initial aim of our work was to identify new Myc interactors on chromatin, starting from a Mass Spectrometry-based approach in a human B-lymphocyte cell line. Among the Myc-interacting proteins identified, we focused our attention on two lymphocyte specific transcription factors, called Ikaros and Aiolos, to characterize their functional and molecular cooperation with Myc.

2. MATERIALS AND METHODS

2.1. Cell lines

P493-6 cells (Pajic et al., 2000) were cultured in RPMI 1640 medium, with 10% tetracycline-free fetal bovine serum, 2 mM glutamine, 100 U/ml penicillin/streptomycin and 0.1 mM non-essential amino acids (NEAA, Lonza). For Low Myc conditions, p493-6 cells were treated with 200 ng/ml tetracycline (Tet) (Sigma) for 8h.

HEK293T cells were grown in DMEM medium, with 10% fetal bovine serum, 2 mM glutamine and 100 U/ml penicillin/streptomycin.

BH1 cells were gently provided by the Kastner and Chan laboratory in France (Heizmann et al, 2013). Cells were amplified in IMDM medium, with 10% tetracycline-free fetal bovine serum, 2 mM glutamine, 100 U/ml penicillin/streptomycin, 50 μM beta-mercaptoethanol and 7% supernatant of J558L cells producing IL7. To activate IkarosER, we added OHT to the medium at a final concentration of 400 nM and to induce Tet-Myc expression we added 400 ng/ml of doxycycline (Dox).

Raji and Daudi Burkitt's lymphoma cell lines were cultured in RPMI 1640 medium with 10% fetal bovine serum, 2 mM glutamine, 1 mM Sodium Pyruvate, 10 mM Hepes and 100 U/ml penicillin/streptomycin.

Namalwa Burkitt's lymphoma cell line was cultured in RPMI 1640 medium with 10% fetal bovine serum, 2 mM glutamine and 100 U/ml penicillin/streptomycin.

Ramos Burkitt's lymphoma cell line was cultured in MEM medium with 10% fetal bovine serum, 2 mM glutamine, 1 mM sodium pyruvate, 10 mM Hepes and 100 U/ml penicillin/streptomycin.

Multiple myeloma cell lines (H929, MM1S, JJN3, KMS11) were cultured in RPMI 1640 medium with 10% fetal bovine serum, 2 mM glutamine and 100 U/ml penicillin/streptomycin.

697 and REH pre-B ALL cell lines were cultured in RPMI 1640 medium, 20% fetal bovine serum, 2 mM glutamine and 100 U/ml penicillin/streptomycin.

Sup-15 pre-B ALL cell line was cultured in McCoy's medium with 20% fetal bovine serum, 2 mM glutamine, 100 U/ml penicillin/streptomycin.

Ba/f3 cell line was cultured in RPMI 1640 medium with 10% fetal bovine serum, 10% supernatant of WEHI-3B cells, 2mM glutamine and 100 U/ml penicillin/streptomycin.

2.2. Cell transfection

3 x 10^6 HEK293T cells were plated in a 10 cm dish the day before the transfection. Cells were transiently transfected with pcDNA3 vectors expressing Ikaros, Aiolos or FLAG-Myc in different combinations using the calcium phosphate protocol (Graham & van der Eb, 1973).

To prepare the Ikaros and Aiolos vectors used for transfection, total RNA was extracted from p493-6 cells (Quick-RNA^{TM} MiniPrep, Zymo Research) and retrotranscribed into complementary DNA (cDNA) using the Reverse Transcriptase enzyme (ImProm-II^{TM}, Promega). The cDNA corresponding to the entire Ikaros and Aiolos genes was amplified using the primers reported in table 1 and the p493-6 cDNA as template. The PCR product was run on agarose gel and the correct band was purified (QiAquick Gel Extraction kit, Quiagen) and inserted in the pcDNA3 vector using the XbaI and BamHI restriction enzymes (NEB); plasmids were then sequenced to check if they were correct.

The pSLIK-Tet-Myc-Hygro vector was prepared with a two-step cloning protocol: first, hMyc cDNA was inserted into the pEN-Tmcs vector and then it was transferred into the pSLIK vector through the Gateway Recombination technology. The primers used to clone the hMyc cDNA are reported in table 1.

2.3. Cell transduction

HEK293T cells were transfected with the pSLIK vector together with the packaging vectors psPax2 and pMD2.G to produce the lentiviral supernatant that was collected 48h later.

Subsequently, 10^6 BH1 cells were resuspended in 1 ml of viral supernatant and centrifuged for 1.5h, 1800 rpm, for spin-infection. After 2h hours of recovery in the incubator, cells were resuspended in fresh medium and, 24h later, hygromycin was added for selection.

2.4. Proliferation assays

For the growth curves, 600000 BH1 cells were plated in 6-well plates with 2 ml of medium containing or not OHT and/or Dox. Cells were counted every two days, in triplicate, up to ten days.

For the cell cycle analysis, BH1 cells were plated at a concentration of 300000 cells/ml in a 6-well plate in presence or absence of OHT and/or Dox. 24h later, BrdU (B9285, Sigma) was added to each well at a final concentration of 10 µg/ml, for 20 minutes. Cells were then collected, washed with PBS and fixed with cold ethanol. After one wash in PBS 1% bovine serum albumin (BSA), cells were resuspended in 1 ml of denaturing solution (2N HCl) and left at room temperature for 20 minutes; subsequently, cells were neutralized with 3 ml 0.1 M $NA_2B_4O_7$ pH 8.5 and washed with PBS 1% BSA. Cells are then stained with the anti-BrdU antibody (BD Bioscience) at a final concentration of 5 µg/ml for 1h light protected, washed again with PBS 1% BSA and incubated wit the secondary donkey-anti-mouse antibody conjugated with ALexaFLuo647 (Invitrogen) at a final concentration of 20 µg/ml for 1h, light protected. Finally, cells are washed with PBS 1% BSA and resuspended in 500 µl of PBS with propidium iodide (PI, 2.5 µg/ml) and RNaseA (250µg/ml) overnight, before the acquisition with the MACSQuant® Analyzer. All the samples were then analyzed with the FlowJo X software.

2.5. Chromatin proteomics (ChroP)

2.5.1. Chromatin Immunoprecipitation (ChIP)

10^8 p493-6 cells were crosslinked with 1% Formaldehyde (FA) for 10 minutes; the reaction was blocked adding 125 mM glycine for 5 minutes. After a wash with PBS, cells were pelleted by centrifugation, shock-frozen in dry ice and conserved at -80°C until use. Thawed cells were resuspended in Lysis Buffer (150 mM NaCl, 15 mM TrisHCl pH 7.6, 60 mM KCl, 2 mM EDTA, 0.5 mM EGTA, 0.3M sucrose, 0.4% NP-40) plus complete EDTA-free protease inhibitors (Roche), 1 mM DTT, 0.2 mM spermine, 1 mM spermidine, 0.5 mM PMSF. After a wash in Buffer D (15 mM NaCl, 15 mM TrisHCl pH 7.6, 60 mM KCl, 0.3 M sucrose), DNA digestion was performed with Micrococcal Nuclease (MNase), for 1h at 37°C in the proper buffer (20 mM Tris-HCl pH 7.6, 5 mM $CaCl_2$); subsequently, the reaction was stopped adding EDTA at a final concentration of 50 mM and an aliquot of the sample was checked on agarose gel.

IP buffer, composed of two parts of SDS buffer (100 mM NaCl, 50 mM Tris-HCl pH 8.1, 0.5% SDS) and one part of Triton dilution buffer (100 mM Tris-HCl pH 8.5, 100 mM NaCl, 5 mM EDTA, 5% Triton X-100), plus protease inhibitors, was added after digestion and a rapid cycle of sonication was performed to completely break the nuclei. An aliquot was kept as input; 20 µg of antibodies were added to the rest (anti-Myc, N262, Santa Cruz; anti-rabbit IgG, Santa Cruz) and incubated overnight at 4°C. Immunocomplexes were recovered adding dynabeads (Life Technologies) for 4h and then washed five times with RIPA buffer (50 mM Hepes pH 7.6, 500 mM LiCl, 1 mM EDTA, 1% NP-40, 0.7% Na-Deoxycholate) and once with TE 50mM NaCl. 10% of the material was processed to perform quantitative PCR and 10% was used for western blot; the rest of the material was decrosslinked, prepared for electrophoresis and loaded on a 4-12% pre-cast gel (NuPAGE Novex Bis-Tris Gel, Invitrogen).

2.5.2. In-gel digestion for MS

In-gel digestion of the samples was performed as previously reported (Shevchenko et al., 2006; Soldi & Bonaldi, 2014) with few modifications.

Each lane of the gel was divided into 9 bands as shown in figure 11; each band was chopped in pieces of approximately 1x1 mm and transferred in microcentrifuge tubes. The gel pieces were washed with destaining buffer (25 mM NH_4HCO_3, 50% EtOH) at 25°C until the Blue Coomassie staining was completely removed. They were then dehydrated in 100% EtOH and dried in a speed-vac. The samples were rehydrated in reduction buffer (10 mM DTT, 50 mM NH_4HCO_3) and incubated 1h at 56°C. Afterwards, alkylation buffer (55 mM iodoacetamide in 50 mM NH_4HCO_3) was added and samples were incubated for 45' at 25°C, protected from light. The gel pieces were washed with digestion buffer (50 mM NH_4HCO_3 in ddH_2O, pH 8) for 20' at 25°C. The samples were again subjected to a couple of cycles of dehydration with EtOH and washed with digestion buffer, then they were dried in a speed-vac and rehydrated in the trypsin solution (12.5 ng/µl trypsin, Promega, in 50 mM NH_4HCO_3) and incubated for 20' at 4°C. Trypsin was then removed and digestion buffer was added for an overnight incubation at 37°C. The reaction was stopped adding trifluoroacetic acid (TFA); the samples were spinned down and the gel pieces were transferred in a new tube. The peptides were extracted from the gel by adding extraction buffer (3% TFA, 30% acetonitrile –ACN-) for 10' at 25°C, shacking; gel pieces were spinned down and the supernatant was collected and added to the previous one (this operation was repeated twice). The same was done using 100% ACN. Finally, the collected supernatant was dried in a speed-vac to remove ACN. Lyophilized samples were desalted and concentrated on C18-Stage Tips (Rappsilber et al., 2007). The elution was carried out with a highly organic solvent (80% ACN) followed by lyophilisation. Prior to LC-MS/MS analysis, samples were resuspended in 1% TFA in ddH2O.

2.5.3. Liquid chromatography and tandem Mass Spectrometry (LC-MS/MS)

Samples were prepared and analyzed by Liquid Chromatography and Tandem Mass Spectrometry (LC-MS/MS) as previously described (Soldi & Bonaldi, 2013).

Peptide mixtures were separated via nano-flow liquid chromatography (LC) using an Agilent 1100 Series (Agilent Technologies Waldbronn, Germany) coupled to a 7-tesla linear ion trap–Fourier transform–ion cyclotron resonance (LTQ-FT-ICR) Ultra mass spectrometer (Thermo-Fisher Scientific, Bremen, Germany). The nano-flow LC system was operated in a one-column set-up with a 15 cm analytical column (75 mm inner diameter, 350 mm outer diameter) packed with C18 resin (ReproSil, Pur C18AQ 3 mm, Dr. Maisch, Ammerbuch Germany). The sample was injected into an aqueous solution at a flow rate of 500 nl/min. Peptides were separated with a gradient of 0%–36% over 120 min followed by gradients of 36%–60% for 10 min and 60%– 80% over 5 min at a flow rate of 250 nl/min. A nanoelectrospray ion source (Proxeon, Odense, Denmark) was used with a spray voltage of 2.4 kV. No sheath, sweep, or auxiliary gasses were used, and the capillary temperature was set at 190 °C. The mass spectrometer was operated in data-dependent mode to automatically switch between MS and MS/MS acquisition. In the mass spectrometer, full scan MS spectra (200–1650 *m/z*) were acquired with a resolution of 100,000 at 400 *m/z*, setting an Acquisition Gain Control target of 1,000,000. The five most intense ions were isolated for fragmentation in the linear ion trap using collision-induced dissociation at a target value of 5000. Singly charged precursor ions were excluded. In the MS/MS method, a dynamic exclusion of 60 s was applied, and the total cycle time was 2 s. The collision gas pressure was 1.3 millitorr, and the normalized collision energy using wide band activation mode was 35%. The ion selection threshold is 250 counts with an activation q=0.25. An activation time of 30 ms was applied in MS/MS acquisitions.

2.5.4. Protein identification by MaxQuant software and data analysis

MS analyses were performed as previously described (Soldi & Bonaldi, 2013) in collaboration with Tiziana Bonaldi's group.

Protein interactors from the cross-linking ChIPs were identified and quantified using MaxQuant software (version 1.3.0.5) (http://www.maxquant.org/downloads.htm). MS/MS spectra were recorded in "centroid" mode, and the six most abundant peaks per 100 Da mass intervals were selected for search. The MS/MS spectra were searched against a HUMAN 1401 database (51195 entries), using Andromeda search engine (Cox et al., 2011) MaxQuant analysis included an initial search with a precursor mass tolerance of 20 ppm, and the results were used for subsequent mass recalibration. Peptide identification was based on a main search with mass deviation of the precursor ion of 7 ppm, and the fragment mass tolerance was set at 0.5 Da. The mass accuracy of the precursor ions was improved by the time-dependent recalibration. Enzyme specificity was set to trypsin, allowing two missed cleavages and cleavage at the N-terminus of proline. A false discovery rate (FDR) of 0.01 for proteins and peptides is applied, and a minimum peptide length of 6 amino acids is required. Carbamidomethylation of cysteine was selected as a fixed modification, and oxidation of methionine and acetylation of the protein N-terminus were included as variable modifications. Peptide and protein identifications were performed automatically with MaxQuant using default settings. Additional option for Label Free Quantification (LFQ) and Match between run were selected. In particular, for the Match between run the precursor masses were matched in a 2-min retention time window (after realignment of the runs) based on the accurate mass measurement.

Contaminants, hits to the reverse database (reversed) and proteins identified only by site were filtered out in each label-free Myc ChIP experiment. Proteins were accepted if they were identified with at least two peptides, one of which was unique, in each experiment. For each protein, the LFQ ratio was calculated dividing the LFQ value in the Myc ChIP over the LFQ value in the IgG ChIP. Proteins present in at least two out of three replicates

were selected as putative Myc interactors, considering all the proteins identified only in Myc-ChIP experiments, and also the proteins identified in both Myc-ChIP and IgG-ChIP with a LFQ ratio>=2.5.

2.6. ChIP-qPCR

To check the quality of the Myc-ChIP, we analyzed regions on Myc-bound promoters (Nucleolin, IFRD2) and a non-targeted region as a negative control (acetylcholine receptor). The qPCR mix was composed of 6 µl of DNA, 4 µl of 2 µM primers mix, 10 µl of Syber Green mix (Applied Biosystem), for a total volume of 20 µl. The primers used are listed in table 1.

2.7. Western Blot (WB)

Cells were resuspended in lysis buffer (150 mM NaCl, 1% NP-40, 0.5% Sodium Deoxycholate, 0.1% SDS, 50 mM Tris pH 7.5) supplemented with protease inhibitors (Roche) and sonicated; protein concentration was determined by Bradford-based Protein Assay kit (Bio-Rad).

Cell lysates were loaded on a 12% polyacrylamide gel. After the electrophoresis, proteins were transferred on a nitrocellulose membrane that was blocked for 1h with 5% milk in TBS-T (10 mM TrisHCl, 100 mM NaCl, 0.1% Tween at pH 7.4) and subsequently incubated with the proper primary and secondary antibodies. The signal was detected using the Enhanced Chemioluminescence kit (Bio-Rad) and analyzed with ChemiDoc XRS+ imaging system and Image Lab software (Bio-Rad).

Antibodies: anti-Myc (9E10), anti-Myc Y69 (ab32072, Abcam) anti-Ikaros (H-100, Santa Cruz), anti-Ikaros (A303-516A, Bethyl laboratories), anti-Aiolos (ab64400, Abcam), anti-FLAG (ab1162, Abcam), anti-Vinculin (Sigma), anti-ACL (A303-866A, Bethyl laboratories), anti-DNA-PK (A300-516A-T, Bethyl laboratories), anti-Ruvbl1 (A304-716-

A-T, Bethyl laboratories), anti-Ruvbl2 (A302-536A-T, Bethyl laboratories), anti-NCL (A300-711A-T, Bethyl laboratories), anti-Rbbp4 (ab79416, Abcam), anti-Ifi16 (sc8023, Santa Cruz), anti-CHD4 (A300-081A-T, Bethyl laboratories).

2.8. Co-Immunoprecipitation (coIP)

Endogenous Ikaros and Aiolos were immunoprecipitated in p493-6 cells, in HEK293T cells, in multiple myeloma cell lines and in Burkitt's lymphoma cell lines using the sc13039 (H-100, Santa Cruz) and ab64400 (Abcam) antibodies respectively. Myc was immunoprecipitated with the N262 (sc764, Santa Cruz) antibody.

Ikaros was immunoprecipitated in BH1 cells using the ab191394 (Abcam) antibody and in pre-B ALL cell lines using the anti-Ikaros antibody from Bethyl Laboratories (A303-516A).

$30x10^6$ cells were resuspended in 1ml of NHEN buffer (150 mM NaCl, 0.5% NP-40, 10% glycerol, 1 mM EDTA, 20 mM HEPES pH 7.5 and complete EDTA-free protease inhibitors (Roche) and briefly sonicated for 30 seconds with 30% amplitude. 2µg of the specific antibody was added to 2 mg of protein lysate and left for 3h at 4°C on a wheel. Sepharose beads conjugated with G protein (Invitrogen) were added for 2 additional hours to recover the immunocomplexes. After five washes with wash buffer (150 mM NaCl, 0.1% Tween, 10% glycerol, 1 mM EDTA, 20 mM HEPES pH 7.5), the beads were resuspended in sample buffer, boiled at 95°C to elute the proteins and ran on SDS-PAGE for western blot analysis.

2.9. ChIP-sequencing (ChIP-seq)

The ChIP experimental protocol previously described in this session was followed with minor modifications. In particular, DNA was fragmented by 8 cycles (30" ON + 30" OFF, 30% Amplitude) of sonication instead of being digested with MNase, in order to obtain

DNA fragments of a size between 200 and 300 bp. After overnight incubation with the antibody, G protein-conjugated beads (Invitrogen), pre-blocked with BSA and *E. coli* tRNA were added to the lysates for 2h at 4°C and then washed three times with Mixed Micelle buffer (150 mM NaCl, 20 mM Tris-HCl pH 8.1, 50 mM EDTA, 0.2% NaN_3, 2% Triton-X 100, 0.2% SDS, 5% w/v sucrose), two times with buffer 500 (0.1% DOC, 1 mM EDTA, 50 mM HEPES, 500 mM NaCl, 1% Triton-X 100, 0.2% NaN_3), two times with LiCl buffer (0.5% DOC, 1 mM EDTA, 250 mM LiCl, 0.5% NP-40, 10 mM Tris-HCl pH 8, 0.2% NaN_3) and once with TE buffer (10 mM Tris pH 8, 1 mM EDTA). Beads and inputs were then resuspended in 200 µl of TE with 2% SDS and decrosslinked overnight at 65°C. The day after, DNA was purified (PCR purification kit, Qiagen) eluted in 50 µl and dosed with the Qubit fluorimeter; an aliquot of DNA was diluted 1:5 and analysed by qPCR.

2.10. ChIP-seq analysis

ChIP-seq Next-Generation Sequencing (NGS) reads sequenced with the Illumina HiSeq2000 were filtered using the fastq_masker tool (setting the options to –q 20 – r N) of the FASTX-Toolkit 0.0.13.2 (http://hannonlab.cshl.edu/fastx_toolkit/). Their quality was evaluated and confirmed using the FastQC application (http://www.bioinformatics.barbraham.ac.uk/projects/fastqc/).

ChIP-seq NGS reads were aligned to the hs19 genome through the BWA-0.6.2-r126 aligner using default settings (Li & Durbin, 2010). Peaks were called using the MACS software (v2.0.9) (Zhang et al., 2008). Only peaks with *P* values $<1 \times 10^{-5}$ were retained (positive peaks). Normalized reads count within a genomic region was obtained by normalizing the number of reads in a particular region on the total number of aligned reads in the sequencing library. Peak enrichment was determined as log2(ChIPw - inputw), in which ChIPw and inputw is the normalized count of reads in the peak region in the ChIP and in the corresponding input sample. Promoters are defined as regions from -2 kb to +1

kb around the TSS. All the alignments and peak calling were performed using HTS-flow, a web tool for the management and the analysis of NGS data (Bianchi et al., 2016). Bioinformatic analyses were performed in collaboration with Vera Pendino.

2.11. RNA extraction and analysis: quantitative PCR (qPCR) and RNA-seq.

Total RNA was purified onto RNeasy columns (Qiagen), or using the Maxwell ® 16 LEV simplyRNA cell kit.

For qPCR analysis, the complementary DNA (cDNA) was synthetized using the ImPromII kit (Promega). 10 ng of cDNA were used for each qPCR reaction together with the FAST SYBER Green Master mix (Applied Biosystem) and 0.4 μM primers in a total volume of 20 μl.

For the RNA-seq, RNA quality was checked with the Agilent 2100 Bioanalyser (Agilent Technologies). Libraries for RNA-seq were then prepared with the TruSeq Stranded Total RNA sample Prep Kits (Illumina) following manufacturer instruction. RNA libraries were sequenced in a 50 bp pair-end mode with 60 milion reads depth.

2.12. RNA-seq data analysis

The samples sequenced with the Illumina HiSeq2000 were filtered using the fastq_masker tool (setting the options to –q 20 – r N) of the FASTX-Toolkit 0.0.13.2 (http://hannonlab.cshl.edu/fastx_toolkit/). Their quality was evaluated and confirmed using the FastQC application (http://www.bioinformatics.barbraham.ac.uk/projects/fastqc/).

NGS reads from the p493-6 samples were aligned to the hs19 reference genome, while the reads from the BH1 cells were aligned to the mm9 genome using the TopHat aligner (version 2.0.6) with default parameters (Trapnell et al., 2009). In case of duplicated reads, only one read was kept. Read counts were associated to each gene (gene annotation from

UCSC derived GTF gene) using the featureCounts software (http://bioinf.wehi.edu.au/featureCounts/). Absolute gene expression was defined determining the number of exonic reads per kilobase per million of total reads aligned on exons (eRPKM). Differentially expressed genes (DEGs) were identified using the Bioconductor package DESeq2 (Love et al., 2014) considering genes whose q-value relative to the control was lower than 0.05.

All the alignments, absolute quantifications and identification of DEGs were performed using HTS-flow, a web tool for the management and the analysis of NGS data (Bianchi et al., 2016). Bioinformatics and statistical analysis, including heatmaps, hierarchical clustering of RNA-Seq data were performed using R and Bioconductor packages (R Core Team 2011).

RNA-seq of p493-6 cells with high or low Myc level was performed on four biological replicates (cells treated and collected at different moments). RNA-seq of BH1 cells with different treatments was performed on three technical replicates (three aliquots of cells treated and collected at the same time). Bioinformatic analyses were performed in collaboration with Vera Pendino.

2.13. Motif analysis

Sequences of 200 bp around the summits of the peaks are considered for each ChIP-seq and analyzed with the MEME Suite web portal (v4.12.0) (Bailey et al., 2009), that uses different motif discovery tools such as DREME (Bailey, 2011) and MEME-ChIP (Machanick & Bailey, 2011).

2.14. Functional annotation

Functional annotation analysis to determine enriched classes of genes was performed using the Molecular Signature Database (MSigDB, v6.1) of the GSEA Broad Institute

(Subramanian et al., 2005), considering in particular the overlap with the Canonical Pathways and the Hallmark gene sets.

2.15. List of primers

Cloning			
Gene name	**Specie**	**Forward**	**Reverse**
Ikaros	human	CGTAGGATCCACCATGGATGCTGATGAGGG	TACGTCTAGATTAGCTCATGTGGAAGC
Aiolos	human	CGTAGGATCCACCATGGAAGATATACAAAC	TACGTCTAGATCACTTCAGCAGGGCTC
c-Myc	human	CGTAACTAGTACCATGCCCCTCAACGTTAG	TACGGCGGCCGCTTACGCACAAGAGTTCC

ChIP			
Gene name	**Specie**	**Forward**	**Reverse**
Nucleolin	human	TTTTGCGACGCGTACGAG	ACTAGGGCCGATACCGCC
IFRD2	human	CGTGCCCCAGCAGTCATT	GCAGTGGGCAGCGAGC
AchR	human	CCTTCATTGGGATCACCACG	AGGAGATGAGTACCAGCAGGTTG
AMICA1	human	AGGAACCACAAGAAGGCTGA	GGGACCCTCTTACGTGACAA
SYK	human	CTGTGTGGTTTGAGCGTGAT	ACATCCCTGGGCCATTAGAG
QPCTL	human	ACCAATCCCCTGCCTACATC	GTTGGTTCCCCTGAGAATGG

Gene expression			
Gene name	**Specie**	**Forward**	**Reverse**
RPPO	mouse/human	TTCATTGTGGGAGCAGAC	CAGCAGTTTCTCCAGAGC
TBP	mouse	TAATCCCAAGCGATTTGCTG	CAGTTGTCCGTGGCTCTCTT
c-Myc	human	GATTCTCTGCTCTCCTCGACGG	AGAAGGTGATCCAGACTCTGACC
c-Myc	mouse	TTTTTGTCTATTTGGGGACAGTG	CATCGTCGTGGCTGTCTG
Ikaros	mouse	TCCAGATGAAGGGGATGAGC	CTTTCTGGGTAAAGGAGGCC
St6Galnac4	human	TGGTCTACGGGATGGTCA	CTGCTCATGCAAACGGTACAT
Rrp9	human	AGAGACCGCACAGGAAAAGA	ACTTCTGCAACCTGCCTCTC
Igll1*	mouse	GGACTTGAGGGTCAATGAAGCTC	GTGGGATGATCTGGAACAGGAG
Lig4*	mouse	CATGTCCCCTTTGCAGACTT	TTTCTGTTCTTATGAAGGGCATC
Rag1*	mouse	AGAGAGCAAGGAGAGAGTAGACAGCA	GGTGTTGAATTTCATCGGGTGC
Syk	mouse	TTCAACCCCTATGAGCCAAC	GGCAGGGCTTCTCTCTGAA
Vpreb*	mouse	CATCAGCCACCATTAGCATC	ACCCTGGTGCTTGTCTGAGT
Ccnd2*	mouse	GATCCGAACGAGACCAAGAA	CCCTCTGGCTCACTTCTCAG
Blnk*	mouse	GAGAGGGAACGGAGAGGACT	GGTTGTGCTGGTGACTGTTG

*From Ferreiros-Vidal et al, 2013

Table 1. List of primers. List of primers used for cloning, ChIP-qPCR and gene expression analysis.

3. RESULTS

3.1 Identification of Myc interactors through mass spectrometry analysis

3.1.1. Myc modulation in p493-6 cells

As a system in which Myc levels can be easily modulated, thus facilitating the validation of Myc interactions and the study of their biological role, we chose to use the p493-6 line. P493-6 cells were derived from a human B cell line (EREB2-5), previously derived from primary human tonsil B-cells immortalized with a conditional form of the Epstein-Bar virus (EBV) protein EBNA2 (Kempkes et al., 1995). EBV infection initiates cell cycle entry of resting B lymphocytes in a way that is strictly dependent on the viral protein EBNA2. In particular, in the EREB2-5 cell line, the EBNA2 protein was engineered and fused with the ligand binding domain of the estrogen receptor, thus activation of EBNA2 and cell proliferation depend on the presence of estrogens. In the absence of EBNA2 activity, the endogenous Myc, that is shown to be an EBNA2 direct target, is not expressed; conversely, upon estrogen stimulation, EBNA2 regulates Myc expression inducing cell cycle entry (Kaiser et al., 1999). Subsequently, EREB2-5 cells were stably transfected with a vector expressing an exogenous Myc transgene under the control of a Tet-OFF system to obtain the final p493-6 cell line (figure 7); the suppression of Myc expression upon tetracycline (Tet) withdrawal treatment rapidly causes cell cycle arrest (Pajic et al., 2000). Since EBV infection is often associated with the onset of Burkitt's lymphoma (BL) and since this cell line showed typical BL features in terms of cell morphology, expression of surface antigens and Myc expression level, p493-6 cells have commonly been considered an *in vitro* model of BL.

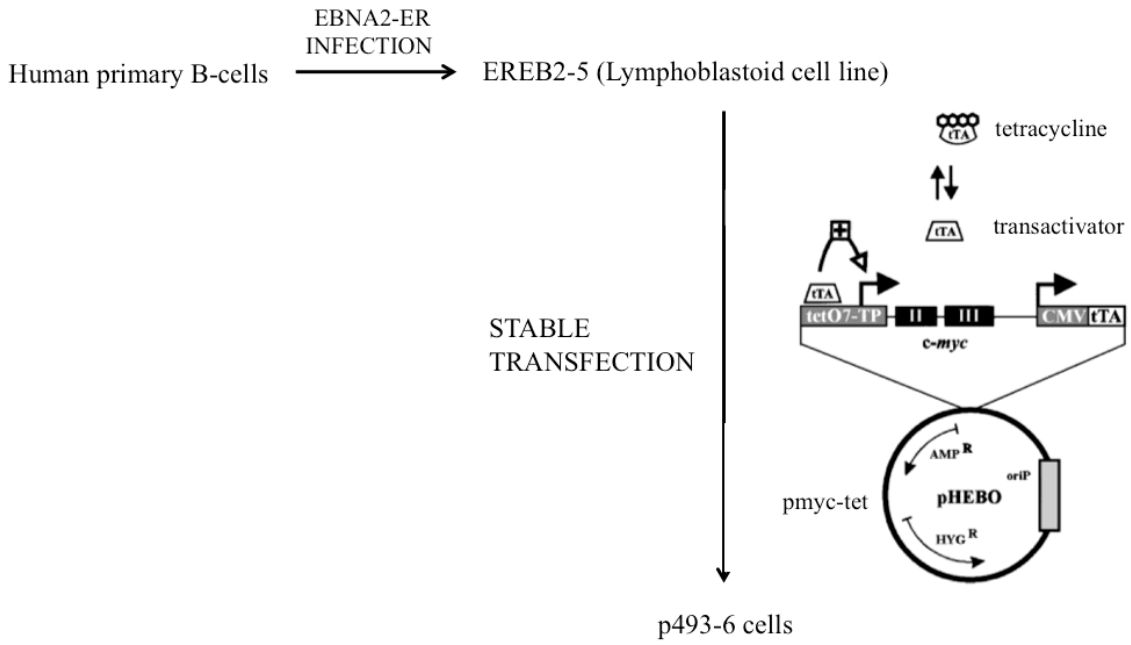

Figure 7. p493-6 cell line. Human B cells were immortalized with a conditional form of the Epstein-Bar Virus (EBV) protein EBNA2. Subsequently, they were stably transfected with a vector expressing an exogenous Myc transgene under the control of a Tet-OFF system (adapted from Pajic 2000).

This system would allow us to easily obtain a cell line with high or low Myc levels just adding Tet to the medium. In particular, we decided to compare cells proliferating in the absence of Tet (i.e. maximal Myc expression) with parallel cultures treated with Tet for 8h, in order to decrease Myc protein level of around ten times in the shorter time frame possible to avoid secondary effects due, for example, to the block of cell cycle. So, from now on, we will refer to "high Myc conditions" for untreated cells and "low Myc conditions" for cells treated with 200 ng/ml Tet for 8h (figure 8).

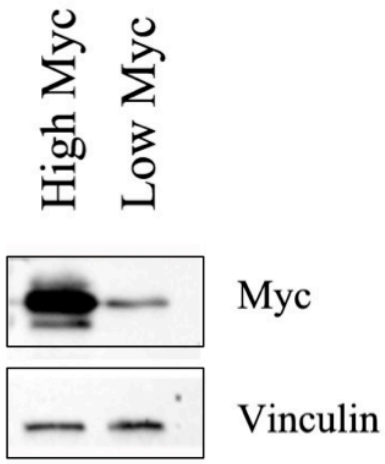

Figure 8. Myc level modulation in p493-6 cells. Exogenous Myc level is under the control of a Tet-off system. High Myc= non-treated cells; low Myc= cell treated for 8h with 200 ng/ml Tet.

3.1.2. Setting of the label-free ChroP technique.

In order to identify new Myc interactors on chromatin, we took advantage of the Chromatin Proteomics (ChroP) technique that combines chromatin immunoprecipitation (ChIP) and Mass Spectrometry (MS) (Soldi & Bonaldi, 2014) (figure 9). We performed this experiment in p493-6 cells with high Myc level, using a label-free MS approach. Basically, we chemically crosslinked proteins and DNA with formaldehyde and performed immunoprecipitation using an antibody that specifically recognizes Myc, as usually done in chromatin immunoprecipitation (ChIP) experiments to identify protein-DNA interactions, but instead of Myc-associated DNA we analyzed Myc-associated proteins by mass spectrometry (figure 9).

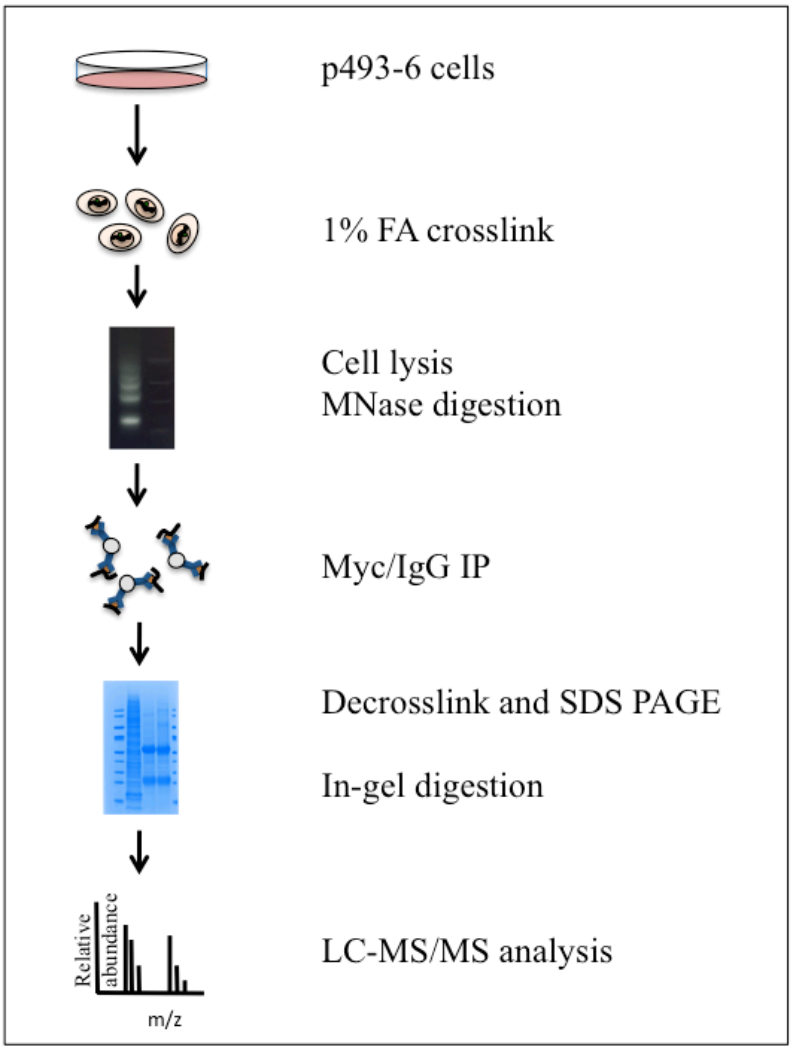

Figure 9. Label free ChroP scheme. Cells are crosslinked with formaldehyde (FA) and treated with MNAse to fragment DNA. Specific antibodies are added to the cell lysate; immune-complexes are then recovered by adding beads and washed. Part of the material is kept for the controls (WB and qPCR), while the rest is loaded on a gel and processed for MS analysis

We first verified the quality of the immunoprecipitation by performing quantitative PCR (qPCR) and WB on part of the recovered material (DNA and protein, respectively). By ChIP-qPCR we verified that, in the Myc-ChIP, the recovery of DNA corresponding to promoters of known MYC targets (*Nucleolin, IFRD2*) (Sabò et al., 2014) was enriched compared to a negative control region (*AchR* promoter), while these levels were comparable to background with the mock IgG-ChIP (figure 10). Moreover, we verified by western blot that the Myc protein was only immunoprecipitated when the anti-Myc antibody was added, while it was not present in the non-specific IgG-ChIP (figure 11).

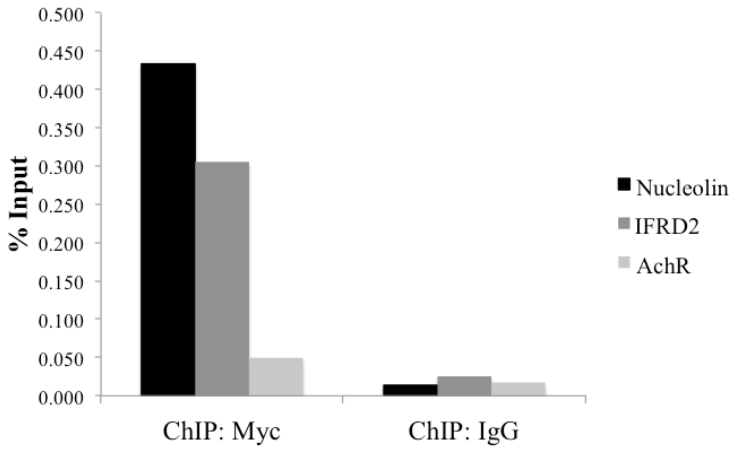

Figure 10. Preliminary ChIP control: qPCR. 10% of the material recovered after the immunoprecipitation was used to extract DNA and verify specific enrichment of known Myc bound regions (Nucleolin and IFRD2) in the Myc IP compared to the IgG IP. The non-bound acetylcholine receptor promoter (AchR) was used as negative control. Here it is shown one experiment representative of the three replicates.

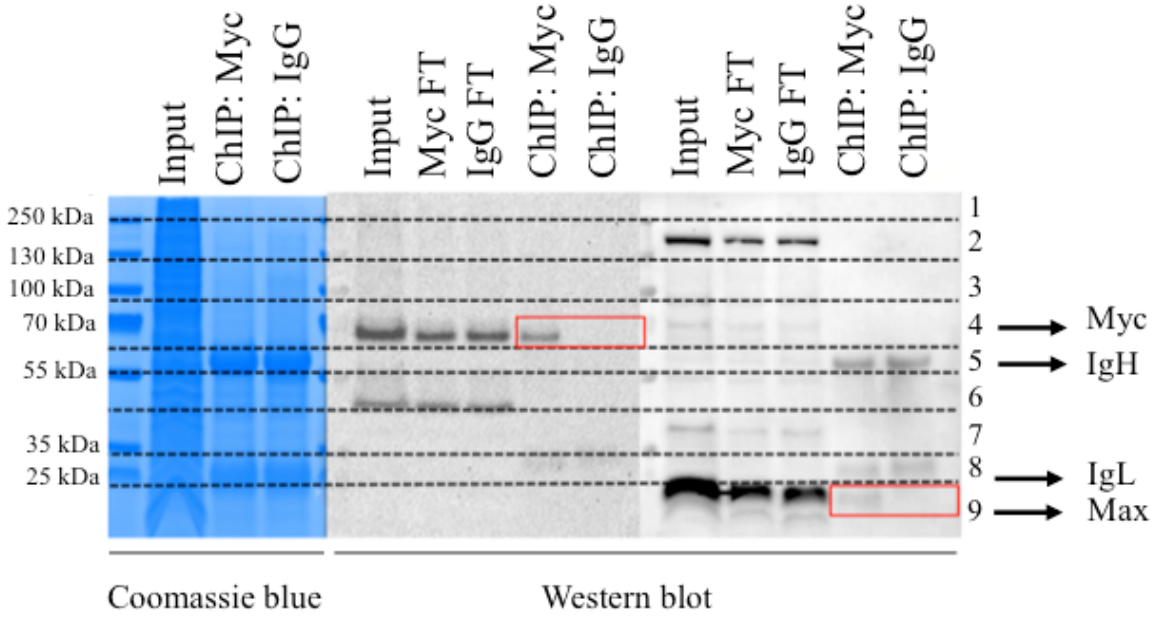

Figure 11. Preliminary ChIP control: WB. 10% of the material recovered after the immunoprecipitation was used to perform a ChIP-WB, while the rest was loaded on gel, stained with coomassie blue and processed for MS analysis. Each lane was divided into 9 parts according to the molecular weight. IgH= immunoglobulin heavy chain of the antibody used for the IP; IgL= immunoglobulin light chain chain of the antibody used for the IP; FT=Flow Through. The loaded input and FT correspond to 2.5% of the material used for the IP. Here it is shown one experiment representative of the three replicates.

Although the western blot showed that we were recovering only a fraction of the Myc protein with the ChIP (as revealed by presence of Myc also in the unbound flow through samples), we judged the amount, specificity and quality of the immunoprecipitated material good enough to proceed with the mass spectrometry. On the same gel used to perform the ChIP-WB, we also loaded all of the remaining immunoprecipitated material for MS analysis: in this way, after development of the WB and coomassie blue staining, respectively, we could use the WB as a precise reference to identify the positions of Myc and Max on the gel (figure 11). Based on this, each lane of the coomassie gel has been divided into 9 different bands taking care of separating Myc (band 4) and Max (band 9) from the heavy and light chains (bands 5 and 8, respectively) of the antibody used for the immunoprecipitation, to avoid signal masking during MS analysis due to the high amount of IgG peptides (figure 11). Each band was cut and processed for MS analysis as described in the material and methods. We performed the ChroP experiment in triplicate, always comparing the Myc-ChroP with a mock, non-specific IgG-ChroP as negative control.

3.1.3. Identification of new Myc interactors

The MS data were analyzed with the MaxQuant software (http://www.maxquant.org/downloads.htm) and only proteins identified with at least two peptides, of which at least 1 is a unique peptide (a peptide that identifies a certain protein in an unambiguous way), have been selected as reliable, following the standard parameters. Proteins identified only in Myc-ChIP experiments or in both Myc-ChIP and IgG-ChIP but with a Myc/IgG ratio of protein amount (Label Free Quantfication, LFQ) $\geq$ 2.5 were considered putative Myc interactors. Using these criteria, we identified a total of 423 candidates, 24 of which were in common within all the 3 experiments, while 51 were found in 2 out of 3 experiments (figure 12).

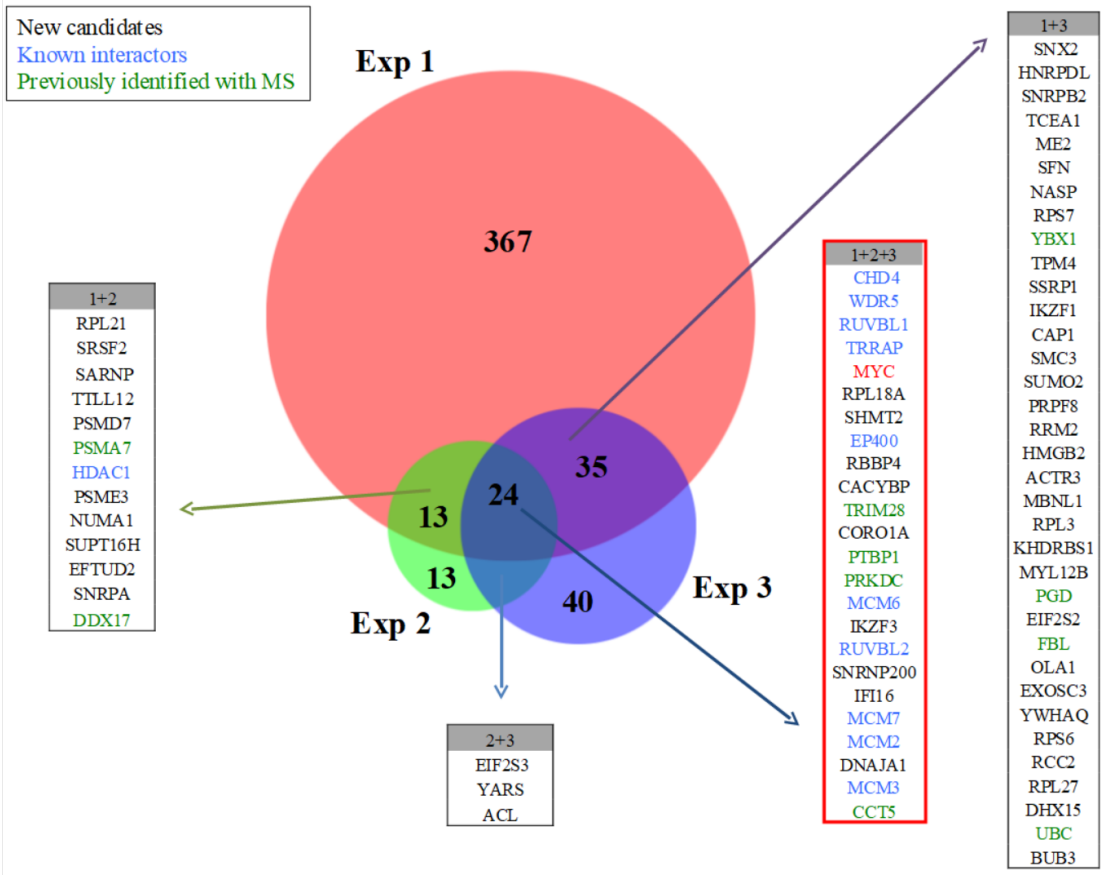

Figure 12. Label free ChroP results. The number of candidates identified in the three experiments was quite different (439 in the first replicate, 53 in the second and 102 in the third), nevertheless 24 proteins were present in all the replicates (1+2+3, red square), while 51 proteins were identified at least in two out of three experiments (1+2, 2+3, 1+3). Proteins written in blue are known Myc interactors; proteins written in green were identified as putative Myc interactors in other MS datasets (Koch et al., 2007; Agrawal et al., 2010), even if the interaction was not validated yet; proteins written in black are the new candidates, not previously reported as Myc ligands.

As expected, Myc was always found with 12 peptides in all the three replicates and only in the Myc-ChIP samples. Several known Myc interacting proteins were identified in at least two independent experiments, validating the reliability of the results: components of the Tip60/NuA4 complex such as TRRAP (McMahon et al. 1998), EP400 (Tworkowski et al., 2008), RUVBL1, RUVBL2 (Frank et al., 2003), as well as WDR5 (Thomas et al., 2015), HDAC1 (Garcia-Sanz et al., 2014), MCM2-7 (Dominguez-Sola et al., 2007), CHD4/Mi-2b (Koch et al., 2007). Moreover, some putative Myc interactors identified also in othe MS-based studies, although not yet validated, were present in our lists: PSMA7, FBL, PRKDC, CCT5, TRIM28 (Koch et al., 2007), DDX17, YBX1, PGD, UBC, PTBP1 (Agrawal et al.,

2010) (figure 12). Unexpectedly, Max was identified only in the first replicate (with 5 peptides) but was missing in the others; this is probably due to technical problems related to the MS analysis, since Max is visible by ChIP-WB and its presence is necessary for Myc to bind the DNA regions (Amati et al., 1992) that resulted enriched by qPCR in our control experiment (figure 10).

Looking at the proteins that were identified in at least two out of three experiments and considering in particular the proteins with a function that could be related to Myc transcriptional activity, some new interesting candidates emerged: IKZF3, IKZF1, RBBP4, SUPT16H, SSRP1, IFI16, YWHAQ, SFN (figure 13).

Ikaros family	IKZF3 (Aiolos)	IKZF1 (Ikaros)		
NuRD complex	RBBP4	HDAC1	CHD4 (mi-2)	Trim28
FACT complex	SUPT16H	SSRP1		
Gamma-interferon-inducible protein 16	IFI16			
14-3-3 proteins	YWHAQ	SFN		

Identified in 3 out of 3 experiments
Identified in 2 out of 3 experiments

Figure 13. Top candidates selected from the label free ChroP results. Proteins identified in at least two out of three replicates, the function of which could be related to Myc transcriptional activity. Different subunits of the same complexes and families are found; already known Myc interactors are indicated in blue.

RBBP4 is a subunit of the NuRD complex (Allen et al., 2013) and several NuRD subunits, including HDAC1/2, TIP48/49 and TRIM28, were already identified as Myc interactors (Koch et al., 2007). SUPT16H and SSRP1 are the two subunits of the facilitates chromatin transcription (FACT) complex, which is a histone chaperone implicated in nucleosome reorganization (Winkler & Luger, 2011). IFI16 is a nuclear protein involved in

transcriptional regulation; in particular, it seems to be a transcriptional repressor that also binds the c-*myc* promoter, interfering with its transcription (Egistelli et al., 2009). YWHAQ and SNF are two members of the 14-3-3 family (14-3-3 theta and sigma respectively) of regulatory proteins: they can interact with many binding partners regulating their activity and thus being involved in many cellular functions such as cell cycle regulation, metabolism control, apoptosis and gene transcription (Obsilová et al., 2008). Aiolos (IKZF3) and Ikaros (IKZF1) are lymphocyte specific transcription factors, able to interact with each other and considered tumor suppressors (Georgopoulos, 2017).

3.1.4. Validation of Myc interactors

We performed ChIP-WB experiments for a first validation of Myc interaction with the cofactors identified by MS. If we immunoprecipitate Myc, we can see a coimmunoprecipitation signal for Nucleolin (NCL), Ruvbl1 and Ifi16, thus, in these cases, the interaction seems to be validated (figure 14A). The specificity of the result is less clear for Aiolos, since a band appears also in the negative control and for ACLY, since it coimmunoprecipitates with Myc in a similar manner when Myc is present at high or low level. Finally, for DNA-PK, Rbbp4, Chd4, Parp1 and Ikaros, no interaction was visible, while for Ruvbl2, the signal could be masked by the heavy chain of the antibody used for the ChIP (figure 14A). We also tried the reciprocal approach by immunoprecipitating Ikaros and Aiolos: in this case, Myc clearly coimmunoprecipitates with both of them when present at high level (figures 14B and C). The same strategy could be tried also for the other candidates to understand if the lack of interaction signal was due to technical issues. Further ChIP-WB experiments, together with coimmunoprecipitations in native conditions are needed to set clear conclusions.

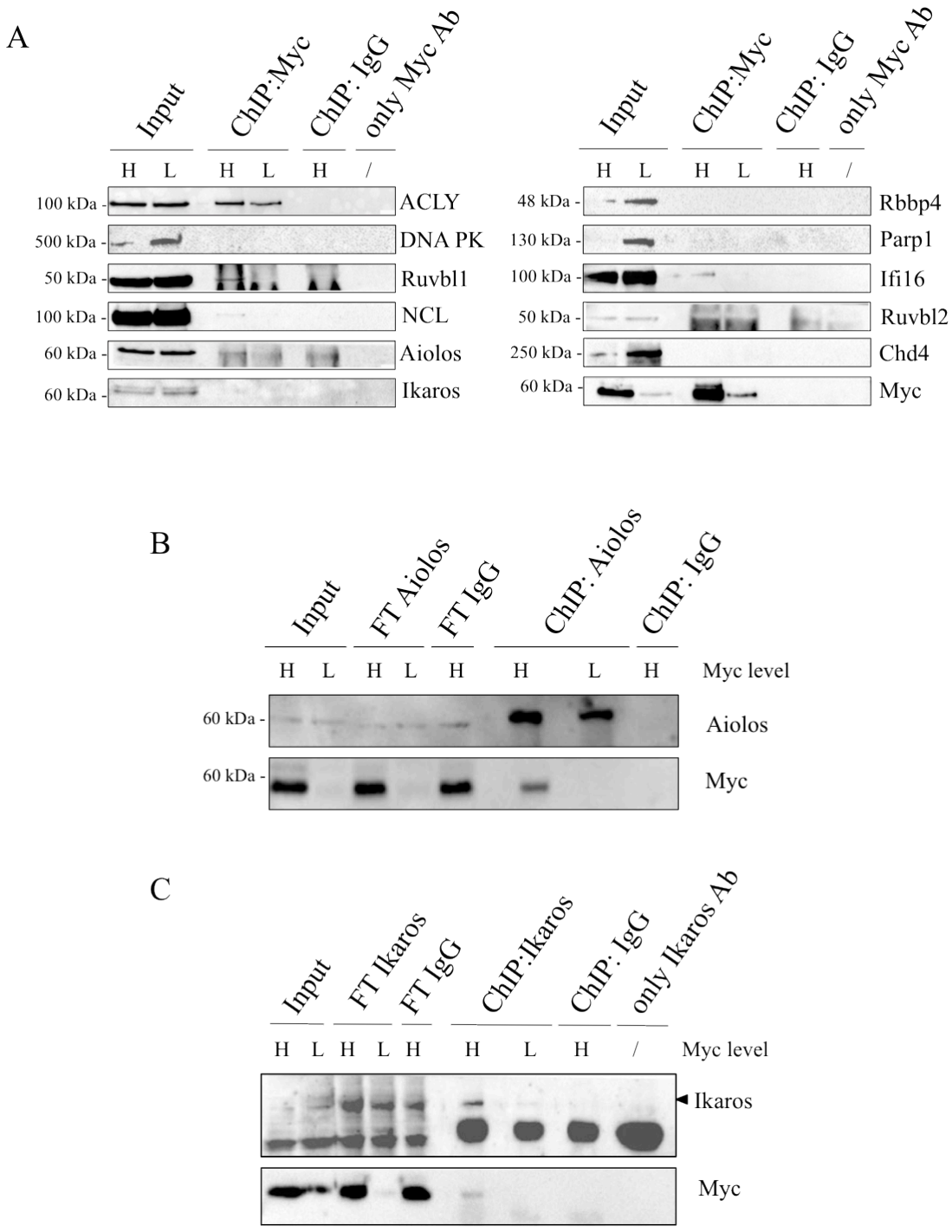

Figure 14. Validation of Myc interactors by ChIP-WB in p493-6 cells. ChIP-WB after Myc (A), Aiolos (B) or Ikaros (C) immunoprecipitation in p493-6 cells with high (H) or low (L) Myc levels. FT= flowthrough. The loaded input and FT correspond to 3% of the material used for the ChIP. Here it is shown one experiment representative of two replicates.

Since, according to the information found in literature, the putative interplay between Myc and Ikaros/Aiolos appeared to be particularly interesting and, in addition, the first ChIP-WB validation of these interactions was promising, we decided to focus our attention on these two proteins, as exposed in the next paragraphs.

3.2. Ikaros, Aiolos and Myc interaction in p493-6 cells

3.2.1. Ikaros and Aiolos coimmunoprecipitate with Myc

In order to validate the interaction of Myc with Ikaros and Aiolos, we checked if these proteins coimmunoprecipitate also in native conditions, in absence of formaldehyde crosslinking. We thus performed a co-immunoprecipitation (coIP) experiment in p493-6 cells with high (non-treated) or low (8h Tet) Myc levels. By immunoprecipitating either Ikaros or Aiolos, we could see their reciprocal interaction in either high or low Myc conditions, as expected (figure 15A and B); Myc was detected in the same immune-precipitate, but not in the IgG control IP, only when expressed at high levels, indicating that its interaction with both proteins was specific. By immunoprecipitating Myc, instead, the results were not so clear: Aiolos was still visible but with a faint band, while Ikaros could not be distinguished from the background (figure 15C). This could be due to technical issues and/or to the fact that only a small part of the overexpressed Myc is bound by Ikaros and Aiolos, thus making it difficult to detect the interaction in this direction; in fact, although the bands corresponding to the immunoprecipitated Ikaros, Aiolos and Myc appeared to be similar in figure 15A and B, Ikaros and Aiolos levels in the input are much lower than Myc. Most noteworthy here, Ikaros and Aiolos protein levels did not change upon modulation of Myc (at least after 8h), suggesting that Ikaros and Aiolos are not regulated by Myc (figure 15).

Myc and Aiolos coimmunoprecipitation was also visible by adding the Benzonase nuclease to the cell lysate, thus suggesting that the two proteins can interact in a DNA independent way.

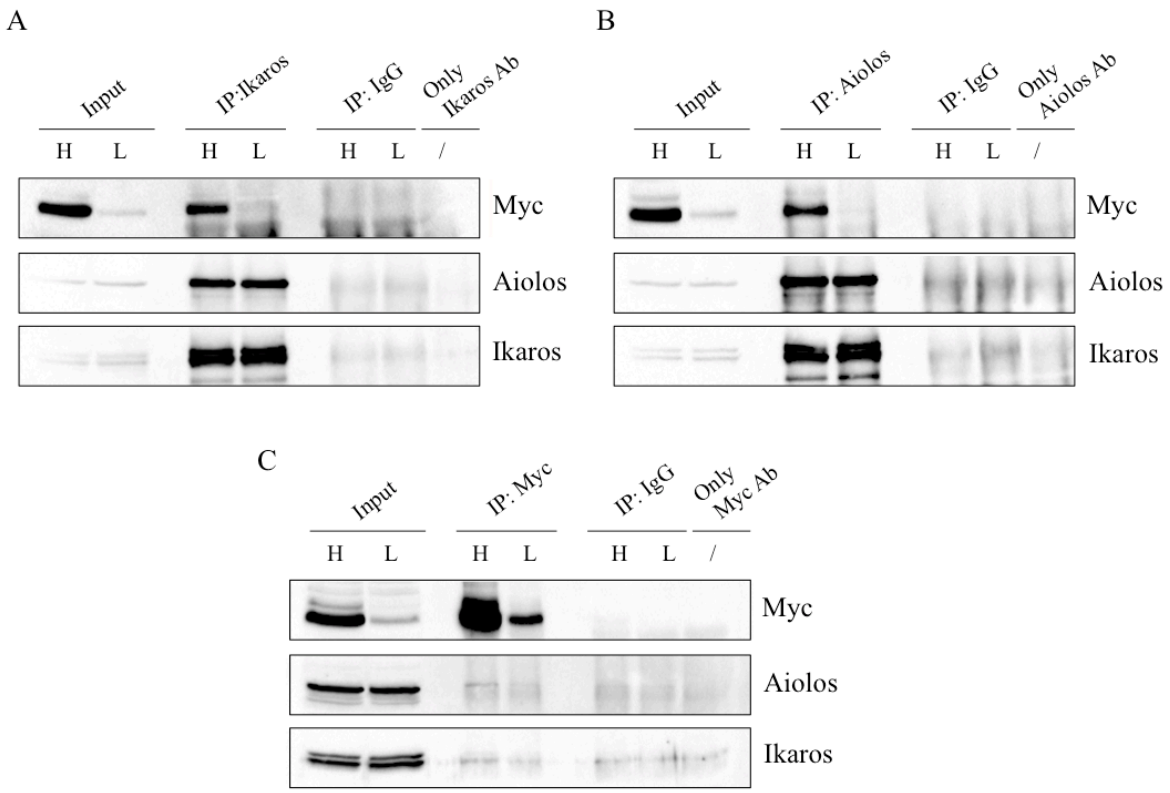

Figure 15. Myc, Ikaros and Aiolos coimmunoprecipitation in p493-6 cells. Immunoprecipitation of the endogenous Ikaros (A) and Aiolos (B) in p493-6 cells with high (H) or low (L) Myc levels. (C) Myc immunoprecipitation in p493-6 cells with high (H) or low (L) Myc levels. The loaded input is 2.5% of the material used for the IP. Low Myc conditions are obtained treating cells for 8h with 200 ng/ml Tet. Here it is shown one experiment representative of several biological replicates.

The interaction of Ikaros/Aiolos with Myc was also visible by coimmunoprecipitation in different lymphocytic cell lines such as Burkitt's lymphoma cells (Daudi, Raji, Namalwa, Ramos) (figure 16A), Multiple Myeloma cells (H929, JJN3, KMS11) (figure 16B) and pre-B ALL cells (697, REH, Sup-b15) (figure 16C).

Altogether, these results confirmed that a protein-protein interaction does occur between Myc, Ikaros and Aiolos.

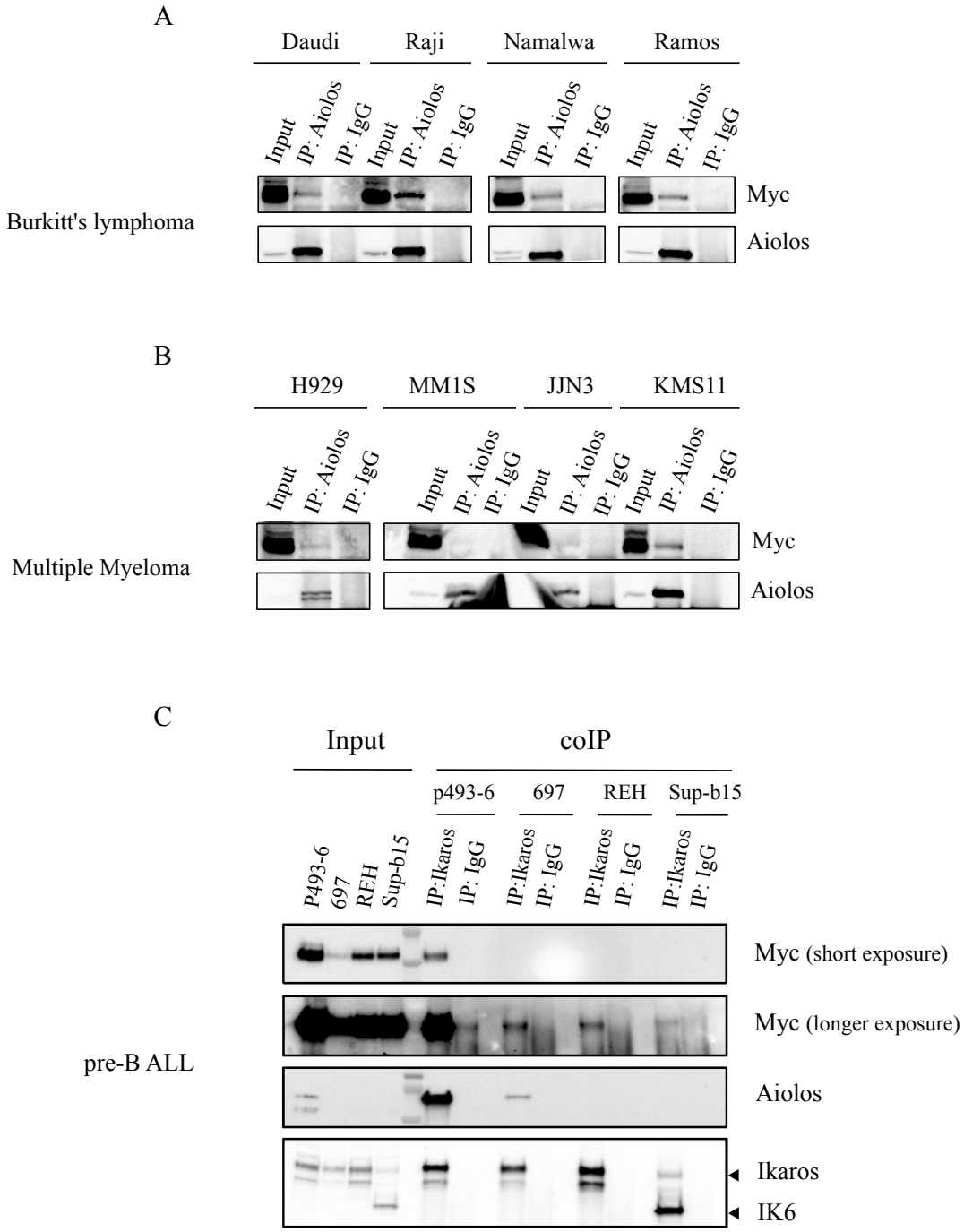

Figure 16. Myc, Ikaros and Aiolos coimmunoprecipitation in different cell lines. (A) Immunoprecipitation of endogenous Aiolos in Burkitt's lymphoma cell lines. (B) Immunoprecipitation of endogenous Aiolos in Multiple Myeloma cell lines; in MM1S we could not detect the co-immunoprecipitated Myc. (C) Immunoprecipitation of endogenous Ikaros in pre-B ALL cell lines. (IK6: Ikaros dominant negative isoform 6). The loaded input corresponds to 2.5% of the material used for the IP. CoIPs shown in panels A and B were done as single experiments, while the coIP in panel C is representative of two replicates.

Subsequently, we asked whether Ikaros and Aiolos were able to bind Myc independently from each other. We already observed that in cell lines in which Aiolos is not present or is

expressed at very low levels, such as REH and Sup-b15 pre-B ALL cell lines, the interaction between Ikaros and Myc was still visible (figure 16C). To answer this question more precisely, we set an *ad hoc* experiment taking advantage of HEK293T cells, which express neither of the two lymphocytic transcription factors. We thus cloned Ikaros and Aiolos cDNAs in the pcDNA3 vector, choosing the *IKZF1.1* and *IKZF3.1* isoforms, which are the most common of either factor. We transfected HEK293T cells with plasmids allowing the overexpression of FLAG-Myc, Ikaros and Aiolos alone or in different combinations and immunoprecipitated either FLAG-Myc, Ikaros or Aiolos in native conditions. When all the constructs were co-transfected, the three factors always co-immunoprecipitated (figure 17). Similarly, Myc and Aiolos reciprocally co-precipitated with anti-Aiolos and anti-Myc antibodies when co-expressed, with or without co-transfection of Ikaros. Most noteworthy, co-immunoprecipitation of Aiolos with FLAG-Myc and, reciprocally, FLAG-Myc with Aiolos consistently decreased upon co-expression of Ikaros. Conversely, co-precipitation of FLAG-Myc and Ikaros was weak on its own, but reinforced by co-expression of Aiolos (figure 17). Altogether, these results suggested that, Aiolos homodimers can interact with Myc, while Ikaros may require dimerization with Aiolos for effective interaction.

It is noteworther here that, in apparent contrast with the above conclusion, Ikaros and Myc interacted also in systems where Aiolos was present at very low levels, like REH and Sup-b15 cells (figure 16C), as mentioned before; moreover no difference in Ikaros-Myc interaction was observed in Ba/f3 cells (where Aiolos was not detectable either at protein or RNA level), infected or not with an Aiolos-expressing vector (figure 18).

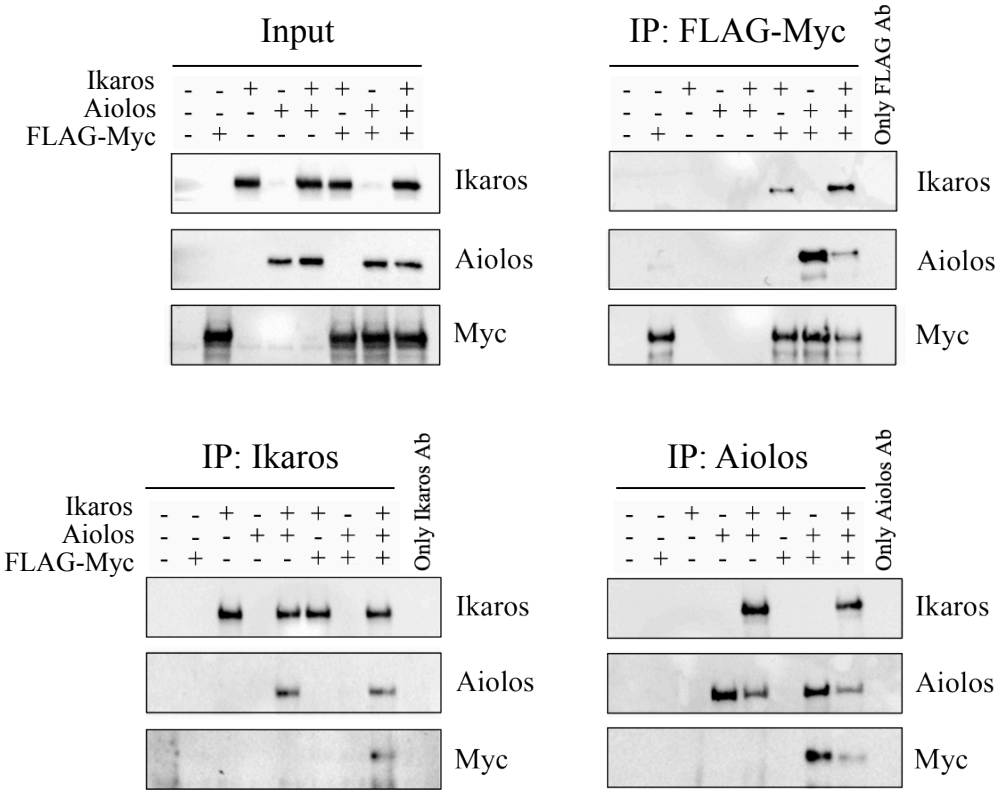

Figure 17. Coimmunoprecipitations in HEK293T cells. HEK293T cells were transfected with the pcDNA3 vector overexpressing FLAG-Myc, Ikaros and Aiolos in different combinations, and the three factors were immunoprecipitated, as indicated, in native conditions. The loaded input corresponds to 2.5% of the material used for the IP. Here it is shown one experiment representative of three biological replicates.

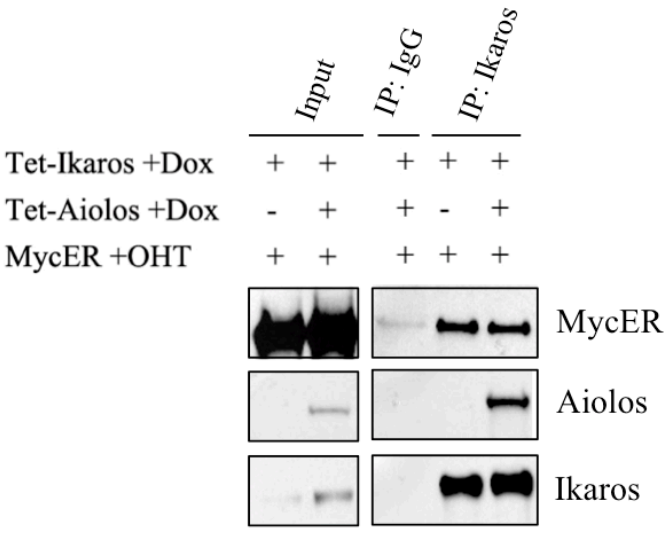

Figure 18. Coimmunoprecipitation in Ba/f3 cells. Ba/f3 were infected with vectors expressing a Tet-inducible Ikaros, an OHT activatable MycER, and with or without a Tet-inducible Aiolos. Anti-Ikaros or anti-IgG antibodies were used for the immunoprecipitation in native conditions. The loaded input corresponds to 2.5% of the material used for the IP. This coIP was done as single experiment.

3.2.2. Genome-wide distribution of Ikaros, Aiolos and Myc

Since Ikaros and Aiolos were identified as Myc interactors on chromatin, we analyzed their genomic distribution in p493-6 cells through ChIP-seq experiments, using the cognate antibodies. We also performed ChIP-seq using an antibody recognizing acetylated lysine 27 in histone 3 (H3K27Ac) to identify active chromatin regions, and in particular active promoters and enhancers (Creyghton et al., 2010). We collected p493-6 cells with high (non-treated) or low (8h Tet) Myc levels and crosslinked them with formaldehyde before proceeding with the ChIP protocol. Prior to sequencing, we verified Myc binding by qPCR at known target promoters (Nucleolin, IFRD2) and the absence of binding in the acetylcholine receptor (AchR) promoter, as we previously did for the ChroP. As expected, the binding was higher in high Myc conditions, reduced in low Myc conditions and close to zero in the negative controls (figure 19).

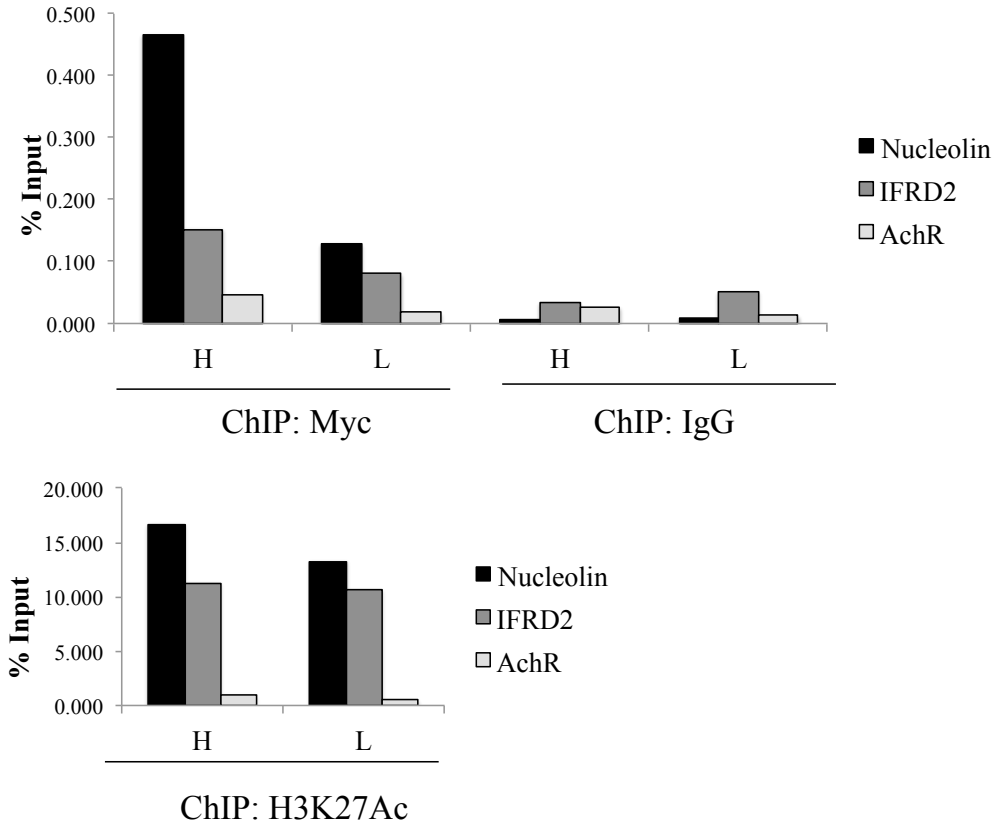

Figure 19. ChIP-qPCR on Myc-ChIP and H3K27Ac-ChIP. ChIP-qPCR on active chromatin regions bound by Myc (Nucleolin, IFRD2) and on an inactive, non-bound region (AchR) as a negative control. H= High Myc; L= low Myc.

After sequencing of the immunoprecipitated DNA and peak calling, we retrieved a total of 22202 and 1555 peaks for Myc in high and low Myc conditions, respectively, and around 20000 peaks for either Ikaros or Aiolos, in either high or low Myc conditions (figure 20). Thus, as expected, the number of Myc peaks strongly decreased at low Myc levels, while peak numbers for Ikaros and Aiolos remained essentially unchanged. As already reported, Myc peaks mostly localized at promoters (Lin et al., 2012; Sabò et al., 2014) even if, when present at high levels, the percentage of peaks at distal sites increased. Conversely, Ikaros and Aiolos peaks seemed to be equally distributed among promoters, gene bodies and intergenic regions (Ferreirós-Vidal et al., 2013; Schjerven et al., 2017; Schwickert et al., 2014), in proportions that did not vary with Myc levels (figure 20).

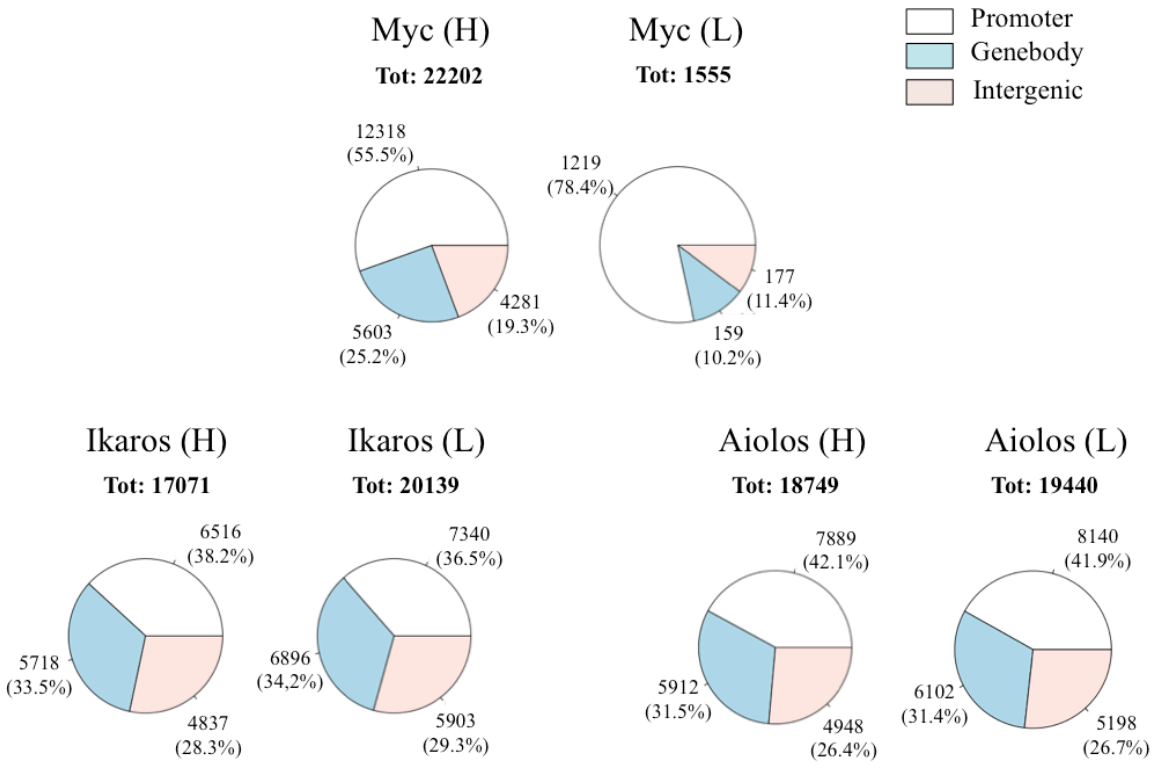

Figure 20. ChIP-seq peak numbers and annotation. Number of peaks retrieved in Myc (pvalue 10^{-5}), Ikaros and Aiolos (pvalue 10^{-10}) ChIP-seq and their localization in promoters, gene bodies or intergenic regions. Promoters: -2kb to +1kb from the TSS; gene body: more than 1kb away from the TSS; intergenic: all the rest; H= high Myc; L= low Myc.

Motif analysis of the sequences underlying the peak summits (200 bp) identified the known consensus for both Ikaros and Aiolos (Molnár & Georgopoulos, 1994) in Ikaros and Aiolos ChIP-seq peaks, and the E-box in Myc peaks, thus confirming the specificity of the identified regions (figure 21).

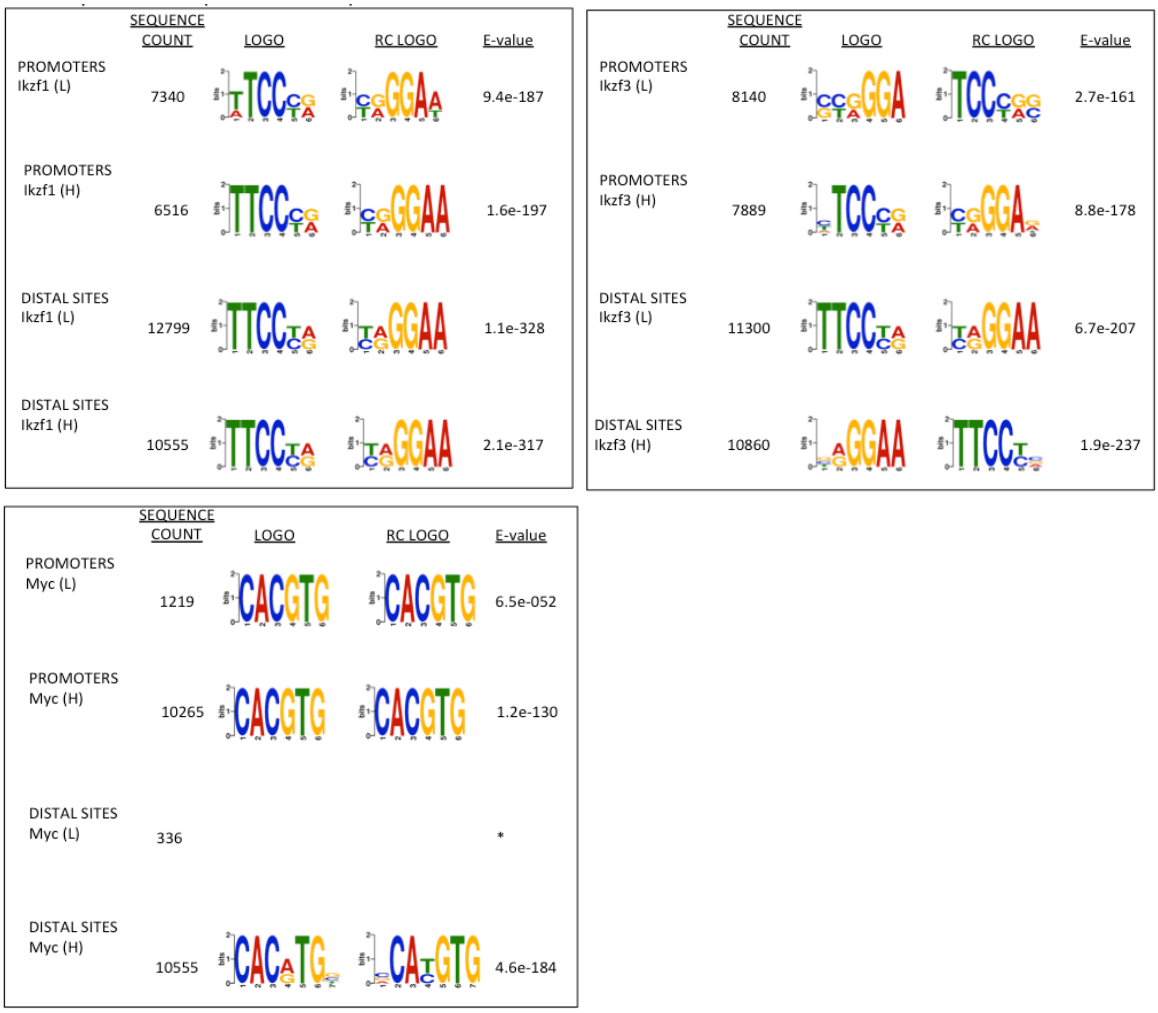

Figure 21. Motif analysis on sequences underlying Ikaros, Aiolos and Myc peaks. 200 bp sequences around the peak summits are considered for each ChIP-seq and analyzed with *de novo* motif discovery programs. Here the enriched motifs identified by DREME are reported for all the sets of regions except for Myc (L) distal sites: in this case DREME did not identify any motif, while the E-box has been retrieved by MEME-ChIP. The e-value and the number of regions used for the analysis are reported. (H)=high Myc; (L)=low Myc.

We then focused our attention on promoters and performed a functional analysis to identify the most enriched classes of genes bound by each transcription factor. Functional analysis

of Ikaros bound genes identified the main biological functions promoted by Ikaros in p493-6. The top ten classes included, in particular, cell cycle regulation, apoptosis and genes related to the immune system (figure 22A and E). All these classes well describe Ikaros specific activity in lymphocytes and its role in the negative regulation of cell cycle, particularly at the G1-S transition. STAT5 signaling pathways (in top 15 results) are also enriched, in accordance with the evidence that Ikaros compete with this transcription factor to regulate common target genes (Katerndahl et al., 2017). Functional analysis of Aiolos bound genes identified mostly the same classes enriched for Ikaros targets, according to the fact that most of target genes are in common (figure 22B and F). Functional analysis on genes bound by Myc (when present at high level) identified classes of genes related to protein and RNA metabolism and ribosomal biogenesis, that were also identified in other cell lines (Sabò et al., 2014; Walz et al., 2014) (figure 22C and G).

Since genes bound by all the three transcription factors are mostly a subset of Myc-bound genes (figure 22D), functional analysis of these common genes did not add relevant information.

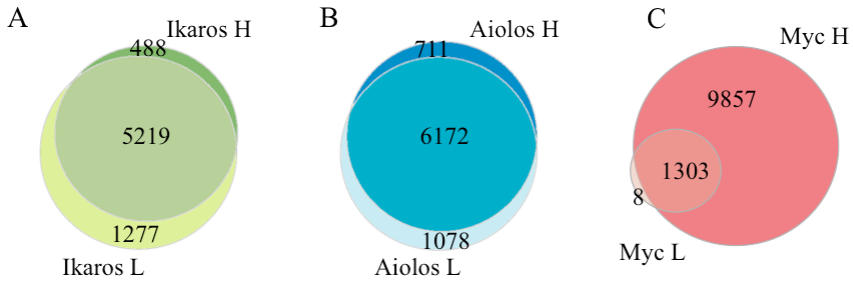

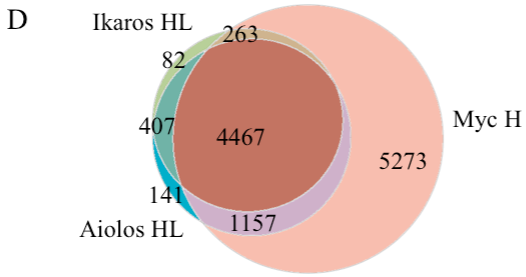

E

Ikaros	
Gene Name	qvalue
IMMUNE SYSTEM	1.83E-36
E2F TARGETS	8.15E-26
CELL CYCLE	6.22E-24
ADAPTIVE IMMUNE SYSTEM	3.39E-21
CELL CYCLE MITOTIC	2.36E-18
CYTOKINE SIGNALING IN IMMUNE SYSTEM	7.38E-18
G2M CHECKPOINT	1.00E-15
TNFA SIGNALING VIA NFKB	2.39E-14
SIGNALLING BY NGF	3.00E-14
DNA REPLICATION	6.66E-14

F

Aiolos	
Gene Name	qvalue
IMMUNE SYSTEM	1.39E-53
ADAPTIVE IMMUNE SYSTEM	8.95E-35
CELL CYCLE	3.60E-27
E2F TARGETS	9.80E-27
SIGNALLING BY NGF	1.44E-24
CELL CYCLE MITOTIC	5.34E-24
HALLMARK MITOTIC SPINDLE	5.48E-22
MAPK SIGNALING PATHWAY	3.59E-20
METABOLISM OF LIPIDS AND LIPOPROTEINS	3.59E-20
TNFA SIGNALING VIA NFKB	8.77E-20

G

Myc	
Gene Name	qvalue
MYC TARGETS V1	6.05E-83
METABOLISM OF PROTEINS	8.47E-49
MTORC1 SIGNALING	1.25E-46
METABOLISM OF RNA	2.53E-35
MYC TARGETS V2	3.96E-35
REACTOME TRANSLATION	1.83E-34
KEGG RIBOSOME	1.31E-33
3' UTR MEDIATED TRANSLATIONAL REGULATION	3.91E-31
HALLMARK E2F TARGETS	1.87E-30
REACTOME INFLUENZA LIFE CYCLE	7.48E-29

Figure 22. Bound genes overlap and functional annotation. A) Venn diagram showing the overlap of the genes whose promoters is bound by Ikaros either in high (H) or low (L) Myc conditions. B) Intersection of genes, the promoter of which is bound by Aiolos in H and L Myc conditions. C) Intersection of the genes, the promoter of which is bound by Myc in H and L Myc conditions. (D) Intersection of genes whose promoter is bound by Ikaros HL, Aiolos HL and Myc H. Functional annotations of genes bound by Ikaros HL (E), by Aiolos HL (F) or by Myc H (G); genes are ranked for their enrichment level and the top 2500 genes are used for the functional analysis.

To further control the quality of the peaks identified for Ikaros and Aiolos, we selected some of the most enriched promoters in the ChIP-seq data (*AMICA1, SYK, QPCTL*) (figure 23) and tested them by ChIP-qPCR. The enrichment was visible only in Ikaros- and Aiolos-ChIP and not in the negative control (IgG), thus providing a first validation of the ChIP-seq results (figure 24). Although the qPCR results suggested a higher Ikaros and Aiolos enrichment on their target genes when Myc was present at low levels, this effect was not significant at a genome-wide level (figure 25).

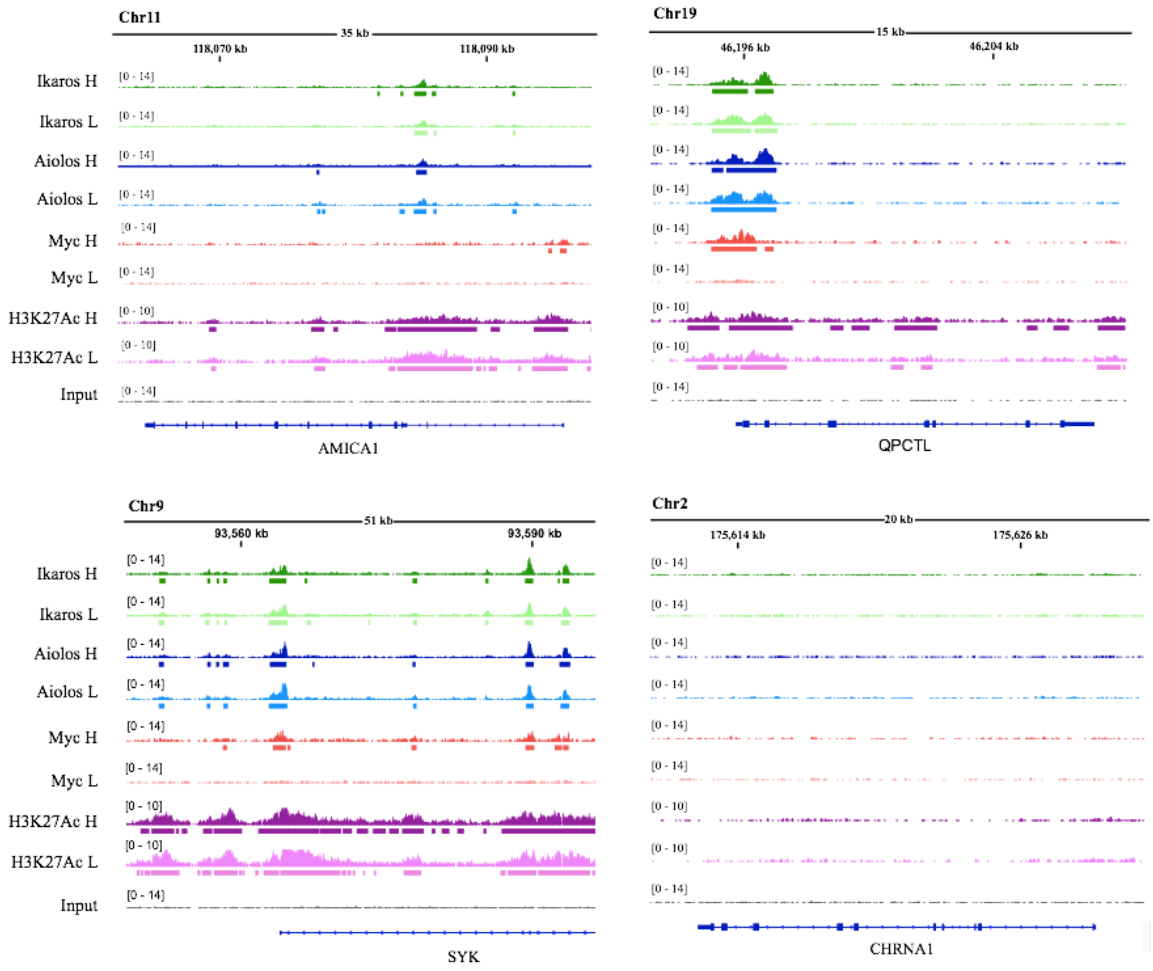

Figure 23. Target gene tracks. ChIP-seq tracks visualized with the genome browser, showing the enrichment of Ikaros, Aiolos, Myc and H3K27Ac on Ikaros/Aiolos target genes (*AMICA1, QPCTL, SYK*) and on one negative control region (AchR-*CHRNA1*)

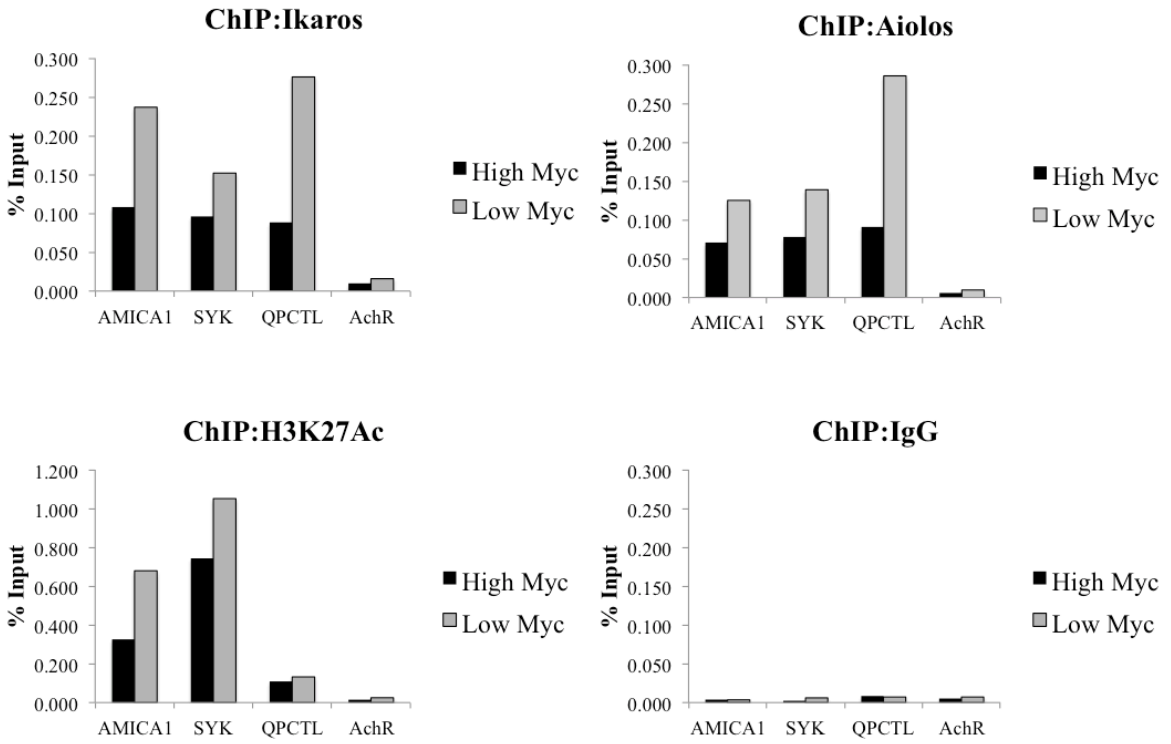

Figure 24. Validation of Ikaros and Aiolos bound regions by ChIP-qPCR. ChIP-qPCR on promoters bound by Ikaros and Aiolos (*AMICA1, SYK, QPCTL*) and on the non-bound region AchR. The oligos used for the qPCR are designed according to ChIP-seq results. Here it is shown one experiment representative of two replicates.

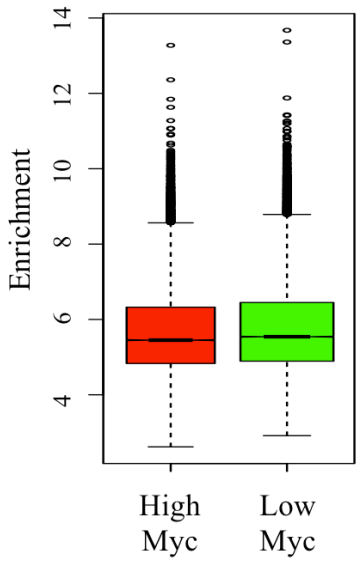

Figure 25. Ikaros binding intensity in high and low Myc conditions. Box-plot representing the enrichment of Ikaros on its own peaks in high and low Myc conditions.

Peak distributions in our ChIP-seq datasets were consistent with their numbers: in particular, Myc peaks identified in the low Myc condition were a subset of those identified at high Myc levels; Ikaros and Aiolos, instead, shared most of the bound regions in both conditions. Moreover, around 70% of Ikaros and Aiolos peaks on promoters were shared with Myc, while around 40% of the promoters bound by Myc in high Myc condition were also bound by Ikaros and Aiolos. These overlaps decreased when considering distal sites, with 20-30% of peaks in common between Ikaros/Aiolos and Myc (figure 26).

The levels of overlap between the transcription factors and H3K27Ac is also visualized in figure 27. In all cases, the great majority of the peaks were found in active chromatin regions, as identified by H3K27Ac. If it is well established that Myc can only bind to already opened chromatin (Guccione et al., 2006), for Ikaros and Aiolos this is less clear: in fact, as we mentioned in the introduction, Ikaros was mainly known as transcriptional repressor and it was identified as bound to close chromatin regions, in particular at centromeric repeated sequences (Brown et al., 1997). In our cells, Ikaros and Aiolos appeared to be mostly bound to active promoters and enhancers, as reported also in other published datasets (Schwickert et al., 2014), nevertheless, they can bind regions in which H3K27Ac is absent too, particularly at distal sites (figure 27). In summary, ChIP-seq results showed that Ikaros, Aiolos and Myc share most of bound regions, particularly at promoters, but also at distal sites.

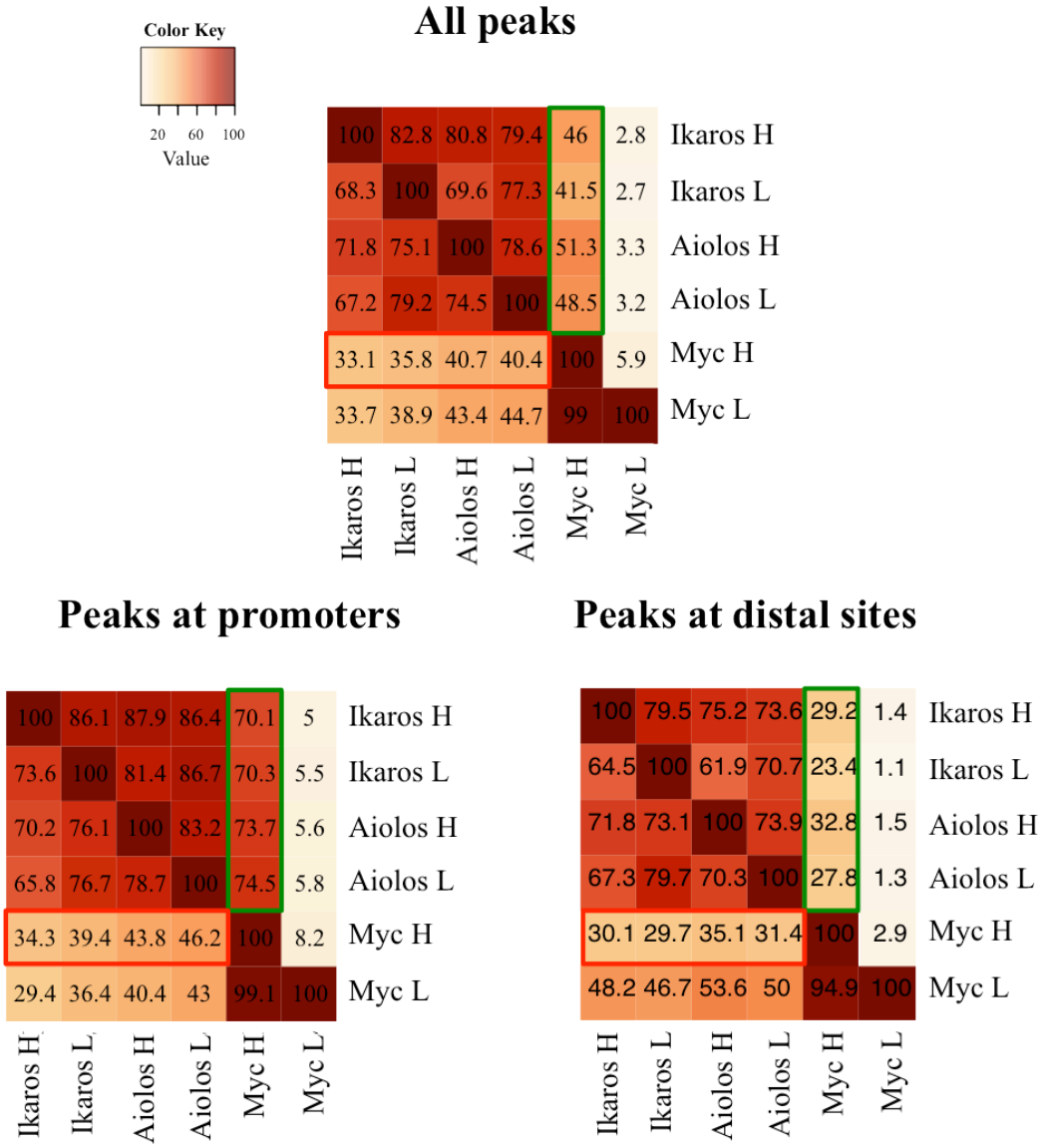

Figure 26. Overlap of Ikaros, Aiolos and Myc peaks in p493-6 cells. Percentages of peaks overlapping among the different samples, considering all the peaks, only peaks on promoters or only peaks on distal sites. For each column, the percentage of peaks overlapping (at least 1 bp) with the reference sample is reported. In green rectangles, the percentage of Ikaros and Aiolos peaks also bound by Myc H are highlighted, while in red rectangles are Myc H peaks also bound by Ikaros and Aiolos. H=High Myc; L=low Myc.

Figure 27. Intensity and distribution of ChIP-seq peaks. Each row of the heatmaps represents a genomic interval (3 kb width centered on the peak). Every annotated promoter (-2000/+1000 bp from TSS) or every distal site (non-promoter region) in chromosome 1, identified as Ikaros-, Aiolos- or Myc-associated by ChIP-seq in at least one of the experimental samples is reported. For the same interval, distribution of Ikaros, Aiolos, Myc and H3K27Ac is indicated. The white-red color code of the read count part is referred to the coverage on each region (white: not enriched; pink: poorly enriched; red: enriched). In the peak calling part, red means that a peak is called by the MACS software, white means that no peaks are called. In the last two columns, annotated genes (exons in red, introns in pink; + sense, - antisense strand) are also reported. All the lanes are ranked on the basis of Myc H enrichment. H=high Myc; L= low Myc.

3.2.3. Identification of direct Myc-regulated genes.

To identify direct Myc target genes we decided to couple DNA binding and transcriptional regulation and we performed RNA-seq in p493-6 cells with high and low Myc levels, preparing four biological replicates for each condition. We identified a total of 4447 differentially expressed genes (DEGs), of which 2429 were downregulated genes (log2Foldchange lower than -0.5) and 2018 were upregulated genes (log2Foldchange higher than 0.5) (figure 28).

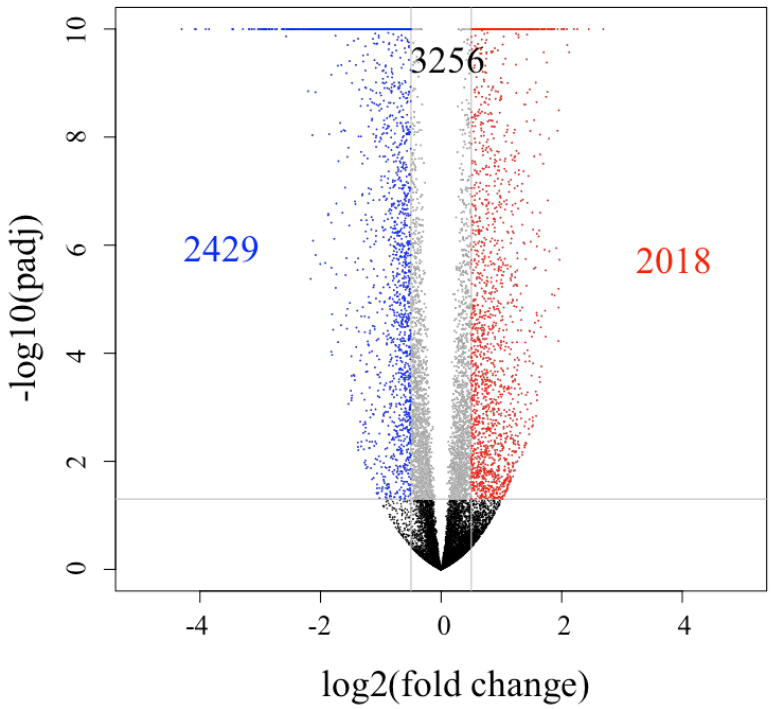

Figure 28. Myc deregulated genes in p493-6 cells. Volcano plot representing deregulated genes upon Myc downregulation (8h Tet). Genes are considered deregulated if they have an adjusted pvalue (padj)<0.05 and a log2(fold change) expression >0.5 (in red) or <-0.5 (in blue). –log 10 (Padj) values are saturated to a maximum value of 10.

In this system, DEGs are defined as genes the expression of which changes upon Myc inhibition, thus the upregulated genes are Myc target genes that are repressed by Myc, and vice-versa. Functional analysis confirmed that the DEGs identified belong to classes of genes that are usually regulated by Myc (figure 29).

DEG DOWN	
Gene Set Name	FDR q-value
MYC_TARGETS_V2	6.69E-26
MYC_TARGETS_V1	1.15E-10
MTORC1_SIGNALING	3.83E-10
TRNA_AMINOACYLATION	1.24E-08
TRANSMEMBRANE TRANSPORT OF SMALL MOLECULES	1.24E-08
TRANSCRIPTION	3.64E-08
RNA POL I RNA POL III AND MITOCHONDRIAL TRANSCRIPTION	5.23E-08
METABOLISM OF VITAMINS AND COFACTORS	9.01E-08
RNA POL I TRANSCRIPTION INITIATION	1.20E-07
SLC MEDIATED TRANSMEMBRANE TRANSPORT	1.24E-07

DEG UP	
Gene Set Name	FDR q-value
INTERFERON GAMMA RESPONSE	2.64E-40
IMMUNE SYSTEM	4.03E-33
INTERFERON ALPHA RESPONSE	1.81E-22
ALLOGRAFT REJECTION	1.71E-17
CYTOKINE SIGNALING IN IMMUNE SYSTEM	2.20E-15
IL2 STAT5 SIGNALING	2.70E-15
TNFA SIGNALING VIA NFKB	2.70E-15
HALLMARK APOPTOSIS	2.00E-14
DEVELOPMENTAL BIOLOGY	7.46E-14
CXCR4 PATHWAY	2.91E-12

Figure 29. Functional analysis of Myc DEGs in p493-6 cells. Upregulated and downregulated genes identified by RNA-seq in p493-6 cells, with high or low Myc levels, belong to classes that are usually related to Myc functions.

Subsequently, we combined ChIP-seq and RNA-seq data to determine the correlation between DNA binding and gene regulation. In figure 30, the percentages of DEGs and no DEGs that are bound by Myc, Ikaros or Aiolos in each experimental condition are represented. We can see that Myc preferentially binds genes that are downregulated upon its inactivation. This is in accordance with previous results reporting that an increase in Myc occupancy at promoters correlates with Myc target gene activation (de Pretis et al., 2017; Walz et al., 2014). Conversely, the same does not seem to be true true for Ikaros and Aiolos.

We are currently performing knock down experiments for Ikaros and Aiolos to obtain the list of genes that transcriptionally respond to their modulation. By intersecting the ChIP-seq data and the complete transcriptional data, we hope to identify genes directly regulated by Myc and Ikaros/Aiolos, in order to study possible regulatory interactions.

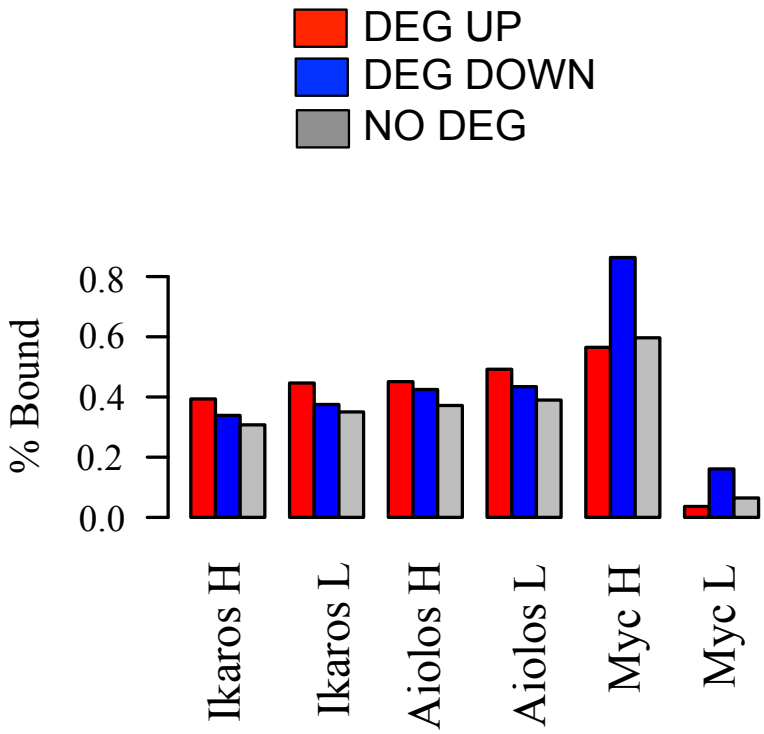

Figure 30. Percentages of DEGs and NO DEGs bound by Ikaros, Aiolos and Myc in p493-6 cells. The percentages of DEGs and NO DEGs identified by RNA-seq in p493-6 cells with high or low Myc, the promoter of which is bound by Ikaros, Aiolos or Myc are represented. H=high Myc level; L=low Myc level.

3.3. Combined activation of Ikaros and Myc in BH1 cells

3.3.1. IkarosER and Tet-Myc inducible system

p493-6 cells constituted a valid system at the beginning of this project; nevertheless, they showed some limitations during the validation of candidate Myc interactors. For example, their growth is strictly dependent upon expression of the exogenous tet-Myc protein,

downregulation of which causes cell cycle arrest. Moreover, they also express high levels of Ikaros and Aiolos that are not easily modulated.

For these reasons, we decided to take advantage of BH1 cells, a murine pre-B cell line expressing a conditional IkarosER chimera, in which Ikaros is fused to the ligand-binding domain of the extrogen receptor (IkarosER) (Heizmann et al., 2013). BH1 cells were originally derived from transgenic mice in which the last exon of the Ikaros allele was flanked by loxP sites, allowing a Cre-dependent deletion that creates an Ikaros null allele: inactivation of Ikaros allowed immortalization and expansion of pre-B cells *in vitro* in presence of interleukin 7 (IL-7), followed by transduction with a retroviral vector expressing the GFP marker and IkarosER. Since these cells appeared very sensible to Ikaros induction and died in few hours after OHT treatment, a second plasmid constitutively expressing Bcl2-dsRed was also introduced (figure 31) (Heizmann et al., 2013).

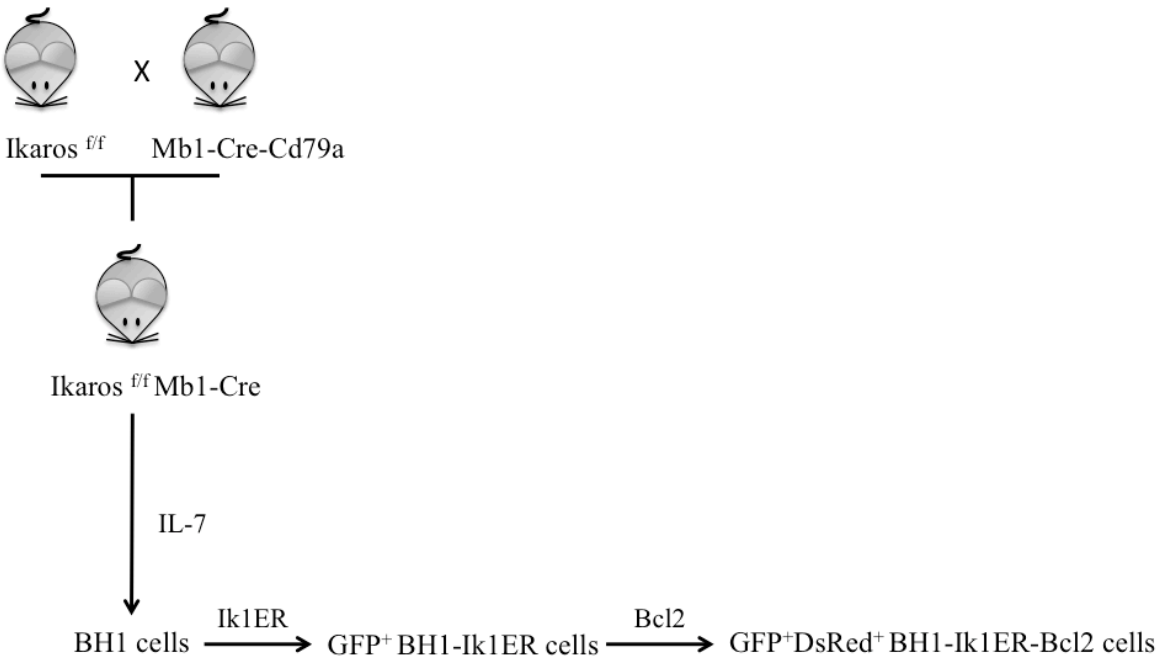

Figure 31. Generation of the BH1 cell line. BH1 cells derived from mice in which the endogenous Ikaros has been floxed out through Mb1 Cre recombinase. Ikaros$^{f/f}$ cells obtained from the bone marrow of these mice were subsequently infected with vectors expressing IkarosER and Bcl2 **(**Heizmann et al., 2013**).**

We first verified that, in our hands, BH1 cells behaved as expected (Heizmann et al., 2013) and checked GFP expression, using parental cells without the IkarosER-GFP vector as negative control. All the cells were GFP positive, although two distinct populations with high and low levels of GFP were visible, corresponding presumably to high and low levels of IkarosER expression, respectively (figure 32). This could be due to a partial leakiness of the IkarosER protein: since it is reported that Ikaros induction blocks the cell cycle thus giving a disadvantage to the cells, it is possible that cells tend to lose the vector when kept in culture. In order to check this assumption, we sorted the different populations and tested them separately.

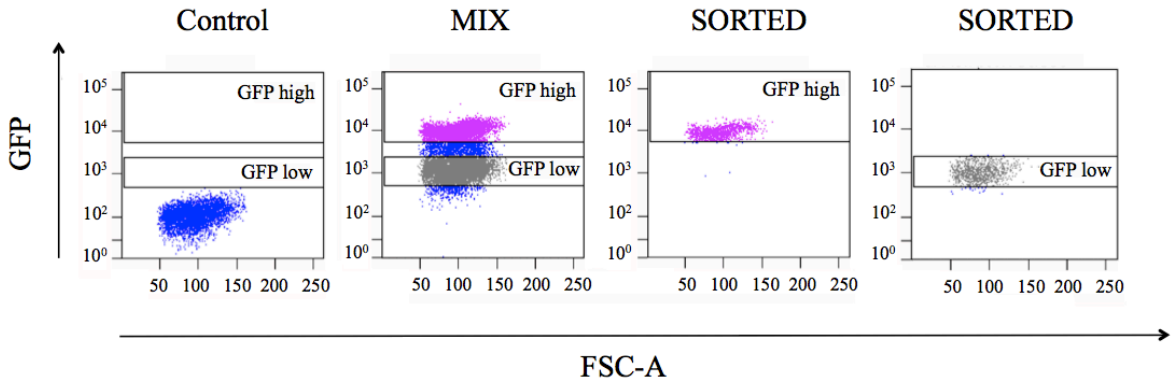

Figure 32. GFP level in BH1 cells. All the BH1 cells were GFP positive compared to the negative control lacking the IkarosER-GFP vector. Nevertheless, two different populations with high or low GFP levels were identified and sorted.

We added ethanol or OHT to the medium of each population (high GFP, low GFP and the initial mixture) and followed cell counts over time: only cells with high GFP stopped proliferating upon IkarosER activation (figure 33), consistent with our hypothesis that low-GFP cells had lost activity. In all subsequent experiments, we used only the bright GFP population.

We also checked the effects of Ikaros activation in presence or absence of interleukin 7 (IL7). As expected, while Ikaros activation per se blocked cell growth, in absence of IL7, the effect was even more dramatic whether or not Ikaros was activated (figure 34) (Heizmann et al., 2013).

We then checked the expression of some Ikaros target genes after 24h of OHT treatment (Ferreirós-Vidal et al., 2013; Heizmann et al., 2013): as expected *Lig4*, *Syk* and *Blnk* were upregulated upon IkarosER activation, while *Igll1*, *Vpreb*, *Ccnd2* and endogenous *Myc* were downregulated. Moreover, we also observed that the transcriptional effects of Ikaros activation were increased in case of IL7 withdrawal (figure 35), as previously reported (Heizmann et al., 2013).

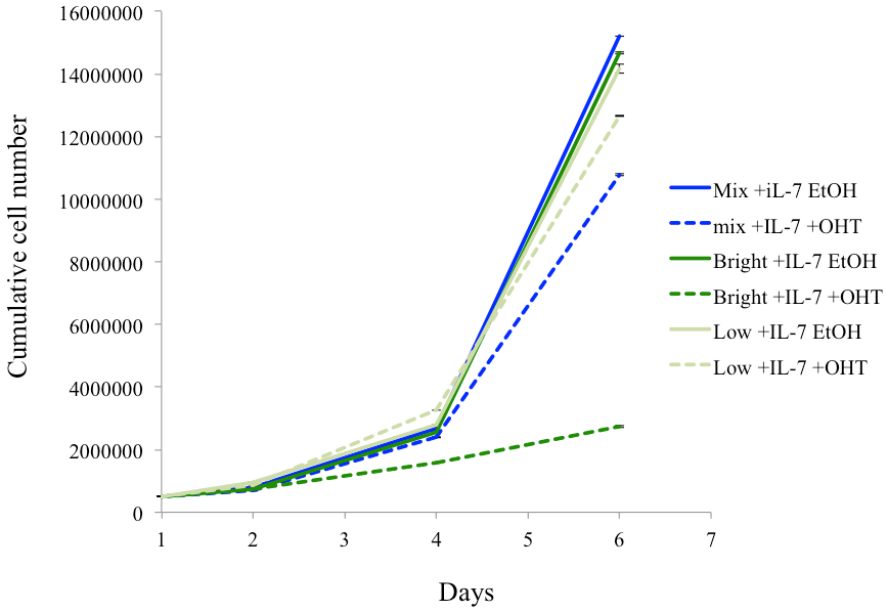

Figure 33. Effects of Ikaros levels on BH1 cell growth. Cells sorted for high or low GFP and the initial mix were treated with 400 nM OHT or ethanol and counted to perform a growth curve. Average and standard deviation of technical replicates are shown. This growth curve was done as a single experiment.

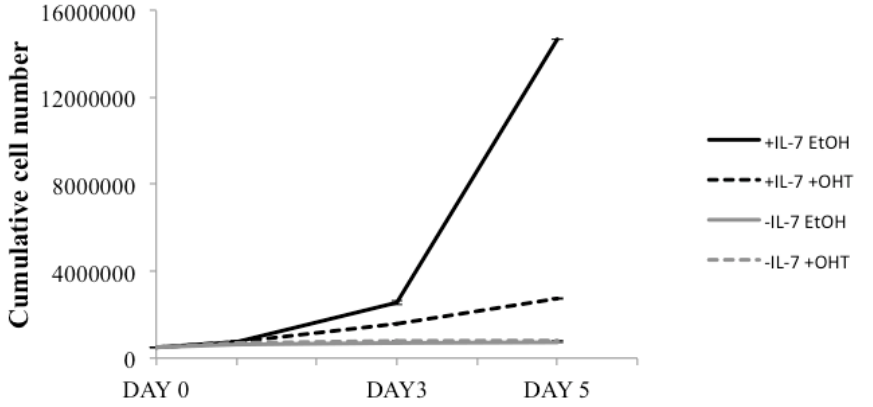

Figure 34. Effect of IL7 on BH1 cell growth. BH1 cells were grown in presence or absence of IL7 and activated or not with OHT to perform a growth curve. Average and standard deviation of technical replicates are shown. This growth curve was done as a single experiment.

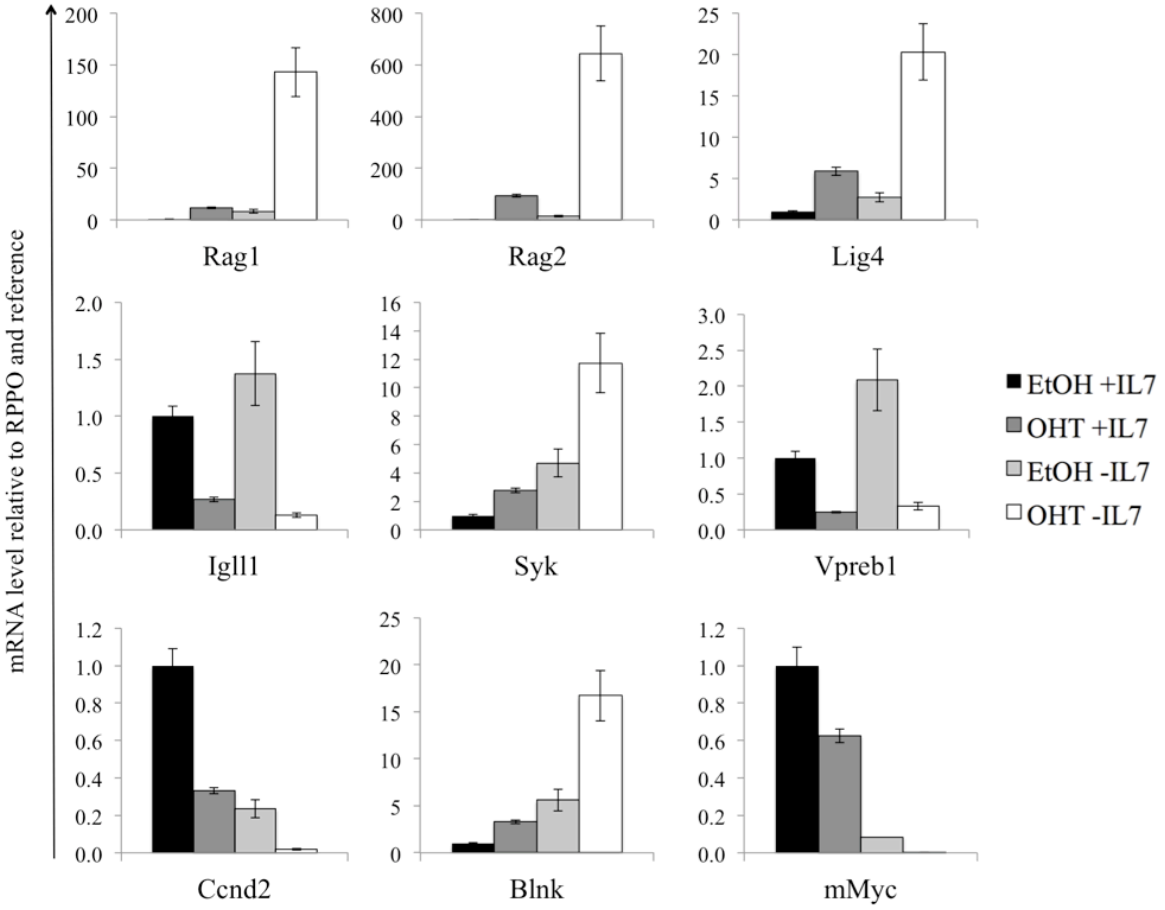

Figure 35. Regulation of Ikaros target genes in BH1 cells. BH1 cells were cultured in presence or absence of IL7 in the medium and treated with 400 nM OHT or ethanol; 24h later, cells were collected for RNA extraction and the expression of known Ikaros target genes was checked by RT-qPCR. Average and standard deviation of technical triplicates are shown. This was done as a single experiment.

In order to be able to modulate also Myc expression in this system, we transduced BH1 cells with a pSLIK vector expressing a human Tet-inducible *c-Myc* cDNA. To test the efficiency of Tet-Myc induction, we treated cells with 400 ng/ml Dox for 24h, checking the level of the exogenous human Myc expression and the regulation of known Myc target genes (Nucleolin, St6galnac4 and Rrp9) by qPCR. The results showed that Myc was well induced upon Dox treatment and that its target genes were upregulated, as expected, compared to non-treated cells (figure 36).

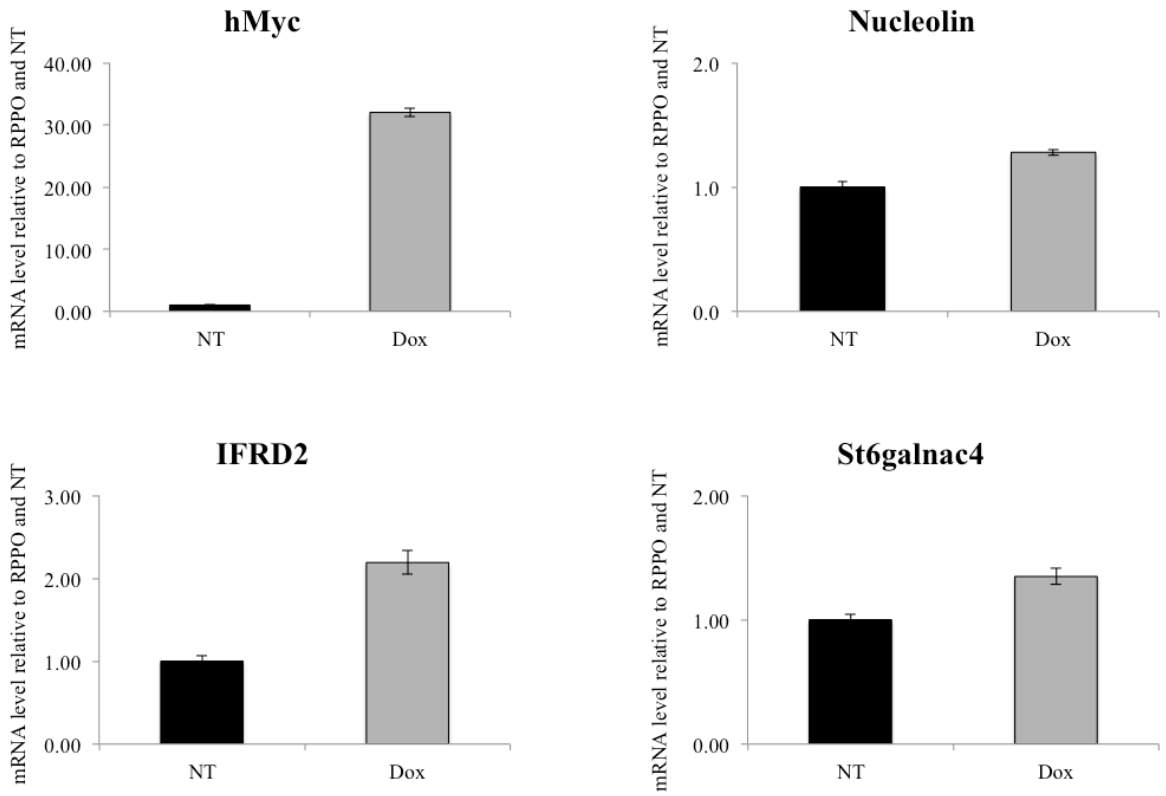

Figure 36. Inducible expression of Tet-Myc in BH1 cells. BH1 cells transduced with Tet-Myc psLIK vector were treated with 400 ng/ml Dox for 24h. Cells were collected for RNA extraction and the expression of the exogenous human Myc and of known Myc target genes (Nucleolin, IFRD2, St6galnac4) was checked by qPCR. NT=non-treated cells; Dox=cells treated with Dox. Average and standard deviation of technical triplicates are shown.

Once we established the system, we performed a coIP experiment to check if the Ikaros/Myc interaction was maintained in these cells and with the Ikaros protein fused to the ER domain. We thus treated cells with OHT to induce IkarosER activation and with Doxycycline (Dox) to induce Myc expression and we immunoprecipitated Ikaros. The result showed that Myc coimmunoprecipitated with IkarosER, thus confirming the possibility to use this system (figure 37).

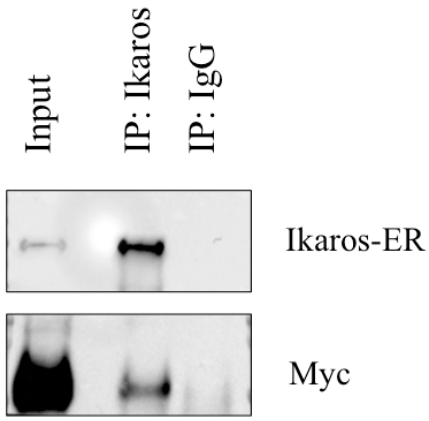

Figure 37. IkarosER and Myc coimmunoprecipitation in BH1 cells. Cells were treated with 400nM OHT and 400 ng/ml Dox for 24h to activate IkarosER and induce Myc expression, respectively, and were collected to perform the coIP in native conditions. The loaded input is 2.5% of the material used for the IP. This coIP was done as a single experiment.

Subsequently, we treated cells with OHT, with Dox or both to check the effects of the single and double activations at protein and mRNA level. By western blot analysis, we observed that IkarosER seemed to be stabilized by OHT addition; the level of overexpressed Myc was not much higher than the endogenous one and, finally, the endogenous Myc was clearly downregulated by IkarosER activation, in particular at 24h (figure 38A). By qPCR, we checked the expression levels of the exogenous Myc (hMyc), of the endogenous Myc (mMyc) and of some target genes specific for Myc (*St6galnac4, Rrp9*) and for Ikaros (*Igll1, Lig4*). The exogenous human Myc was specifically induced in presence of Dox at all the time points, with a decrease of the induction after 24h; the endogenous murine Myc was downregulated in presence of Tet-induced Myc and even more when IkarosER was active, particularly after 24h. qPCR results were in accordance with the western blot in terms of endogenous and exogenous Myc expression levels and all the tested target genes were regulated as expected (figure 38B) (Ferreirós-Vidal et al., 2013; Heizmann et al., 2013).

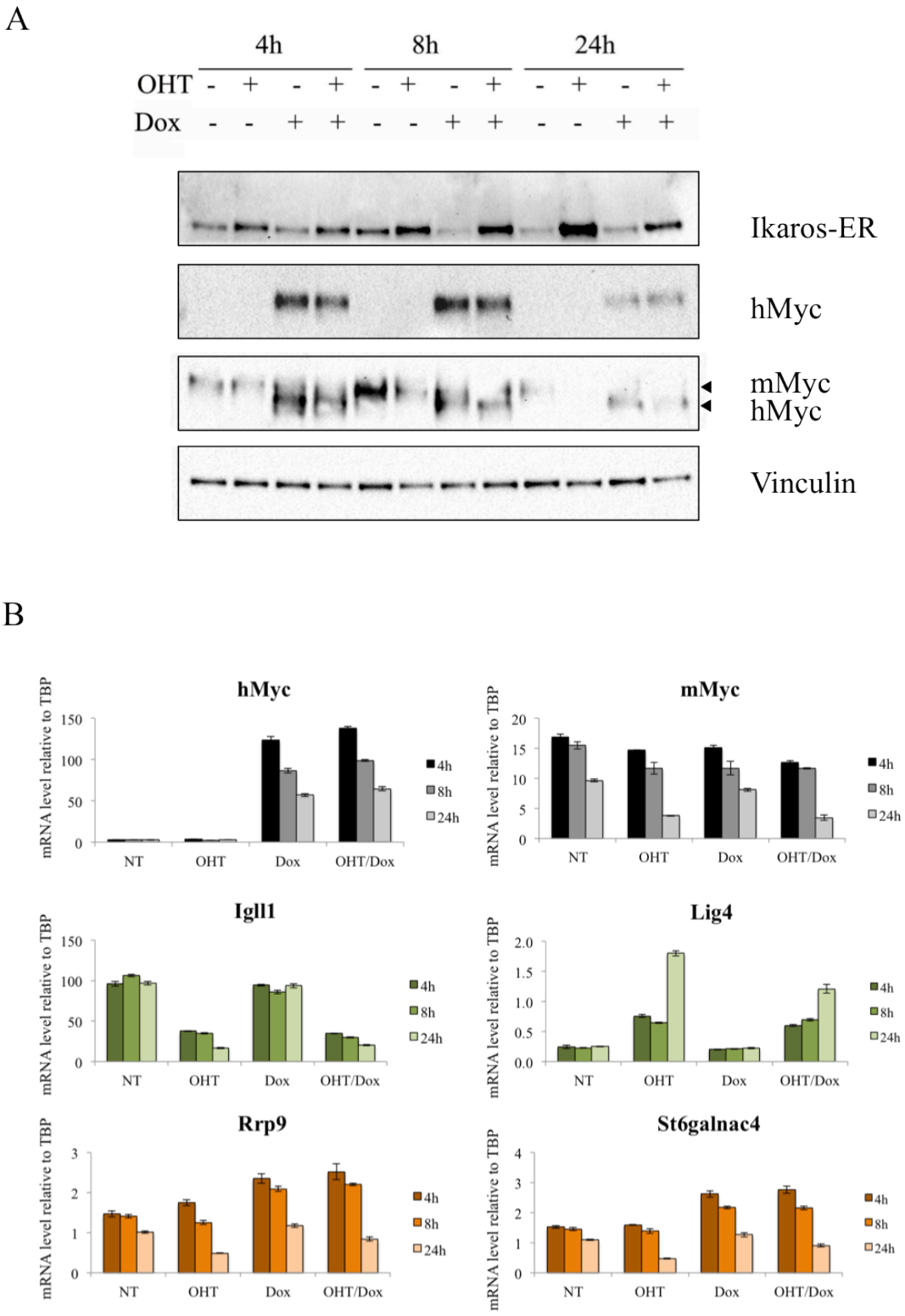

Figure 38. BH1 treatment controls. BH1 cells were left non-treated (NT) or treated with OHT, Dox or both. Cells were collected after 4h, 8h and 24h for RNA and protein extraction. (A) Western blot showing the levels of IkarosER, exogenous Myc (hMyc) and endogenous Myc (mMyc) in all the conditions. (B) RT-qPCR to check the expression of the exogenous Myc (hMyc), endogenous Myc (mMyc), Ikaros target genes (*Igll1, Lig4*) and Myc target genes (*Rrp9, St6galnac4*). Average and standard deviation of technical replicates are shown. This experiment is representative of two biological replicates.

3.3.2. Ikaros and Myc have an opposite effect on cell proliferation

In order to characterize the phenotypic effect of single versus combined activation of Ikaros and Myc in BH1 cells, we treated them with OHT, Dox or both, in presence or absence of IL7, and followed cell growth for ten days. In presence of IL7, as expected, IkarosER activation arrested cell proliferation, while Myc induction increased it. Interestingly, the activation of both Ikaros and Myc together resulted in an intermediate effect (figure 39A). Since it is known that Ikaros activation causes Myc downregulation (Ma et al., 2010) that can contribute to cell cycle arrest, it is reasonable that Myc overexpression is able to partially rescue the phenotype. Without IL7, we observed an initial decrease in cell number, possibly due cell death, even if more detailed analysis are needed to define it precisely; subsequently, non-treated cells or cells with activated IkarosER stopped growing, while Myc overexpression kept the cells proliferating, even if less than in presence of IL7, thus suggesting that Myc expression partially overcome the absence of survival and proliferative stimuli due to IL7 withdrawal (figure 39B).

BH1 cells constitutively express Bcl2, thus the decrease in proliferation observed with the growth curves should be mainly due to a cytostatic effect rather than to apoptosis. To verify this, we also measured BrdU incorporation in the same conditions after 24h of treatments. As expected, when IkarosER was active, the entry into the S phase was reduced and cells accumulated in G1; Myc induction increased the percentage of cells in S phase, while the double activation resulted in an intermediate effect (figure 40A). Again, without IL7 in the medium, cells are completely blocked in G1, unless Myc is overexpressed (figure 40B). Apoptotic events are not present at a significant level and does not seem to change after 24h of treatments, with or without IL7, at least measuring the subG1 population based on propidium iodide (PI) incorporation (figure 41); nevertheless, more specific assays are needed to study cell death in detail.

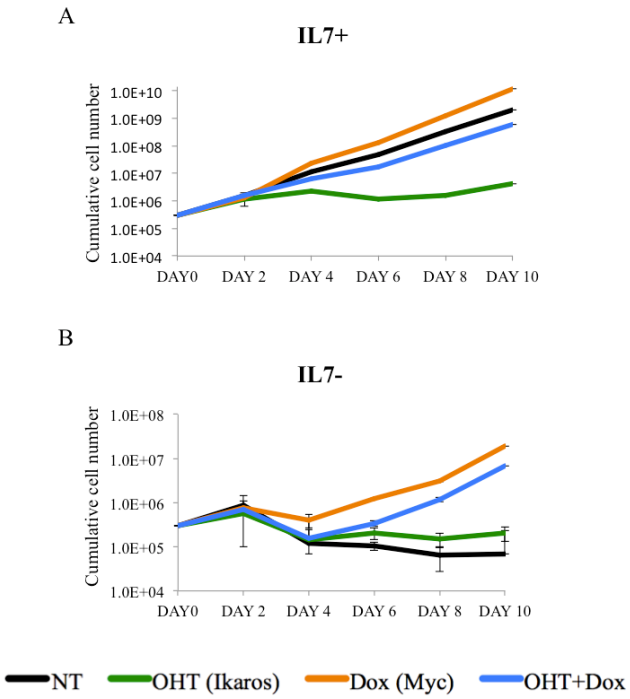

Figure 39. Growth curves upon IkarosER and/or Myc activation in BH1 cells. Cells are treated with OHT, Dox or both to perform the growth curves with (A) or without IL7 (B) in the medium. Average and standard deviation of three technical replicates are shown. This experiment is representative of three biological experiments.

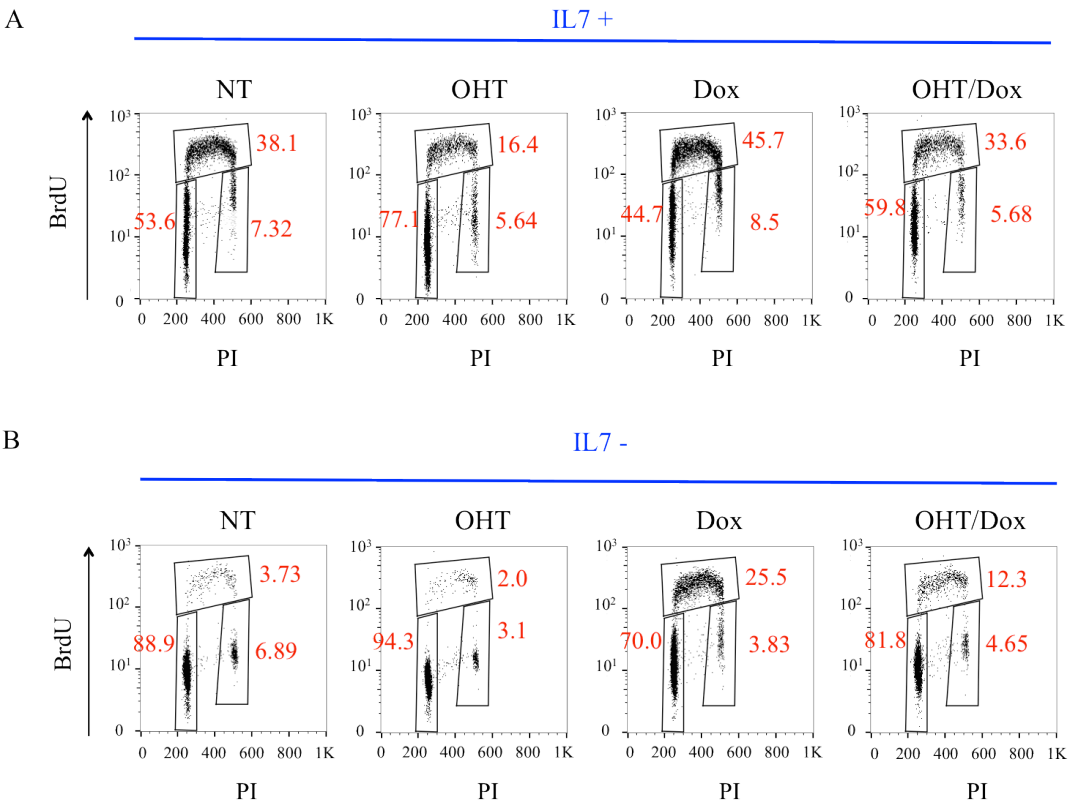

Figure 40. BrdU incorporation. Cells were treated with OHT, Dox or both, with (A) or without (B) IL7 in the medium and BrdU incorporation after 24h of treatment was measured. The percentage of BrdU-positive cells in S phase, as well as in G1 and G2 phases is reported. Cells were previously gated to exclude debris and aggregates. This experiment is representative of three biological replicates.

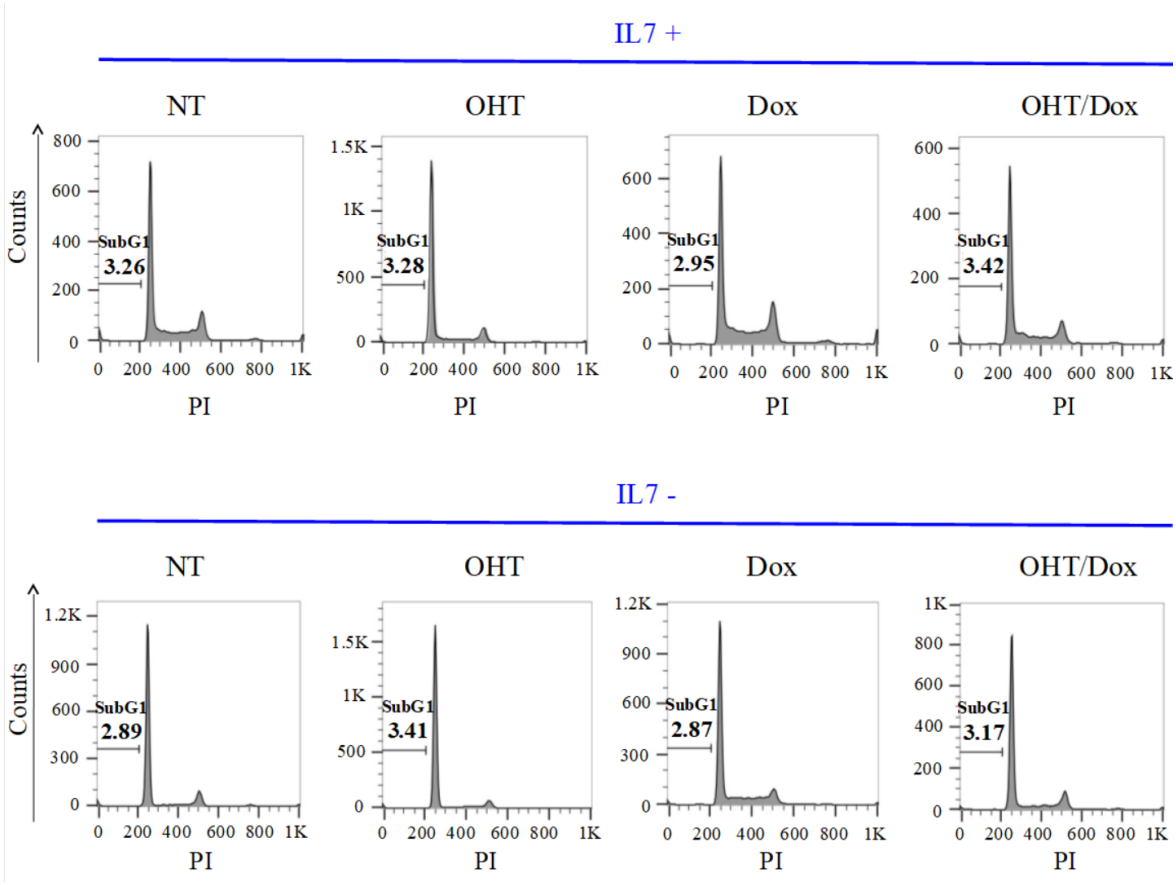

Figure 41. Evaluation of cell death. Cells were treated with OHT, Dox or both, with (A) or without (B) IL7 in the medium; 24h later, cells were subjected to a BrdU pulse and collected. While stained to measure BrdU incorporation, cells were incubated overnight with propidium iodide (PI) to determine the DNA content. In this figure, the percentage of cells in subG1, corresponding to dead cells, was measured according to PI incorporation.

3.3.3. Transcriptional effect of Ikaros and Myc induction

In order to identify the transcriptional programs behind the observed phenotypes, we collected cells at 4h, 8h and 24h after treatment with OHT, Dox or both to analyze the complete transcriptional profile of Ikaros/Myc response.

From an initial qPCR analysis of the samples, Ikaros and Myc target genes resulted to be regulated as expected; on the other hand, the effect of the double activation was not clear, at least for these selected target genes (figure 38B).

Subsequently, we profiled the total RNA in all these conditions, performing RNA-seq in triplicate.

Analysis of genes that were deregulated in treated cells at each time point compared to the relative non-treated control, showed a substantial effect of IkarosER, but very little effects of Myc activation alone on gene expression (figure 42). The latter was expected in the conditions used here, as the exogenous Myc was induced in proliferating cells that already expressed endogenous Myc, with relatively modest changes in total Myc levels (figure 38A). However, co-activation of Tet-Myc and IkarosER allowed sustained Myc expression in the presence of IkarosER activity, causing significant effects on both cell growth (as described above, figure 39) and gene expression, especially at 24h (figures 43 and 44). In figure 43, all the samples were compared and clusterized according to the similarity of their expression profiles. In this heatmap, samples in which only Myc is induced (red) are close to non-treated samples (grey); conversely, samples in which only IkarosER (green) or both IkarosER and Myc (blue) are activated share a high similarity at 4h and 8h, while they are well separated at 24h.

The effect of Myc on Ikaros response is described more precisely in figure 44, which compare the response to co-activation of both factors (Y-axes) relative to IkarosER alone (X-axes), revealing a decrease in the extent of gene expression changes in the presence of Myc, particularly at 24h.

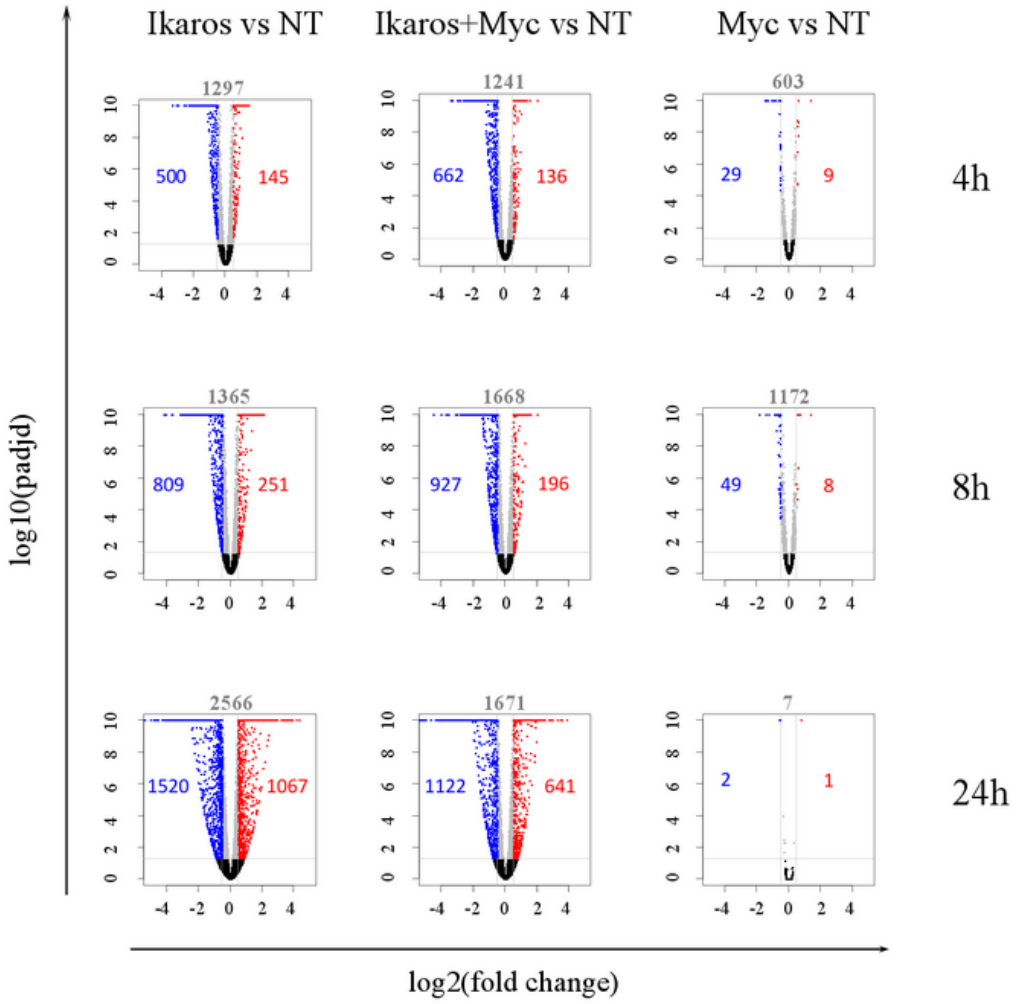

Figure 42. DEGs identified in BH1 cells upon IkarosER and/or Tet-Myc induction. Volcano plots representing DEGs identified with RNA-seq experiments in BH1 cells. Only genes that were significantly deregulated (qvalue <0.05) were considered. DEGs with log2(fold change) <0.5 are downregulated genes (in blue), while DEGs with log_2(fold change) >0.5 are upregulated genes (in red). –log10(padj) values are saturated at a maximum value of 10.

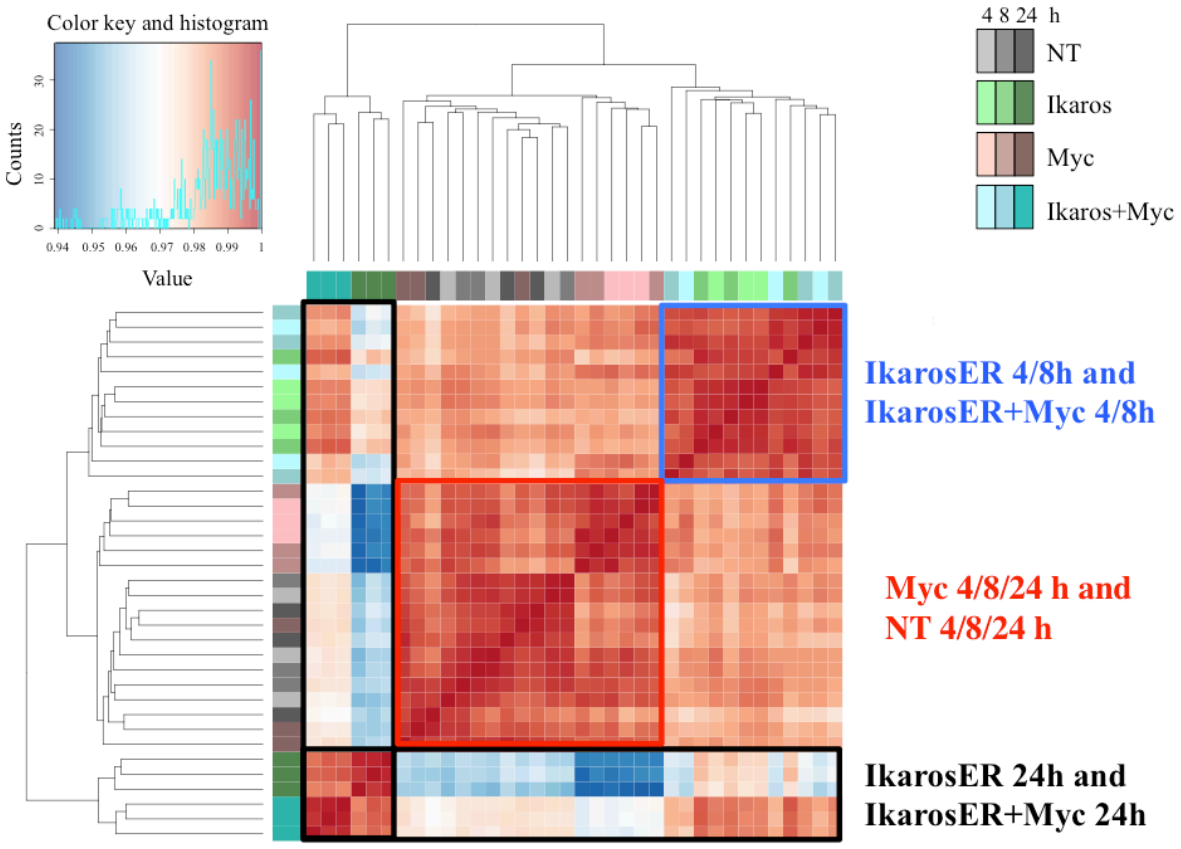

Figure 43. Correlation heatmap of RNA-seq samples upon IkarosER and/or Myc activation in BH1 cells. Heatmap representing the correlation and clusterization of all RNA-seq replicates in BH1 cells upon activation of Myc and/or IkarosER. In the colored squares inside the heatmap the major clusters are highlighted: non-treated cells (NT) or cells with only Myc clusterize together at 4, 8 and 24h (red square inside the heatmap); samples in which only IkarosER or IkarosER plus Myc are induces appeared similar at 4 and 8h (blue square inside the heatmap); conversely, at 24h, samples with only IkarosER or IkarosER plus Myc activated, clusterize separatly suggesting a major effect on the transcriptional activity (black square inside the heatmap).

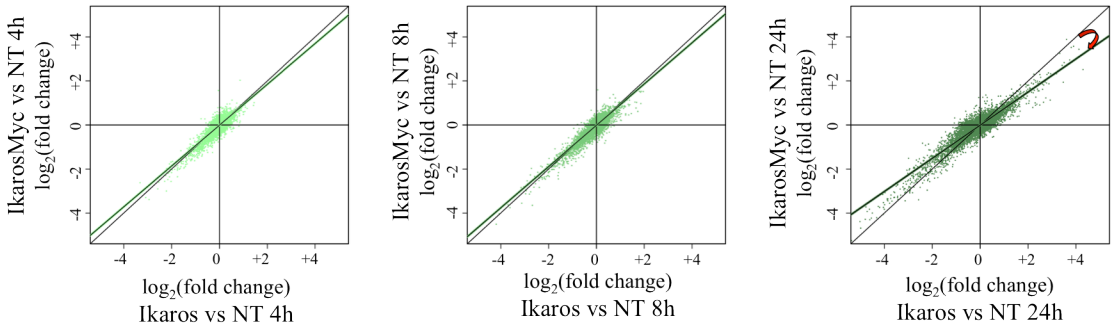

Figure 44. Correlation plots of gene expression upon IkarosER or IkarosER plus Myc activation in BH1 cells. The effect due to the co-activation of IkarosER and Myc (Y-axes) relative to IkarosER alone (X-axes) at 4, 8 and 24h is represented.

This behavior suggests that after 24h we are observing a general effect probably due to the opposite transcriptional program promoted by the two transcription factors. Since we are particularly interested in studying variations directly caused by the protein-protein interaction between Ikaros and Myc, we decided to focus on target genes already regulated at early time points.

We started considering genes that were deregulated upon IkarosER activation alone, reasonably corresponding to Ikaros target genes (figure 45A); among them, we identified the ones whom expression was also significantly different between the condition in which both IkarosER and Myc were activated and that with only IkarosER activation (figure 45B). Finally, we focused our attention on the genes that were behaving in this way along the entire time course, that were presumably the most direct (being already modulated at earlier time points) and consistent, retrieving a total of 113 genes (figure 45C).

By analyzing more in detail the change in the expression level of these target genes, we can observe that around 80% of them are anti-regulated by IkarosER and Myc and, in particular, the majority is positively regulated by IkarosER and more downregulated in presence of Myc (figure 46). The complete list of genes divided in the four classes depicted in figure 46 is reported in Table 2. In the supplementary table 1, the complete data relative to log2(FoldChange) of the 113 DEGs upon IkarosER and/or Myc activation at all the time points are available

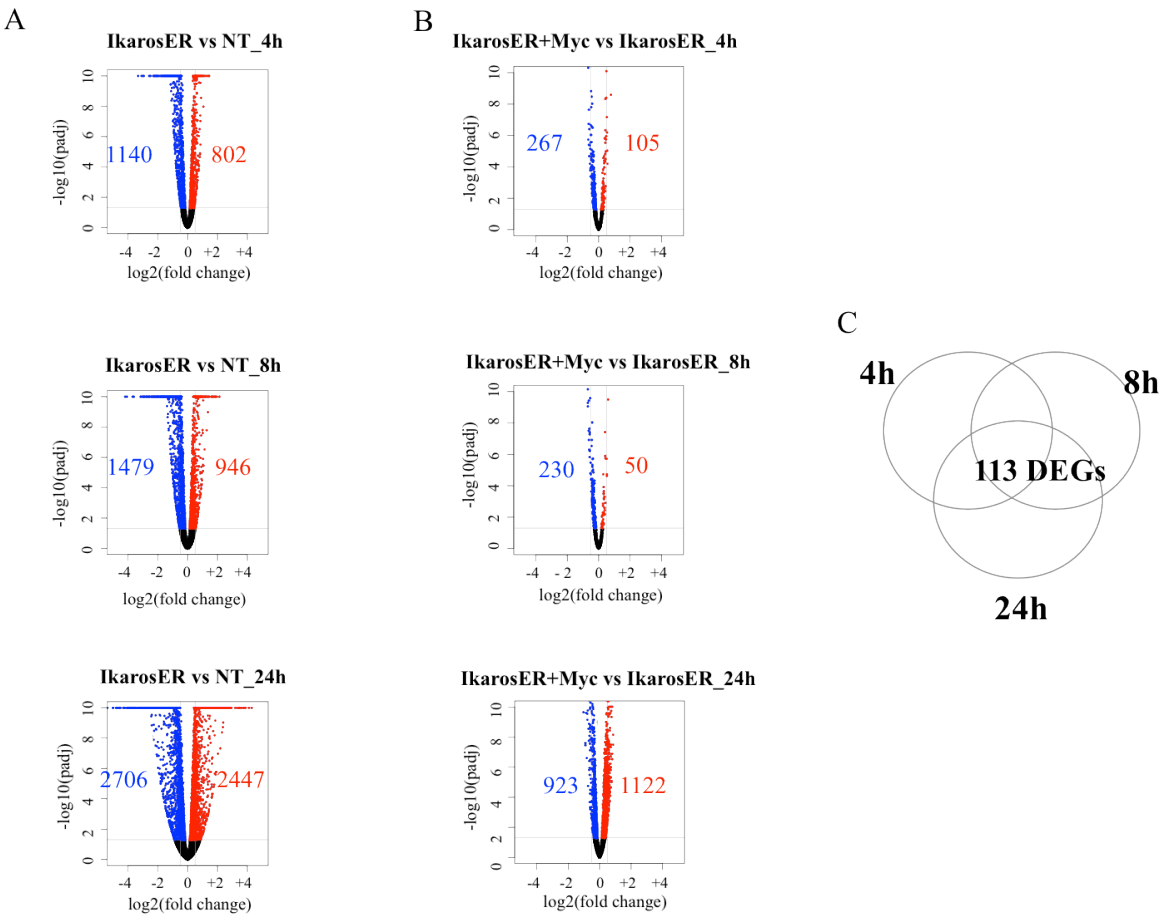

Figure 45. Ikaros and Myc common target genes in BH1 cells. Among genes significantly deregulated upon IkarosER activation (pvalue<0.05, without treshold on the log2(FoldChange) values) (A), we selected genes that were deregulate when both IkarosER and Myc were activated compared to IkarosER activation alone (B). The overlap of the DEGs identified in each time point resulted in 113 genes (C).

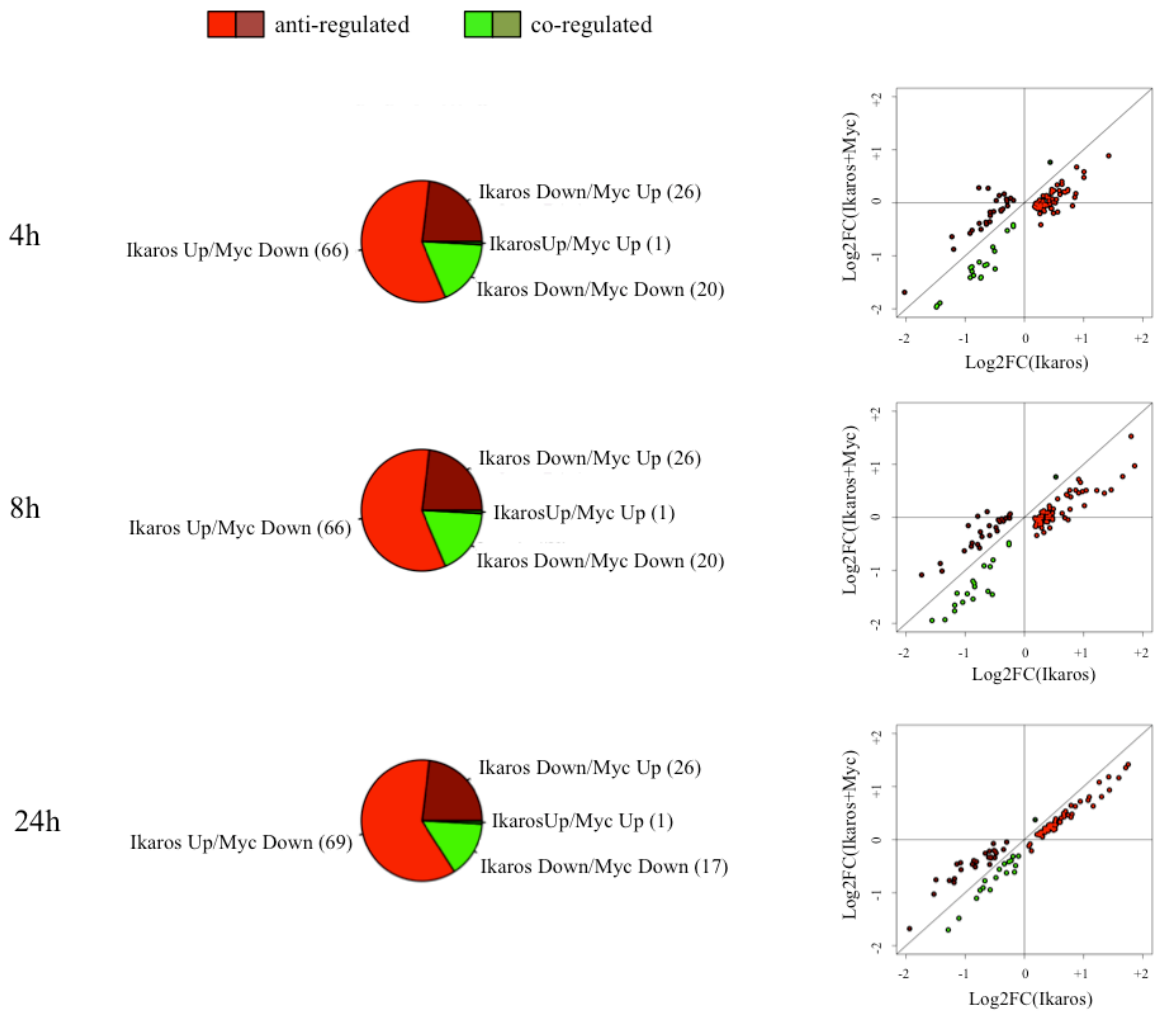

Figure 46. Genes anti-regulated and co-regulated by IkarosER and Myc in BH1 cells. The pie charts (on the left) represent the fractions of genes anti- or co-regulated by IkarosER and Myc; the same classes are also represented on the scatter plots (on the right) with the log2(fold change) of DEGs in the IkarosER plus Myc samples (y axis) compared to the log2(fold change) of DEGs in presence of IkarosER alone (x axis). Only DEGs with a qvalue <0.05 were considered. Three genes, Lbh, Prox1 and Trp53i11 showed a different behaviour at 24h compared to the other time points.

Interestingly, among the genes antagonistically regulated by IkarosER and Myc, were genes involved in the regulation of cell cycle. In particular, *Asb2* (Guibal et al., 2001), *Btg1* (Zhu et al., 2013), *Cdkn1b* (Polyak et al., 1994) and *Rbm5* (Sutherland et al., 2005), that favor cell cycle arrest, were upregulated by IkarosER and downregulated in presence of Myc, in accordance with the expectations; vice-versa, *Ccnd1* (Baldin et al., 1993), that is required for the G1/S transition, was downregulated by IkarosER alone and less downregulated in presence of Myc.

Many antagonistically regulated genes were also related to lipid metabolism and transport: *Abcd1* (Wiesinger et al., 2013), *Acox3* (Ferdinandusse et al., 2017), *Cerk* (Ordoñez et al., 2017), *Pyct1a* (Hoover-Fong et al., 2014) and *Spns3* (Perland et al., 2017). Myc involvement in lipid metabolism has been reported in different systems: in general, Myc seems to favor fatty acid biosynthesis during cell growth and to influence the lipid composition of cells during tumorigenesis (Dang 2013; Edmunds et al., 2014; Hall et al., 2016). Ikaros role in the regulation of these pathways had not been deeply investigated; a connection between Ikaros and cholesterol biosynthesis was only provided by experiments performed in pituatury gland cells, in which Ikaros seemed to upregulate the expression of *LDL-R* and to regulates other genes involved in cholesterol homeostasis such as *SREBP2* and *HmGCoAR* (Loeper et al., 2008).

In addition, genes related to energy stress were also identified: *Prkaa2* encodes for a catalytic subunit of the AMPK energy-stress sensor that is activated in low energy conditions (Ross et al., 2016), while *Deptor* encodes for an inhibitor of the mTORC1/2 complexes (Catena & Fanciulli, 2017), thus blocking energy consuming pathways. Both of them were downregulated by IkarosER alone and less downregulated when also Myc is present. Ikaros implication in the regulation of cellular homeostasis was proposed by a recent study according to which Ikaros exerts its tumor suppressor function, at least in part, by acting as a metabolic gatekeeper. In particular, the suggested hypothesis would be that Ikaros can restrict glucose uptake and metabolism, thus limiting glucose and energy supply to levels not sufficient for malignant transformation. The identification of *Foxo1*, that promotes gluconeogenesis (Zhang et al., 2006), might be related to this concept, too; nevertheless, Foxo1 also plays crucial roles in early steps of B cell development as well as in peripheral immune functions (Dengler et al., 2008), thus the regulation of this gene exerted by IkarosER and Myc could have multiple implications.

Due to the complex and still not completely disentangled mechanisms that regulate cell metabolism and to the multiple feedback loops that control cellular homeostasis, it is

difficult to predict, at a first glance, the direction in which we expect to find these target genes regulated by either Ikaros and Myc; nevertheless, the fact that many of them belong to classes of genes that are functionally related with the known activities of the two transcription factors suggests that it could be worth to investigate more in depth the meaning of these findings.

Finally, genes that resulted co-regulated by IkarosER and Myc appeared to have in general a less defined function and no particular classes of genes emerged.

In summary, these results are in accordance with the opposite functions exerted by Ikaros and Myc in pre-B cells, particularly in cell cycle regulation and metabolic pathways. Further studies are needed to investigate the mechanism behind the regulation of these common target genes.

Ikaros UP Myc down	Ikaros DOWN/ Myc UP	Ikaros UP Myc UP	Ikaros DOWN Myc DOWN
2610008E11Rik	Abcb1b	Mtrr	Alpk2
Abcd1	Abcc1		Apba1
Ackr4	Acy1		Atp6v0a1
Acox3	Atg9b		Cd248
Adamtsl2	Bcl11a		Cyth4
Aim1	Ccnd1		Gab2
Ankrd44	D8Ertd82e		Il5ra
Ap3m2	Deptor		Kctd12b
Arid3b	Dfna5		Klf3
Asb2	Fgd2		Pcdh17
Atg9a	Frrs1		Ppp1r18
Baz2a	Kdelc1		Rasgrp3
Bcl2l1	Mmp15		Rgs2
Btg1	Nr1d1		Rnf150
Calcoco1	Nrp2		Slc37a2
Cblb	Pdzrn3		Tmem108
Cd37	Prkaa2		Tmtc1
Cdkn1b	Prrg4		(Lbh)
Cerk	Ptpn14		(Prox1)
Chd3	Rasd2		(Trp53i11)
Cklf	Sdc1		
Cpm	Slc19a2		
Cr2	Slc39a10		
Dennd1c	Tbkbp1		
Dgka	Xxylt1		
Dopey2	Zfp365		

Dyrk1b Endou Ero1lb Fam214a Fam63b Fchsd1 Foxo1 Gdi1 Git2 Gltscr1 H2-Oa H2-Ob Ifi203 Il16 Jakmip1 Kmt2e Map4k2 Mbd4 Natd1 Neil1 Pcyt1a Pecam1 Pias3 Pink1 Plekhg2 Pyhin1 Rab43 Rag1 Rbm5 Rprl1 Serinc5 Siglecg Slc12a6 Spns3 Tbx6 Tuba1a Ypel3 Zfp821 Zfp831 Zhx3 (Lbh) (Prox1) (Trp53i11)			

Table 2. Lists of genes anti-regulated and co-regulated by Ikaros and Myc. Ikaros and Myc common target genes are listed according to the direction of their regulation. Genes in brackets (Lbh, Prox1, Trp53i11) have a different behaviour at 24h compared to 4h and 8h. The complete table reporting the log2(FoldChange) upon Ikaros and/or Myc activation is available in the supplementary table 1.

4. DISCUSSION

4.1. Identification of new Myc interactors using a MS-based approach.

Myc is a key transcription factor that regulates many physiological cell functions and with the diffusion of high throughput sequencing techniques, such as ChIP-seq and RNA-seq, Myc activity has been deeply studied at a genomic scale. Our group recently proposed that the process of Myc binding site recognition on chromatin initially occurs in a sequence-independent manner (Sabò & Amati, 2014), probably supported by the interaction with other proteins (Richart et al., 2016; Thomas et al., 2015). This, together with the observation that Myc can bind most of the active chromatin sites, but only part of them is actually regulated, strengthens the idea that many cofactors can be implicated in supporting and regulating Myc activity on DNA. In this contest, the identification of Myc interactors becomes particularly interesting to better clarify the complex and largely unknown network of Myc cooperations (Tu et al., 2015).

Myc interactors have been studied with different techniques, the most used of which are two-hybrid assay, in vitro pull-down and co-immunoprecipitation. With the advent of mass-spectrometry, new approaches have been exploited to identify Myc cofactors. Indeed, mass spectrometry introduced the possibility to gain a broader (-omic) idea of the dynamic interactions in cells and an easier way to detect not only associations within single proteins, but also within multiprotein complexes.

Until now, three published studies used MS-based approaches to investigate the Myc interactome. In the first paper, Koch et al. performed Tag-affinity-immunoprecipitation experiments in colorectal cancer cells and identified 221 proteins, some of which were validated by co-immunoprecipitation and two-hybrid assay (H. Koch et al., 2007). In the second paper, Agrawal et al. used a similar approach in human fibroblasts. They performed

tandem-affinity-immunoprecipitation both in label free conditions and with the stable isotope labeling with amino acids in cell culture (SILAC) MS approach, identifying a total of 418 putative Myc interactors (Agrawal et al., 2010). Finally, in the third paper, Dingar et al used a different technique called BioID proximity-based biotin labeling: the protein of interest (in this case Myc) is fused with a mutant *Escherichia coli* biotin ligase that biotinilates the surrounding proteins so that they can be easily purified with a streptavidin-sepharose matrix. With this method, they identified 134 proteins in 293T-Rex cells (Dingar et al., 2015). The comparison of the data obtained from these three different studies revealed that the overlap was quite small: only three proteins have been identified in all of them: MAX, TRRAP and EP400 (Dingar et al., 2015). This high variability is partly expected since they used different techniques: different methods can be more useful to identify particular type of proteins (soluble proteins with tag affinity purification or proteins in less soluble compartments with BioID). Even more important can be the type of cells that are used for the analysis, since many interactors can be cell-type specific.

In our work, we used the ChroP technique (Soldi & Bonaldi, 2014b) to specifically identify Myc interactors on chromatin. The ChroP technique involves cell crosslinking with formaldehyde (FA): the FA crosslink has many advantages, in fact it can stabilize protein interactions with DNA and, being FA a very small molecule, it can also stabilize the interaction within very close aminoacids, thus allowing the use of stronger detergents during the washing steps of the immunoprecipitation protocol. The same concept was recently used to study the estrogen receptor interactome, with the rapid immunoprecipitation mass spectrometry of endogenous proteins (RIME) technique (Mohammed et al., 2013) and other similar methods have been used in mammalian cells (TChP, Pourfarzad et al., 2013), in Drosophila (ChIP-MS, Wang et al., 2013) as well as in yeast (CHAP-Ms, Byrum et al., 2012), highlighting the high potential of this kind of approach.

In our experiments, we have quite a high variability between biological replicates that could be due partly to the intrinsic variability of the MS technique, but also to the fact that, by crosslinking proteins to DNA, stochastic or weak interactions difficult to reproduce can be stabilized too. Moreover, the presence of the FA could affect the MS detection of some peptides and the immunoprecipitation efficiency by masking recognized epitopes (Mohammed et al., 2016). For example, unexpectedly, we only identified Max in the first replicate: this is probably a technical artifact, since its presence is instead visible by ChIP-WB and Myc binding to DNA, that we detected by ChIP-qPCR (figure 10), is possible only through the interaction with Max (Amati et al., 1992). Nevertheless, we identified 24 proteins in common between all the three biological replicates and 51 proteins in common between at least two out of three experiments (figure 12). Among them, we identified 10 already known Myc interactors (WDR5, RUVBL1/2, TRRAP, EP400, MCM2/3/6/7, HDAC1), mostly detected in all three replicates; additionally, we found 10 other proteins (PSMA7, DDX17, TRIM28, PTBP1, PRKDC, CCT5, YBX1, PGD, FBL, UBC) that were already identified in the previously mentioned proteomic datasets (Agrawal et al., 2010; H. Koch et al., 2007), but not yet validated (figure 12). The complete list of the identified Myc interactors is reported in the supplementary table 2. In that table, Myc interactors identified in our and other published MS datasets are reported and ranked according to the number of times they have been identified (see also the Appendix). We can see that MAX, EP400 and TRRAP are actually at the top positions, since they have been retrieved in all (or most of) the cases (figure 53).

Among the new putative interactors identified with the label free ChroP technique, we defined the top candidates, that were judged of particular interest according to the information found in literature (figure 13). In particular, Ifi16 is considered a potent transcriptional repressor and, being able to bind regulatory regions of Myc promoter could be involved in the auto-regulation of this oncogene. In fact, an increase of Myc level in cells induces a feedback loop to control Myc expression itself; although the exact

mechanism behind this autoregulation is still not clear, it can require the formation of complexes between Myc and other cellular factors (Egistelli et al., 2009; Penn et al., 1990). Of notice, we identified multiple proteins belonging to the same complexes. For example we found many subunits of the NuRD complex, some of which were already known to interact with Myc (HDAC1, TRIM28, CHD4), while RBBP4 has been identified for the first time here. YWHAQ and SFN are two members of the 14-3-3 family of scaffold proteins, involved in many cell functions among which cell cycle regulation, metabolism, apoptosis and gene transcription (Obsilová et al., 2008). Of particular interest is the identification of both subunits of the facilitate chromatin transcription complex (FACT), SUPT16H and SSRP. The FACT complex is a nucleosome chaperone implicated in chromatin remodeling and associated with the acceleration of tumorigenic transformation; in particular, it seems to exert its activity on genes related to cell proliferation, cell death and cell differentiation and it has been reported to regulate the expression of its target genes through the interaction with transcription factors such as Myc itself (Garcia et al., 2013). Finally, Ikaros and Aiolos belong to the same family of transcription factors involved in lymphocyte development and differentiation, and are the candidates we chose for further validation and functional studies.

4.2. Interplay between Ikaros/Aiolos and Myc

Among the newly identified Myc interactors, we focused our attention on Ikaros and Aiolos, that were found in two and three of our MS triplicates, respectively. The identification of two members of the same family, that are known to form either homo-or heterodimers, as putative Myc interactors suggests that a relevant complex can be formed. Interestingly, Ikaros/Aiolos and Myc seem to be implicated in the same cellular functions, but playing opposite roles. First of all, they all are transcription factors, able to either activate or repress genes (Schwickert et al., 2014; Wanzel, 2003). One of the main

functions that characterize Myc and Ikaros/Aiolos activity is the regulation of cell proliferation: while Myc induces cell cycle progression (Amati et al., 1998), Ikaros decreases cell proliferation by blocking cells in G1 phase (figure 40) (Gómez-del Arco et al., 2004). They also play crucial role in cell differentiation: Myc expression can affect this process depending on the cellular contest, for example it can block differentiation of plasma cells (Calame et al., 2000), while it promotes differentiation of HSC (Wilson et al., 2004) and B-cell early progenitors (Habib et al., 2007). Ikaros and Aiolos, instead, tend to promote cell differentiation: Ikaros particularly at earlier stages of hematopoiesis (Heizmann et al., 2013), Aiolos mostly during maturation of B lymphocytes (Cortes and Georgopoulos, 2004). Moreover, it is well known that Myc regulates cell metabolism to favor energy supply, in particular during tumorigenesis (Hsieh et al., 2015), while recently, it has been proposed that Ikaros could, at least in part, act as a tumor suppressor by creating a metabolic barrier that keeps the energy supply under the level necessary for malignant transformation (Chan et al., 2017). These behaviors are examples of Myc oncogenic potential (Dang, 2012) in opposition to Ikaros and Aiolos that, instead, are mostly considered tumor suppressors (Winandy et al., 1995). Altogether these observations lead to the hypothesis that Ikaros/Aiolos and Myc could actually compete to regulate each other activities.

Nevertheless, the picture could be even more complex since while Ikaros/Aiolos act as tumor suppressors in B cell progenitors, they could be oncogenic in mature B cells. Indeed, they are expressed at high levels in mature B cells and in the correspondent lymphomas, where Myc generally plays a crucial role in tumor proliferation, and their expression seems to be necessary for tumor maintenance (Bjorklund et al., 2015). For example, multiple myeloma, as well as other blood malignancy deriving from mature B cells, is treated with Lenalidomide, that specifically induces Ikaros and Aiolos ubiquitination and subsequent degradation (Kronke et al., 2014; Lu et al., 2014). For this reason, we cannot exclude that, at later stages of B lymphopoiesis, Ikaros/Aiolos and Myc could also cooperate. These

observations imply that we have to consider very carefully the system we choose for our studies because experiments performed at different stages of B cell development could potentially lead to opposite results.

In this contest, the first system we used was the p493-6 cell line. P493-6 are human mature B cells expressing high levels of endogenous Ikaros and Aiolos, and with a highly overexpressed exogenous Tet-Myc.

The second system we used, BH1 cells, are murine pre-B cells transduced with inducible Ikaros and Myc.

Finally, pre-B ALL cell lines could also be considered as suitable models for future studies on Ikaros/Myc interaction in a pathological condition that is known to be strictly dependent on Ikaros activity (Mullighan et al., 2009).

After the MS identification of Ikaros and Aiolos, we validated their interaction with Myc by co-immunoprecipitation in native conditions. Of particular interest is the fact that Myc interaction with Ikaros/Aiolos is observed not only by overexpressing all the transcription factors in a host system (HEK293T cells, figure 17), but also at an endogenous level in different lymphocytic cell lines such as, p493-6, Burkitt's lymphoma (Daudi, Raji, Namalwa, Ramos), multiple myeloma (H929, JJN3, KMS11), pre-B ALL (697, REH, Sup-b15), Ba/f3 and BH1 cells, strengthening the idea that it is quite conserved across different B cell subtypes and differentiation stages (figures 15, 16 and 18).

We tried to define more precisely the interplay of the three proteins by testing Myc interaction with Ikaros and Aiolos separately. Overall the results we obtained suggested that Aiolos is able to bind Myc also in the absence of Ikaros, while the vice-versa is still not completely clear (figures 17 and 18).

The identification of the domains responsible for Ikaros/Aiolos/Myc interaction would be very interesting to better understand the structure of this complex and for further functional studies. Although we tried some preliminary experiments in that direction, we did not obtained reliable results, thus a more detailed analysis is needed.

ChIP-seq data in p493-6 cells also supported the idea of a co-binding between Ikaros, Aiolos and Myc on chromatin. Indeed, the overlap of the sites bound by Ikaros, Aiolos and Myc is quite high, both on promoters and distal sites (figures 26-27). Of notice is the fact that Ikaros and Aiolos distribution on chromatin does not seem to be macroscopically influenced upon Myc modulation, thus we exclude a broad effect on their DNA-binding ability. In order to explore a possible correlation between Ikaros/Aiolos co-binding with Myc and transcriptional regulation, we also performed RNA-seq in p493-6 cells with high and low Myc levels, to define Myc target genes in this system. From the integration of ChIP-seq and RNA-seq data in these conditions we observed that, while Myc preferentially binds to Myc-induced target genes, as expected (de Pretis et al., 2017), Ikaros/Aiolos enrichment is the same on promoters of Myc target and non-target genes (figure 30). Taken these observations together, the most probable scenario is that Myc interaction with Ikaros/Aiolos could only affect a subset of common target genes. To verify this hypothesis and to identify the putative common target genes, we are planning to perform RNA-seq experiments in p493-6 cells, in presence or absence of Ikaros/Aiolos so that, together with the dataset that we already have, we would be able to identify genes that are bound and regulated by all the factors in an antagonistic or common direction.

We also tried to define Myc and Ikaros common target genes in BH1 cells, where we were able to easily modulate both Ikaros and Myc levels. Myc induction in this system appeared to be less efficient than expected (figures 38 and 42); nevertheless, we observed the opposite effect exerted by Ikaros and Myc on cell proliferation (figures 39 and 40) and on the regulation of their transcriptional programs (figures 43 and 44). The fact that Ikaros is able to repress Myc by directly binding to its promoter (Ma et al., 2010) imposes to be very careful in the interpretation of the obtained data, to distinguish between a general effect due to the transcriptional interplay of these factors and the direct effects possibly dependent on a protein-protein interaction. RNA-seq data allowed us to select genes that were regulated by both Ikaros and Myc at short time points, thus presumably coinciding

with direct target genes (figure 45). Interestingly, most of these genes were anti-regulated by Ikaros and Myc, while a smaller percentage was constituted by co-regulated genes (figure 46). Among the anti-regulated targets, we found genes involved in cell cycle control (*Asb2, Btg1, Cdkn1b, Rbm5, Ccnd1*), in metabolism of lipids (*Abcd1, Acox3, Cerk, Pyct1a, Spns3, Nr1d1*) and in the regulation of energy homeostasis (*Prkaa2, Deptor, Foxo1*). These classes of genes are consistent with the key role played by Ikaros and Myc in cell cycle regulation and can also be related to the newly suggested role of Ikaros as a metabolic gate keeper and a regulator of energy metabolism. (Chan et al., 2017). In some cases, such as for targets involved in cell cycle regulation, the direction of Ikaros- and Myc-dependent regulation is clear and in accordance with the expectations. In the other cases, the meaning of Ikaros/Myc antagonistic regulation needs to be investigated more in depth.

Moreover, once we will have the complete datasets of RNA-seq and ChIP-seq in both our systems (p493-6 and BH1 cells), it would be interesting to compare Ikaros transcriptional activity in mature B cells and pre-B cells and, particularly, the interplay between Ikaros and Myc at different B cell developmental stages.

Further studies on the mechanisms that drive the expression of these common target genes will shed light on the role of Ikaros-Myc interaction in transcriptional regulation. For example, Myc-mediated transcriptional repression has been suggested to occur also by antagonizing the activity of other transcription factors such as Miz-1: Myc binding to Miz-1 would cause the release of Miz-1 cofactors p300 and Npm, and the recruitment of chromatin repressors (Staller al., 2001; Brenner et al., 2005). Similarly, Ikaros can regulate its target genes by competing with other transcription factors, such as STAT5, in different ways: either by binding to the same DNA motif or by recruiting on chromatin histone modifier that can promote transcriptional activation or repression (Katerndahl et al., 2017). Thus it is reasonable that the interaction between Myc and Ikaros/Aiolos on promoters of common target genes could imply similar mechanisms to determine the final direction of

transcriptional regulation. To assess this idea, we will select a subset of the antagonistically regulated genes (according to their fold change variation, biological function, presence of Ikaros and Myc motifs in their promoters) for which we will accurately characterize the dynamic of Myc and Ikaros binding to their promoters along with their transcriptional response, both by ChIP- and RT-qPCR and by Luciferase assays.

In conclusion, we identified an interaction between Myc, Ikaros and Aiolos, and are working to better define its biological role. By unveiling the mechanism driving Myc-Ikaros interplay, we would also be able to consider if and how targeting Ikaros (and Aiolos) activity could impact Myc-dependent tumorigenesis.

5. APPENDIX

5.1. Experimental design

Besides the label-free ChroP, we also performed a Stable Isotope Labeling by Amino acids in Cell culture (SILAC) ChroP experiment, in p493-6 cells, with the aim of increasing the accuracy of Myc interactors identification using different MS techniques.

For the SILAC approach, two cell populations are grown separately in medium containing light (L) (12C6 and 14N4) or heavy (H) (13C6 and 15N4) lysine (Lys) and arginine (Arg). After the ChIP, the two samples are mixed in a 1:1 proportion and analyzed together: the m/z ratio obtained with the MS analysis will reveal to which population each protein belongs (figure 47) (Soldi & Bonaldi, 2013).

Moreover, differently from the label-free ChroP, for the SILAC ChroP we performed the Myc-ChIP in both high and low Myc conditions. Indeed, this technique should be particularly sensible in comparing the proteome deriving from two different conditions, since the two samples are mixed and analyzed together. We performed it in two replicates called forward (FWD) and reverse (REV): in the forward experiment, the high Myc cell population was associated with heavy Arg and Lys and the low Myc condition with light aminoacids, while in the reverse experiment it was the opposite. We expected specific Myc interactors to be more abundantly immunoprecipitated when Myc was present at high level and thus to be identified as proteins with a heavy/light (H/L) (FWD experiment) or light/heavy (L/H) (REV experiment) ratio greater than 1.

Subsequently, we compared the results that we obtained with the SILAC and label-free approaches together with previously published datasets in which Myc interactors were identified with other MS-based techniques.

From this comparison we retrieved a list of the most reliable Myc cofactors candidates to test them with a functional siRNA-based screen.

The functional screen will allow us to identify Myc cofactors implicated in Myc's transcriptional activity. To this aim, we used a 3T9 cell line, expressing an exogenous human MycER chimaera that can be activated adding OHT to the medium (Littlewood et al., 1995). These cells have been engineered using the CRISPR-Cas9 technique (Ran et al., 2013) to insert the NanoLuc luciferase reporter gene under the control of a Myc target gene promoter and thus, if we transfect cells with an siRNA able to silence a cofactor which is necessary for Myc transcriptional activity, we should see a variation of the NanoLuc signal upon OHT activation.

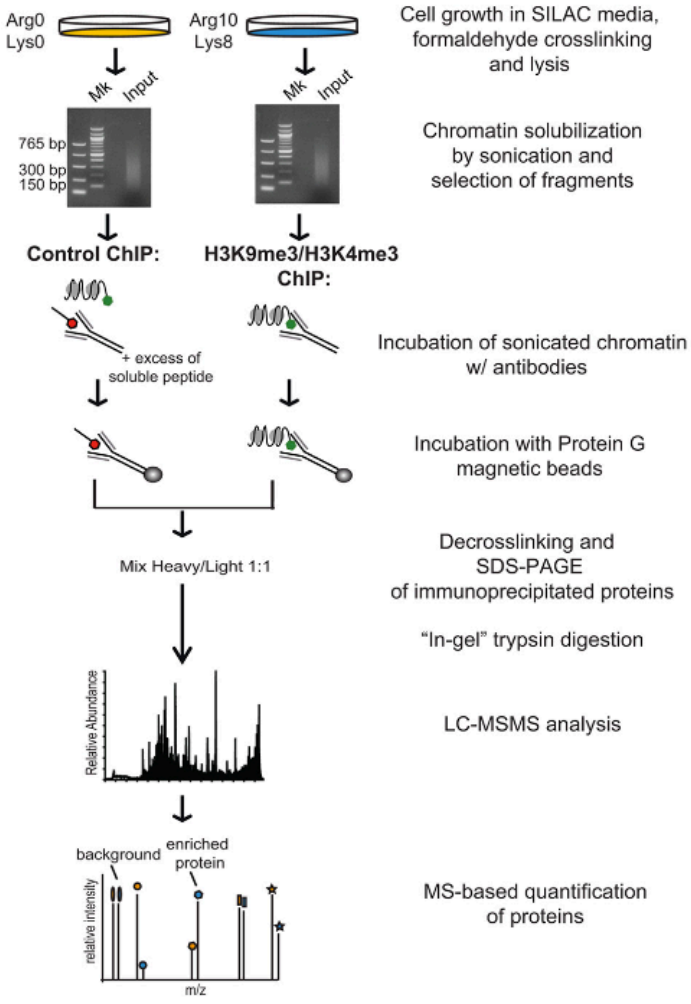

Figure 47. SILAC ChroP scheme. Two different cell populations are separately grown in SILAC medium containing light or heavy aminoacids. The cell lisates are fragmented with the MNase enzyme and the Myc antibody is added to perform the ChIP. Immunocomplexes are recovered with the beads and washed. The material recovered from the two samples are mixed in a 1:1 proportion and processed for MS analysis. After the MS analysis, each peptide could be associated to the heavy or light population according to its m/z ratio (adapted from Soldi & Bonaldi, 2013).

5.2. Materials and methods

5.2.1. Cell culture

P493-6 cells were grown for at least eight replication cycles in RPMI medium with 10% Tet-free dyalized fetal bovin serum, 2 mM glutamine, 100 U/ml penicillin/streptomycin and 0.1 mM non-essential amino acids (NEAA, Lonza), with the addition of light (12C6 and 14N4) or heavy (13C6 and 15N4) Lys (146 mg/L) and Arg (84 mg/L). For Low Myc conditions, p493-6 cells were treated with 200 ng/ml tetracycline (Tet) (Sigma) for 8h.

BZ1 cells were grown in DMEM medium with 10% fetal bovine serum, 2 mM glutamine, 10 U/ml penicillin/streptomycin.

5.2.2. SILAC ChroP

The ChroP protocol was followed as described in previous material and methods session. Myc-ChIP in cells with high or low Myc conditions were performed separately but the recovered material was then mixed in a 1:1 proportion before being loaded on gel and processed for MS analysis.

5.2.3. MS analysis

In-gel digestion and MS analysis were performed as previously described.

5.2.4. siRNA tranfection

2500 BZ1 cells were plated in each well of a white 96 multiwell plate and transfected with 3 pmol siRNA and 0.3 µl RNAiMax transfection reagent.

5.2.5. Luciferase and resazurin measurement

Resazurin was resuspended at a final concentration of 100 µM in PBS. The transfection medium was taken out of the wells except for 50 µl to which was added the same volume of the resazurin solution. Cells are left in the incubator for 2h and then, after 30 minutes at room temperature, the resazurin luminescence was read with a Tecan spectrophotometer (excitation λ: 535 nm; emission λ: 590 nm).

After the resazurin measurement, 50 µl of solution per well were substituted with 50 µl of the Nanoglo mix (buffer+reagent) (Nano-Glo® Luciferase Assay System, Promega), the plate was shacked for few minutes and the nanoLuc luminescence was read with the Tecan spectrophotometer.

5.3. Results

5.3.1. Setting of the SILAC ChroP

Since cells need to be cultured in the SILAC medium, we performed a growth curve to check if this could affect their growth. We plated and counted separately cells with the normal medium, with the SILAC medium containing light aminoacids and with the SILAC medium containing heavy aminoacids and we did not observe any significant difference (figure 48).

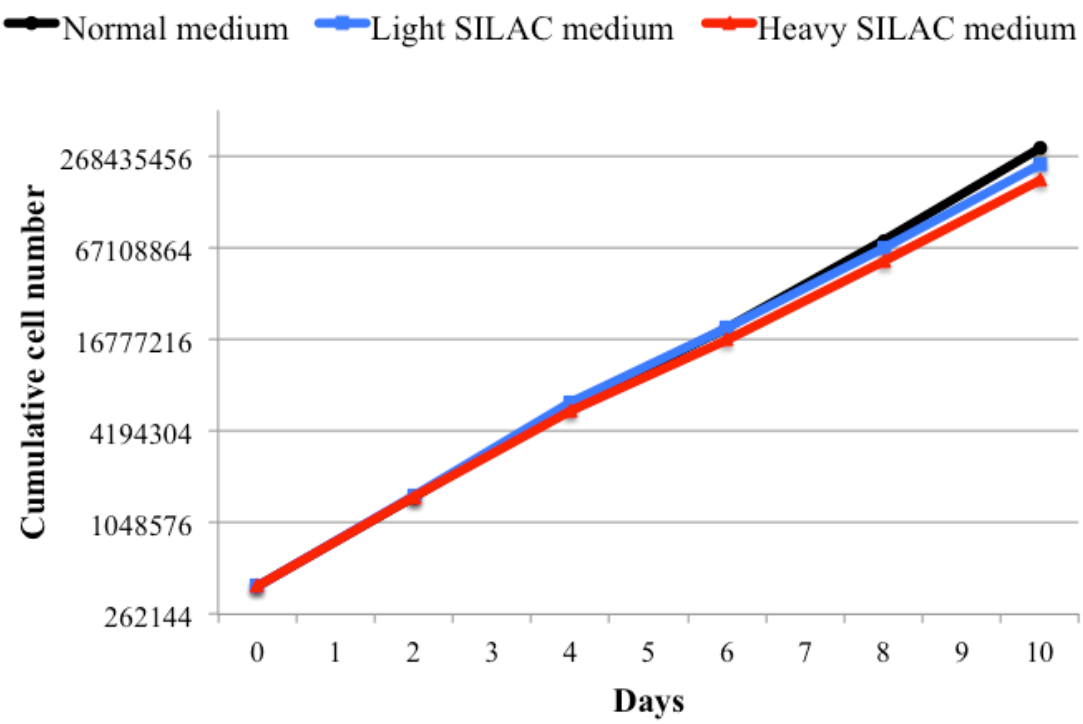

Figure 48. Growth curve with SILAC medium. P493-6 cells were cultured with normal medium, with the SILAC medium containing light aminoacids or with the SILAC medium containing heavy aminoacids and counted every two days to perform the growth curve.

The next step consisted in verifying if the incorporation of heavy aminoacids by the cells actually occurred. To this aim, we collected cells grown in heavy and light SILAC medium after eight replication cycles, we prepared the cell lysates and part of the material was used to obtain an heavy:light 1:1 mix; the samples were then loaded on acrylamide gel and processed for the MS analysis (figure 49A). The distribution of proteins identified with a

H/L ratio in the mixed sample confirmed that it was actually a 1:1 mix, thus half of the material incorporated heavy aminoacids (figure 49C). Moreover, more than 96% of the peptides identified in the heavy sample fully incorporated heavy aminoacids indicating that the labeling was working efficiently (figure 49B).

A

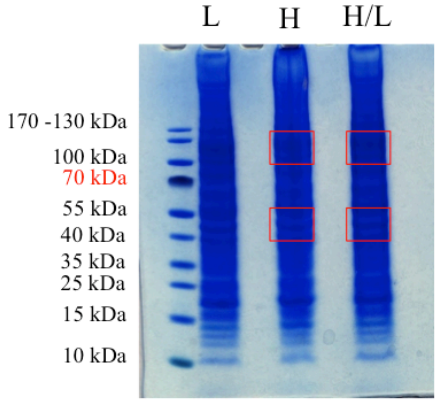

B

Heavy aminoacids incorporation

All peptides	6468	
Only Arg & Lys	6342	
Only Heavy	6128	96.63 %
Only Light	1	0.02 %
SILAC pairs	65	1.02 %
All 0	148	2.33 %
	6342	100 %

C

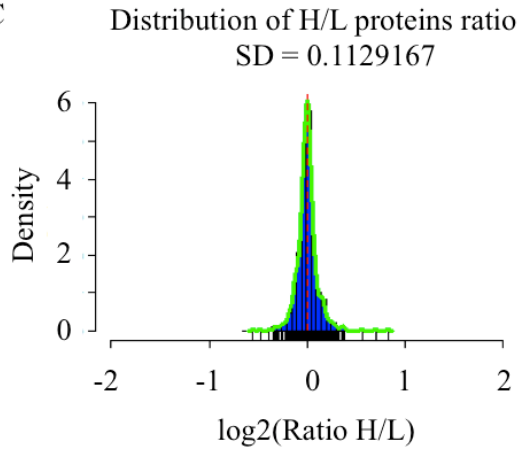

Figure 49. Incorporation test. (A) Protein lysates obtained from cells grown in light medium (L), heavy medium (H) or a 1:1 mix of light and heavy lysates (H/L) have been separated by SDS-PAGE and dyed with Coomassie Blue. The red squares indicate the bands that have been cut and analyzed by MS. **(B)** Summary of the peptides identified in the Heavy sample: more than 96% of the peptides incorporated the heavy aminoacids. **(C)** Distribution of the proteins with a H/L ratio, identified in the H/L sample: the low standard deviation (SD) indicates that it is actually a 1:1 mix of light and heavy protein lysates.

We controlled the efficiency of the ChIP by western blot and ChIP-qPCR. As expected, the enrichment of Myc-bound regions (Nucleolin, IFRD2) observed by ChIP-qPCR was correlated to the Myc protein level detected by western blot (figure 50). The rest of the material was mixed in a 1:1 heavy:light ratio and loaded on the gel for Coomassie Blue staining and sample processing.

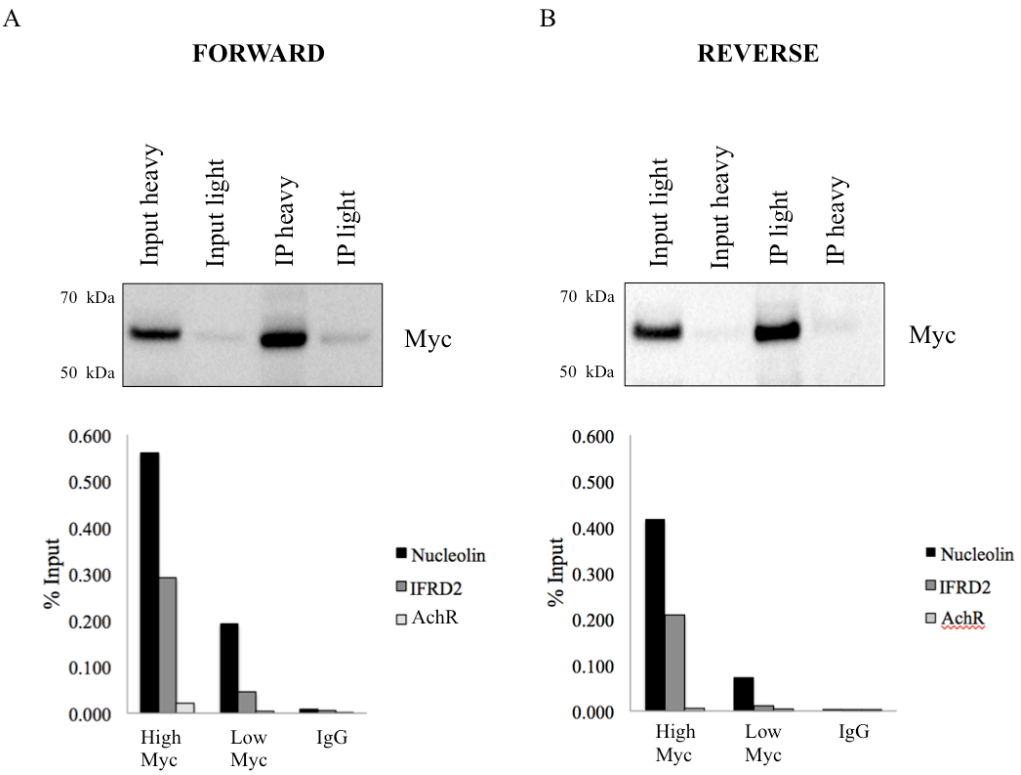

Figure 50. Myc enrichment in SILAC ChroP experiments. Myc enrichment evaluated by ChIP-WB (upper part) and ChIP-qPCR (lower part) in forward (A) and reverse (B) experiments; Nucleolin and IFRD2 are known Myc-bound promoters used as positive controls, while the acetylcholine receptor promoter (AchR) is not bound by Myc and used as negative control. The loaded input corresponds to 2.5% of the material used for the IP. IP=immunoprecipitated proteins.

5.3.2. SILAC MS results

The number of peptides identified in the input was similar in both forward (FWD) and reverse (REV) experiments; conversely, analysis of reverse Myc-ChroP resulted in lower number of proteins compared to the forward experiment. However, in both replicates Myc has been identified with a good number of peptides (9 and 12 for FWD and REV, respectively) and has a good and comparable H/L ratio value in the two experiments (log 2 H/L ratio FWD=2.34; log2 H/L ratio REV=-3.2). Moreover, the majority of the proteins identified in REV experiment are present also in the FWD experiment (86%) (figure 51). Of the 44 proteins identified in both the replicates, 22 had a H/L higher than 1 (log2=0) and can be considered “enriched” .

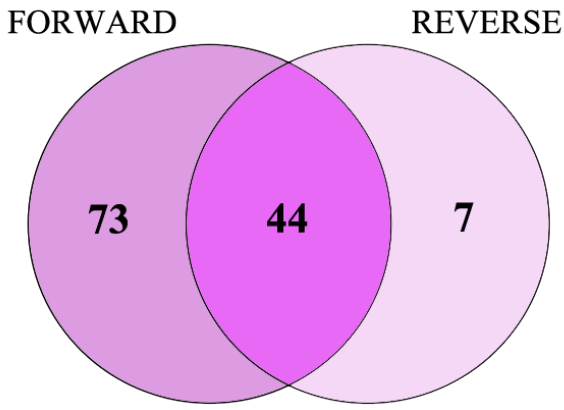

Figure 51. SILAC MS results. In the forward experiments, a higher number of proteins have been identified compared to the reverse replicate; nevertheless, the overlap in quite good. Of the 44 proteins in common, 22 have a H/L ration >0 and can be considered "enriched".

We enlarged our list of candidates considering not only the common ones, but all the proteins identified in the FWD experiment with a H/L ratio >1 and all the proteins identified in the REV experiment with a H/L ratio <1 in the reverse replicate, retriving a total of 68 proteins.

5.3.3. Integration of the MS data

The number of putative candidates identified with the SILAC technique (68 proteins in total) was much lower than the one identified with the label-free approach (468 proteins). Nevertheless, 27 candidates were in common within the two approaches, some of which were already known Myc interactors (i.e. Max, WDR5, TRRAP, MCM3) (figure 52).

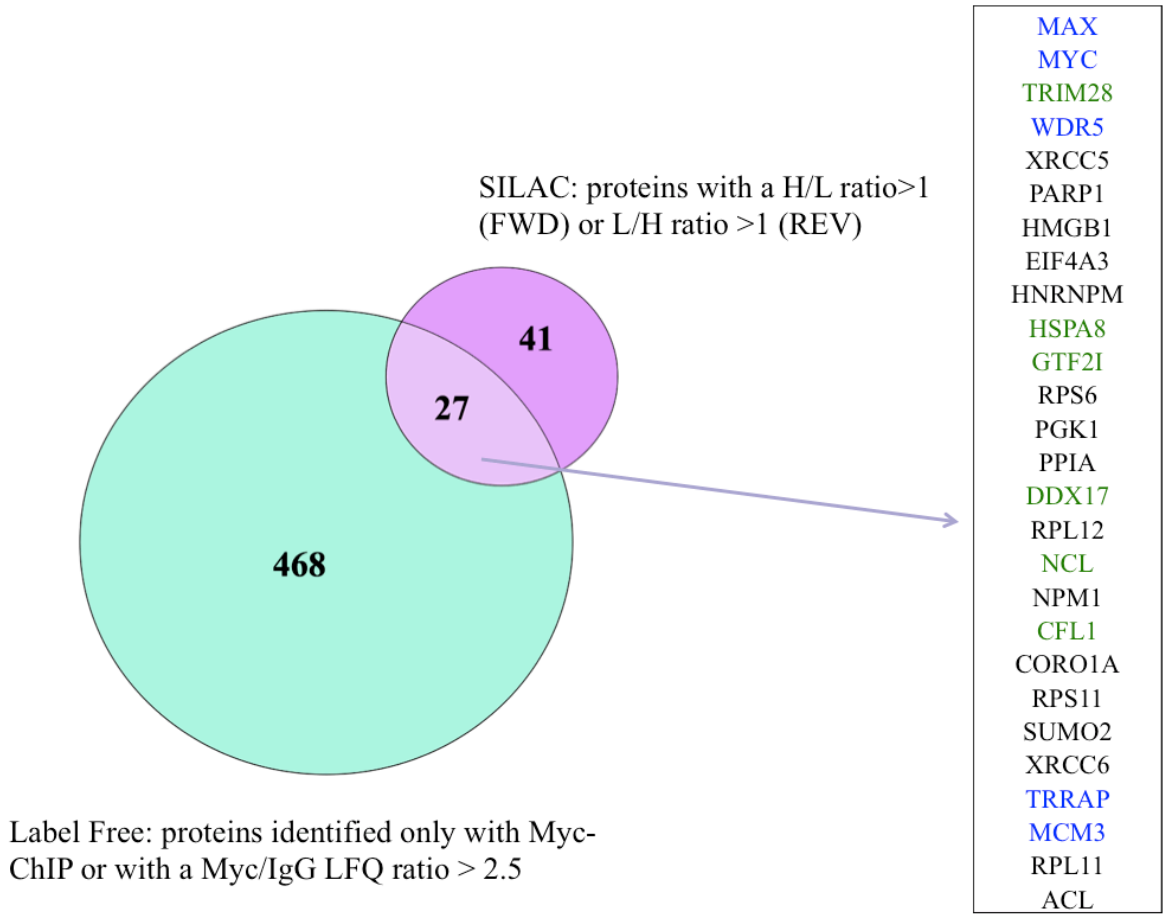

Figure 52. Label-free and SILAC MS results. Total number of putative Myc interactors identified with the label free and SILAC ChroP. The 27 proteins reported on the right were identified with both SILAC and label free techniques. Already known interactors are highlighted in blue, while proteins identified as putative Myc interactors in other MS datasets (Koch et al., 2007; Agrawal et al., 2010), even though the interaction was not yet validated, are highlighted in green.

To enlarge our dataset, we decided to consider all the interactors identified with both our label-free and SILAC experiments and to include the already published MS datasets (Agrawal et al., 2010; Dingar et al., 2015; Koch et al., 2007) and the Myc interactors reported in the Human Protein Reference Database (HPRD) (http://www.hprd.org/) (Peri et al., 2003). We ranked all these proteins according to the number of times they were identified and selected the ones that were identified at least twice, of which at least once in our data (figure 53).

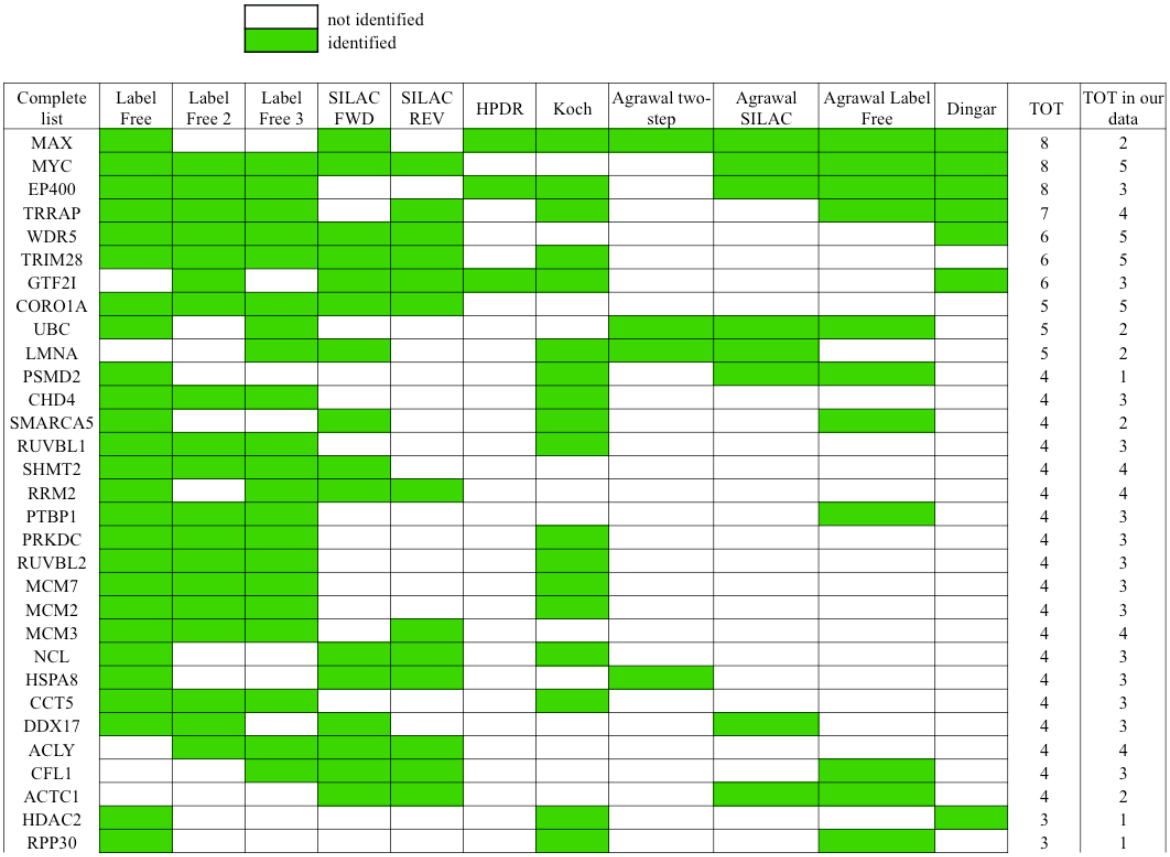

Complete list	Label Free	Label Free 2	Label Free 3	SILAC FWD	SILAC REV	HPDR	Koch	Agrawal two-step	Agrawal SILAC	Agrawal Label Free	Dingar	TOT	TOT in our data
MAX	■			■		■	■	■	■	■	■	8	2
MYC	■	■	■	■	■				■	■	■	8	5
EP400	■	■	■			■	■		■	■	■	8	3
TRRAP	■	■	■		■		■			■	■	7	4
WDR5	■	■	■	■	■						■	6	5
TRIM28	■	■	■	■	■		■					6	5
GTF2I		■		■	■	■	■				■	6	3
CORO1A	■	■	■	■	■							5	5
UBC	■		■					■	■	■		5	2
LMNA			■	■			■	■	■			5	2
PSMD2	■						■		■	■		4	1
CHD4	■	■	■				■					4	3
SMARCA5	■			■			■			■		4	2
RUVBL1	■	■	■				■					4	3
SHMT2	■	■	■	■								4	4
RRM2	■		■	■	■							4	4
PTBP1	■	■	■							■		4	3
PRKDC	■	■	■				■					4	3
RUVBL2	■	■	■				■					4	3
MCM7	■	■	■				■					4	3
MCM2	■	■	■				■					4	3
MCM3	■	■	■		■							4	4
NCL	■			■	■		■					4	3
HSPA8	■			■	■			■				4	3
CCT5	■	■	■				■					4	3
DDX17	■	■		■					■			4	3
ACLY		■	■	■	■							4	4
CFL1			■	■	■					■		4	3
ACTC1				■	■				■	■		4	2
HDAC2	■						■				■	3	1
RPP30	■						■			■		3	1

Figure 53. Enlarged list of Myc interactors. Part of the Supplementary 2 table in which are reported all the putative Myc interactors identified in our data and in already published datasets (Koch et al., 2007; Agrawal et al., 2010; Dingar et al., 2015; Peri et al., 2003). All the proteins were ranked according to the number of times they have been identified. The ones identified at least twice and at least once in our datasets, were selected to be tested with the functional screen. Green= identified; white= not identified.

5.3.4. Functional screen set up

In order to functionally assess the role of the identified Myc interactors on its transcriptional activity we decided to set up a siRNA-based screen.

We took advantage of immortalized murine fibroblasts, the BZ1 cell line, in which the exogenous human MycER is under the control of the Rosa26 promoter. The MycER protein is a chimaera that can be activated adding OHT to the medium, inducing its translocation from cytoplasm to nucleus and thus a rapid activation of Myc transcriptional activity (Littlewood et al.,1995). These cells have been further engineered using the CRISPR-Cas9 technique to insert the NanoLuc luciferase reporter gene under the control of the promoter of a Myc induced gene, St6galnac4. In this system, Myc activation by

OHT will lead to the upregulation of the reporter gene, which is easily readable thanks to the luminescence properties of the luciferase. Knock down of the selected candidates will lead to a decrease or increase in luminescence if they co-activate or antagonize Myc activity on that promoter (figure 54)

We decided to activate cells for 24h with a low dose of OHT (25 nM) to avoid the saturation of the system. Moreover, we used resazurin as a normalizer for cell number and viability.

Preliminary controls in non-transfected cells and in cells transfected with a siRNA against Myc, treated with OHT for 24h confirmed that the nanoLuc signal of the reporter gene strongly increases with MycER activation, while it does not change when cells are transfected with the siMyc (figure 55A). Conversely, the resazurin signal remains constant, as expected from a normalizer (figure 55B). We concluded that the system is working and can be used to test our siRNA library.

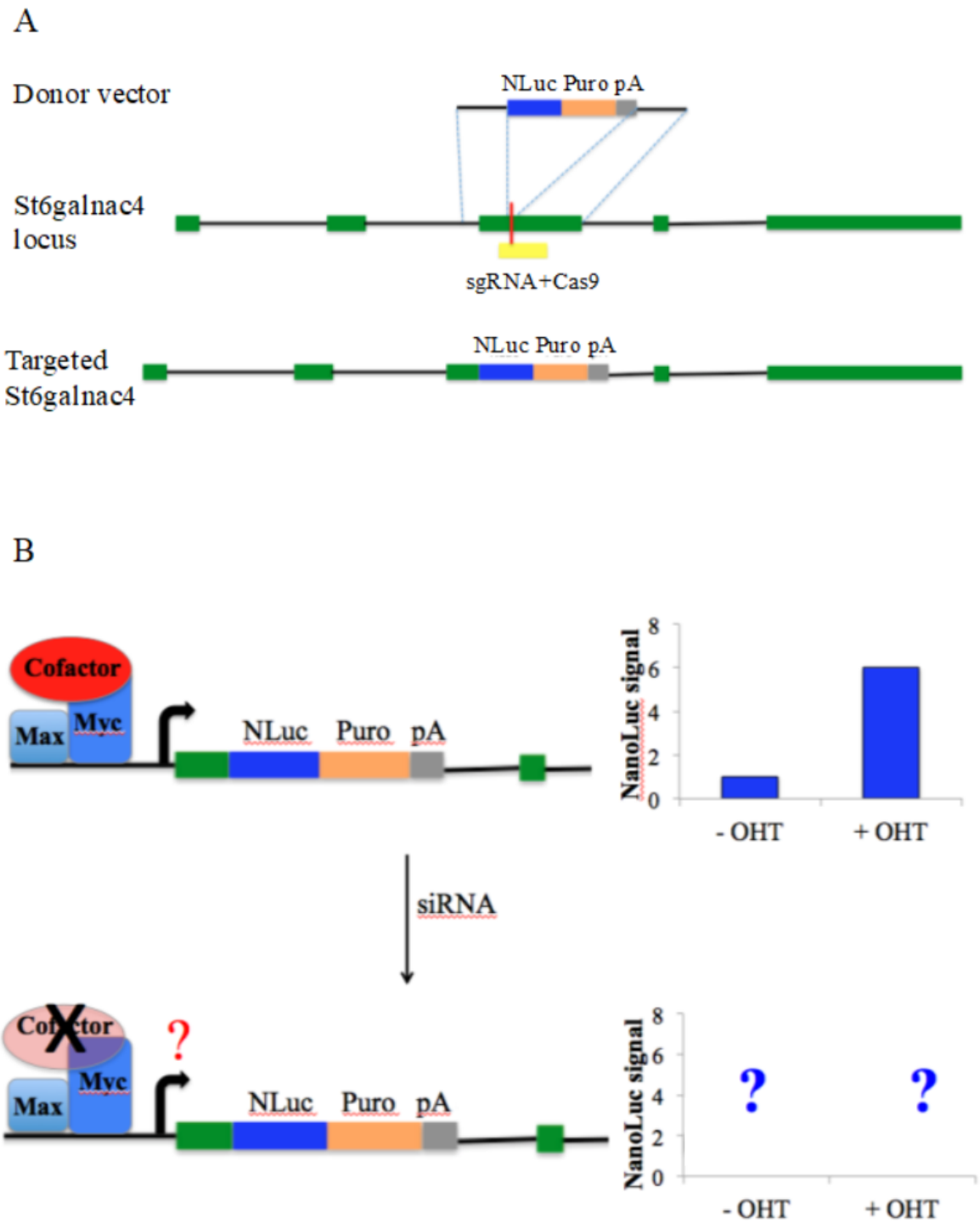

Figure 54. Functional screen setup. (A) BZ1 fibroblasts expressing an exogenous hMycER were engineered to have the NanoLuc luciferase reporter gene under the control of the St6galnac4 Myc target gene. (B) Screen model: the reporter gene is expressed at a basal level in normal conditions and is upregulated when OHT is added to the medium; if cells are transfected with an siRNA which silences a Myc cofactor, a change in the luciferase levels should be observed.

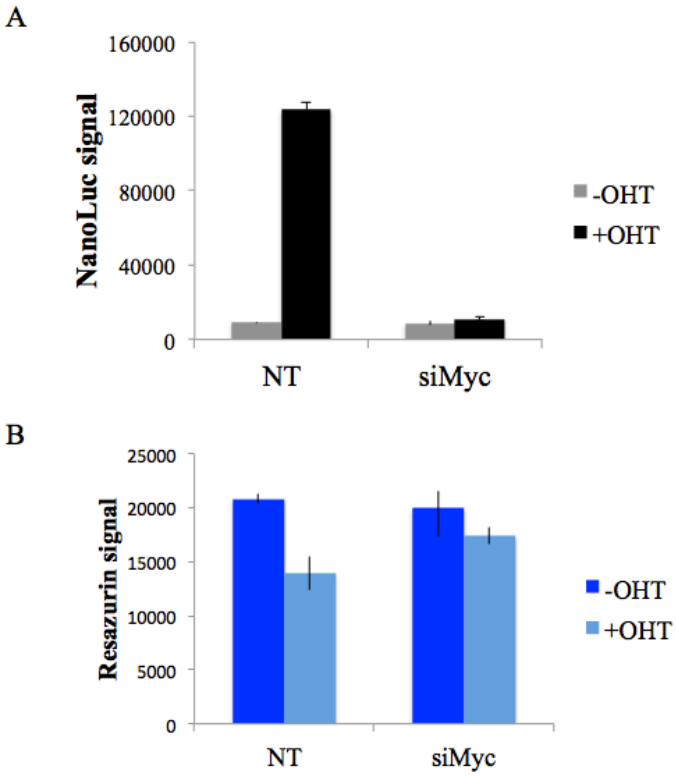

Figure 55. Preliminary controls. Non-transfected cells (NT) and cells transfected with an siRNA against Myc were treated with OHT for 24h. As expected, the NanoLuc signal significantly increases upon induction in non-transfected cells, while it does not change when the siMyc is present (A). Conversely, the resazurin signal remains constant, thus it can be used as normalizer for cell number and viability (B).

5.4.5. Screen results

We bought an siRNAs library against our list of candidates and performed the screen in two replicates. We plated cells in 96 multiwell plates and transfected them with the siRNAs. The day after, we added OHT to the medium (or ethanol in control cells) and after 24h we read the nanoLuciferase signal by spectrophotometer to evaluate the induction of the reporter gene in Myc activated cells respect to controls. Unfortunately, the two replicates we prepared did not seem to correlate very well and it was hard to identify real candidates for further validation. Moreover, the few siRNAs that induced a consistent downregulation of the reporter signal in both replicates were, apart from the positive controls (siMyc and siMax), mostly against ribosomal proteins, so we could not distinguish if the effect was specific for Myc activity or due to a more general impairment in protein translation (figure 56).

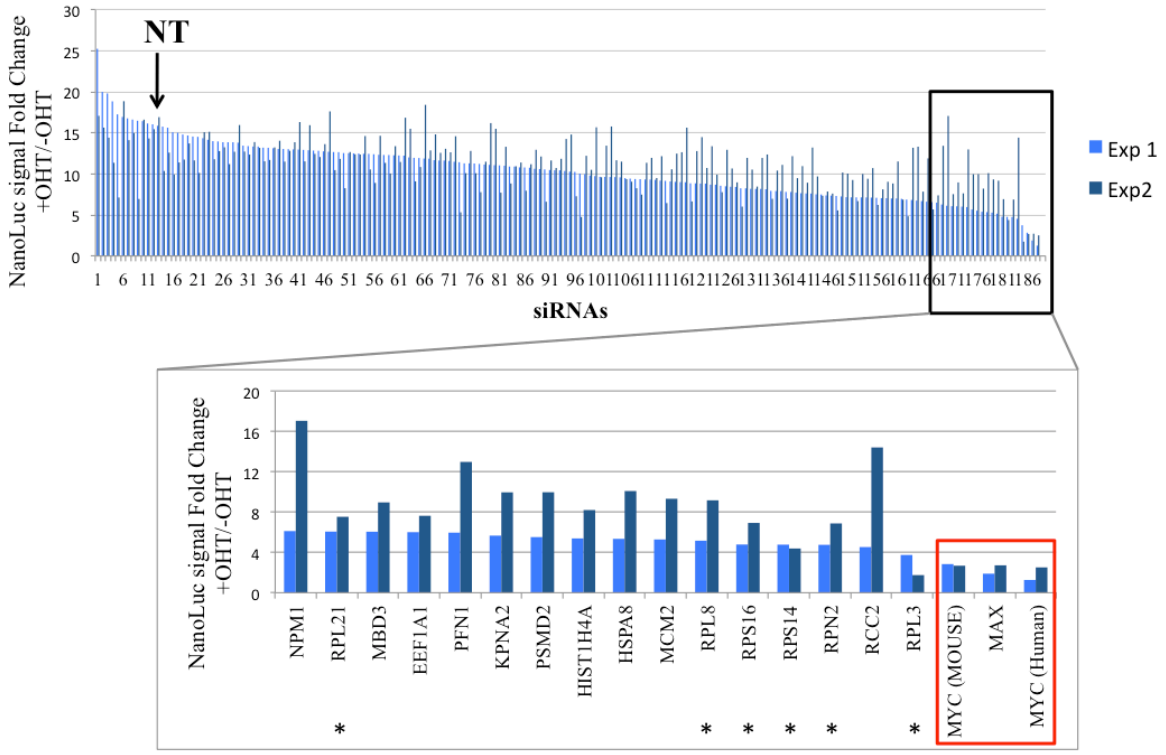

Figure 56. Functional screen results. The results obtained from the two replicates (dark blue and light blue) do not correlate so well. Moreover, most of the siRNAs that induce a reduction of the reporter signal in both the experiments are targeting ribosomal proteins (*).

In conclusion, we set up a system that is potentially very useful as a functional screen to identify genes implicated in Myc activity, but we still need to fix some technical problems. Along this line we are preparing another cell line bearing an additional reporter (Renilla luciferase) under the control of a housekeeper gene that can be used as an internal normalizer for unspecific effects on transcription/translation.

References

Agrawal, P., Yu, K., Salomon, A. R., & Sedivy, J. M. (2010). Proteomic profiling of Myc-associated proteins. *Cell Cycle*, *9*(24), 4908–4921. http://doi.org/10.4161/cc.9.24.14199

Allen, H. F., Wade, P. A., & Kutateladze, T. G. (2013). The NuRD architecture. *Cellular and Molecular Life Sciences : CMLS*, *70*(19), 3513–24. http://doi.org/10.1007/s00018-012-1256-2

Allman, D., & Pillai, S. (2008). Peripheral B cell subsets. *Current Opinion in Immunology*, *20*(2), 149–57. http://doi.org/10.1016/j.coi.2008.03.014

Amati, B., Alevizopoulos, K., & Vlach, J. (1998). Myc and the cell cycle. *Frontiers in Bioscience : A Journal and Virtual Library*, *3*, d250–68. Retrieved from http://www.ncbi.nlm.nih.gov/pubmed/9468463

Amati, B., Brooks, M. W., Levy, N., Littlewood, T. D., Evan, G. I., & Land, H. (1993a). Oncogenic activity of the c-Myc protein requires dimerization with Max. *Cell*, *72*(2), 233–45. Retrieved from http://www.ncbi.nlm.nih.gov/pubmed/8425220

Amati, B., Dalton, S., Brooks, M. W., Littlewood, T. D., Evan, G. I., & Land, H. (1992). Transcriptional activation by the human c-Myc oncoprotein in yeast requires interaction with Max. *Nature*, *359*(6394), 423–426. http://doi.org/10.1038/359423a0

Amati, B., Littlewood, T. D., Evan, G. I., & Land, H. (1993b). The c-Myc protein induces cell cycle progression and apoptosis through dimerization with Max. *The EMBO Journal*, *12*(13), 5083–7. Retrieved from http://www.ncbi.nlm.nih.gov/pubmed/8262051

Andresen, C., Helander, S., Lemak, A., Farès, C., Csizmok, V., Carlsson, J., … Sunnerhagen, M. (2012). Transient structure and dynamics in the disordered c-Myc transactivation domain affect Bin1 binding. *Nucleic Acids Research*, *40*(13), 6353–66. http://doi.org/10.1093/nar/gks263

Arabi, A., Wu, S., Ridderstråle, K., Bierhoff, H., Shiue, C., Fatyol, K., … Wright, A. P. H. (2005). c-Myc associates with ribosomal DNA and activates RNA polymerase I transcription. *Nature Cell Biology*, *7*(3), 303–10. http://doi.org/10.1038/ncb1225

Avitahl, N., Winandy, S., Friedrich, C., Jones, B., Ge, Y., & Georgopoulos, K. (1999). Ikaros sets thresholds for T cell activation and regulates chromosome propagation. *Immunity*, *10*(3), 333–43. Retrieved from http://www.ncbi.nlm.nih.gov/pubmed/10204489

Bahram, F., von der Lehr, N., Cetinkaya, C., & Larsson, L. G. (2000). c-Myc hot spot mutations in lymphomas result in inefficient ubiquitination and decreased proteasome-mediated turnover. *Blood*, *95*(6), 2104–10. Retrieved from http://www.ncbi.nlm.nih.gov/pubmed/10706881

Bailey, T. L. (2011). DREME: motif discovery in transcription factor ChIP-seq data. *Bioinformatics*, *27*(12), 1653–1659. http://doi.org/10.1093/bioinformatics/btr261

Bailey, T. L., Boden, M., Buske, F. A., Frith, M., Grant, C. E., Clementi, L., … Noble, W. S. (2009). MEME SUITE: tools for motif discovery and searching. *Nucleic Acids Research*, *37*(Web Server), W202–W208. http://doi.org/10.1093/nar/gkp335

Baldin, V., Lukas, J., Marcote, M. J., Pagano, M., & Draetta, G. (1993). Cyclin D1 is a nuclear protein required for cell cycle progression in G1. *Genes & Development*, *7*(5), 812–21. http://doi.org/10.1101/GAD.7.5.812

Baudino, T. A., McKay, C., Pendeville-Samain, H., Nilsson, J. A., Maclean, K. H., White, E. L., … Cleveland, J. L. (2002). c-Myc is essential for vasculogenesis and angiogenesis during development and tumor progression. *Genes & Development*, *16*(19), 2530–43. http://doi.org/10.1101/gad.1024602

Bianchi, V., Ceol, A., Ogier, A. G. E., de Pretis, S., Galeota, E., Kishore, K., … Pelizzola,

M. (2016). Integrated Systems for NGS Data Management and Analysis: Open Issues and Available Solutions. *Frontiers in Genetics*, *7*, 75. http://doi.org/10.3389/fgene.2016.00075

Bissonnette, R. P., Echeverri, F., Mahboubi, A., & Green, D. R. (1992). Apoptotic cell death induced by c-myc is inhibited by bcl-2. *Nature*, *359*(6395), 552–554. http://doi.org/10.1038/359552a0

Bjorklund, C. C., Lu, L., Kang, J., Hagner, P. R., Havens, C. G., Amatangelo, M., … Thakurta, a G. (2015). Rate of CRL4(CRBN) substrate Ikaros and Aiolos degradation underlies differential activity of lenalidomide and pomalidomide in multiple myeloma cells by regulation of c-Myc and IRF4. *Blood Cancer Journal*, *5*(July), e354. http://doi.org/10.1038/bcj.2015.66

Blackwell, T. K., Huang, J., Ma, A., Kretzner, L., Alt, F. W., Eisenman, R. N., & Weintraub, H. (1993). Binding of myc proteins to canonical and noncanonical DNA sequences. *Molecular and Cellular Biology*, *13*(9), 5216–24. Retrieved from http://www.ncbi.nlm.nih.gov/pubmed/8395000

Blackwell, T. K., Kretzner, L., Blackwood, E. M., Eisenman, R. N., & Weintraub, H. (1990). Sequence-specific DNA binding by the c-Myc protein. *Science (New York, N.Y.)*, *250*(4984), 1149–51. Retrieved from http://www.ncbi.nlm.nih.gov/pubmed/2251503

Bottardi, S., Mavoungou, L., Bourgoin, V., Mashtalir, N., Affar, E. B., & Milot, E. (2013). Direct Protein Interactions Are Responsible for Ikaros-GATA and Ikaros-Cdk9 Cooperativeness in Hematopoietic Cells. *Molecular and Cellular Biology*, *33*(16), 3064–3076. http://doi.org/10.1128/MCB.00296-13

Bottardi, S., Mavoungou, L., & Milot, E. (2015). IKAROS: A multifunctional regulator of the polymerase II transcription cycle. *Trends in Genetics*, *31*(9), 500–508. http://doi.org/10.1016/j.tig.2015.05.003

Bottardi, S., Mavoungou, L., Pak, H., Daou, S., Bourgoin, V., Lakehal, Y. a, … Milot, E. (2014). The IKAROS interaction with a complex including chromatin remodeling and transcription elongation activities is required for hematopoiesis. *PLoS Genetics*, *10*(12), e1004827. http://doi.org/10.1371/journal.pgen.1004827

Bottardi, S., Zmiri, F. a, Bourgoin, V., Ross, J., Mavoungou, L., & Milot, E. (2011). Ikaros interacts with P-TEFb and cooperates with GATA-1 to enhance transcription elongation. *Nucleic Acids Research*, *39*(9), 3505–19. http://doi.org/10.1093/nar/gkq1271

Bouchard, C., Marquardt, J., Brás, A., Medema, R. H., & Eilers, M. (2004). Myc-induced proliferation and transformation require Akt-mediated phosphorylation of FoxO proteins. *The EMBO Journal*, *23*(14), 2830–40. http://doi.org/10.1038/sj.emboj.7600279

Brenner, C., Deplus, R., Didelot, C., Loriot, A., Viré, E., De Smet, C., … Fuks, F. (2005). Myc represses transcription through recruitment of DNA methyltransferase corepressor. *The EMBO Journal*, *24*(2), 336–46. http://doi.org/10.1038/sj.emboj.7600509

Brown, K. E., Guest, S. S., Smale, S. T., Hahm, K., Merkenschlager, M., & Fisher, A. G. (1997). Association of transcriptionally silent genes with Ikaros complexes at centromeric heterochromatin. *Cell*, *91*(6), 845–54. Retrieved from http://www.ncbi.nlm.nih.gov/pubmed/9413993

Busslinger, M. (2004). Transcriptional Control of Early B Cell Development. *Annual Review of Immunology*, *22*(1), 55–79. http://doi.org/10.1146/annurev.immunol.22.012703.104807

Byrum, S. D., Raman, A., Taverna, S. D., & Tackett, A. J. (2012). ChAP-MS: A Method for Identification of Proteins and Histone Posttranslational Modifications at a Single Genomic Locus. *Cell Reports*, *2*(1), 198–205. http://doi.org/10.1016/j.celrep.2012.06.019

Caballero, R., Setien, F., Lopez-Serra, L., Boix-Chornet, M., Fraga, M. F., Ropero, S., … Ballestar, E. (2007). Combinatorial effects of splice variants modulate function of Aiolos. *Journal of Cell Science*, *120*(15), 2619–2630. http://doi.org/10.1242/jcs.007344

Calado, D. P., Sasaki, Y., Godinho, S. A., Pellerin, A., Köchert, K., Sleckman, B. P., … Rajewsky, K. (2012). The cell-cycle regulator c-Myc is essential for the formation and maintenance of germinal centers. *Nature Immunology*, *13*(11), 1092–100. http://doi.org/10.1038/ni.2418

Cancro, M. P., & Kearney, J. F. (2004). B cell positive selection: road map to the primary repertoire? *Journal of Immunology (Baltimore, Md. : 1950)*, *173*(1), 15–9. Retrieved from http://www.ncbi.nlm.nih.gov/pubmed/15210753

Cariappa, A., Tang, M., Parng, C., Nebelitskiy, E., Carroll, M., Georgopoulos, K., & Pillai, S. (2001). The follicular versus marginal zone B lymphocyte cell fate decision is regulated by Aiolos, Btk, and CD21. *Immunity*, *14*(5), 603–15. Retrieved from http://www.ncbi.nlm.nih.gov/pubmed/11371362

Carsetti, R., Köhler, G., & Lamers, M. C. (1995). Transitional B cells are the target of negative selection in the B cell compartment. *The Journal of Experimental Medicine*, *181*(6), 2129–40. Retrieved from http://www.ncbi.nlm.nih.gov/pubmed/7760002

Carugo, A., Genovese, G., Seth, S., Nezi, L., Rose, J. L., Bossi, D., … Draetta, G. F. (2016). In Vivo Functional Platform Targeting Patient-Derived Xenografts Identifies WDR5-Myc Association as a Critical Determinant of Pancreatic Cancer. *Cell Reports*, *16*(1), 133–147. http://doi.org/10.1016/j.celrep.2016.05.063

Casola, S., Otipoby, K. L., Alimzhanov, M., Humme, S., Uyttersprot, N., Kutok, J. L., … Rajewsky, K. (2004). B cell receptor signal strength determines B cell fate. *Nature Immunology*, *5*(3), 317–327. http://doi.org/10.1038/ni1036

Catena, V., & Fanciulli, M. (2017). Deptor: not only a mTOR inhibitor. *Journal of Experimental & Clinical Cancer Research*, *36*(1), 12. http://doi.org/10.1186/s13046-016-0484-y

Chan, L. N., Chen, Z., Braas, D., Lee, J.-W., Xiao, G., Geng, H., … Müschen, M. (2017). Metabolic gatekeeper function of B-lymphoid transcription factors. *Nature*, *542*(7642), 1–5. http://doi.org/10.1038/nature21076

Cheng, S.-W. G., Davies, K. P., Yung, E., Beltran, R. J., Yu, J., & Kalpana, G. V. (1999). c-MYC interacts with INI1/hSNF5 and requires the SWI/SNF complex for transactivation function. *Nature Genetics*, *22*(1), 102–105. http://doi.org/10.1038/8811

Churchman, M. L., Low, J., Qu, C., Paietta, E. M., Kasper, L. H., Chang, Y., … Mullighan, C. G. (2015). Efficacy of Retinoids in IKZF1-Mutated BCR-ABL1 Acute Lymphoblastic Leukemia. *Cancer Cell*, *28*(3), 343–356. http://doi.org/10.1016/j.ccell.2015.07.016

Cobb, B. S., Morales-Alcelay, S., Kleiger, G., Brown, K. E., Fisher, A. G., & Smale, S. T. (2000). Targeting of Ikaros to pericentromeric heterochromatin by direct DNA binding. *Genes & Development*, *14*(17), 2146–60. Retrieved from http://www.ncbi.nlm.nih.gov/pubmed/10970879

Conacci-Sorrell, M., McFerrin, L., & Eisenman, R. N. (2014). An Overview of MYC and Its Interactome. *Cold Spring Harbor Perspectives in Medicine*, *4*(1), a014357. http://doi.org/10.1101/cshperspect.a014357

Cortés, M., & Georgopoulos, K. (2004). Aiolos is required for the generation of high affinity bone marrow plasma cells responsible for long-term immunity. *The Journal of Experimental Medicine*, *199*(2), 209–19. http://doi.org/10.1084/jem.20031571

Cortes, M., Wong, E., Koipally, J., & Georgopoulos, K. (1999). Control of lymphocyte development by the Ikaros gene family. *Current Opinion in Immunology*, *11*(2), 167–71. Retrieved from http://www.ncbi.nlm.nih.gov/pubmed/10322160

Cox, J., Neuhauser, N., Michalski, A., Scheltema, R. A., Olsen, J. V, & Mann, M. (2011).

Andromeda: a peptide search engine integrated into the MaxQuant environment. *Journal of Proteome Research*, *10*(4), 1794–805. http://doi.org/10.1021/pr101065j

Creyghton, M. P., Cheng, A. W., Welstead, G. G., Kooistra, T., Carey, B. W., Steine, E. J., … Jaenisch, R. (2010). Histone H3K27ac separates active from poised enhancers and predicts developmental state. *Proceedings of the National Academy of Sciences of the United States of America*, *107*(50), 21931–6. http://doi.org/10.1073/pnas.1016071107

Cyster, J. G. (2010). B cell follicles and antigen encounters of the third kind. *Nature Immunology*, *11*(11), 989–96. http://doi.org/10.1038/ni.1946

Dalla-Favera, R., Bregni, M., Eriksont, J., Pattersonf, D., Gallo, R. C., & Crocet, C. M. (1982). Human c-myc onc Gene is Located on the Region of Chromosome 8 that is Translocated in Burkitt Lymphoma Cells. *Proceedings of the National Academy of Sciences*, *79*(December), 7824–7827. http://doi.org/10.1073/pnas.79.24.7824

Dang, C. V. (2012). MYC on the Path to Cancer. *Cell*, *149*, 22–35. http://doi.org/10.1016/j.cell.2012.03.003

Davis, A. C., Wims, M., Spotts, G. D., Hann, S. R., & Bradley, A. (1993). A null c-myc mutation causes lethality before 10.5 days of gestation in homozygotes and reduced fertility in heterozygous female mice. *Genes & Development*, *7*(4), 671–82. Retrieved from http://www.ncbi.nlm.nih.gov/pubmed/8458579

de Pretis, S., Kress, T. R., Morelli, M. J., Sabò, A., Locarno, C., Verrecchia, A., … Pelizzola, M. (2017). Integrative analysis of RNA polymerase II and transcriptional dynamics upon MYC activation. *Genome Research*, *27*(10), 1658–1664. http://doi.org/10.1101/gr.226035.117

Delgado, M. D., & Leon, J. (2010). Myc Roles in Hematopoiesis and Leukemia. *Genes & Cancer*, *1*(6), 605–616. http://doi.org/10.1177/1947601910377495

Delmore, J. E., Issa, G. C., Lemieux, M. E., Rahl, P. B., Shi, J., Jacobs, H. M., … Mitsiades, C. S. (2011). BET Bromodomain Inhibition as a Therapeutic Strategy to Target c-Myc. *Cell*, *146*(6), 904–917. http://doi.org/10.1016/j.cell.2011.08.017

Dengler, H. S., Baracho, G. V, Omori, S. A., Bruckner, S., Arden, K. C., Castrillon, D. H., … Rickert, R. C. (2008). Distinct functions for the transcription factor Foxo1 at various stages of B cell differentiation. *Nature Immunology*, *9*(12), 1388–98. http://doi.org/10.1038/ni.1667

Dews, M., Homayouni, A., Yu, D., Murphy, D., Sevignani, C., Furth, E. E., … Mendell, J. T. (2009). Augmentation of tumor angiogenesis by a Myc-activated microRNA cluster, *38*(9), 1060–1065. http://doi.org/10.1038/ng1855.Augmentation

Dingar, D., Kalkat, M., Chan, P.-K., Srikumar, T., Bailey, S. D., Tu, W. B., … Raught, B. (2015). BioID identifies novel c-MYC interacting partners in cultured cells and xenograft tumors. *Journal of Proteomics*, *118*, 95–111. http://doi.org/10.1016/j.jprot.2014.09.029

Diolaiti, D., McFerrin, L., Carroll, P. A., & Eisenman, R. N. (2015). Functional interactions among members of the MAX and MLX transcriptional network during oncogenesis. *Biochimica et Biophysica Acta*, *1849*(5), 484–500. http://doi.org/10.1016/j.bbagrm.2014.05.016

Dominguez-Sola, D., Victora, G. D., Ying, C. Y., Phan, R. T., Saito, M., Nussenzweig, M. C., & Dalla-Favera, R. (2012). The proto-oncogene MYC is required for selection in the germinal center and cyclic reentry. *Nature Immunology*, *13*(11), 1083–1091. http://doi.org/10.1038/ni.2428

Dominguez-Sola, D., Ying, C. Y., Grandori, C., Ruggiero, L., Chen, B., Li, M., … Dalla-Favera, R. (2007). Non-transcriptional control of DNA replication by c-Myc. *Nature*, *448*(7152), 445–451. http://doi.org/10.1038/nature05953

Donato, E., Croci, O., Sabò, A., Muller, H., Morelli, M. J., Pelizzola, M., & Campaner, S. (2017). Compensatory RNA polymerase 2 loading determines the efficacy and transcriptional selectivity of JQ1 in Myc-driven tumors. *Leukemia*, *31*(2), 479–490. http://doi.org/10.1038/leu.2016.182

Dovat, S. (2013). Ikaros: the enhancer makes the difference. *Blood*, *122*(18), 3091–2. http://doi.org/10.1182/blood-2013-09-526343
Eberhardy, S. R., & Farnham, P. J. (2001). c-Myc Mediates Activation of the *cad* Promoter via a Post-RNA Polymerase II Recruitment Mechanism. *Journal of Biological Chemistry*, *276*(51), 48562–48571. http://doi.org/10.1074/jbc.M109014200
Eberhardy, S. R., & Farnham, P. J. (2002). Myc recruits P-TEFb to mediate the final step in the transcriptional activation of the cad promoter. *The Journal of Biological Chemistry*, *277*(42), 40156–62. http://doi.org/10.1074/jbc.M207441200
Edmunds, L. R., Sharma, L., Kang, A., Lu, J., Vockley, J., Basu, S., … Prochownik, E. V. (2014). c-Myc Programs Fatty Acid Metabolism and Dictates Acetyl-CoA Abundance and Fate. *Journal of Biological Chemistry*, *289*(36), 25382–25392. http://doi.org/10.1074/jbc.M114.580662
Egistelli, L., Chichiarelli, S., Gaucci, E., Eufemi, M., Schininà, M. E., Giorgi, A., … Cervoni, L. (2009). IFI16 and NM23 bind to a common DNA fragment both in the P53 and the cMYC gene promoters. *Journal of Cellular Biochemistry*, *106*(4), 666–72. http://doi.org/10.1002/jcb.22053
Eischen, C. M., Packham, G., Nip, J., Fee, B. E., Hiebert, S. W., Zambetti, G. P., & Cleveland, J. L. (2001). Bcl-2 is an apoptotic target suppressed by both c-Myc and E2F-1. *Oncogene*, *20*(48), 6983–6993. http://doi.org/10.1038/sj.onc.1204892
Evan, G. I., Wyllie, A. H., Gilbert, C. S., Littlewood, T. D., Land, H., Brooks, M., … Hancock, D. C. (1992). Induction of apoptosis in fibroblasts by c-myc protein. *Cell*, *69*(1), 119–28. Retrieved from http://www.ncbi.nlm.nih.gov/pubmed/1555236
Fanidi, A., Harrington, E. A., & Evan, G. I. (1992). Cooperative interaction between c-myc and bcl-2 proto-oncogenes. *Nature*, *359*(6395), 554–556. http://doi.org/10.1038/359554a0
Felsher, D. W. (2010). MYC Inactivation Elicits Oncogene Addiction through Both Tumor Cell-Intrinsic and Host-Dependent Mechanisms. *Genes & Cancer*, *1*(6), 597–604. http://doi.org/10.1177/1947601910377798
Felsher, D. W., & Bishop, J. M. (1999). Transient excess of MYC activity can elicit genomic instability and tumorigenesis. *Proceedings of the National Academy of Sciences of the United States of America*, *96*(7), 3940–4. Retrieved from http://www.ncbi.nlm.nih.gov/pubmed/10097142
Feng, X.-H., Liang, Y.-Y., Liang, M., Zhai, W., & Lin, X. (2002). Direct interaction of c-Myc with Smad2 and Smad3 to inhibit TGF-beta-mediated induction of the CDK inhibitor p15(Ink4B). *Molecular Cell*, *9*(1), 133–43. Retrieved from http://www.ncbi.nlm.nih.gov/pubmed/11804592
Ferdinandusse, S., Denis, S., van Roermund, C. W. T., Preece, M. A., Koster, J., Ebberink, M. S., … Wanders, R. J. A. (2017). A novel case of ACOX2 deficiency leads to recognition of a third human peroxisomal acyl-CoA oxidase. *Biochimica et Biophysica Acta (BBA) - Molecular Basis of Disease*. http://doi.org/10.1016/j.bbadis.2017.12.032
Fernandez, P. C., Frank, S. R., Wang, L., Schroeder, M., Liu, S., Greene, J., … Amati, B. (2003). Genomic targets of the human c-Myc protein. *Genes & Development*, *17*(9), 1115–29. http://doi.org/10.1101/gad.1067003
Ferreirós-Vidal, I., Carroll, T., Taylor, B., Terry, A., Liang, Z., Bruno, L., … Merkenschlager, M. (2013). Genome-wide identification of Ikaros targets elucidates its contribution to mouse B-cell lineage specification and pre-B-cell differentiation. *Blood*, *121*(10), 1769–82. http://doi.org/10.1182/blood-2012-08-450114
Fink, E. C., & Ebert, B. L. (2015). The novel mechanism of lenalidomide activity. *Blood*, *126*(21), 2366–2369. http://doi.org/10.1182/blood-2015-07-567958
Frank, S. R., Parisi, T., Taubert, S., Fernandez, P., Fuchs, M., Chan, H.-M., … Amati, B. (2003). MYC recruits the TIP60 histone acetyltransferase complex to chromatin. *EMBO Reports*, *4*(6), 575–580. http://doi.org/10.1038/sj.embor.embor861

Frisch, S. M., & Schaller, M. D. (2014). The wind god promotes lung cancer. *Cancer Cell*, *25*(5), 551–2. http://doi.org/10.1016/j.ccr.2014.04.022
Frye, M., Gardner, C., Li, E. R., Arnold, I., & Watt, F. M. (2003). Evidence that Myc activation depletes the epidermal stem cell compartment by modulating adhesive interactions with the local microenvironment. *Development (Cambridge, England)*, *130*(12), 2793–808. Retrieved from http://www.ncbi.nlm.nih.gov/pubmed/12736221
Gabay, M., Li, Y., & Felsher, D. W. (2014). MYC Activation Is a Hallmark of Cancer Initiation and Maintenance. *Cold Spring Harbor Perspectives in Medicine*, *4*(6), a014241–a014241. http://doi.org/10.1101/cshperspect.a014241
Gao, Ping, E. Al. (2009). c-Myc suppression of miR-23 enhances mitochondrial glutaminase and glutamine metabolism. *Nature*, *458*(7239), 762–765. http://doi.org/10.1038/nature07823.c-Myc
Garcia-Sanz, P., Quintanilla, A., Lafita, M. C., Moreno-Bueno, G., García-Gutierrez, L., Tabor, V., … Leon, J. (2014). Sin3b interacts with Myc and decreases Myc levels. *The Journal of Biological Chemistry*, *289*(32), 22221–36. http://doi.org/10.1074/jbc.M113.538744
Garcia, H., Miecznikowski, J. C., Safina, A., Commane, M., Ruusulehto, A., Kilpinen, S., … Gurova, K. V. (2013). Facilitates chromatin transcription complex is an "accelerator" of tumor transformation and potential marker and target of aggressive cancers. *Cell Reports*, *4*(1), 159–73. http://doi.org/10.1016/j.celrep.2013.06.013
Gartel, A. L., Ye, X., Goufman, E., Shianov, P., Hay, N., Najmabadi, F., & Tyner, A. L. (2001). Myc represses the p21(WAF1/CIP1) promoter and interacts with Sp1/Sp3. *Proceedings of the National Academy of Sciences of the United States of America*, *98*(8), 4510–5. http://doi.org/10.1073/pnas.081074898
Georgopoulos, K. (2017). The making of a lymphocyte: the choice among disparate cell fates and the IKAROS enigma. *Genes & Development*, *31*(5), 439–450. http://doi.org/10.1101/gad.297002.117
Georgopoulos, K., Bigby, M., Wang, J. H., Molnar, A., Wu, P., Winandy, S., & Sharpe, A. (1994). The Ikaros gene is required for the development of all lymphoid lineages. *Cell*, *79*(1), 143–56. Retrieved from http://www.ncbi.nlm.nih.gov/pubmed/7923373
Georgopoulos, K., Moore, D. D., & Derfler, B. (1992). Ikaros, an early lymphoid-specific transcription factor and a putative mediator for T cell commitment. *Science (New York, N.Y.)*, *258*(5083), 808–12. Retrieved from http://www.ncbi.nlm.nih.gov/pubmed/1439790
Georgopoulos, K., Winandy, S., & Avitahl, N. (1997). The role of the Ikaros gene in lymphocyte development and homeostasis. *Annual Review of Immunology*, *15*(1), 155–176. http://doi.org/10.1146/annurev.immunol.15.1.155
Gómez-del Arco, P., Maki, K., & Georgopoulos, K. (2004). Phosphorylation controls Ikaros's ability to negatively regulate the G(1)-S transition. *Molecular and Cellular Biology*, *24*(7), 2797–807. Retrieved from http://www.ncbi.nlm.nih.gov/pubmed/15024069
Gomez-Roman, N., Grandori, C., Eisenman, R. N., & White, R. J. (2003). Direct activation of RNA polymerase III transcription by c-Myc. *Nature*, *421*(6920), 290–294. http://doi.org/10.1038/nature01327
Gowda, C., Soliman, M., Kapadia, M., Ding, Y., Payne, K., & Dovat, S. (2017). Casein Kinase II (CK2), Glycogen Synthase Kinase-3 (GSK-3) and Ikaros mediated regulation of leukemia. *Advances in Biological Regulation*, *3*, 1–10. http://doi.org/10.1016/j.jbior.2017.06.001
Graham, F. L., & van der Eb, A. J. (1973). Transformation of rat cells by DNA of human adenovirus 5. *Virology*, *54*(2), 536–9. Retrieved from http://www.ncbi.nlm.nih.gov/pubmed/4737663
Grandori, C., Cowley, S. M., James, L. P., & Eisenman, R. N. (2000). The Myc/Max/Mad

Network and the Transcriptional Control of Cell Behavior. *Annual Review of Cell and Developmental Biology*, *16*(1), 653–699. http://doi.org/10.1146/annurev.cellbio.16.1.653

Guccione, E., Martinato, F., Finocchiaro, G., Luzi, L., Tizzoni, L., Dall' Olio, V., … Amati, B. (2006). Myc-binding-site recognition in the human genome is determined by chromatin context. *Nature Cell Biology*, *8*(7), 764–770. http://doi.org/10.1038/ncb1434

Guibal, F. C., Moog-Lutz, C., Smolewski, P., Gioia, Y. Di, Darzynkiewicz, Z., Lutz, P. G., & Cayre, Y. E. (2001). ASB-2 Inhibits Growth and Promotes Commitment in Myeloid Leukemia Cells*. http://doi.org/10.1074/jbc.M108476200

Habib, T., Park, H., Tsang, M., de Alborán, I. M., Nicks, A., Wilson, L., … Iritani, B. M. (2007). Myc stimulates B lymphocyte differentiation and amplifies calcium signaling. *The Journal of Cell Biology*, *179*(4), 717–31. http://doi.org/10.1083/jcb.200704173

Hahm, K., Cobb, B. S., McCarty, A. S., Brown, K. E., Klug, C. A., Lee, R., … Smale, S. T. (1998). Helios, a T cell-restricted Ikaros family member that quantitatively associates with Ikaros at centromeric heterochromatin. *Genes and Development*, *12*(6), 782–796. http://doi.org/10.1101/gad.12.6.782

Hahm, K., Ernst, P., Lo, K., Kim, G. S., Turck, C., & Smale, S. T. (1994). The lymphoid transcription factor LyF-1 is encoded by specific, alternatively spliced mRNAs derived from the Ikaros gene. *Molecular and Cellular Biology*, *14*(11), 7111–23. Retrieved from http://www.ncbi.nlm.nih.gov/pubmed/7935426

Hall, Z., Ament, Z., Wilson, C. H., Burkhart, D. L., Ashmore, T., Koulman, A., … Griffin, J. L. (2016). Myc Expression Drives Aberrant Lipid Metabolism in Lung Cancer. *Cancer Research*, *76*(16), 4608–18. http://doi.org/10.1158/0008-5472.CAN-15-3403

Hardy, B. R. R., Carmack, C. E., Shinton, S. A., Kemp, J. D., & Hayakawa, K. (1991). Resolution and Characterization of Pro-B and Pre-Pro-B Cell Stages in Normal Mouse, (May).

Harker, N., Naito, T., Cortes, M., Hostert, A., Hirschberg, S., Tolaini, M., … Kioussis, D. (2002). The CD8alpha gene locus is regulated by the Ikaros family of proteins. *Molecular Cell*, *10*(6), 1403–15. Retrieved from http://www.ncbi.nlm.nih.gov/pubmed/12504015

Hateboer, G., Timmers, H. T., Rustgi, A. K., Billaud, M., van 't Veer, L. J., & Bernards, R. (1993). TATA-binding protein and the retinoblastoma gene product bind to overlapping epitopes on c-Myc and adenovirus E1A protein. *Proceedings of the National Academy of Sciences of the United States of America*, *90*(18), 8489–93. Retrieved from http://www.ncbi.nlm.nih.gov/pubmed/7690963

Heizmann, B., Kastner, P., & Chan, S. (2013). Ikaros is absolutely required for pre-B cell differentiation by attenuating IL-7 signals. *The Journal of Experimental Medicine*, *210*(13), 2823–32. http://doi.org/10.1084/jem.20131735

Hemann, M. T., Bric, A., Teruya-Feldstein, J., Herbst, A., Nilsson, J. A., Cordon-Cardo, C., … Lowe, S. W. (2005). Evasion of the p53 tumour surveillance network by tumour-derived MYC mutants. *Nature*, *436*(7052), 807–811. http://doi.org/10.1038/nature03845

Hess, J., Werner, A., Wirth, T., Melchers, F., Jäck, H. M., & Winkler, T. H. (2001). Induction of pre-B cell proliferation after de novo synthesis of the pre-B cell receptor. *Proceedings of the National Academy of Sciences of the United States of America*, *98*(4), 1745–50. http://doi.org/10.1073/pnas.041492098

Honma, Y., Kiyosawa, H., Mori, T., Oguri, A., Nikaido, T., Kanazawa, K. Y., … Wanaka, A. (1999). Eos: A novel member of the Ikaros gene family expressed predominantly in the developing nervous system. *FEBS Letters*, *447*(1), 76–80. http://doi.org/10.1016/S0014-5793(99)00265-3

Hoover-Fong, J., Sobreira, N., Jurgens, J., Modaff, P., Blout, C., Moser, A., … Pauli, R. M. (2014). Mutations in PCYT1A, Encoding a Key Regulator of Phosphatidylcholine

Metabolism, Cause Spondylometaphyseal Dysplasia with Cone-Rod Dystrophy. *The American Journal of Human Genetics*, *94*(1), 105–112. http://doi.org/10.1016/j.ajhg.2013.11.018

Horiuchi, D., Anderton, B., & Goga, A. (2014). Taking on challenging targets: making MYC druggable. *American Society of Clinical Oncology Educational Book. American Society of Clinical Oncology. Meeting*, *34*, e497–502. http://doi.org/10.14694/EdBook_AM.2014.34.e497

Hosokawa, Y., Maeda, Y., Takahashi, E., Suzuki, M., & Seto, M. (1999). Human Aiolos, an Ikaros-Related Zinc Finger DNA Binding Protein: cDNA Cloning, Tissue Expression Pattern, and Chromosomal Mapping. *Genomics*, *61*(3), 326–329. http://doi.org/10.1006/geno.1999.5949

Hsieh, A. L., Walton, Z. E., Altman, B. J., Stine, Z. E., & Dang, C. V. (2015). MYC and metabolism on the path to cancer. *Seminars in Cell & Developmental Biology*, *43*, 11–21. http://doi.org/10.1016/j.semcdb.2015.08.003

Hu, Y., Zhang, Z., Kashiwagi, M., Yoshida, T., Joshi, I., Jena, N., … Georgopoulos, K. (2016). Superenhancer reprogramming drives a B-cell-epithelial transition and high-risk leukemia. *Genes and Development*, *30*(17), 1971–1990. http://doi.org/10.1101/gad.283762.116

Iritani, B. M., & Eisenman, R. N. (1999). c-Myc enhances protein synthesis and cell size during B lymphocyte development. *Proceedings of the National Academy of Sciences of the United States of America*, *96*(23), 13180–5. Retrieved from http://www.ncbi.nlm.nih.gov/pubmed/10557294

Izumi, H., Molander, C., Penn, L. Z., Ishisaki, A., Kohno, K., & Funa, K. (2001). Mechanism for the transcriptional repression by c-Myc on PDGF beta-receptor. *Journal of Cell Science*, *114*(Pt 8), 1533–44. Retrieved from http://www.ncbi.nlm.nih.gov/pubmed/11282029

Joshi, I., Yoshida, T., Jena, N., Qi, X., Zhang, J., Van Etten, R. A., & Georgopoulos, K. (2014). Loss of Ikaros DNA-binding function confers integrin-dependent survival on pre-B cells and progression to acute lymphoblastic leukemia. *Nature Immunology*, *15*(3), 294–304. http://doi.org/10.1038/ni.2821

Jung, L. A., Gebhardt, A., Koelmel, W., Ade, C. P., Walz, S., Kuper, J., … Eilers, M. (2017). OmoMYC blunts promoter invasion by oncogenic MYC to inhibit gene expression characteristic of MYC-dependent tumors. *Oncogene*, *36*(14), 1911–1924. http://doi.org/10.1038/onc.2016.354

Kaiser, C., Laux, G., Eick, D., Jochner, N., Bornkamm, G. W., & Kempkes, B. (1999). The proto-oncogene c-myc is a direct target gene of Epstein-Barr virus nuclear antigen 2. *Journal of Virology*, *73*(5), 4481–4. Retrieved from http://www.ncbi.nlm.nih.gov/pubmed/10196351

Katerndahl, C. D. S., Heltemes-Harris, L. M., Willette, M. J. L., Henzler, C. M., Frietze, S., Yang, R., … Farrar, M. A. (2017). Antagonism of B cell enhancer networks by STAT5 drives leukemia and poor patient survival. *Nature Immunology*, *18*(6), 694–704. http://doi.org/10.1038/ni.3716

Kato, G. J., Barrett, J., Villa-Garcia, M., & Dang, C. V. (1990). An amino-terminal c-myc domain required for neoplastic transformation activates transcription. *Molecular and Cellular Biology*, *10*(11), 5914–20. Retrieved from http://www.ncbi.nlm.nih.gov/pubmed/2233723

Kelley, C. M., Ikeda, T., Koipally, J., Avitahl, N., Wu, L., Georgopoulos, K., & Morgan, B. A. (1998). Helios, a novel dimerization partner of Ikaros expressed in the earliest hematopoietic progenitors. *Current Biology : CB*, *8*(9), 508–15. Retrieved from http://www.ncbi.nlm.nih.gov/pubmed/9560339

Kempkes, B., Spitkovsky, D., Jansen-Dürr, P., Ellwart, J. W., Kremmer, E., Delecluse, H. J., … Hammerschmidt, W. (1995). B-cell proliferation and induction of early G1-regulating proteins by Epstein-Barr virus mutants conditional for EBNA2. *The EMBO*

Journal, *14*(1), 88–96. Retrieved from http://www.ncbi.nlm.nih.gov/pubmed/7828599
Kim, J., Sif, S., Jones, B., Jackson, A., Koipally, J., Heller, E., … Georgopoulos, K. (1999). Ikaros DNA-Binding Proteins Direct Formation of Chromatin Remodeling Complexes in Lymphocytes. *Immunity*, *10*(3), 345–355. http://doi.org/10.1016/S1074-7613(00)80034-5
King, L. B., & Monroe, J. G. (2014). Immunobiology of the immature B cell: plasticity in the B-cell antigen receptor-induced response fine tunes negative selection. *Immunological Reviews*, *176*(3), 86–104. http://doi.org/10.1034/j.1600-065X.2000.00609.x
Kioussis, D. (2007). Aiolos: An Ungrateful Member of the Ikaros Family. *Immunity*, *26*(3), 275–277. http://doi.org/10.1016/j.immuni.2007.03.003
Klug, C. A., Morrison, S. J., Masek, M., Hahm, K., Smale, S. T., & Weissman, I. L. (1998). Hematopoietic stem cells and lymphoid progenitors express different Ikaros isoforms, and Ikaros is localized to heterochromatin in immature lymphocytes. *Proceedings of the National Academy of Sciences of the United States of America*, *95*(2), 657–62. Retrieved from http://www.ncbi.nlm.nih.gov/pubmed/9435248
Koch, H., Zhang, R., Verdoodt, B., Bailey, A., Zhang, C.-D., Yates, J. R., … Hermeking, H. (2007). Large-Scale Identification of c-MYC-Associated Proteins Using a Combined TAP/MudPIT Approach. *Cell Cycle*, *6*(2), 205–217. http://doi.org/10.4161/cc.6.2.3742
Koh, C. M., Sabò, A., & Guccione, E. (2016). Targeting MYC in cancer therapy: RNA processing offers new opportunities. *BioEssays*, *38*(3), 266–275. http://doi.org/10.1002/bies.201500134
Koipally, J., & Georgopoulos, K. (2000). Ikaros interactions with CtBP reveal a repression mechanism that is independent of histone deacetylase activity. *Journal of Biological Chemistry*, *275*(26), 19594–19602. http://doi.org/10.1074/jbc.M000254200
Koipally, J., & Georgopoulos, K. (2002). Ikaros-CtIP Interactions Do Not Require C-terminal Binding Protein and Participate in a Deacetylase-independent Mode of Repression*. http://doi.org/10.1074/jbc.M202079200
Koipally, J., Heller, E. J., Seavitt, J. R., & Georgopoulos, K. (2002). Unconventional Potentiation of Gene Expression by Ikaros. *Journal of Biological Chemistry*, *277*(15), 13007–13015. http://doi.org/10.1074/jbc.M111371200
Koipally, J., Renold, A., Kim, J., & Georgopoulos, K. (1999). Repression by Ikaros and Aiolos is mediated through histone deacetylase complexes. *The EMBO Journal*, *18*(11), 3090–3100. http://doi.org/10.1093/emboj/18.11.3090
Kress, T. R., Sabò, A., & Amati, B. (2015). MYC: connecting selective transcriptional control to global RNA production. *Nature Reviews Cancer*, *15*(10), 593–607. http://doi.org/10.1038/nrc3984
Kronke, J., Hurst, S. N., & Ebert, B. L. (2014). Lenalidomide induces degradation of IKZF1 and IKZF3. *Oncoimmunology*, *3*(7), e941742. http://doi.org/10.4161/21624011.2014.941742
Kurland, J. F., & Tansey, W. P. (2008). Myc-Mediated Transcriptional Repression by Recruitment of Histone Deacetylase. *Cancer Research*, *68*(10), 3624–3629. http://doi.org/10.1158/0008-5472.CAN-07-6552
Levine, M. H., Haberman, A. M., Sant'Angelo, D. B., Hannum, L. G., Cancro, M. P., Janeway, C. A., & Shlomchik, M. J. (2000). A B-cell receptor-specific selection step governs immature to mature B cell differentiation. *Proceedings of the National Academy of Sciences of the United States of America*, *97*(6), 2743–8. http://doi.org/10.1073/pnas.050552997
Li, H., & Durbin, R. (2010). Fast and accurate long-read alignment with Burrows-Wheeler transform. *Bioinformatics (Oxford, England)*, *26*(5), 589–95. http://doi.org/10.1093/bioinformatics/btp698
Li, Y., Casey, S. C., & Felsher, D. W. (2014). Inactivation of MYC reverses

tumorigenesis, *276*(1), 52–60. http://doi.org/10.1111/joim.12237.Inactivation
Li, Y. S., Wasserman, R., Hayakawa, K., & Hardy, R. R. (1996). Identification of the earliest B lineage stage in mouse bone marrow. *Immunity*, *5*(6), 527–535. http://doi.org/10.1016/S1074-7613(00)80268-X
Liang, Z., Brown, K. E., Carroll, T., Taylor, B., Vidal, I. F., Hendrich, B., … Merkenschlager, M. (2017). A high-resolution map of transcriptional repression. *eLife*, *6*, 1–24. http://doi.org/10.7554/eLife.22767
Lin, C. Y., Lovén, J., Rahl, P. B., Paranal, R. M., Burge, C. B., Bradner, J. E., … Young, R. A. (2012). Transcriptional Amplification in Tumor Cells with Elevated c-Myc. *Cell*, *151*(1), 56–67. http://doi.org/10.1016/j.cell.2012.08.026
Lin, K. I., Lin, Y., & Calame, K. (2000). Repression of c-myc is necessary but not sufficient for terminal differentiation of B lymphocytes in vitro. *Mol Cell Biol*, *20*(23), 8684–8695. http://doi.org/10.1128/MCB.20.23.8684-8695.2000
Little, C. D., Nau, M. M., Carney, D. N., Gazdar, A. F., & Minna, J. D. (1983). Amplification and expression of the c-myc oncogene in human lung cancer cell lines. *Nature*, *306*(5939), 194–6. Retrieved from http://www.ncbi.nlm.nih.gov/pubmed/6646201
Littlewood, T. D., Hancock, D. C., Danielianl, P. S., & Parker, M. G. (1995). A modified oestrogen receptor ligand-binding domain as an improved switch for the regulation of heterologous proteins. *Nucleic Acids Research*, *23*, 1686–1690. Retrieved from https://www.ncbi.nlm.nih.gov/pmc/articles/PMC306922/pdf/nar00010-0050.pdf
Liu, Y.-Y., Ge, C., & Tian, H. (2017). The transcription factor FOXN3 inhibits cell proliferation by downregulating E2F5 expression in hepatocellular carcinoma cells, *7*(28), 1285–1297. http://doi.org/10.18632/oncotarget.9780
Lo, K., Landau, N. R., & Smale, S. T. (1991). LyF-1, a transcriptional regulator that interacts with a novel class of promoters for lymphocyte-specific genes. *Molecular and Cellular Biology*, *11*(10), 5229–43. Retrieved from http://www.ncbi.nlm.nih.gov/pubmed/1922043
Loeper, S., Asa, S. L., & Ezzat, S. (2008). Ikaros Modulates Cholesterol Uptake: A Link between Tumor Suppression and Differentiation. *Cancer Res*, *68*(10), 3715–23. http://doi.org/10.1158/0008-5472.CAN-08-0103
Love, M. I., Huber, W., & Anders, S. (2014). Moderated estimation of fold change and dispersion for RNA-seq data with DESeq2. *Genome Biology*, *15*(12), 550. http://doi.org/10.1186/s13059-014-0550-8
Lu, G., Middleton, R. E., Sun, H., Naniong, M., Ott, C. J., Mitsiades, C. S., … Kaelin, W. G. (2014). The myeloma drug lenalidomide promotes the cereblon-dependent destruction of Ikaros proteins. *Science (New York, N.Y.)*, *343*(6168), 305–9. http://doi.org/10.1126/science.1244917
Ma, S., Pathak, S., Mandal, M., Trinh, L., Clark, M. R., & Lu, R. (2010). Ikaros and Aiolos Inhibit Pre-B-Cell Proliferation by Directly Suppressing c-Myc Expression. *Molecular and Cellular Biology*, *30*(17), 4149–4158. http://doi.org/10.1128/MCB.00224-10
Ma, S., Pathak, S., Trinh, L., & Lu, R. (2008). Interferon regulatory factors 4 and 8 induce the expression of Ikaros and Aiolos to down-regulate pre-B-cell receptor and promote cell-cycle withdrawal in pre-B-cell development. *Blood*, *111*(3), 1396–1403. http://doi.org/10.1182/blood-2007-08-110106
Machanick, P., & Bailey, T. L. (2011). MEME-ChIP: motif analysis of large DNA datasets. *Bioinformatics (Oxford, England)*, *27*(12), 1696–7. http://doi.org/10.1093/bioinformatics/btr189
Mårtensson, I.-L., Almqvist, N., Grimsholm, O., & Bernardi, A. I. (2010). The pre-B cell receptor checkpoint. *FEBS Letters*, *584*(12), 2572–9. http://doi.org/10.1016/j.febslet.2010.04.057
Mårtensson, I.-L., Keenan, R. A., & Licence, S. (2007). The pre-B-cell receptor. *Current*

Opinion in Immunology, *19*(2), 137–142. http://doi.org/10.1016/j.coi.2007.02.006
McKeown, M. R., & Bradner, J. E. (2014). Therapeutic strategies to inhibit MYC. *Cold Spring Harbor Perspectives in Medicine*, *4*(10), a014266–a014266. http://doi.org/10.1101/cshperspect.a014266
McMahon, S. B., Van Buskirk, H. A., Dugan, K. A., Copeland, T. D., & Cole, M. D. (1998). The novel ATM-related protein TRRAP is an essential cofactor for the c-Myc and E2F oncoproteins. *Cell*, *94*(3), 363–74. Retrieved from http://www.ncbi.nlm.nih.gov/pubmed/9708738
Melchers, F., Karasuyama, H., Haasner, D., Bauer, S., Kudo, A., Sakaguchi, N., … Rolink, A. (1993). The surrogate light chain in B-cell development. *Immunology Today*, *14*(2), 60–8. http://doi.org/10.1016/0167-5699(93)90060-X
Melchers, F., Rolink, A., Grawunder, U., Winkler, T. H., Karasuyama, H., Ghia, P., & Andersson, J. (1995). Positive and negative selection events during B lymphopoiesis. *Current Opinion in Immunology*, *7*(2), 214–227. http://doi.org/10.1016/0952-7915(95)80006-9
Melchers, F., ten Boekel, E., Seidl, T., Kong, X. C., Yamagami, T., Onishi, K., … Andersson, J. (2000). Repertoire selection by pre-B-cell receptors and B-cell receptors, and genetic control of B-cell development from immature to mature B cells. *Immunological Reviews*, *175*, 33–46. Retrieved from http://www.ncbi.nlm.nih.gov/pubmed/10933589
Mertz, J. A., Conery, A. R., Bryant, B. M., Sandy, P., Balasubramanian, S., Mele, D. A., … Sims, R. J. (2011). Targeting MYC dependence in cancer by inhibiting BET bromodomains. *Proceedings of the National Academy of Sciences of the United States of America*, *108*(40), 16669–74. http://doi.org/10.1073/pnas.1108190108
Meyer, N., & Penn, L. Z. (2008). Reflecting on 25 years with MYC. *Nature Reviews Cancer*, *8*(12), 976–990. http://doi.org/10.1038/nrc2231
Mohammed, H., D'Santos, C., Serandour, A. A., Ali, H. R., Brown, G. D., Atkins, A., … Carroll, J. S. (2013). Endogenous Purification Reveals GREB1 as a Key Estrogen Receptor Regulatory Factor. *Cell Reports*, *3*(2), 342–349. http://doi.org/10.1016/j.celrep.2013.01.010
Mohammed, H., Taylor, C., Brown, G. D., Papachristou, E. K., Carroll, J. S., & D'Santos, C. S. (2016). Rapid immunoprecipitation mass spectrometry of endogenous proteins (RIME) for analysis of chromatin complexes. *Nature Protocols*, *11*(2), 316–326. http://doi.org/10.1038/nprot.2016.020
Molnár, A., & Georgopoulos, K. (1994). The Ikaros gene encodes a family of functionally diverse zinc finger DNA-binding proteins. *Molecular and Cellular Biology*, *14*(12), 8292–303. Retrieved from http://www.ncbi.nlm.nih.gov/pubmed/7969165
Molnár, A., Wu, P., Largespada, D. A., Vortkamp, A., Scherer, S., Copeland, N. G., … Georgopoulos, K. (1996). The Ikaros gene encodes a family of lymphocyte-restricted zinc finger DNA binding proteins, highly conserved in human and mouse. *Journal of Immunology (Baltimore, Md. : 1950)*, *156*(2), 585–92. Retrieved from http://www.ncbi.nlm.nih.gov/pubmed/8543809
Morgan, B., Sun, L., Avitahl, N., Andrikopoulos, K., Ikeda, T., Gonzales, E., … Georgopoulos, K. (1997). Aiolos, a lymphoid restricted transcription factor that interacts with Ikaros to regulate lymphocyte differentiation. *The EMBO Journal*, *16*(8), 2004–2013. http://doi.org/10.1093/emboj/16.8.2004
Mullighan, C. G., Miller, C. B., Radtke, I., Phillips, L. A., Dalton, J., Ma, J., … Downing, J. R. (2008). BCR–ABL1 lymphoblastic leukaemia is characterized by the deletion of Ikaros. *Nature*, *453*(7191), 110–114. http://doi.org/10.1038/nature06866
Mullighan, C., Su, X., Zhang, J., Radtke, I., Letha, P., Christopher, M., … Mary, V. (2009). Deletion of IKZF1 and Prognosis in Acute Lymphoblastic Leukemia. *N Engl J Med*, *360*(5), 470–480. http://doi.org/10.1056/NEJMoa0808253
Nair, S. K., & Burley, S. K. (2003). X-ray structures of Myc-Max and Mad-Max

recognizing DNA. Molecular bases of regulation by proto-oncogenic transcription factors. *Cell*, *112*(2), 193–205. Retrieved from http://www.ncbi.nlm.nih.gov/pubmed/12553908

Nau, M. M., Brooks, B. J., Battey, J., Sausville, E., Gazdar, A. F., Kirsch, I. R., … Minna, J. D. (1985). L-myc, a new myc-related gene amplified and expressed in human small cell lung cancer. *Nature*, *318*(6041), 69–73. Retrieved from http://www.ncbi.nlm.nih.gov/pubmed/2997622

Ng, S. Y.-M., Yoshida, T., & Georgopoulos, K. (2007). Ikaros and chromatin regulation in early hematopoiesis. *Current Opinion in Immunology*, *19*(2), 116–22. http://doi.org/10.1016/j.coi.2007.02.014

Ng, S. Y.-M., Yoshida, T., Zhang, J., & Georgopoulos, K. (2009). Genome-wide Lineage-Specific Transcriptional Networks Underscore Ikaros-Dependent Lymphoid Priming in Hematopoietic Stem Cells. *Immunity*, *30*(4), 493–507. http://doi.org/10.1016/j.immuni.2009.01.014

Nichogiannopoulou, a, Trevisan, M., Friedrich, C., & Georgopoulos, K. (1998). Ikaros in hemopoietic lineage determination and homeostasis. *Seminars in Immunology*, *10*, 119–125. http://doi.org/10.1006/smim.1998.0113

Nie, Z., Hu, G., Wei, G., Cui, K., Yamane, A., Resch, W., … Levens, D. (2012). c-Myc Is a Universal Amplifier of Expressed Genes in Lymphocytes and Embryonic Stem Cells. *Cell*, *151*(1), 68–79. http://doi.org/10.1016/j.cell.2012.08.033

Nutt, S. L., Hodgkin, P. D., Tarlinton, D. M., & Corcoran, L. M. (2015). The generation of antibody-secreting plasma cells. *Nature Reviews Immunology*, *15*(3), 160–171. http://doi.org/10.1038/nri3795

Obsilová, V., Silhan, J., Boura, E., Teisinger, J., & Obsil, T. (2008). 14-3-3 proteins: a family of versatile molecular regulators. *Physiological Research*, *57 Suppl 3*, S11–21. Retrieved from http://www.ncbi.nlm.nih.gov/pubmed/18481918

Oestereich, W., & Einmann. (2012). Ikaros changes the face of NuRD remodeling. *Nature Publishing Group*, *13*(168), 678–689. http://doi.org/10.1038/ni.2191

Ordoñez, M., Presa, N., Trueba, M., & Gomez-Muñoz, A. (2017). Implication of Ceramide Kinase in Adipogenesis. *Mediators of Inflammation*, *2017*, 9374563. http://doi.org/10.1155/2017/9374563

Pajic, A., Spitkovsky, D., Christoph, B., Kempkes, B., Schuhmacher, M., Staege, M. S., … Eick, D. (2000). Cell cycle activation by c-myc in a burkitt lymphoma model cell line. *International Journal of Cancer*, *87*(6), 787–93. Retrieved from http://www.ncbi.nlm.nih.gov/pubmed/10956386

Pelanda, R., & Torres, R. M. (2012). Central B-cell tolerance: where selection begins. *Cold Spring Harbor Perspectives in Biology*, *4*(4), 1–15. http://doi.org/10.1101/cshperspect.a007146

Penn, L. J., Brooks, M. W., Laufer, E. M., & Land, H. (1990). Negative autoregulation of c-myc transcription. *The EMBO Journal*, *9*(4), 1113–21. Retrieved from http://www.ncbi.nlm.nih.gov/pubmed/2182320

Perdomo, J., Holmes, M., Chong, B., & Crossley, M. (2000). Eos and Pegasus, two members of the Ikaros family of proteins with distinct DNA binding activities. *Journal of Biological Chemistry*, *275*(49), 38347–38354. http://doi.org/10.1074/jbc.M005457200

Peri, S., Navarro, J. D., Amanchy, R., Kristiansen, T. Z., Jonnalagadda, C. K., Surendranath, V., … Pandey, A. (2003). Development of human protein reference database as an initial platform for approaching systems biology in humans. *Genome Research*, *13*(10), 2363–71. http://doi.org/10.1101/gr.1680803

Perland, E., Bagchi, S., Klaesson, A., & Fredriksson, R. (2017). Characteristics of 29 novel atypical solute carriers of major facilitator superfamily type: evolutionary conservation, predicted structure and neuronal co-expression. *Open Biology*, *7*(9). http://doi.org/10.1098/rsob.170142

Peukert, K., Staller, P., Schneider, A., Carmichael, G., Hänel, F., & Eilers, M. (1997). An alternative pathway for gene regulation by Myc. *The EMBO Journal*, *16*(18), 5672–5686. http://doi.org/10.1093/emboj/16.18.5672

Pieper, K., Grimbacher, B., & Eibel, H. (2013). B-cell biology and development. *The Journal of Allergy and Clinical Immunology*, *131*(4), 959–71. http://doi.org/10.1016/j.jaci.2013.01.046

Pillai, S., & Cariappa, A. (2009). The follicular versus marginal zone B lymphocyte cell fate decision. *Nature Reviews Immunology*, *9*(11), 767–777. http://doi.org/10.1038/nri2656

Polyak, K., Lee, M. H., Erdjument-Bromage, H., Koff, A., Roberts, J. M., Tempst, P., & Massagué, J. (1994). Cloning of p27Kip1, a cyclin-dependent kinase inhibitor and a potential mediator of extracellular antimitogenic signals. *Cell*, *78*(1), 59–66. http://doi.org/10.1016/0092-8674(94)90572-X

Pourfarzad, F., Aghajanirefah, A., de Boer, E., Ten Have, S., Bryn van Dijk, T., Kheradmandkia, S., … Grosveld, F. (2013). Locus-Specific Proteomics by TChP: Targeted Chromatin Purification. *Cell Reports*, *4*(3), 589–600. http://doi.org/10.1016/J.CELREP.2013.07.004

Prochownik, E. V., & Li, Y. (2007). The Ever Expanding Role for c-Myc in Promoting Genomic Instability. *Cell Cycle*, *6*(9), 1024–1029. http://doi.org/10.4161/cc.6.9.4161

Rahl, P. B., & Young, R. A. (2014). MYC and Transcription Elongation. *Cold Spring Harbor Perspectives in Medicine*, *4*(1), a020990. http://doi.org/10.1101/cshperspect.a020990

Ran, F. A., Hsu, P. D., Wright, J., Agarwala, V., Scott, D. A., & Zhang, F. (2013). Genome engineering using the CRISPR-Cas9 system. *Nature Protocols*, *8*(11), 2281–2308. http://doi.org/10.1038/nprot.2013.143

Rappsilber, J., Mann, M., & Ishihama, Y. (2007). Protocol for micro-purification, enrichment, pre-fractionation and storage of peptides for proteomics using StageTips. *Nature Protocols*, *2*(8), 1896–1906. http://doi.org/10.1038/nprot.2007.261

Richart, L., Carrillo-de Santa Pau, E., Río-Machín, A., de Andrés, M. P., Cigudosa, J. C., Lobo, V. J. S.-A., & Real, F. X. (2016). BPTF is required for c-MYC transcriptional activity and in vivo tumorigenesis. *Nature Communications*, *7*, 10153. http://doi.org/10.1038/ncomms10153

Rieder, S. A., & Shevach, E. M. (2013). Eos, goddess of treg cell reprogramming. *Immunity*, *38*(5), 849–50. http://doi.org/10.1016/j.immuni.2013.05.001

Rohban, S., & Campaner, S. (2015). Myc induced replicative stress response: How to cope with it and exploit it. *Biochimica et Biophysica Acta (BBA) - Gene Regulatory Mechanisms*, *1849*(5), 517–524. http://doi.org/10.1016/j.bbagrm.2014.04.008

Ross, F. A., MacKintosh, C., & Hardie, D. G. (2016). AMP-activated protein kinase: a cellular energy sensor that comes in 12 flavours. *The FEBS Journal*, *283*(16), 2987–3001. http://doi.org/10.1111/febs.13698

Roy, A. L., Carruthers, C., Gutjahr, T., & Roeder, R. G. (1993). Direct role for Myc in transcription initiation mediated by interactions with TFII-I. *Nature*, *365*(6444), 359–361. http://doi.org/10.1038/365359a0

Sabbattini, P., Lundgren, M., Georgiou, A., Chow, C. M., Warnes, G., & Dillon, N. (2001). Binding of Ikaros to the λ5 promoter silences transcription through a mechanism that does not require heterochromatin formation. *EMBO Journal*, *20*(11), 2812–2822. http://doi.org/10.1093/emboj/20.11.2812

Sabo, A., & Amati, B. (2014). Genome Recognition by MYC. *Cold Spring Harbor Perspectives in Medicine*, *4*(2), a014191–a014191. http://doi.org/10.1101/cshperspect.a014191

Sabò, A., Kress, T. R., Pelizzola, M., de Pretis, S., Gorski, M. M., Tesi, A., … Amati, B. (2014). Selective transcriptional regulation by Myc in cellular growth control and lymphomagenesis. *Nature*, *511*(7510), 488–492. http://doi.org/10.1038/nature13537

Schjerven, H., Ayongaba, E. F., Aghajanirefah, A., McLaughlin, J., Cheng, D., Geng, H., … Müschen, M. (2017). Genetic analysis of Ikaros target genes and tumor suppressor function in BCR-ABL1 $^{+}$ pre–B ALL. *The Journal of Experimental Medicine*, *214*(3), jem.20160049. http://doi.org/10.1084/jem.20160049

Schwab, M., Ellison, J. A. Y., Bishop, J. M., Rosenaut, W., & Varmust, H. E. (n.d.). Enhanced expression of the human gene N-myc consequent to amplification of DNA may contribute to malignant progression of neuroblastoma W **, (August 1984), 4940–4944.

Schwickert, T. A., Tagoh, H., Gültekin, S., Dakic, A., Axelsson, E., Minnich, M., … Busslinger, M. (2014). Stage-specific control of early B cell development by the transcription factor Ikaros. *Nature Immunology*, *15*(3), 283–293. http://doi.org/10.1038/ni.2828

Shapiro-Shelef, M., & Calame, K. (2005). Regulation of plasma-cell development. *Nature Reviews Immunology*, *5*(3), 230–242. http://doi.org/10.1038/nri1572

Sheiness, D., & Bishop, J. M. (1979). DNA and RNA from uninfected vertebrate cells contain nucleotide sequences related to the putative transforming gene of avian myelocytomatosis virus. *Journal of Virology*, *31*(2), 514–21. Retrieved from http://www.ncbi.nlm.nih.gov/pubmed/225569

Sheiness, D., Fanshier, L., & Bishop, J. M. (1978). Identification of nucleotide sequences which may encode the oncogenic capacity of avian retrovirus MC29. *Journal of Virology*, *28*(2), 600–10. Retrieved from http://www.ncbi.nlm.nih.gov/pubmed/214581

Shevchenko, A., Tomas, H., Havlis, J., Olsen, J. V, & Mann, M. (2006). In-gel digestion for mass spectrometric characterization of proteins and proteomes. *Nature Protocols*, *1*(6), 2856–2860. http://doi.org/10.1038/nprot.2006.468

Shim, H., Chun, Y. S., Lewis, B. C., & Dang, C. V. (1998). A unique glucose-dependent apoptotic pathway induced by c-Myc. *Proceedings of the National Academy of Sciences of the United States of America*, *95*(4), 1511–6. Retrieved from http://www.ncbi.nlm.nih.gov/pubmed/9465046

Shrivastava, A., Saleque, S., Kalpana, G. V, Artandi, S., Goff, S. P., & Calame, K. (1993). Inhibition of transcriptional regulator Yin-Yang-1 by association with c-Myc. *Science (New York, N.Y.)*, *262*(5141), 1889–92. Retrieved from http://www.ncbi.nlm.nih.gov/pubmed/8266081

Smith, a P., Verrecchia, A., Fagà, G., Doni, M., Perna, D., Martinato, F., … Amati, B. (2009). A positive role for Myc in TGFbeta-induced Snail transcription and epithelial-to-mesenchymal transition. *Oncogene*, *28*(November 2008), 422–430. http://doi.org/10.1038/onc.2008.395

Soldi, M., & Bonaldi, T. (2013). The Proteomic Investigation of Chromatin Functional Domains Reveals Novel Synergisms among Distinct Heterochromatin Components. *Molecular & Cellular Proteomics*, *12*(3), 764–780. http://doi.org/10.1074/mcp.M112.024307

Soldi, M., & Bonaldi, T. (2014). The ChroP Approach Combines ChIP and Mass Spectrometry to Dissect Locus-specific Proteomic Landscapes of Chromatin. *Journal of Visualized Experiments*, (86). http://doi.org/10.3791/51220

Song, C., Gowda, C., Pan, X., Ding, Y., Tong, Y., Tan, B. H., … Dovat, S. (2015). Targeting casein kinase II restores Ikaros tumor suppressor activity and demonstrates therapeutic efficacy in high-risk leukemia. *Blood*, *126*(15), 1813–1822. http://doi.org/10.1182/blood-2015-06-651505

Soucek, L., Whitfield, J., Martins, C. P., Finch, A. J., Murphy, D. J., Sodir, N. M., … Evan, G. I. (2008). Modelling Myc inhibition as a cancer therapy. *Nature*, *455*(7213), 679–683. http://doi.org/10.1038/nature07260

Soucek, L., Whitfield, J. R., Sodir, N. M., Massó-Vallés, D., Serrano, E., Karnezis, A. N., … Evan, G. I. (2013). Inhibition of Myc family proteins eradicates KRas-driven lung

cancer in mice. *Genes and Development*, *27*(5), 504–513. http://doi.org/10.1101/gad.205542.112
Sridharan, R., & Smale, S. T. (2007). Predominant interaction of both Ikaros and Helios with the NuRD complex in immature thymocytes. *Journal of Biological Chemistry*, *282*(41), 30227–30238. http://doi.org/10.1074/jbc.M702541200
Staller, P., Peukert, K., Kiermaier, A., Seoane, J., Lukas, J., Karsunky, H., … Eilers, M. (2001). Repression of p15INK4b expression by Myc through association with Miz-1. *Nature Cell Biology*, *3*(4), 392–399. http://doi.org/10.1038/35070076
Stojanova, A., Tu, W. B., Ponzielli, R., Kotlyar, M., Chan, P.-K., Boutros, P. C., … Penn, L. Z. (2016). MYC interaction with the tumor suppressive SWI/SNF complex member INI1 regulates transcription and cellular transformation. *Cell Cycle (Georgetown, Tex.)*, *15*(13), 1693–705. http://doi.org/10.1080/15384101.2016.1146836
Stone, J., de Lange, T., Ramsay, G., Jakobovits, E., Bishop, J. M., Varmus, H., & Lee, W. (1987). Definition of regions in human c-myc that are involved in transformation and nuclear localization. *Molecular and Cellular Biology*, *7*(5), 1697–709. Retrieved from http://www.ncbi.nlm.nih.gov/pubmed/3299053
Strasser, A., Harris, A. W., Bath, M. L., & Cory, S. (1990). Novel primitive lymphoid tumours induced in transgenic mice by cooperation between myc and bcl-2. *Nature*, *348*(6299), 331–333. http://doi.org/10.1038/348331a0
Subramanian, A., Tamayo, P., Mootha, V. K., Mukherjee, S., Ebert, B. L., Gillette, M. A., … Mesirov, J. P. (2005). Gene set enrichment analysis: A knowledge-based approach for interpreting genome-wide expression profiles. *Proceedings of the National Academy of Sciences*, *102*(43), 15545–15550. http://doi.org/10.1073/pnas.0506580102
Sun, J., Matthias, G., Mihatsch, M. J., Georgopoulos, K., & Matthias, P. (2003). Lack of the transcriptional coactivator OBF-1 prevents the development of systemic lupus erythematosus-like phenotypes in Aiolos mutant mice. *Journal of Immunology (Baltimore, Md. : 1950)*, *170*(4), 1699–706. Retrieved from http://www.ncbi.nlm.nih.gov/pubmed/12574333
Sun, L., Liu, A., & Georgopoulos, K. (1996). Zinc finger-mediated protein interactions modulate Ikaros activity, a molecular control of lymphocyte development. *The EMBO Journal*, *15*(19), 5358–69. Retrieved from http://www.ncbi.nlm.nih.gov/pubmed/8895580
Sutherland, L. C., Rintala-Maki, N. D., White, R. D., & Morin, C. D. (2005). RNA binding motif (RBM) proteins: A novel family of apoptosis modulators? *Journal of Cellular Biochemistry*, *94*(1), 5–24. http://doi.org/10.1002/jcb.20204
Tansey, W. P. (2014). Mammalian MYC Proteins and Cancer. *New Journal of Science*, *2014*, 1–27. http://doi.org/10.1155/2014/757534
Terada, L. S., & Liu, Z. (2014). Aiolos and Lymphocyte Mimicry in Lung Cancer. *Mol Cell Oncol*, *1*(July 2014), 2–3.
Thomas, L. R., Wang, Q., Grieb, B. C., Phan, J., Foshage, A. M., Sun, Q., … Tansey, W. P. (2015). Interaction with WDR5 Promotes Target Gene Recognition and Tumorigenesis by MYC. *Molecular Cell*, *58*(3), 440–452. http://doi.org/10.1016/j.molcel.2015.02.028
Thompson, E. C., Cobb, B. S., Sabbattini, P., Meixlsperger, S., Parelho, V., Liberg, D., … Merkenschlager, M. (2007). Ikaros DNA-Binding Proteins as Integral Components of B Cell Developmental-Stage-Specific Regulatory Circuits. *Immunity*, *26*(3), 335–344. http://doi.org/10.1016/j.immuni.2007.02.010
Tian, H., Ge, C., Zhao, F., Zhu, M., Zhang, L., Huo, Q., … Li, J. (2017). Downregulation of AZGP1 by Ikaros and histone deacetylase promotes tumor progression through the PTEN/Akt and CD44s pathways in hepatocellular carcinoma. *Carcinogenesis*, *38*(2), 207–217. http://doi.org/10.1093/carcin/bgw125

Trapnell, C., Pachter, L., & Salzberg, S. L. (2009). TopHat: discovering splice junctions with RNA-Seq. *Bioinformatics*, *25*(9), 1105–1111. http://doi.org/10.1093/bioinformatics/btp120

Trimboli, A. J., Fukino, K., de Bruin, A., Wei, G., Shen, L., Tanner, S. M., … Leone, G. (2008). Direct Evidence for Epithelial-Mesenchymal Transitions in Breast Cancer. *Cancer Research*, *68*(3), 937–945. http://doi.org/10.1158/0008-5472.CAN-07-2148

Trinh, L. A., Ferrini, R., Cobb, B. S., Weinmann, A. S., Hahm, K., Ernst, P., … Smale, S. T. (2001). Down-regulation of TDT transcription in CD4 + CD8 + thymocytes by Ikaros proteins in direct competition with an Ets activator, 1817–1832. http://doi.org/10.1101/gad.905601.Although

Tu, W. B., Helander, S., Pilstål, R., Hickman, K. A., Lourenco, C., Jurisica, I., … Penn, L. Z. (2015). Myc and its interactors take shape. *Biochimica et Biophysica Acta (BBA) - Gene Regulatory Mechanisms*, *1849*(5), 469–483. http://doi.org/10.1016/J.BBAGRM.2014.06.002

Tworkowski, K. A., Chakraborty, A. A., Samuelson, A. V, Seger, Y. R., Narita, M., Hannon, G. J., … Tansey, W. P. (2008). Adenovirus E1A targets p400 to induce the cellular oncoprotein Myc. *Proceedings of the National Academy of Sciences of the United States of America*, *105*(16), 6103–8. http://doi.org/10.1073/pnas.0802095105

Vafa, O., Wade, M., Kern, S., Beeche, M., Pandita, T. K., Hampton, G. M., & Wahl, G. M. (2002). c-Myc can induce DNA damage, increase reactive oxygen species, and mitigate p53 function: a mechanism for oncogene-induced genetic instability. *Molecular Cell*, *9*(5), 1031–44. Retrieved from http://www.ncbi.nlm.nih.gov/pubmed/12049739

Vennstrom, B., Sheiness, D., Zabielski, J., & Bishop, J. M. (1982). Isolation and characterization of c-myc, a cellular homolog of the oncogene (v-myc) of avian myelocytomatosis virus strain 29. *Journal of Virology*, *42*(3), 773–9. Retrieved from http://www.ncbi.nlm.nih.gov/pubmed/6284994

Vervoorts, J., Lüscher-Firzlaff, J. M., Rottmann, S., Lilischkis, R., Walsemann, G., Dohmann, K., … Lüscher, B. (2003). Stimulation of c-MYC transcriptional activity and acetylation by recruitment of the cofactor CBP. *EMBO Reports*, *4*(5), 484–90. http://doi.org/10.1038/sj.embor.embor821

Vita, M., & Henriksson, M. (2006). The Myc oncoprotein as a therapeutic target for human cancer. *Seminars in Cancer Biology*, *16*(4), 318–330. http://doi.org/10.1016/j.semcancer.2006.07.015

Walz, S., Lorenzin, F., Morton, J., Wiese, K. E., von Eyss, B., Herold, S., … Eilers, M. (2014). Activation and repression by oncogenic MYC shape tumour-specific gene expression profiles. *Nature*, *511*(7510), 483–487. http://doi.org/10.1038/nature13473

Wang, C. I., Alekseyenko, A. A., LeRoy, G., Elia, A. E., Gorchakov, A. A., Britton, L.-M. P., … Kuroda, M. I. (2013). Chromatin proteins captured by ChIP–mass spectrometry are linked to dosage compensation in Drosophila. *Nature Structural & Molecular Biology*, *20*(2), 202–209. http://doi.org/10.1038/nsmb.2477

Wang, J. H., Avitahl, N., Cariappa, A., Friedrich, C., Ikeda, T., Renold, A., … Georgopoulos, K. (1998). Aiolos regulates B cell activation and maturation to effector state. *Immunity*, *9*(4), 543–553. http://doi.org/10.1016/S1074-7613(00)80637-8

Wang, J. H., Nichogiannopoulou, A., Wu, L., Sun, L., Sharpe, A. H., Bigby, M., & Georgopoulos, K. (1996). Selective defects in the development of the fetal and adult lymphoid system in mice with an Ikaros null mutation. *Immunity*, *5*(6), 537–549. http://doi.org/10.1016/S1074-7613(00)80269-1

Wanzel, M., Herold, S., & Eilers, M. (2003). Transcriptional repression by Myc. *Trends in Cell Biology*, *13*(3), 146–50. Retrieved from http://www.ncbi.nlm.nih.gov/pubmed/12628347

Wargnier, A., Lafaurie, C., Legros-Maïda, S., Bourge, J. F., Sigaux, F., Sasportes, M., & Paul, P. (1998). Down-regulation of human granzyme B expression by

glucocorticoids. Dexamethasone inhibits binding to the Ikaros and AP-1 regulatory elements of the granzyme B promoter. *The Journal of Biological Chemistry*, *273*(52), 35326–31. Retrieved from http://www.ncbi.nlm.nih.gov/pubmed/9857074

Wasylishen, A. R., & Penn, L. Z. (2010). Myc: The Beauty and the Beast. *Genes & Cancer*, *1*(6), 532–541. http://doi.org/10.1177/1947601910378024

Wiesinger, C., Kunze, M., Regelsberger, G., Forss-Petter, S., & Berger, J. (2013). Impaired Very Long-chain Acyl-CoA β-Oxidation in Human X-linked Adrenoleukodystrophy Fibroblasts Is a Direct Consequence of ABCD1 Transporter Dysfunction. *Journal of Biological Chemistry*, *288*(26), 19269–19279. http://doi.org/10.1074/jbc.M112.445445

Wilson, A., Murphy, M. J., Oskarsson, T., Kaloulis, K., Bettess, M. D., Oser, G. M., … Trumpp, A. (2004). c-Myc controls the balance between hematopoietic stem cell self-renewal and differentiation. *Genes & Development*, *18*(22), 2747–63. http://doi.org/10.1101/gad.313104

Winandy, S., Wu, P., & Georgopoulos, K. (1995). A dominant mutation in the Ikaros gene leads to rapid development of leukemia and lymphoma. *Cell*, *83*(2), 289–299. http://doi.org/10.1016/0092-8674(95)90170-1

Winkler, D. D., & Luger, K. (2011). The Histone Chaperone FACT: Structural Insights and Mechanisms for Nucleosome Reorganization. *Journal of Biological Chemistry*, *286*(21), 18369–18374. http://doi.org/10.1074/jbc.R110.180778

Yasuda, T., Sanjo, H., Pagès, G., Kawano, Y., Karasuyama, H., Pouysségur, J., … Kurosaki, T. (2008). Erk kinases link pre-B cell receptor signaling to transcriptional events required for early B cell expansion. *Immunity*, *28*(4), 499–508. http://doi.org/10.1016/j.immuni.2008.02.015

Yoshida, T., Ng, S. Y.-M., Zuniga-Pflucker, J. C., & Georgopoulos, K. (2006). Early hematopoietic lineage restrictions directed by Ikaros. *Nature Immunology*, *7*(4), 382–91. http://doi.org/10.1038/ni1314

Zeller, K. I., Zhao, X., Lee, C. W. H., Chiu, K. P., Yao, F., Yustein, J. T., … Wei, C.-L. (2006). Global mapping of c-Myc binding sites and target gene networks in human B cells. *Proceedings of the National Academy of Sciences*, *103*(47), 17834–17839. http://doi.org/10.1073/pnas.0604129103

Zhang, J., Jackson, A. F., Naito, T., Dose, M., Seavitt, J., Liu, F., … Georgopoulos, K. (2012). Harnessing of the nucleosome-remodeling-deacetylase complex controls lymphocyte development and prevents leukemogenesis. *Nature Immunology*, *13*(1), 86–94. http://doi.org/10.1038/ni.2150

Zhang, L. (2014). Inhibitory effects of transcription factor Ikaros on the expression of liver cancer stem cell marker CD133 in hepatocellular carcinoma., *5*(21), 10621–35. http://doi.org/10.18632/oncotarget.2524

Zhang, N., Ichikawa, W., Faiola, F., Lo, S.-Y., Liu, X., & Martinez, E. (2014). MYC interacts with the human STAGA coactivator complex via multivalent contacts with the GCN5 and TRRAP subunits. *Biochimica et Biophysica Acta*, *1839*(5), 395–405. http://doi.org/10.1016/j.bbagrm.2014.03.017

Zhang, W., Patil, S., Chauhan, B., Guo, S., Powell, D. R., Le, J., … Unterman, T. G. (2006). FoxO1 Regulates Multiple Metabolic Pathways in the Liver. *Journal of Biological Chemistry*, *281*(15), 10105–10117. http://doi.org/10.1074/jbc.M600272200

Zhang, Y., Liu, T., Meyer, C. A., Eeckhoute, J., Johnson, D. S., Bernstein, B. E., … Liu, X. S. (2008). Model-based Analysis of ChIP-Seq (MACS). *Genome Biology*, *9*(9), R137. http://doi.org/10.1186/gb-2008-9-9-r137

Zhang, Z., Xu, Z., Wang, X., Wang, H., Yao, Z., Mu, Y., … Liu, Z. (2013). Ectopic Ikaros Expression Positively Correlates With Lung Cancer Progression. *The Anatomical Record*, *296*(6), 907–913. http://doi.org/10.1002/ar.22700

Zhou, F. E. N., Xu, Y., Qiu, Y., Wu, X., Zhang, Z., & Jin, R. (2013). Ik6 expression

provides a new strategy for the therapy of acute lymphoblastic leukemia, 1373–1379.
Zhu, R., Zou, S.-T., Wan, J.-M., Li, W., Li, X.-L., & Zhu, W. (2013). BTG1 inhibits breast cancer cell growth through induction of cell cycle arrest and apoptosis. *Oncology Reports*, *30*(5), 2137–2144. http://doi.org/10.3892/or.2013.2697
Zhu, Z., Wang, H., Wei, Y., Meng, F., Liu, Z., & Zhang, Z. (2017). Downregulation of PRDM1 promotes cellular invasion and lung cancer metastasis. *Tumor Biology*, *39*(4), 101042831769592. http://doi.org/10.1177/1010428317695929
Zindy, F., Eischen, C. M., Randle, D. H., Kamijo, T., Cleveland, J. L., Sherr, C. J., & Roussel, M. F. (1998). Myc signaling via the ARF tumor suppressor regulates p53-dependent apoptosis and immortalization. *Genes & Development*, *12*(15), 2424–33. Retrieved from http://www.ncbi.nlm.nih.gov/pubmed/9694806
Zuber, J., Shi, J., Wang, E., & Rappaport, A. (2011). RNAi screen identifies Brd4 as a therapeutic target in acute myeloid leukaemia. *Nature*, *478*(7370), 524–528. http://doi.org/10.1038/nature10334.RNAi

Acknowledgments

I would like to thank Bruno for the opportunity he gave me to work in his group during my PhD years.

I would like to thank Arianna for supervising me and being a fundamental reference for my work.

I would like to thank Theresia, for guiding me at the beginning of this project.

I would like to thank Tiziana Bonaldi's group, in particular Monica and Alessio, for the MS analysis.

I would like to thank Vera, who performed the bioinformatic analysis and Annalisa, who lately joined the project, for critical discussions and for sharing the daily life in the lab; thanks to Paola for sharing joy and pain of these years of work.

Thanks to our technicians Mirko and Alessandro for their help and precious tricks, to Andrea for the assistance with the FACS and critical suggestions, to all the members of the IIT groups, particularly to BA group, for the constructive suggestions.

Thanks to Ottavio for sharing these four years of PhD and for bio/info conversations during the long hours on train/metro/tram.

Thanks to Andrea C. who, after introducing me into the research world, remained a strong motivator and supporter at distance.

Many thanks to my family for supporting me anytime.

A special thank to my husband Claudio for his patience and constant presence.

,

Supplementary table 1.

Page 1. DEGs identified by comparing IkarosER plus Myc activation and IkarosER activation alone are reported. For each of them, the log2(fold change) value calculated by comparing IkarosERvsNT, IkarosER+Myc vs IkarosER or Myc vs NT is reported at every time point. Genes are classified in four groups as described in figure 46. The last three genes of the list (Lbh, Prox1, Trp53i11) have a different behaviour at 24h compared to earlier time points

Page 2. Ikaros and Myc common target genes are listed according to the direction of their regulation. Genes in brakets (Lbh, Prox1, Trp53i11) have a different behaviour at 24h compared to 4h and 8h.

Page 3. Functional annotation of Ikaros and Myc common target genes. For each gene, symbol, extended name and function are reported.

	4h			8h			24h		
	Ikaros_vs_NT	IkarosMyc_vs_NT	Myc_vs_NT	Ikaros_vs_NT	IkarosMyc_vs_NT	Myc_vs_NT	Ikaros_vs_NT	IkarosMyc_vs_NT	Myc_vs_NT
Ikaros UP/MycDOWN									
2610008E11Rik	0.327929774	-0.05028815	-0.391030045	0.255566548	-0.086271373	-0.329619492	0.877791713	0.446960184	-0.045289142
Abcd1	0.374771606	0.127494188	-0.184070863	0.421302601	0.21648273	-0.086642653	0.814773717	0.5443528	-0.043573639
Ackr4	0.489981254	-0.196459975	-0.353808606	0.770916602	0.151918379	-0.393109295	1.340584474	0.857570956	0.014668447
Acox3	0.326467491	-0.133860923	-0.239678904	0.281085445	-0.086314449	-0.318163372	0.885122155	0.488437169	-0.098129898
Adamtsl2	0.539906795	0.06322198	-0.211391929	0.683235955	-0.009945773	-0.273962266	0.609975548	0.108365263	-0.077363497
Aim1	0.379704881	0.097833961	-0.204972584	0.369995806	0.086539793	-0.251996926	0.867479039	0.571118414	-0.089380125
Ankrd44	0.458915506	0.184648613	-0.30264765	0.487839863	0.158347692	-0.453438181	0.879230734	0.533092174	-0.157283696
Ap3m2	0.670252087	0.20766236	-0.26474834	0.78272426	0.385188563	-0.298636423	1.322697255	0.983279976	-0.062616271
Arid3b	0.588602689	0.228998232	-0.434212396	0.979077868	0.485254012	-0.378292082	2.190411103	1.60791325	-0.038726217
Ash2	0.850451406	0.102375155	-0.344188482	1.4659589	0.518062292	-0.509092636	3.505340244	2.832154605	-0.061870002
Atg9a	0.310646329	0.020653885	-0.159118628	0.212396683	-0.076163091	-0.063468304	0.551411495	0.221891718	0.027159882
Baz2a	0.254787461	0.050347346	-0.056709886	0.288460897	0.005648382	-0.225659011	0.77278103	0.418366151	-0.031507322
Bcl2l1	0.261466943	-0.204681289	-0.37572559	0.377857554	-0.016747348	-0.374897011	1.474905642	0.925340843	-0.183176425
Btg1	0.273012928	-0.112977567	-0.388910547	0.367581795	-0.079863407	-0.408172993	1.032779374	0.530190654	-0.179656584
Calcoco1	0.43026141	-0.026968322	-0.220921997	0.291765302	-0.198170089	-0.217957169	0.805736093	0.33047559	-0.066984334
Cblb	0.631892872	0.40174452	-0.22272675	0.76552738	0.510609322	-0.269847995	1.718512976	1.254727162	0.002507172
Cd37	0.269918643	-0.034246073	-0.089099456	0.297693853	0.027610382	-0.217478572	0.533426451	0.17150353	-0.105755172
Cdkn1b	0.225673495	-0.115198358	-0.267265388	0.183489907	-0.171763845	-0.23609083	0.695655839	0.272439901	-0.040680259
Cerk	0.463065081	0.252014186	-0.059511707	0.425476838	0.167709648	-0.174091537	0.900153342	0.490613081	-0.179000722
Chd3	0.314943679	0.129712957	-0.043494353	0.288672726	0.09714769	-0.173491333	0.481950241	0.201646036	-0.059516288
Cklf	0.373532481	0.135954382	-0.090796426	0.378504151	0.016933176	-0.117636726	0.838007929	0.528079617	0.000830981
Cpm	1.423716387	0.885593666	-0.322855088	1.861413794	0.969928216	-0.543317184	3.188849919	2.329277725	-0.171855217
Cr2	0.36096313	-0.031602715	-0.256786261	0.411932939	0.018199164	-0.507502507	1.038649586	0.39463341	-0.006312942
Dennd1c	0.415300705	0.033626063	-0.223467635	0.431162648	-0.009661568	-0.340329922	0.915764492	0.421012843	-0.057167848
Dgka	0.461663692	-0.107432331	-0.388840688	0.474737438	-0.010697818	-0.419538148	1.191941171	0.649539742	-0.060582615
Dopey2	0.52165567	-0.001333051	-0.342784432	0.737648204	-0.046402828	-0.379326381	1.606698945	0.959598781	-0.151387164
Dyrk1b	0.561543547	-0.173401721	-0.340172882	0.475492089	-0.046812294	-0.334730311	1.031940313	0.577615144	-0.105728948
Endou	0.331981918	-0.017037379	-0.138852421	0.428681445	-0.199039835	-0.392445408	0.987652596	0.359730512	-0.012370454
Ero1lb	0.498317422	0.229846891	-0.345323221	0.916171026	0.459357511	-0.428316356	2.151015658	1.485239929	-0.100832456
Fam214a	0.191615104	-0.092782651	-0.235084	0.195386117	-0.170925638	-0.241635922	0.668270385	0.307772363	0.00831751
Fam63b	0.195413687	-0.012276451	-0.189735722	0.248729588	-0.139528511	-0.355028426	0.594738495	0.265034596	-0.079429766
Fchsd1	0.360716618	-0.038246862	-0.299115996	0.286858808	-0.130866476	-0.320918299	0.547107566	0.197832913	-0.033202012
Foxo1	0.275662328	-0.013320196	-0.164402249	0.19886185	-0.128038276	-0.382473208	1.061937479	0.547523856	-0.099766686
Gdi1	0.219975056	-0.042886974	-0.205118377	0.251443563	0.010120574	-0.243020582	0.736855734	0.433473312	-0.047509263
Git2	0.202880426	-0.003271104	-0.131330926	0.180989751	-0.030073643	-0.150495125	0.519796543	0.257786935	-0.036810268
Gltscr1	0.600403095	0.157168213	-0.350310814	0.866471058	0.511958999	-0.371798911	1.887168756	1.439928571	-0.07010381
H2-Oa	0.3798625	-0.050786796	-0.2855865	0.475153223	0.07960808	-0.136012391	0.9717152	0.416544575	-0.043507889
H2-Ob	0.460988526	0.206342073	-0.14380916	0.724293965	0.41600554	-0.205835466	1.239269423	0.812611605	-0.141386242
Ifi203	0.311301451	0.038688566	-0.250628398	0.321414419	0.090100196	-0.28968377	0.811579659	0.427320684	-0.010062184
Il16	0.634149705	0.347476429	-0.152970806	0.709895624	0.429658571	-0.21198387	1.340775604	0.916810698	-0.123728807
Jakmip1	0.171720464	-0.072206008	-0.129807166	0.211350754	-0.020128458	-0.157553832	0.423850871	0.194006974	-0.106088826
Kmt2c	0.238424441	-0.058746773	-0.241809622	0.276316681	-0.016788112	-0.287671912	0.666419516	0.320795899	-0.041520148
Map4k2	0.24065611	-0.053756006	-0.191521874	0.32678724	0.123481209	-0.13705562	0.560543388	0.290790424	-0.061142388
Mbd4	0.419025525	0.093449553	-0.245807287	0.403652218	0.089477934	-0.287646591	0.678096315	0.428778114	-0.015098457
Natd1	0.334323493	-0.060917731	-0.339632185	0.364864239	-0.080704725	-0.301224894	1.210180635	0.660301846	-0.091883413
Neil1	0.882211992	0.673067075	-0.068065303	0.915755646	0.716611925	-0.109735383	1.390860892	1.070302296	-0.045221389
Pcyt1a	0.26825637	-0.044779303	-0.319078183	0.20749495	-0.340750485	-0.488567438	0.945574826	0.564037864	-0.173254239
Pecam1	0.279936784	-0.060281549	-0.310122126	0.297811424	-0.009433183	-0.345835127	0.8117710 37	0.454584981	-0.11493943
Pias3	0.449244698	-0.107039554	-0.40959423	0.391686188	-0.088229945	-0.397906724	0.740016336	0.352091903	-0.060188855
Pink1	0.225668155	-0.107743343	-0.212583157	0.246115408	-0.049076667	-0.140450149	0.538696208	0.268664853	-0.052942573
Plekhg2	0.276408971	-0.413698949	-0.646304373	0.328423512	-0.285225863	-0.586819392	0.781217744	0.36726221	-0.141131818
Pyhin1	0.728451565	0.220623156	-0.182966716	1.013069252	0.220002307	-0.295998741	2.605791254	1.616364473	-0.094866778
Rab43	0.553687458	0.336578231	-0.084563626	0.561231257	0.34788463	-0.104716578	1.056438501	0.782345855	-0.083624471
Rag1	0.868092952	0.173414091	-0.191581801	1.659382761	0.770165509	-0.352421021	2.871940905	1.868512041	-0.221369252
Rbm5	0.186068139	-0.015304107	-0.073527418	0.176855262	-0.008834836	-0.101623327	0.486011025	0.180568808	-0.020518752
Rprl1	0.733996122	0.249123458	-0.197787589	0.947227055	0.659076333	-0.086730666	1.576934807	1.287415048	-0.069754239
Serinc5	1.004671295	0.477633053	-0.379925199	1.222387836	0.506667556	-0.430405352	3.422197301	2.709507039	-0.00132975
Siglecg	1.006088803	0.584854039	-0.422363558	1.802125072	1.52767944	-0.30249276	2.526342436	2.163984519	-0.106095328
Slc12a6	0.225887388	0.004139065	-0.154983158	0.255942154	-0.030927505	-0.19070104	0.796282383	0.345435705	-0.067599101
Spns3	0.685953579	0.198283281	-0.29719941	1.042814264	0.507873527	-0.611424689	2.847079627	2.36448936	-0.036127239
Tbx6	0.472301696	0.072936545	-0.160294411	0.636479428	0.075965729	-0.271593458	1.572769495	0.843243466	-0.069392064
Tuba1a	0.336167453	-0.161896079	-0.320332976	0.395544704	-0.014363895	-0.356676228	1.034863869	0.685578001	-0.083933937
Ypel3	0.483561116	0.005006829	-0.279946123	0.43442784	0.04339626	-0.39506584	1.190329405	0.67246835	-0.126069524
Zfp821	0.280963472	-0.068146919	-0.247901744	0.30049144	0.021836079	-0.232505532	0.712434323	0.357986905	-0.087270171
Zfp831	0.812474025	-0.057475369	-0.433059192	1.350278254	0.455309902	-0.317397468	2.322686753	1.264671513	-0.134279496
Zhx3	0.25688548	-0.073252589	-0.25170845	0.275391438	-0.077023178	-0.281809734	0.516893439	0.176047578	-0.161437571
Ikaros DOWN/Myc UP									
Abcb1b	-0.184501518	0.045723285	0.195871745	-0.249817888	-0.01421564	0.180112514	-0.956054629	-0.504776179	0.041021562
Abcc1	-0.341190333	0.165701433	0.278653833	-0.386028252	-0.029408812	0.220745	-1.322066308	-0.514797386	0.082061206
Acy1	-0.284524106	-0.056784066	0.21442374	-0.439831081	-0.047063041	0.342162628	-1.023567293	-0.40822979	0.050411997
Atg9b	-0.642078564	-0.404797545	0.182235649	-0.716857143	-0.363722541	0.230206732	-1.619048403	-0.833475931	0.107988907
Bcl11a	-0.733326465	-0.499974729	0.056276093	-0.757084447	-0.576673683	-0.061162021	-1.173151834	-0.936060546	-0.018925424
Ccnd1	-0.393310819	-0.156223198	0.207481984	-0.592609519	-0.158372769	0.256629731	-1.709970586	-0.789297348	0.086215877
D8Ertd82e	-0.425158035	0.137371034	0.320430813	-0.251839437	0.046541292	0.271537534	-1.046970419	-0.149686995	0.090578571
Deptor	-1.224275192	-0.639613603	0.331354475	-1.736038495	-1.084625629	0.286280151	-2.376573243	-1.620238268	0.167662529
Dfna5	-0.580284786	-0.17595617	0.151677151	-0.587140964	-0.340514679	0.108089702	-1.130299392	-0.694644181	0.06605994
Fgd2	-0.576084548	-0.241097167	0.29275312	-0.744093846	-0.273684619	0.328407445	-2.140412322	-1.131854096	0.113234617
Frrs1	-0.29334019	0.025579351	0.11394422	-0.314394526	-0.01498001	0.048050637	-0.988064012	-0.442113996	0.013401118
Kdelc1	-0.582921232	-0.356212524	0.108615964	-0.790160501	-0.51032218	0.098342778	-1.759353927	-0.928183375	0.075320065
Mmp15	-1.195121224	-0.876241516	0.033444847	-1.421029902	-0.869230452	0.130012571	-3.05692944	-2.054775434	0.003545737
Nr1d1	-0.769964639	0.282383821	0.520014726	-0.948007579	-0.155853153	0.517754929	-2.15578533	-0.871977309	0.162481689
Nrp2	-0.918716375	-0.574515061	0.191211199	-1.391354846	-1.012371865	0.02289976	-2.361105176	-1.472302904	0.102544766
Pdzrn3	-2.024228732	-1.686673486	0.102986905	-2.264819815	-1.909671889	0.109890949	-3.879301485	-3.354763045	-0.049854217
Prkaa2	-0.517405593	-0.165640565	0.051100052	-0.417004426	-0.082627619	0.065561311	-1.128319667	-0.660911207	-0.028558484
Prrg4	-0.884175576	-0.518778816	0.255360109	-0.883429534	-0.482944295	0.225681165	-0.704146612	-0.371714307	0.081378574
Ptpn14	-0.650917374	-0.367236577	0.142805585	-0.896763603	-0.547986964	-0.12388203	-1.659730785	-1.029373077	0.031047087
Rasd2	-0.612418467	0.273948692	0.562358866	-0.629118707	0.106771571	0.609617885	-2.987740467	-1.515128672	0.208425051
Sdc1	-0.397878646	-0.136001221	0.188787304	-0.480566105	-0.190159826	0.264730716	-1.206517686	-0.670325873	0.047351102
Slc19a2	-0.304549181	0.068604407	0.275187327	-0.239532718	0.065564373	0.331971194	-0.599326294	-0.094261403	0.063348583
Slc39a10	-0.364382052	-0.116368547	0.107505163	-0.460215788	-0.257433793	0.066274624	-1.000963508	-0.680207834	-0.034724542
Tbkbp1	-0.762768417	-0.388254184	0.130250817	-1.014564681	-0.631607537	0.054071424	-2.536515278	-1.541562631	0.031556706
Xxylt1	-0.232515615	0.086011027	0.261982785	-0.354623657	-0.071656127	0.150379574	-1.181429565	-0.437652861	0.064783841
Zfp365	-0.4765213	0.042104217	0.233033793	-0.788003655	0.02055114	0.422793221	-2.283282166	-0.922617796	0.059439355
Ikaros UP/Myc UP									
Mtrr	0.434770417	0.763893694	0.175150946	0.530736128	0.762467315	0.244713147	0.364612018	0.749203731	0.079741556
Ikaros DOWN/Myc DOWN									
Alpk2	-1.426335259	-1.88752649	-0.319627808	-1.176703152	-1.654744764	-0.239229409	-0.29855436	-0.98114671	-0.061948622
Apba1	-0.762656193	-1.117967683	-0.148785936	-0.840174272	-1.307008669	-0.256465534	-0.448686014	-0.793923282	-0.145107055
Atp6v0a1	-0.73154847	-1.401545957	-0.532376938	-0.541484159	-1.453752004	-0.542292661	-0.335130251	-1.224142744	-0.208085066
Cd248	-1.475301339	-1.938394988	-0.192461626	-1.560271083	-1.943126261	-0.167923687	-1.617721289	-2.211667853	-0.118544988
Cyth4	-0.886793002	-1.206087561	-0.145945273	-0.965086728	-1.44049949	-0.220207531	-0.847889923	-1.118676155	-0.038473492
Gab2	-0.28950398	-0.523894029	-0.321910506	-0.528706855	-0.803477502	-0.407050395	-0.385461821	-0.632870101	-0.064198646
Il5ra	-0.632477561	-1.162258407	-0.471660104	-0.869582167	-1.200495237	-0.29849865	-0.522231825	-0.834319061	-0.059543823
Kctd12b	-0.738823444	-1.418245289	-0.466055301	-1.341569229	-1.929589771	-0.403021609	-1.394546539	-1.816019033	-0.063506767
Klf3	-0.670024793	-1.179970811	-0.483589263	-1.042523567	-1.599853212	-0.454149949	-0.962287053	-1.43563299	-0.152244381
Pcdh17	-0.915155321	-1.409217751	-0.409188493	-0.867673956	-1.539116669	-0.371615541	-1.15709451	-1.893561933	-0.111486341
Ppp1r18	-0.502738992	-0.912453698	-0.242333997	-0.57873491	-0.9291964	-0.207746162	-0.199596052	-0.621621187	-0.107963077
Rasgrp3	-1.486339227	-1.964708975	-0.27312871	-1.593951708	-2.454725632	-0.28168211	-2.211261325	-2.964153072	-0.161319603
Rgs2	-0.910897416	-1.225557774	-0.224093734	-0.846268948	-1.244782489	-0.10379063	-0.605289228	-1.252903822	-0.02570328
Rnf150	-0.532716238	-0.834189176	-0.19415426	-0.681265437	-0.912480978	-0.284346849	-0.677465796	-0.912257961	-0.057020884
Slc37a2	-0.886279517	-1.293429398	-0.228107173	-1.137962483	-1.430609704	-0.182402357	-1.335788951	-1.552427043	-0.116521589
Tmem108	-0.857858236	-1.369222423	-0.335726382	-1.178782561	-1.763946746	-0.450419917	-1.497990405	-1.910468357	-0.133727539
Tmtc1	-2.218849408	-3.004033171	-0.526997123	-2.680723347	-3.6553773	-0.683938153	-2.572485486	-3.402741933	-0.146307076
Lbh	-0.188292491	-0.414779482	-0.148277353	-0.261468675	-0.480387109	-0.123531595	0.191131659	-0.165278682	-0.088308909
Prox1	-0.494972479	-1.246143491	-0.510061212	-0.614856401	-1.393404554	-0.586538758	0.237854541	-0.424295567	-0.135758323
Trp53i11	-0.187357001	-0.44704639	-0.116102323	-0.260998076	-0.516291274	-0.140865171	0.151094225	-0.243521233	-0.056506412

Page 2

Ikaros UP/Myc DOWN	Ikaros DOWN/ Myc UP	Ikaros UP/Myc UP	Ikaros DOWN/Myc DOWN
2610008E11Rik	Abcb1b	Mtrr	Alpk2
Abcd1	Abcc1		Apba1
Ackr4	Acy1		Atp6v0a1
Acox3	Atg9b		Cd248
Adamtsl2	Bcl11a		Cyth4
Aim1	Ccnd1		Gab2
Ankrd44	D8Ertd82e		Il5ra
Ap3m2	Deptor		Kctd12b
Arid3b	Dfna5		Klf3
Asb2	Fgd2		Pcdh17
Atg9a	Frrs1		Ppp1r18
Baz2a	Kdelc1		Rasgrp3
Bcl2l1	Mmp15		Rgs2
Btg1	Nr1d1		Rnf150
Calcoco1	Nrp2		Slc37a2
Cblb	Pdzrn3		Tmem108
Cd37	Prkaa2		Tmtc1
Cdkn1b	Prrg4		(Lbh)
Cerk	Ptpn14		(Prox1)
Chd3	Rasd2		(Trp53i11)
Cklf	Sdc1		
Cpm	Slc19a2		
Cr2	Slc39a10		
Dennd1c	Tbkbp1		
Dgka	Xxylt1		
Dopey2	Zfp365		
Dyrk1b			
Endou			
Ero1lb			
Fam214a			
Fam63b			
Fchsd1			
Foxo1			
Gdi1			
Git2			
Gltscr1			
H2-Oa			
H2-Ob			
Ifi203			
Il16			
Jakmip1			
Kmt2e			
Map4k2			
Mbd4			
Natd1			
Neil1			
Pcyt1a			
Pecam1			
Pias3			
Pink1			
Plekhg2			
Pyhin1			
Rab43			
Rag1			
Rbm5			
Rprl1			
Serinc5			
Siglecg			
Slc12a6			
Spns3			
Tbx6			
Tuba1a			
Ypel3			
Zfp821			
Zfp831			
Zhx3			
(Lbh)			
(Prox1)			
(Trp53i11)			

Gene symbol	Extended name	Function
Antagonistic UP		
2610008E11Rik	unidentified	/
Abcd1	ATP Binding Cassette Subfamily D Member 1	ABC transporter ikely involved in the peroxisomal transport or catabolism of very long chain fatty acids
Ackr4	Atypical Chemokine Receptor 4	Receptor for C-C type chemokines. This receptor has been shown to bind dendritic cell- and T cell-activated chemokines
Acox3	Acyl-CoA Oxidase 3, Pristanoyl	Desaturation of 2-methyl branched fatty acids in peroxisomes
Adamtsl2	ADAMTS Like 2	Secreted glycoprotein that binds the cell surface and extracellular matrix
Aim1	CRYBG1, Crystallin Beta-Gamma Domain Containing 1	May function as suppressor of malignant melanoma. It may exert its effects through interactions with the cytoskeleton.
Ankrd44	Ankyrin Repeat Domain 44	Putative regulatory subunit of protein phosphatase 6 (PP6) that may be involved in the recognition of phosphoprotein substrates
Ap3m2	Adaptor Related Protein Complex 3 Mu 2 Subunit	Subunit of the heterotetrameric adaptor-related protein comlex 3 (AP-3).The AP-3 complex plays a role in protein trafficking to lysosomes and specialized organelles
Arid3b	AT-Rich Interaction Domain 3B	Member of the ARID (AT-rich interaction domain) family of DNA-binding proteins. Members of the ARID family have roles in embryonic patterning, cell lineage gene regulation, cell cycle control, transcriptional regulation and possibly in chromatin structure modification
Asb2	Ankyrin Repeat And SOCS Box Containing 2	subunit of a multimeric E3 ubiquitin ligase complex that mediates the degradation of actin-binding proteins. This gene plays a role in retinoic acid-induced growth inhibition and differentiation of myeloid leukemia cells
Atg9a	Autophagy Related 9A	Involved in autophagy and cytoplasm to vacuole transport (Cvt) vesicle formation
Baz2a	Bromodomain Adjacent To Zinc Finger Domain 2A	Essential component of the NoRC complex. It plays a central role by being recruited to rDNA and by targeting chromatin modifying enzymes such as HDAC1, leading to repress RNA polymerase I transcription.
Bcl2l1	BCL2 Like 1	Potent inhibitor of cell death
Btg1	BTG Anti-Proliferation Factor 1	Member of an anti-proliferative gene family that regulates cell growth and differentiation. Expression of this gene is highest in the G0/G1 phases of the cell cycle and downregulated when cells progressed through G1.
Calcoco1	Calcium Binding And Coiled-Coil Domain 1	Functions as a coactivator for aryl hydrocarbon and nuclear receptors (NR). Involved in the transcriptional activation of target genes in the Wnt/CTNNB1 pathway
Chn1b	Chi Proto-Oncogene B	Negatively regulates TCR (T-cell receptor), BCR (B-cell receptor) and FCER1 (high affinity immunoglobulin epsilon receptor) signal transduction pathways.
Cd37	Cell Differentiation Antigen 37	Mediate signal transduction events that play a role in the regulation of cell development, activation, growth and motility
Cdkn1b	Cyclin Dependent Kinase Inhibitor 1B	Binds to and prevents the activation of cyclin E-CDK2 or cyclin D-CDK4 complexes, and thus controls the cell cycle progression at G1. The degradation of this protein is required for the cellular transition from quiescence to the proliferative state.
Cerk	Ceramide Kinase	Converts ceramide to ceramide 1-phosphate (C1P), a sphingolipid metabolite
Chd3	Chromodomain Helicase DNA Binding Protein 3	Components of a histone deacetylase complex referred to as the Mi-2/NuRD complex
Cklf	Chemokine Like Factor	Chemoattractant for neutrophils, monocytes and lymphocytes
Cpm	Carboxypeptidase M	Arginine/lysine carboxypeptidase. Its expression is associated with monocyte to macrophage differentiation
Cr2	Complement C3d Receptor 2	Eceptor for Epstein-Barr virus (EBV) binding on B and T lymphocytes
Dennd1c	DENN Domain Containing 1C	Guanine nucleotide exchange factor, regulates endosomal membrane trafficking and is involved in actin polymerization
Dgka	Diacylglycerol Kinase Alpha	Upon cell stimulation converts the second messenger diacylglycerol into phosphatidate, initiating the resynthesis of phosphatidylinositols and attenuating protein kinase C activity.
Dopey2	Dopey Family Member 2	May be involved in protein traffic between late Golgi and early endosomes
Dyrk1b	Dual Specificity Tyrosine Phosphorylation Regulated Kin	Dual-specificity kinase which possesses both serine/threonine and tyrosine kinase activities. Enhances the transcriptional activity of TCF1/HNF1A and FOXO1. promotes expression of the gluconeogenic enzyme glucose-6-phosphatase (G6PC)
Endou	Endonuclease, Poly(U) Specific	Endoribonuclease that cleaves single-stranded RNAs at uridylates and releases products that have 2-3-cyclic phosphate termini
Ero1lb	Endoplasmic Reticulum Oxidoreductase 1 Beta	Oxidoreductase involved in disulfide bond formation in the endoplasmic reticulum.
Fam214a	Family With Sequence Similarity 214 Member A	/
Fam63b	MINDY Lysine 48 Deubiquitinase 2	Can remove ubiquitin from proteins
Fchsd1	FCH And Double SH3 Domains 1	/
Foxo1	Forkhead Box O1	Transcription factor that is the main target of insulin signaling and regulates metabolic homeostasis in response to oxidative stress
Gdi1	GDP Dissociation Inhibitor 1	Regulate the GDP-GTP exchange reaction of members of the rab family that are involved in vesicular trafficking of molecules between cellular organelles
Git2	GIT ArfGAP 2	GIT proteins regulate cytoskeletal dynamics and participate in receptor internalization and membrane trafficking.
Gltscr1	Glioma Tumor Suppressor Candidate Region Gene 1	May play a role in BRD4-mediated gene transcription.
H2-Oa		Heterodimer encoded by H2-Oa and b in the MCH II class region, shown to be physically associated with H2-M in B cells and to downregulate its function
H2-Ob		Heterodimer encoded by H2-Oa and b in the MCH II class region, shown to be physically associated with H2-M in B cells and to downregulate its function
Ifi203	interferon activated gene 203	/
Il16	Interleukin 16	Chemoattractnt, ligand for CD4
Jakmip1	Janus kinase and microtubule interacting protein 1	Associates with microtubules and may play a role in the microtubule-dependent transport of the GABA-B receptor. May play a role in JAK1 signaling and regulate microtubule cytoskeleton rearrangement
Kmt2e	Lysine MEthyltransferase 2E	Histone methyltransferase that specifically mono- and dimethylates Lys-4 of histone G. REgulator of hematopoiesis, cell cycle regulator, required to suppress inappropriate expression of S-phase-promoting genes; overexpression inhibits cell cycle progression
Map4k2	Mitogen-Activated PRotein Kinase Kinase Kinase Kinase	SEr/Thr kinase. REquired for efficient activation of JNKs
Mbd4	Methyl-CpG Binding Domain 4, DNA Glycosylase	Mismatch-specific DNA N-glycosylase involved in DNA repair
Natd1	N-Acetyltransferase Domain Containing 1	/
Neil1	Nei Like DNA Glycosylase 1	Acts as DNA glycosylase that recognizes and removes damaged bases.
Pcyt1a	Phosphate Cytidylyltransferase 1, Choline, Alpha	Involved in the regulation of phosphatidylcholine biosynthesis
Pecam1	Platelet And Endothelial Cell Adhesion Molecule 1	The encoded protein is a member of the immunoglobulin superfamily and is likely involved in leukocyte migration, angiogenesis, and integrin activation.
Pias3	Protein Inhibitor Of Activated STAT 3	E3-type small ubiquitin-like modifier (SUMO) ligase; role as a transcriptional coregulation in various cellular pathways, including the STAT pathway and the steroid hormone signaling pathway.
Pink1	PTEN Induced Putative Kinase 1	Serine/threonine protein kinase that localizes to mitochondria. It is thought to protect cells from stress-induced mitochondrial dysfunction.
Plekhg2	Pleckstrin Homology And RhoGEF Domain Containing G	RhoGTPase that can activate CDC42 by promoting exchange of GDP for GTP on CDC42
Pyhin1	Pyrin And HIN Domain Family Member 1	Tumor suppressor activity of IFN in breast cancer cells. Promotes ubiquitination and subsequent degradation of MDM2, which leads to p53/TP53 stabilization.
Rab43	RAB43, Member RAS Oncogene Family	Rab are key regulators of intracellular membrane trafficking
Rag1	Recombination Activating 1	Involved in activation of immunoglobulin V-D-J recombination
Rbm5	RNA Binding Motif Protein 5	Plays a role in the induction of cell cycle arrest and apoptosis through pre-mRNA splicing of multiple target genes including the tumor suppressor protein p53.
Rprl1	ribonuclease P RNA-like 1	/
Serinc5	Serine Incorporator 5	Enhances the incorporation of serine into phosphatidylserine and sphingolipids
Siglecg	sialic acid binding Ig-like lectin G	B1 cell inhibitory receptor
Slc12a6	Solute Carrier Family 12 Member 6	Mediates electroneutral potassium-chloride cotransport.
Spns3	Sphingolipid Transporter 3	Sphingolipid transporter
Thx6	T-Box 6	Role in the determination of the fate of axial stem cells: neural vs mesodermal
Tuba1a	Tubulin Alpha 1a	Major components of microtubules
Ypel3	Yippee Like 3	Involved in proliferation and apoptosis in myeloid precursor cells.
Zfp821	Zinc Finger Protein 821	/
Zfp831	Zinc Finger Protein 831	/
Zhx3	Zinc Fingers And Homeoboxes 3	Acts as a transcriptional repressor. Involved in the early stages of mesenchymal stem cell (MSC) osteogenic differentiation
Antagonistic DOWN		
Abcb1b	ATP-binding cassette, sub-family B, member 1B	ABC transporter involved in multidrug resistance.
Abcc1	ATP Binding Cassette Subfamily C Member 1	ABC transporter involved in multidrug resistance.
Acy1	Aminoacylase 1	Function in the catabolism and salvage of acylated amino acids.
Atg9b	Autophagy Related 9B	Involved in autophagy and cytoplasm to vacuole transport (Cvt) vesicle formation
Bcl11a	B-Cell CLL/Lymphoma 11A	Transcription factor associated with the BAF SWI/SNF chromatin remodeling complex
Ccnd1	Cyclin D1	This cyclin forms a complex with and functions as a regulatory subunit of CDK4 or CDK6, whose activity is required for cell cycle G1/S transition.
D8Ertd82e	/	/
Deptor	DEP Domain Containing MTOR Interacting Protein	Negative regulator of the mTORC1 and mTORC2 signaling pathways
Dfna5	Non-syndromic hearing impairment protein 5	/
Fgd2	FYVE, RhoGEF And PH Domain Containing 2	May play a role in leukocyte signaling and vesicle trafficking in antigen-presenting cells in the immune system
Frrs1	Ferric Chelate Reductase 1	Reduce ferric to ferrous iron before its transport from the endosome to the cytoplasm
Kdelc1	KDEL Motif Containing 1	Proteins carrying this motif are bound by a receptor in the Golgi apparatus so that the receptor-ligand complex returns to the endoplasmic reticulum.
Mmp15	Matrix Metallopeptidase 15	Involved in the breakdown of extracellular matrix
Nr1d1	Nuclear Receptor Subfamily 1 Group D Member 1	Transcriptional repressor which coordinates circadian rhythm and metabolic pathways in a heme-dependent manner. Also regulates genes involved in metabolic functions, including lipid and bile acid metabolism, adipogenesis, gluconeogenesis and the macrophage inflammatory response
Nrp2	Neuropilin 2	May play a role in cardiovascular development, axon guidance, and tumorigenesis
Pdzrn3	PDZ Domain Containing Ring Finger 3	E3 ubiquitin-protein ligase
Prkaa2	Protein Kinase AMP-Activated Catalytic Subunit Alpha 2	Catalytic subunit of the AMP-activated protein kinase (AMPK
Prrg4	Proline Rich And Gla Domain 4	/
Ptpn14	Protein Tyrosine Phosphatase, Non-Receptor Type 14	May play a role in the regulation of lymphangiogenesis, cell-cell adhesion, cell-matrix adhesion, cell migration, cell growth
Rasd2	RASD Family Member 2	Activator of mechanistic target of rapamycin 1
Sdc1	Syndecan 1	Participates in cell proliferation, cell migration and cell-matrix interactions via its receptor for extracellular matrix proteins
Slc19a2	Solute Carrier Family 19 Member 2	High-affinity transporter for the intake of thiamine.
Slc39a10	Solute Carrier Family 39 Member 10	May act as a zinc-influx transporter.
Tbkbp1	TBK1 Binding Protein 1	Adapter protein which constitutively binds TBK1 and IKBKE playing a role in antiviral innate immunity.
Xxylt1	Xyloside Xylosyltransferase 1	/
Zfp365	Zinc Finger Protein 365	May play a role in uric acid excretion.
Synergic UP		
Mtrr	5-Methyltetrahydrofolate-Homocysteine Methyltransferas	Functions in the synthesis of methionine by regenerating methionine synthase to a functional state.
Synergic DOWN		
Alpk2	Alpha Kinase 2	Kinase that recognizes phosphorylation sites in which the surrounding peptides have an alpha-helical conformation.
Apba1	Amyloid Beta Precursor Protein Binding Family A	Putative function in synaptic vesicle exocytosis
Atp6v0a1	ATPase H+ Transporting V0 Subunit A1	Required for assembly and activity of the vacuolar ATPase
Cd248	CD248 Molecule	May play a role in tumor angiogenesis.
Cyth4	Cytohesin 4	Promotes the activation of ARF factors through replacement of GDP with GTP.
Gab2	GRB2 Associated Binding Protein 2	They act as adapters for transmitting various signals in response to stimuli through cytokine and growth factor receptors
Il5ra	Interleukin 5 Receptor Subunit Alpha	Receptor for interleukin-5.
Kcnf12b	Potassium Channel Tetramerization Domain Containing 1	Auxiliary subunit of GABA-B receptors that determine the pharmacology and kinetics of the receptor response
Klf3	Kruppel Like Factor 3	Binds to the CACCC box of erythroid cell-expressed genes. May play a role in hematopoiesis
Lbh	Limb Bud And Heart Development	Transcriptional activator which may act in mitogen-activated protein kinase signaling pathway.
Pcdh17	Protocadherin 17	Potential calcium-dependent cell-adhesion protein.
Ppp1r18	Protein Phosphatase 1 Regulatory Subunit 18	Protein phosphatase-1
Prox1	Prospero Homeobox 1	May play an essential role during development
Rasgrp3	RAS Guanyl Releasing Protein 3	Guanine nucleotide exchange factor (GEF) for Ras and Rap1.
Rgs2	Regulator Of G Protein Signaling 2	Regulates G protein-coupled receptor signaling cascades
Rnf150	Ring Finger Protein 150	/
Slc37a2	Solute Carrier Family 37 Member 2	Inorganic phosphate and glucose-6-phosphate antiporter.
Tmem108	Transmembrane Protein 108	Regulates the organization and stability of the microtubule
Tmtc1	Transmembrane And Tetratricopeptide Repeat Containing	Endoplasmic reticulum adaptor protein
Trp53i11	Tumor Protein P53 Inducible Protein 11	/

Supplementary table 2. In this table, all Myc interactors identified in our experiments (label free and SILAC) or in already published datasets (Koch et al, 2007; Agrawal et al, 2010; Dingar et al, 2015; HPDR, Peri et al, 2003) are reported. Each column represents one dataset and cells are colored in green if the corresponding protein has been identified in that experiment. The proteins are ranked according to the number of times they have been identified considering all the datasets ("TOT" column). The number of times each protein has been identified in our datasets is also reported ("TOT in our data" column).

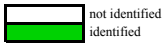

Complete list	Label Free	Label Free 2	Label Free 3	SILAC FWD	SILAC REV	HPDR	Koch	Agrawal two-step	Agrawal SILAC	Agrawal Label Free	Dingar	TOT	TOT in our data
MAX	■			■		■	■	■	■	■	■	8	2
MYC	■	■	■	■	■				■	■	■	8	5
EP400	■	■	■			■	■		■	■	■	8	3
TRRAP	■	■	■		■		■			■	■	7	4
WDR5	■	■	■	■	■						■	6	5
TRIM28	■	■	■	■	■		■					6	5
GTF2I		■		■	■	■	■				■	6	3
CORO1A	■	■	■	■	■							5	5
UBC	■		■					■	■	■		5	2
LMNA			■	■			■	■	■			5	2
PSMD2	■						■		■	■		4	1
CHD4	■	■	■				■					4	3
SMARCA5	■			■			■			■		4	2
RUVBL1	■	■	■				■					4	3
SHMT2	■	■	■	■								4	4
RRM2	■		■	■	■							4	4
PTBP1	■	■	■							■		4	3
PRKDC	■	■	■				■					4	3
RUVBL2	■	■	■				■					4	3
MCM7	■	■	■				■					4	3
MCM2	■	■	■				■					4	3
MCM3	■	■	■		■							4	4
NCL	■			■	■		■					4	3
HSPA8	■			■	■			■				4	3
CCT5	■	■	■				■					4	3
DDX17	■	■		■					■			4	3
ACLY		■	■	■	■							4	4
CFL1			■	■	■					■		4	3
ACTC1				■	■				■	■		4	2
HDAC2	■						■				■	3	1
RPP30	■						■			■		3	1
TF	■				■				■			3	2
ACTL6A	■					■					■	3	1
RPL13	■			■					■			3	2
PML	■					■				■		3	1
RPS16	■			■						■		3	2
YBX1	■		■						■			3	2
SSRP1	■		■	■								3	3
CBFB	■								■	■		3	1
SUMO2	■		■		■							3	3
RPL18A	■	■	■									3	3
RBBP4	■	■	■									3	3
RPL3	■		■	■								3	3
PGD	■		■	■						■		3	2
FBL	■		■				■					3	2
CACYBP	■	■	■									3	3
PSMA7	■	■					■					3	2
RPS6	■		■	■								3	3
HDAC1	■	■					■					3	2
MCM6	■	■	■									3	3
IKZF3	■	■	■									3	3
HMGB1	■			■	■							3	3
SNRNP200	■	■	■									3	3
IFI16	■	■	■									3	3
DNAJA1	■	■	■									3	3
PARP1	■			■	■							3	3
RPL27	■		■	■	■							3	3
NPM1	■			■	■							3	3
HNRNPM	■			■	■							3	3
ACO2		■		■	■							3	3
RPL11			■	■	■							3	3
PGK1			■	■	■							3	3
PCBP1				■	■		■					3	2
PCBP2				■	■					■		3	2
EIF4A1				■	■		■					3	2
PKM2				■	■					■		3	2
CKAP4				■					■	■		3	1
NONO				■			■		■			3	1
FLNA				■					■	■		3	1
HSPB1							■		■	■		3	0
ERBB2IP								■	■	■		3	0
PRKCDBP								■	■	■		3	0
TUBA4A								■	■	■		3	0
ADNP									■	■	■	3	0
SNX2	■		■									2	2
XRN2	■										■	2	1
MSH2	■						■					2	1
RPL31	■			■								2	2
USP7	■										■	2	1
POLR2B	■						■					2	1
CSNK2A1	■					■						2	1
UBTF	■									■		2	1
ZC3H11A	■										■	2	1
KDM1A	■										■	2	1
RFC5	■						■					2	1
NSUN2	■										■	2	1
DDX24	■									■		2	1
SMEK1	■										■	2	1
FIP1L1	■										■	2	1
TCERG1	■										■	2	1
HNRPDL	■		■									2	2
OGT	■										■	2	1
IDH3B	■						■					2	1
SYNCRIP	■			■								2	2
PRPF6	■								■			2	1

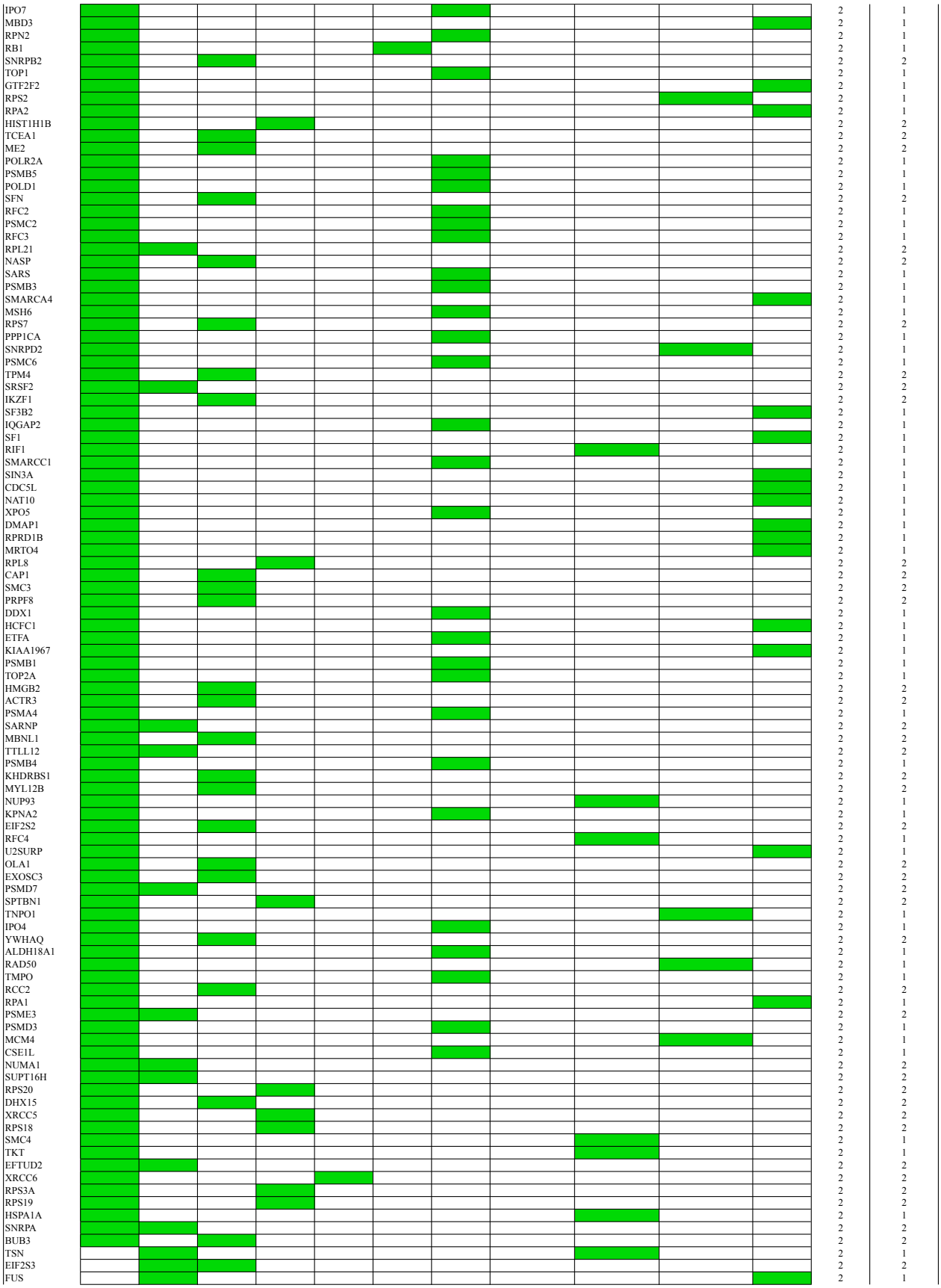
IPO7 2 1
MBD3 2 1
RPN2 2 1
RB1 2 1
SNRPB2 2 2
TOP1 2 1
GTF2F2 2 1
RPS2 2 1
RPA2 2 1
HIST1H1B 2 2
TCEA1 2 2
ME2 2 2
POLR2A 2 1
PSMB5 2 1
POLD1 2 1
SFN 2 2
RFC2 2 1
PSMC2 2 1
RFC3 2 1
RPL21 2 2
NASP 2 2
SARS 2 1
PSMB3 2 1
SMARCA4 2 1
MSH6 2 1
RPS7 2 2
PPP1CA 2 1
SNRPD2 2 1
PSMC6 2 1
TPM4 2 2
SRSF2 2 2
IKZF1 2 2
SF3B2 2 1
IQGAP2 2 1
SF1 2 1
RIF1 2 1
SMARCC1 2 1
SIN3A 2 1
CDC5L 2 1
NAT10 2 1
XPO5 2 1
DMAP1 2 1
RPRD1B 2 1
MRTO4 2 1
RPL8 2 2
CAP1 2 2
SMC3 2 2
PRPF8 2 2
DDX1 2 1
HCFC1 2 1
ETFA 2 1
KIAA1967 2 1
PSMB1 2 1
TOP2A 2 1
HMGB2 2 2
ACTR3 2 2
PSMA4 2 1
SARNP 2 2
MBNL1 2 2
TTLL12 2 2
PSMB4 2 1
KHDRBS1 2 2
MYL12B 2 2
NUP93 2 1
KPNA2 2 1
EIF2S2 2 2
RFC4 2 1
U2SURP 2 1
OLA1 2 2
EXOSC3 2 2
PSMD7 2 2
SPTBN1 2 2
TNPO1 2 1
IPO4 2 1
YWHAQ 2 2
ALDH18A1 2 1
RAD50 2 1
TMPO 2 1
RCC2 2 2
RPA1 2 1
PSME3 2 2
PSMD3 2 1
MCM4 2 1
CSE1L 2 1
NUMA1 2 2
SUPT16H 2 2
RPS20 2 2
DHX15 2 2
XRCC5 2 2
RPS18 2 2
SMC4 2 1
TKT 2 1
EFTUD2 2 2
XRCC6 2 2
RPS3A 2 2
RPS19 2 2
HSPA1A 2 1
SNRPA 2 2
BUB3 2 2
TSN 2 1
EIF2S3 2 2
FUS 2 1

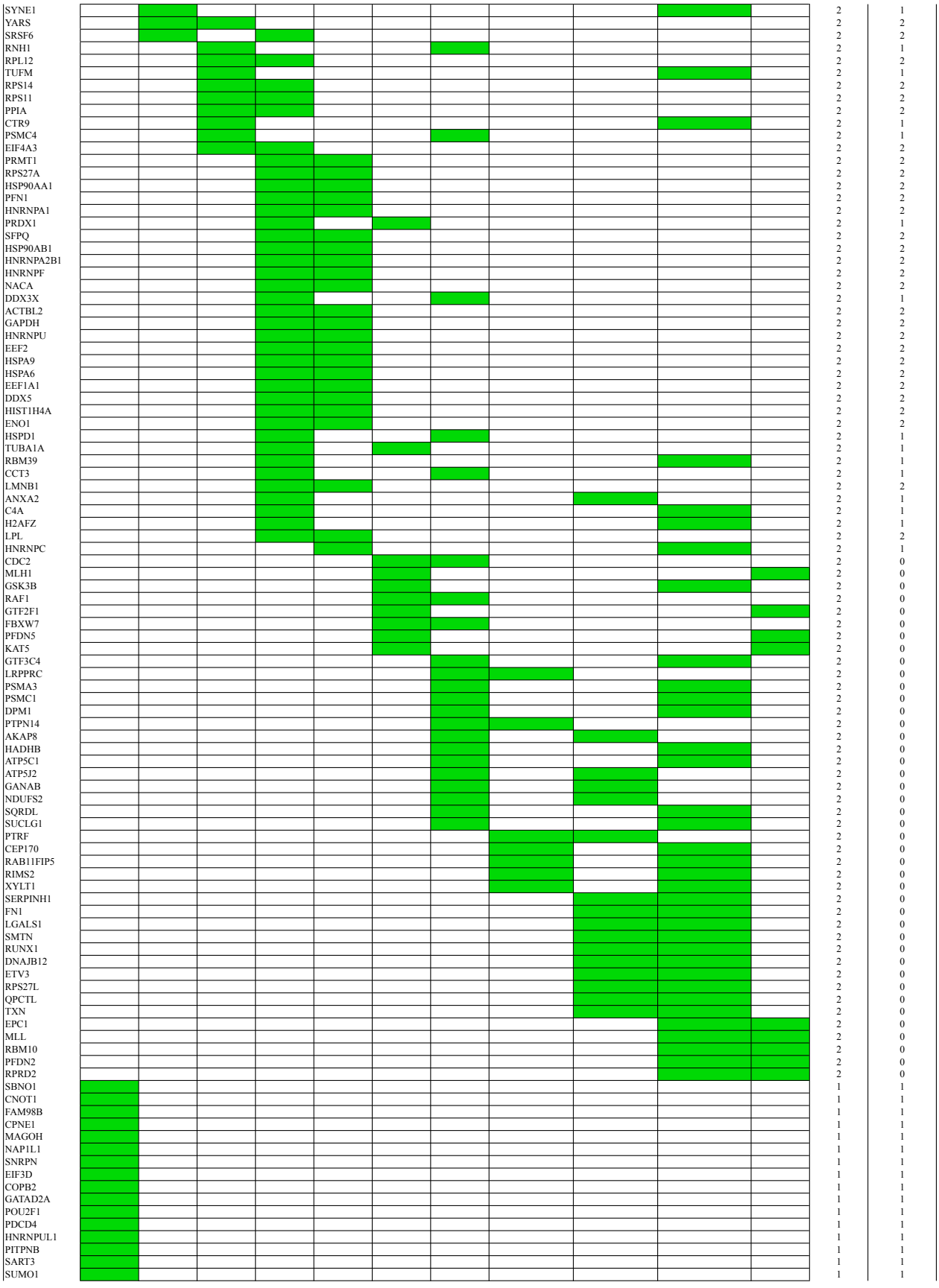

MTHFD2												1	1
GFM1												1	1
ZNF207												1	1
UBR5												1	1
ADAR												1	1
GINS1												1	1
CDK2												1	1
GDI2												1	1
CYFIP2												1	1
CSTF2												1	1
FDPS												1	1
COPS8												1	1
RAB1B												1	1
DNMT1												1	1
DDB1												1	1
DHX8												1	1
IARS2												1	1
C12orf10												1	1
SMARCC2												1	1
PPP1CC												1	1
MRE11A												1	1
ANP32A												1	1
DHX30												1	1
SMARCD2												1	1
FSCN1												1	1
RPL17												1	1
PSMD14												1	1
PRMT5												1	1
HAT1												1	1
SPTBN2												1	1
PPM1G												1	1
RNMT												1	1
SART1												1	1
TIMM44												1	1
RAD21												1	1
DHX16												1	1
AQR												1	1
RNF40												1	1
H2AFY												1	1
PRPF40A												1	1
WDHD1												1	1
RNASEH2A												1	1
GLS												1	1
C3												1	1
HIST1H2BJ												1	1
LTA4H												1	1
AKR1B1												1	1
HIST1H1C												1	1
PGAM1												1	1
RCC1												1	1
SRM												1	1
U2AF2												1	1
UQCRC1												1	1
PYCR1												1	1
RPL9												1	1
TALDO1												1	1
MRPL19												1	1
EMD												1	1
RAD23B												1	1
NAPA												1	1
ADK												1	1
PPP4C												1	1
RAB10												1	1
UBE2N												1	1
RPL26												1	1
RPL23												1	1
RPS25												1	1
RPL10A												1	1
MRPS9												1	1
PFKP												1	1
TOP2B												1	1
YWHAH												1	1
MTAP												1	1
AIMP2												1	1
CBX3												1	1
CUL1												1	1
EXOSC2												1	1
TRIM25												1	1
FRG1												1	1
PDCD11												1	1
PSMD6												1	1
PDS5A												1	1
ANP32E												1	1
ABCF2												1	1
BZW1												1	1
KTN1												1	1
ALYREF												1	1
THOC6												1	1
CCAR1												1	1
ABCF1												1	1
PRPF31												1	1
PSPC1												1	1
GATAD2B												1	1
DOCK2												1	1
ANP32B												1	1
EMG1												1	1
ZNF622												1	1
SMARCD1												1	1
PAWR												1	1
THOC3												1	1
PUS7												1	1
NACC1												1	1

STRBP												1	1
TSNAX												1	1
DNAJC7												1	1
MCMBP												1	1
RBM4												1	1
SRRT												1	1
QTRT1												1	1
MRPL4												1	1
TBL1XR1												1	1
FAM192A												1	1
MRPL46												1	1
PNN												1	1
MOV10												1	1
NIT2												1	1
DIABLO												1	1
DDX21												1	1
PNO1												1	1
SLTM												1	1
PUF60												1	1
NAGK												1	1
RALY												1	1
PSME2												1	1
PSMD13												1	1
COPS3												1	1
SRRM2												1	1
MRPS28												1	1
YARS2												1	1
NOSIP												1	1
PUS1												1	1
C16orf80												1	1
PYCR2												1	1
RPL5												1	1
MCM5												1	1
PRPF4												1	1
EIF3B												1	1
DIS3												1	1
SAFB												1	1
SMCHD1												1	1
WDR82												1	1
GSTP1												1	1
NANS												1	1
PLAA												1	1
OTUB1												1	1
RBM12												1	1
RBM8A												1	1
GLRX3												1	1
ANXA6												1	1
G3BP2												1	1
SUCLA2												1	1
PAPSS1												1	1
ECM29												1	1
MAPK1												1	1
API5												1	1
GALK1												1	1
PARK7												1	1
LUC7L2												1	1
SF3A1												1	1
SRPRB												1	1
U2AF1												1	1
POLR2H												1	1
NUDT5												1	1
EIF3M												1	1
DDX42												1	1
SET												1	1
SUB1												1	1
APEX1												1	1
KIAA0564												1	1
CLIC4												1	1
ISG20												1	1
PSMC5												1	1
MAT2A												1	1
PSMG1												1	1
CDC37												1	1
USP14												1	1
ZC3HAV1L												1	1
RPL7												1	1
ACAA2												1	1
UBAP2L												1	1
PDHB												1	1
DDX46												1	1
SUGT1												1	1
MAGOHB												1	1
PSMB8												1	1
PSIP1												1	1
SYK												1	1
PRDX6												1	1
EIF3K												1	1
USP5												1	1
RPS8												1	1
RAC2												1	1
NAA15												1	1
RNF20												1	1
CAT												1	1
LARP1												1	1
EIF4B												1	1
PRDX3												1	1
FAM120A												1	1
COBRA1												1	1
HNRNPR												1	1
TPR												1	1
RBM25												1	1
LMNB2												1	1

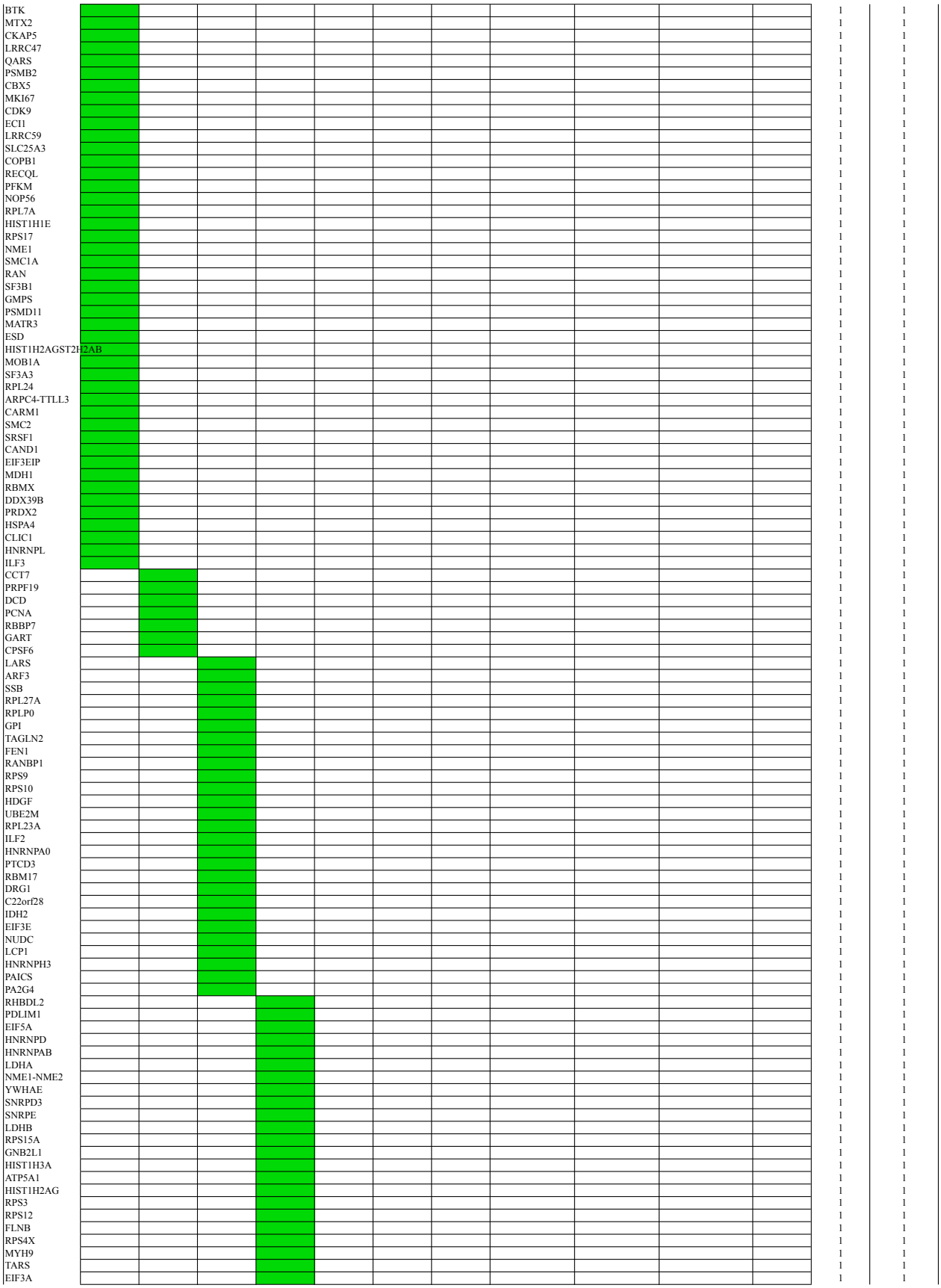
BTK 1 1
MTX2 1 1
CKAP5 1 1
LRRC47 1 1
QARS 1 1
PSMB2 1 1
CBX5 1 1
MKI67 1 1
CDK9 1 1
ECI1 1 1
LRRC59 1 1
SLC25A3 1 1
COPB1 1 1
RECQL 1 1
PFKM 1 1
NOP56 1 1
RPL7A 1 1
HIST1H1E 1 1
RPS17 1 1
NME1 1 1
SMC1A 1 1
RAN 1 1
SF3B1 1 1
GMPS 1 1
PSMD11 1 1
MATR3 1 1
ESD 1 1
HIST1H2AGST2H2AB 1 1
MOB1A 1 1
SF3A3 1 1
RPL24 1 1
ARPC4-TTLL3 1 1
CARM1 1 1
SMC2 1 1
SRSF1 1 1
CAND1 1 1
EIF3EIP 1 1
MDH1 1 1
RBMX 1 1
DDX39B 1 1
PRDX2 1 1
HSPA4 1 1
CLIC1 1 1
HNRNPL 1 1
ILF3 1 1
CCT7 1 1
PRPF19 1 1
DCD 1 1
PCNA 1 1
RBBP7 1 1
GART 1 1
CPSF6 1 1
LARS 1 1
ARF3 1 1
SSB 1 1
RPL27A 1 1
RPLP0 1 1
GPI 1 1
TAGLN2 1 1
FEN1 1 1
RANBP1 1 1
RPS9 1 1
RPS10 1 1
HDGF 1 1
UBE2M 1 1
RPL23A 1 1
ILF2 1 1
HNRNPA0 1 1
PTCD3 1 1
RBM17 1 1
DRG1 1 1
C22orf28 1 1
IDH2 1 1
EIF3E 1 1
NUDC 1 1
LCP1 1 1
HNRNPH3 1 1
PAICS 1 1
PA2G4 1 1
RHBDL2 1 1
PDLIM1 1 1
EIF5A 1 1
HNRNPD 1 1
HNRNPAB 1 1
LDHA 1 1
NME1-NME2 1 1
YWHAE 1 1
SNRPD3 1 1
SNRPE 1 1
LDHB 1 1
RPS15A 1 1
GNB2L1 1 1
HIST1H3A 1 1
ATP5A1 1 1
HIST1H2AG 1 1
RPS3 1 1
RPS12 1 1
FLNB 1 1
RPS4X 1 1
MYH9 1 1
TARS 1 1
EIF3A 1 1

TUBB												1	1
PLEC												1	1
IGHG3												1	1
COL1A1												1	1
CDK1												1	1
HSPA5												1	1
CLTC												1	1
PABPC1												1	1
HIST1H2AC												1	1
SRSF7												1	1
VIM												1	1
TPM3												1	1
C/EBP												1	0
C/EBP												1	0
CREBBP												1	0
EP300												1	0
ELF3												1	0
HSP90A												1	0
KIAA1524												1	0
MEK1												1	0
NFKB3												1	0
NFYB												1	0
PARP10												1	0
RBL1												1	0
SKP2												1	0
TAF1B												1	0
TBP												1	0
SP1												1	0
CSNK2A2												1	0
YY1												1	0
MAD												1	0
TIAM1												1	0
MAPK8												1	0
SH3P9; BIN1												1	0
SMAD2												1	0
TFAP2B												1	0
SMARCB1												1	0
P73												1	0
CCNT1												1	0
MAPK7												1	0
TUBA2												1	0
TUBA1B												1	0
CDC6												1	0
DNMT3A												1	0
SUP73H												1	0
PAF350/400												1	0
SMAD3												1	0
NMI												1	0
ZNF151												1	0
TUBA8												1	0
MYCBP												1	0
RAGE-1												1	0
MYCBP2												1	0
SPAG9												1	0
MINA												1	0
UBB												1	0
CDKN2A												1	0
GCN5L2												1	0
ERK1												1	0
NFYC												1	0
MXI1												1	0
SNIP1												1	0
BCL2												1	0
GCN5L1												1	0
ZNF281												1	0
HECTH9												1	0
DBC-1												1	0
MYBBP1A												1	0
BAF53A												1	0
H2B												1	0
SMARCA6												1	0
MMS19L												1	0
GTF3C1												1	0
GTF3C2												1	0
GTF3C3												1	0
U5-200kD												1	0
U5-116kD												1	0
HNRPF												1	0
HNRPK												1	0
NOL5A												1	0
HSA9761												1	0
ARHGEF2												1	0
DDX15												1	0
DDX20												1	0
DDX52												1	0
HNRPA0												1	0
IMP-1												1	0
IMP-2												1	0
KIAA0332												1	0
RNGTT												1	0
U5-102kD												1	0
XRN1												1	0
AKAP8L												1	0
POLE												1	0
LTAg												1	0
CHTF18												1	0
SMC2L1												1	0
SMC4L1												1	0
KU70												1	0
FANCD2												1	0
ERCC3												1	0
KU80												1	0

MSH3												1	0
EIF3S2												1	0
EF1G												1	0
EIF4ENIF1												1	0
MARS												1	0
MRPS22												1	0
MRPS34												1	0
PELO												1	0
SKP1A												1	0
PSMA1												1	0
PSMA2												1	0
PSMA5												1	0
PSME4												1	0
UBE3C												1	0
UBR2												1	0
FBX29												1	0
PRSS15												1	0
PSMC3												1	0
PSMD4												1	0
SQSTM1												1	0
BCR												1	0
PPP6C												1	0
ARL1												1	0
GCS1												1	0
GSG2												1	0
IRAK1												1	0
MEP50												1	0
NEK9												1	0
PLK1												1	0
RPN1												1	0
DNAJA2												1	0
DNAJB6												1	0
TCP1												1	0
CCT2												1	0
DNAJA3												1	0
CCT4												1	0
CCT6A												1	0
CCT8												1	0
HSPH1												1	0
IRS4												1	0
C1QBP												1	0
IKBKAP												1	0
CYR61												1	0
RIN1												1	0
SHOC2												1	0
14-3-3												1	0
TUBAL1												1	0
COPG												1	0
COPG2												1	0
KPNB1												1	0
MYO9B												1	0
NUP133												1	0
SLC25A12												1	0
SLC25A13												1	0
XPO1												1	0
ABCB7												1	0
ARF4												1	0
ATP1A1												1	0
ATP2A2												1	0
DNCH1												1	0
IPO13												1	0
IPO9												1	0
KPNA4												1	0
MYO5C												1	0
MYO9A												1	0
NUP153												1	0
PLEKHC1												1	0
RANBP2												1	0
SEC61A2												1	0
SLC25A1												1	0
SLC25A11												1	0
TUBG1												1	0
TUBGCP2												1	0
XPOT												1	0
ALDH1B1												1	0
NDUFS3												1	0
OAT												1	0
P4HA1												1	0
AASS												1	0
ASS												1	0
CEPT1												1	0
GCDH												1	0
IDH3A												1	0
IDH3G												1	0
NDUFA5												1	0
NDUFA8												1	0
NDUFS1												1	0
PLOD3												1	0
PPT1												1	0
PTE1												1	0
PTGES2												1	0
SPTLC1												1	0
GCN1L1												1	0
IQGAP3												1	0
C1ORF25												1	0
FLJ20272												1	0
HIGD1A												1	0
ILVBL												1	0
SLIT2												1	0
SSR4												1	0
ZNF121												1	0
LMO7												1	0

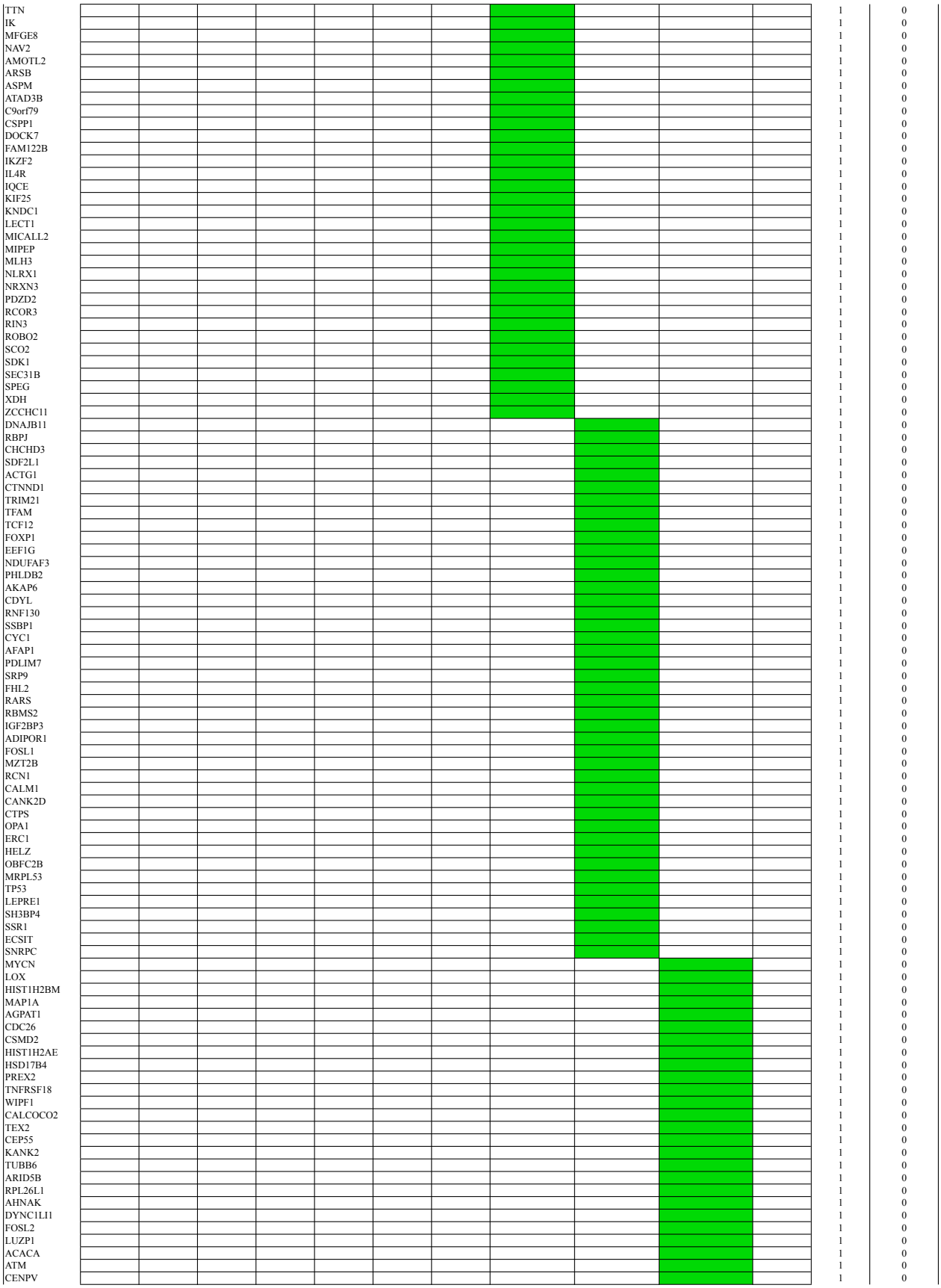
TTN 1 0
IK 1 0
MFGE8 1 0
NAV2 1 0
AMOTL2 1 0
ARSB 1 0
ASPM 1 0
ATAD3B 1 0
C9orf79 1 0
CSPP1 1 0
DOCK7 1 0
FAM122B 1 0
IKZF2 1 0
IL4R 1 0
IQCE 1 0
KIF25 1 0
KNDC1 1 0
LECT1 1 0
MICALL2 1 0
MIPEP 1 0
MLH3 1 0
NLRX1 1 0
NRXN3 1 0
PDZD2 1 0
RCOR3 1 0
RIN3 1 0
ROBO2 1 0
SCO2 1 0
SDK1 1 0
SEC31B 1 0
SPEG 1 0
XDH 1 0
ZCCHC11 1 0
DNAJB11 1 0
RBPJ 1 0
CHCHD3 1 0
SDF2L1 1 0
ACTG1 1 0
CTNND1 1 0
TRIM21 1 0
TFAM 1 0
TCF12 1 0
FOXP1 1 0
EEF1G 1 0
NDUFAF3 1 0
PHLDB2 1 0
AKAP6 1 0
CDYL 1 0
RNF130 1 0
SSBP1 1 0
CYC1 1 0
AFAP1 1 0
PDLIM7 1 0
SRP9 1 0
FHL2 1 0
RARS 1 0
RBMS2 1 0
IGF2BP3 1 0
ADIPOR1 1 0
FOSL1 1 0
MZT2B 1 0
RCN1 1 0
CALM1 1 0
CANK2D 1 0
CTPS 1 0
OPA1 1 0
ERC1 1 0
HELZ 1 0
OBFC2B 1 0
MRPL53 1 0
TP53 1 0
LEPRE1 1 0
SH3BP4 1 0
SSR1 1 0
ECSIT 1 0
SNRPC 1 0
MYCN 1 0
LOX 1 0
HIST1H2BM 1 0
MAP1A 1 0
AGPAT1 1 0
CDC26 1 0
CSMD2 1 0
HIST1H2AE 1 0
HSD17B4 1 0
PREX2 1 0
TNFRSF18 1 0
WIPF1 1 0
CALCOCO2 1 0
TEX2 1 0
CEP55 1 0
KANK2 1 0
TUBB6 1 0
ARID5B 1 0
RPL26L1 1 0
AHNAK 1 0
DYNC1LI1 1 0
FOSL2 1 0
LUZP1 1 0
ACACA 1 0
ATM 1 0
CENPV 1 0

CHAF1B												1	0
CNOT4												1	0
DDX51												1	0
FANCM												1	0
FZD10												1	0
NPTX2												1	0
OBSCN												1	0
OPHN1												1	0
PDLIM4												1	0
SGOL2												1	0
SNRPF												1	0
ABCA1												1	0
ABRA												1	0
ADAMTS20												1	0
ANLN												1	0
AP4B1												1	0
ARG1												1	0
ASXL1												1	0
ATP6V1D												1	0
BAT2												1	0
BCMO1												1	0
BPTF												1	0
C14orf43												1	0
C18orf22												1	0
C20orf160												1	0
C20orf20												1	0
C2orf89												1	0
C3orf15												1	0
CEP192												1	0
CPSF2												1	0
CYP2U1												1	0
DENND3												1	0
DHX58												1	0
DIP2B												1	0
DIRAS2												1	0
EHHADH												1	0
ETV6												1	0
EXOSC1												1	0
FAM117B												1	0
FRMD6												1	0
FZR1												1	0
H3F3B												1	0
HCFC2												1	0
HIRA												1	0
HOXB5												1	0
IL1B												1	0
INSM1												1	0
ITGAL												1	0
KALRN												1	0
KCNG3												1	0
KIAA0922												1	0
KIAA1274												1	0
KLF10												1	0
LBX2												1	0
LRP1B												1	0
MAGEB10												1	0
MAP3K1												1	0
MAP3K7												1	0
MATN4												1	0
MCF2L2												1	0
MCTP2												1	0
MED12L												1	0
MIB1												1	0
MKL1												1	0
MRPL14												1	0
MTRF1												1	0
MYO18A												1	0
NAIP												1	0
NCOR1												1	0
NPC1L1												1	0
PLEKHH1												1	0
POP4												1	0
PPA2												1	0
PPP2R3B												1	0
PRG4												1	0
PRKAR1B												1	0
PRR11												1	0
RAG1												1	0
RALGAPA1												1	0
RUNX2												1	0
SAMD9L												1	0
SETX												1	0
SH3RF1												1	0
SHANK2												1	0
SIPA1L3												1	0
SNX19												1	0
ST3GAL3												1	0
ST6GALNAC6												1	0
TAF2												1	0
TENC1												1	0
TRAK1												1	0
USP10												1	0
WDFY3												1	0
ZBTB40												1	0
ZC3H7B												1	0
ZFHX3												1	0
ZNF354B												1	0
ZNF541												1	0
ZNF586												1	0
ZNF703												1	0
ZNF740												1	0
IGF2BP2												1	0

RBM9												1	0
PDS5B												1	0
NCOR2												1	0
IMMT												1	0
GFPT1												1	0
PHF6												1	0
ATP5O												1	0
SMC6												1	0
YAF2												1	0
CDC42EP1												1	0
CLEC11A												1	0
HIST1H1A												1	0
JUN												1	0
KIAA0319												1	0
NOMO2												1	0
PLOD2												1	0
SDF4												1	0
TPP1												1	0
TRPM1												1	0
ZC3H18												1	0
BAHCC1												1	0
C2orf29												1	0
CACNA1G												1	0
CALD1												1	0
CROCC												1	0
DACT1												1	0
DYNLRB1												1	0
FAF2												1	0
FAM116B												1	0
FASTKD1												1	0
FLJ45139												1	0
GLTSCR1												1	0
IL16												1	0
KARS												1	0
KIAA2026												1	0
KIF20B												1	0
LGALS7												1	0
LIMS1												1	0
MAGI1												1	0
MUC5AC												1	0
OTUD4												1	0
PDHA2												1	0
PHF20												1	0
PLA2G4A												1	0
PPIP5K2												1	0
RPS21												1	0
RRP1B												1	0
SEC11C												1	0
SHE												1	0
SMYD4												1	0
TBL2												1	0
TDG												1	0
UQCRFS1												1	0
ZFP106												1	0
HOXA10												1	0
CDV3												1	0
MAST4												1	0
MUC3A												1	0
TUBB3												1	0
ABCA9												1	0
ABCB1												1	0
ACACB												1	0
AGK												1	0
AHNAK2												1	0
AIFM2												1	0
AJAP1												1	0
ALPK3												1	0
ARFGAP1												1	0
ARID4B												1	0
BRWD1												1	0
BUB1												1	0
C2orf16												1	0
CDK5RAP2												1	0
CLSTN1												1	0
CNTN5												1	0
CSF1												1	0
CTBP1												1	0
CYBA												1	0
DDX47												1	0
DNAH8												1	0
DUSP15												1	0
ELFN1												1	0
ERP44												1	0
EXPH5												1	0
FERMT3												1	0
FLJ44674												1	0
FOXC2												1	0
FRMPD4												1	0
GABRR1												1	0
GEMIN5												1	0
GPR158												1	0
HK1												1	0
KIF12												1	0
LCN12												1	0
MAP3K5												1	0
MAP7D1												1	0
MFHAS1												1	0
MYO1D												1	0
NAV3												1	0
NFIL3												1	0
NPR1												1	0
NRD1												1	0

NUP98												1	0
ODZ2												1	0
PADI2												1	0
PITX2												1	0
POLG												1	0
POLR3A												1	0
RFX2												1	0
RRM1												1	0
SACS												1	0
SBNO2												1	0
SDHA												1	0
SLC25A10												1	0
SUCLG2												1	0
TMPRSS11A												1	0
TNR												1	0
TPH1												1	0
TRAP1												1	0
UBA1												1	0
USP36												1	0
USP48												1	0
XKRX												1	0
ZNF238												1	0
ZZEF1												1	0
ZBTB33												1	0
TAFL6												1	0
BRD4												1	0
TAF9B												1	0
FAM48A												1	0
TAF5L												1	0
EPC2												1	0
TADA1												1	0
VPS72												1	0
DIDO1												1	0
ARID1A												1	0
PPP1R10												1	0
SUPT7L												1	0
CCDC101												1	0
ING3												1	0
SUPT3H												1	0
TAF10												1	0
MED1												1	0
TAF12												1	0
YEATS4												1	0
KDM3B												1	0
CHD8												1	0
RBM27												1	0
RDBP												1	0
TRIM24												1	0
SIN3B												1	0
MBTD1												1	0
YEATS2												1	0
SPEN												1	0
TASA2B												1	0
PES1												1	0
TADA3												1	0
SNW1												1	0
MGA												1	0
LRWD1												1	0
ARID3B												1	0
TRIM33												1	0
TAF9												1	0
BAG2												1	0
SETD1A												1	0
BAP1												1	0
ZMYM2												1	0
ATXN7L2												1	0
WDR36												1	0
VBP1												1	0
SUGP1												1	0
SMARCE1												1	0
ARID1B												1	0
THAP11												1	0
TCF20												1	0
ZMYND8												1	0
PFDN6												1	0
WHSC2												1	0
UTP14A												1	0
NOC3L												1	0
XAB2												1	0
KANSL3												1	0
MGEA5												1	0
MLL4												1	0
HMGXB4												1	0
CCDC99												1	0
ZC3H14												1	0
WAC												1	0
MEAF6												1	0
JMJD1C												1	0
CDC73												1	0
CCNK												1	0
CFDP1												1	0
IRF2BP2												1	0
TPX2												1	0
LIN54												1	0
LUC7L3												1	0
USP22												1	0
NFRKB												1	0
PPIL1												1	0
DPY30												1	0
NUP50												1	0
ELAC2												1	0
NFIA												1	0

WIZ												1	0
WRNIP1												1	0
DGCR14												1	0
HEXIM1												1	0
WDR3												1	0
NCAPH												1	0
MED23												1	0
TBPL1												1	0
CPSF7												1	0
PRPF3												1	0
TLE3												1	0